The Functional Competence of Animal Cells in Culture: Analysis of the Microsome Proteome

A thesis submitted to the University of Kent for the degree of Doctor of Philosophy in the Faculty of Science, Technology and Medical Studies.

2003

Daniel Alete

RESEARCH SCHOOL OF
BIOSCIENCES
UNIVERSITY OF KENT
AT CANTERBURY

Declaration

No part of this thesis has been submitted in support of an application for any degree or qualification of the University of Kent or any other University or institute of learning.

Daniel Alete
30th October 2003

This thesis is dedicated to the memory of
Pauline Elizabeth Alete
1940 – 1991

Acknowledgements

I would like to extend by gratitude toward my supervisors, Dr Mark Smales and Dr David James for the opportunity to work in their laboratory, and for their endless patience. I would also like to thank Prof. John Birch and Dr Andrew Racher at Lonza Biologics for their help and advice. Thanks also to the members of the DCJ lab (past and present), Michele Underhill, Elisabeth Sage, Kym Baker, Clare Coley, and Mark Weeks for making the lab such an enjoyable place to be. Thank you also to my family for their support throughout the last three years. Finally, thank you to Julia for her endless encouragement, support, and love through the toughest of times. You are very special.

Contents

List of Figures

List of Tables

Abbreviations

μ	Specific growth rate
ACN	Acetonitrile
ADP	Adenosine-5'-diphosphate
AMP	Adenosine-5'-monophophate
APS	Ammonium persulphate
ATP	Adenosine-5'-triphosphate
ATPase	Adenosine triphosphatase
BSA	Bovine serum albumin
CHAPS	3,3'-Cholamidopropyl-dimethylammonio-1-propanesulfonate
CHO	Chinese hamster ovary
CnBr	Cyanogen bromide
cpm	Counts per minute
ddH_20	Double distilled water (18 MΩ cm purity)
dFCS	Dialysed foetal calf serum
DDM	n-Dodecyl b-D-Maltoside
2DE	Two-dimensional electrophorsesis
DEPC	Diethyl pyrocarbonate
DHFR	Dihydrofolate reductase
DMEM	Dulbecco's minimum essential medium
DMSO	Dimethylsulphoxide
DNA	Deoxyribonucleic acid
DTT	Dithiothreitol
ECL	Enhanced chemiluminescence
EDTA	Ethylenediaminetetra-acetic acid
ELISA	Enzyme linked immunosorbent assay
ER	Endoplasmic reticulum
ERGIC	ER-golgi intermediate compartment
ESI	Electrospray ionisation
EthBr	Ethidium Bromide
FPLC	Fast performance liquid chromatography
GRP78	Glucose regulated protein 78

GRP94	Glucose regulated protein 94
GS	Glutamine synthetase
HRP	Horse radish peroxidase
HSP60	Heat shock protein 60
HSP70	Heat shock protein 70
IAA	Idoacetic acid
IEF	Isoelectric focusing
IgG	Immunoglobulin G
IMDM	Iscoves modified Dulbecco's medium
IPG	Immobilised pH gradient
kB	Kilobase
kDa	Kilodaltons
M	Molarity (moles/litre)
mab	Monoclonal antibody
MALDI	Matrix assisted laser desorption ionisation
mRNA	Messenger ribonucleic acid
MS	Mass spectrometry
MSX	Methionine sulphoxamine
NAD(H)	Nicotinamide adenosine dinucleotide (reduced)
NS0	Non-secreting murine myeloma cell
PAGE	polyacrylamide gel electrophoresis
PBS	Phosphate buffered saline
PDI	Protein disulphide isomerase
pI	Isoelectric point
PMF	Peptide mass fingerprint
PST	Peptide sequence tag
qMab	Cell specific productivity
RNA	Ribonucleic acid
RT	Room temperature
rpm	Revolutions per minute
SDS	Sodium dodecyle sulphate
TBS	Tris Buffered saline
T_d	Doubling time
TE	Tris-EDTA

TEA	Triethanolamine
TEMED	N, N, N',N'-Tetramethylethylenediamine
TFA	Trifloracetic acid
TGS	Tris glycine SDS electrophoresis buffer (pre-mixed)
TIMP-1	Metalloproteinase inhibitor 1
TMB	3,3'5,5'-tetramethylbenzidine
TOF	Time-of-flight
UPR	Unfolded protein response
VCC	Viable cell concentration

Abstract

It has previously been reported that the efficient folding, transport and modifications of recombinant proteins are major bottlenecks in limiting high level productivity with respect to the manufacture of recombinant proteins by mammalian cells in culture. However, the potential for manipulating specific productivity by altering the complement of proteins that make up secretory pathway, such as chaperones and foldases, is largely unknown and open to question. In this study a series of murine myeloma cell lines (NS0), and Chinese hamster ovary cell lines (CHO), have been generated expressing the cB72.3 monoclonal antibody. These cell lines exhibited a range of productivities from 0 – 300 mg L^{-1} and 100 – 1000 mg L^{-1} respectively, and were fully characterised during this study using targeted proteome analysis. During this investigation the following questions were addressed; (1) Do cell lines selected for high level productivity have altered expression of secretory pathway components?, (2) are specific metabolic processes such as protein transport and degradation up or down regulated as a result of high level productivity? , and (3) are changes in protein expression conserved between different cell types producing the same recombinant protein (e.g CHO vs NS0)? NS0 and CHO cells were grown under batch culture conditions and harvested at mid-exponential phase (μmax) for analysis. Analysis of the heavy and light chain antibody mRNA levels and cell size of each cell line showed that there was no correlation between cell specific productivity and mRNA levels. A comparative semi-quantitative proteomic analysis was then performed on the microsome fractions generated from NS0 and CHO cell lines, then the resulting analysis revealed 8 proteins whose expression levels were correlated with cellular recombinant protein productivity (7 up-regulated and 1 down) among clonal populations of the NS0 cell line. Seven regulated proteins (4 up and 3 down) were also observed between CHO cell lines producing the same IgG4 recombinant protein. The majority of changes observed in protein expression were cell line specific (not correlated with productivity) and were not conserved between clonal populations or cell lines. This implies that each cell line has a 'bias' to its range of proteins involved in integrated functions such as productivity and metabolism. Identification of the regulated proteins by MALDI-ms revealed that the majority of these proteins are involved in the generation of ATP, suggesting that the up-regulation of a cells metabolic capacity is required for high level productivity. The data presented in this thesis clearly demonstrate that any strategy aimed

at improving productivity by multi-gene engineering of specific proteins within the secretory pathway is unlikely to succeed.

Chapter 1 Introduction

1.0 Recombinant protein production from mammalian cell systems

Processes for recombinant protein production by mammalian cells in culture were originally developed for the production of virus vaccines such as the polio vaccine, developed in monkey kidney cells in 1954 (Birch, 1999). This was followed by the first large scale industrial production of foot-and-mouth vaccine in baby hamster kidney (BHK) cells by suspension culture (Birch, 1999). Soon after, methods were developed for producing clinically useful human proteins such as interferons (Lubiniecki, 1998). Further advances in recombinant DNA (rDNA) and hybridoma technology have greatly expanded the range of products produced in animal cells. Furthermore, rDNA technology has the potential to produce large quantities of previously scarce or completely novel proteins as therapeutics or diagnostic tools.

The growth of recombinant proteins as a class of therapeutic molecules has greatly accelerated over the past five years. Approximately 50 different recombinant proteins have been licensed for use in the US and Europe, and account for revenues estimated to be in excess of $12 billion (Kelley, 2001). A list of licensed rDNA biologicals (as at the end of 2001) expressed by mammalian cells is presented in table 1.1

Table 1.1 Licensed/approved rDNA biologicals expressed by mammalian cells (Adapted from Chu & Robinson, 2001., Lubiniecki, 1998).

Product	Year	Cell System	Application
Actilyse (tPA)	1987	CHO	Blood clot removal
Saizen (hGH)	1989	C127	Growth disorders
Eposin (EPO)	1990	CHO	Anaemia
Follistim (FSH)	1996	CHO	Infertility
Novo Seven (Factor VII)	1996	BHK	Haemophilia
Verluma (mab)	1996	Mammalian cells	Cancer imaging
VAQTA (vaccine)	1996	MRC-5 diploid fibroblasts	Immunisation for hepatitis A
Avonex (Interferon β)	1996	CHO	Multiple Sclerosis
Benefix (coagulation factor IX)	1997	CHO	Haemophilia
Rituxan (mab to CD20)	1997	CHO	Non-hodgkin B cell lymphoma
Rotashield (vaccine)	1997	FRhL-2	Immunisation for rotavirus
Simulect (mab)	1998	NS0	Prophylaxis of acute organ rejection
Synagis (mab)	1998	NS0	Prophylaxis of respiratory synctial virus
Remicade (mab)	1998	NS0	Crohn's disease
Herceptin	1998	CHO	Metastatic breast cancer
Enbrel (chimeric mab)	1998	CHO	Rheumatoid arthritis
Wellferon (interferon α)	1999	Human Lymphoblastoid Cell line	Hepatitis C
ReFacto	2000	CHO	Acute myocardial infarction

BHK, baby hamster kidney; CHO, Chinese hamster ovary; NS0 non-secreting murine myeloma

Prokaryotic systems (i.e bacterial cultures) can be employed for the production of recombinant proteins, however these systems are mainly used for the production of small protein products. The advantage of mammalian cell systems for the production of heterologous proteins are that they contain the complement of organelles and enzymes

required to permit physiological protein folding and ensure correct post-translational modification. Such modifications include glycosylation, phosphorylation of tyrosine, serine and threonine residues, addition of fatty acid chains, and macromolecular assembly prior to secretion (Geisse et al., 1996). In general prokaryotic systems are unable to undertake these tasks. Protein structure, and the pattern of post-traslational modifications, are crucial factors that influence characteristics such as biological activity, trafficking, immunogenicity and clearance rate *in vivo* of biotherapeutics (Barnes et al., 2003; Geisse et al., 1996). Small variations in the very specific modifications of recombinant proteins may result in dramatic changes in their properties (i.e. stability, solubility and efficacy *in vivo*). Thus, if proteins obtained from cell cultures are to be used for such medical purposes as diagnostics, prophylactics, or therapeutic agents, it is of great importance that they reflect their naturally occurring counterparts to the highest possible degree. This requires correct and undisturbed functioning of the protein processing components that constitute the secretory pathway. Indeed, inefficient functioning of the secretory pathway is currently thought to be a major bottle-neck in efforts to increase the productivity of mammalian cell systems (Downham et al., 1996).

1.1 Protein synthesis and secretion in eukaryotic cells

In order to improve our understanding of the factors that may influence the production of recombinant proteins in mammalian cells, it is necessary to examine the processes involved in protein synthesis, modification and transport. This serves to highlight the large number of proteins that are involved in protein synthesis and the complexity of their organisation within the secretory pathway.

1.1.1 Introduction to the secretory pathway

The secretory pathway of eukaryotic cells underlies the targeting of newly synthesised proteins, the generation and maintainance of subcellular compartments and organelles, and proper cell growth and division. The secretory pathway was originally defined in 1975 using pancreatic exocrine cells (Palade, 1975). This pathway is highly compartmentalized, creating an optimal milieu for a broad spectrum of reactions. In mammalian cells, it consists of a complex system of endomembranes which include the

endoplasmic reticulum (ER), ER/golgi intermediate compartment (ERGIC), *cis*, *medial* and *trans* golgi network and the plasma membrane (Figure 1.1), which are responsible for the synthesis, modification, sorting, and transport of secretory and membrane proteins. Over the years morphological analysis by many investigators has resulted in a general description and understanding of the organelles involved in the secretory pathway. Furthermore, the need for vascular carriers to ferry protein cargo between topologically separate components has been widely published (Palade, 1975; Saraste and Kuismanen, 1984). The development of yeast mutants defective in specific transport steps in secretion in the 1980's offered a powerful approach to dissect the components of the secretory machinery. These studies revealed that the described vesicular transport mechanism is conserved universally from fungal to neuronal cells (Bennett and Scheller, 1993; Novick et al., 1980). Additional studies involving the reconstitution of vesicular transport *in vitro* clearly identified the cytosolic factors and membrane components required for vesicle formation, docking and fusion (Rothman, 1994; Rothman and Wieland, 1996). More recently, chimeric proteins tagged with green fluorescent protein have made it possible to follow membrane transport *in vivo* (Presley, 1997), allowing further characterisation of the processes involved in the secretory pathway.

1.1.2 Protein translocation into the ER

The entry station for all proteins destined for the secretory pathway (including secretory proteins, plasma membrane proteins, and proteins destined for various compartments of the endomembrane system) is the endoplasmic reticulum (ER). The ER is responsible for the synthesis and translocation of proteins and the release of properly processed, folded and assembled proteins to allow transport to their destinations. The function of the ER can be divided up into three main sections that are performed by different sets of resident proteins. These include; (i) protein translocation across the ER membrane, (ii) facilitation of proper folding, maturation and modification of newly synthesised proteins, and (iii) the export of proteins from the ER to the *cis*-golgi. Translocation across, or integration into, the endoplasmic reticulum (ER) membrane is the first event in the intracellular sorting of numerous proteins in eukaryotic cells. Proteins that are translocated across the ER include virtually all secreted proteins in addition to lumenal

proteins of the ER, nuclear envelope, golgi apparatus, lysosomes and endosomes (Gilmore, 1993)

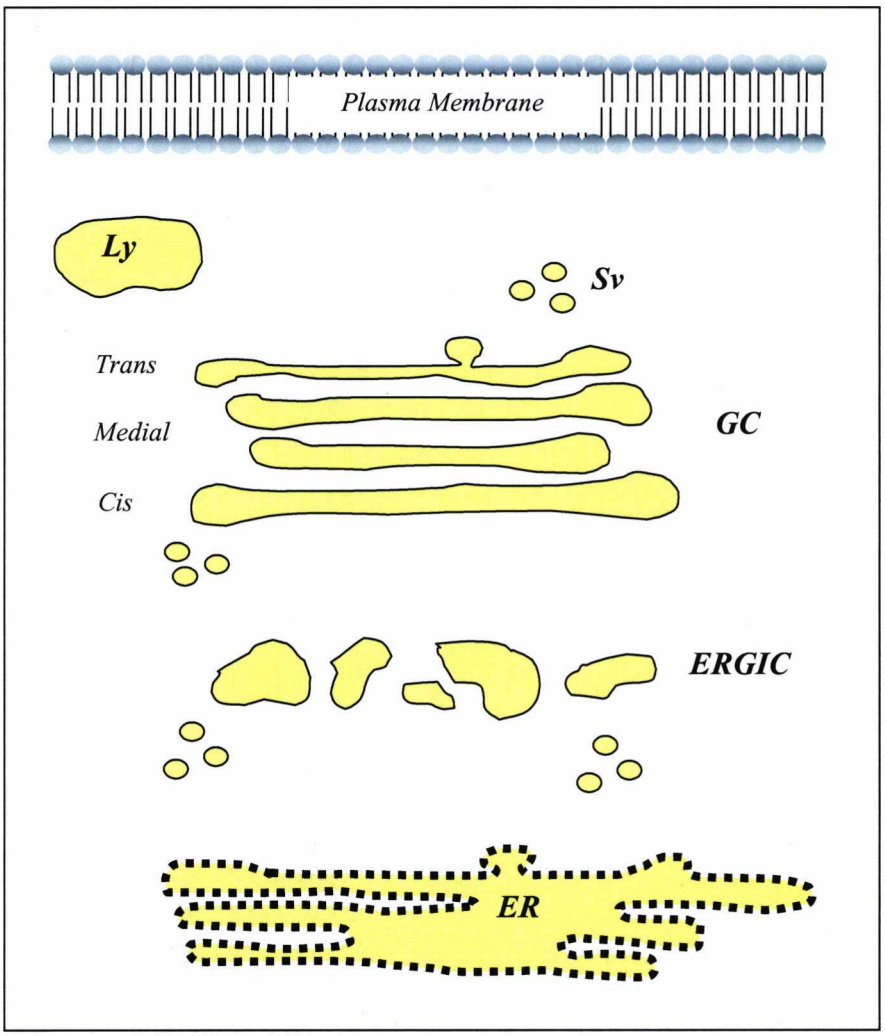

Figure 1.1 Schematic representation of the secretory pathway. ***ER***, endoplasmic reticulum; ERGIC, ER-Golgi-Intermediate- Compartment; ***GC***, golgi complex; ***Sv***, secretory vesicle; ***Ly***, lysosome.

Translocation can occur either co-translationally or post-translationally. Post-translational translocation is less common, and usually only occurs with small proteins (<100 amino acids). The majority of polypeptides which form secretory and membrane proteins are translocated co-translationally with the ribosome synthesizing the secretory protein tightly bound to the ER membrane.

As the polypeptide of a secretory protein is synthesized, a sequence of around 6-20 amino acids at the N-terminus of the polypeptide chain, termed 'the signal sequence', directs the ribosome to the ER membrane (Nothwehr, 1990). Targeting of the nascent polypeptide to the ER membrane via the signal sequence is accomplished by the combined function of the signal recognition particle (SRP) and its membrane receptor, termed either docking protein or SRP receptor (Rapoport, 1992). SRP is a small ribonucleoprotein that is comprised of one molecule of 7S RNA (around 300 nucleotides) and six distinct polypeptides of 9, 14, 19, 54, 68, and 72 kDa (High, 1995; Lodish, 1995). As the signal sequence emerges from the ribosome it is bound by the 54 kDa subunit of SRP leading to the arrest of elongation after about 70-100 amino acids. Arrest of polypeptide elongation is mediated by the 9 and 14 kDa components of SRP (Lodish, 1995). Once SRP is bound and elongation has been arrested, the complex consisting of the nascent polypeptide, the ribosome, and bound SRP is specifically targeted via the 68 and 72 kDa components, to SRP receptors located on the ER membrane. The SRP receptor consists of α and β subunits of 640 and 300 amino acids respectively (Rapoport, 1992). Contact between the SRP ribosome complex and the SRP receptor triggers the exchange of GTP for GDP bound to the α subunit of the receptor. The receptor in a GTP bound state tenaciously binds SRP, which releases its grip on the signal peptide. The freed signal peptide swiftly binds to the translocation machinery. The α subunit of the receptor then hydrolyses its bound GTP to GDP which releases SRP. The delay in GTP hydrolysis gives the signal peptide time to find its new partner. The interval is sufficiently long to ensure that the signal peptide is not recaptured by SRP (Gilmore, 1993; High, 1995; Rapoport, 1992).

Once the signal sequence intitiates translocation, the polypeptide chain passes directly from the large ribosomal subunit through the ER membrane via the translocation machinery termed the translocon. The translocon is a protein linked channel in the membrane through which the nascent polypeptide traverses. Little is known about the precise composition of the translocon, but two components have been shown to play a major role in translocation. The translocating chain-associating membrane (TRAM) protein is a multi-spanning integral membrane protein found in the rough ER of mammals (Rothblatt et al., 1994). It is thought to bind the N-terminal portion of the signal sequence of the nascent polypeptide chain (High, 1995). The second component thus far identified is the mammalian homologue of yeast Sec61, called Sec61 α. In mammalian cells Sec61 α

has been shown to be part of a complex consisting of three integral membrane proteins Sec61 α, Sec61 β, and Sec61 γ (High, 1995). The Sec61 complex primarily interacts with the core of the nascent polypeptide chain (Rapoport, 1992). The Sec61 complex and TRAM therefore appear to cooperate in order to facilitate the transfer of the polypeptide chain through the membrane (Gilmore, 1993). As the nascent polypeptide chain emerges from the translocon, the signal sequence is cleaved and rapidly degraded by the signal peptidase complex. Concurrently the transfer of dolichol-linked core oligosaccharide precursors occurs from dolichol to the appropriate asparagine residues on the nascent polypeptide by the oligosacharyltransferase complex (OST) (Rothblatt et al., 1994). A schematic representation of the translocon is shown in figure 1.2.

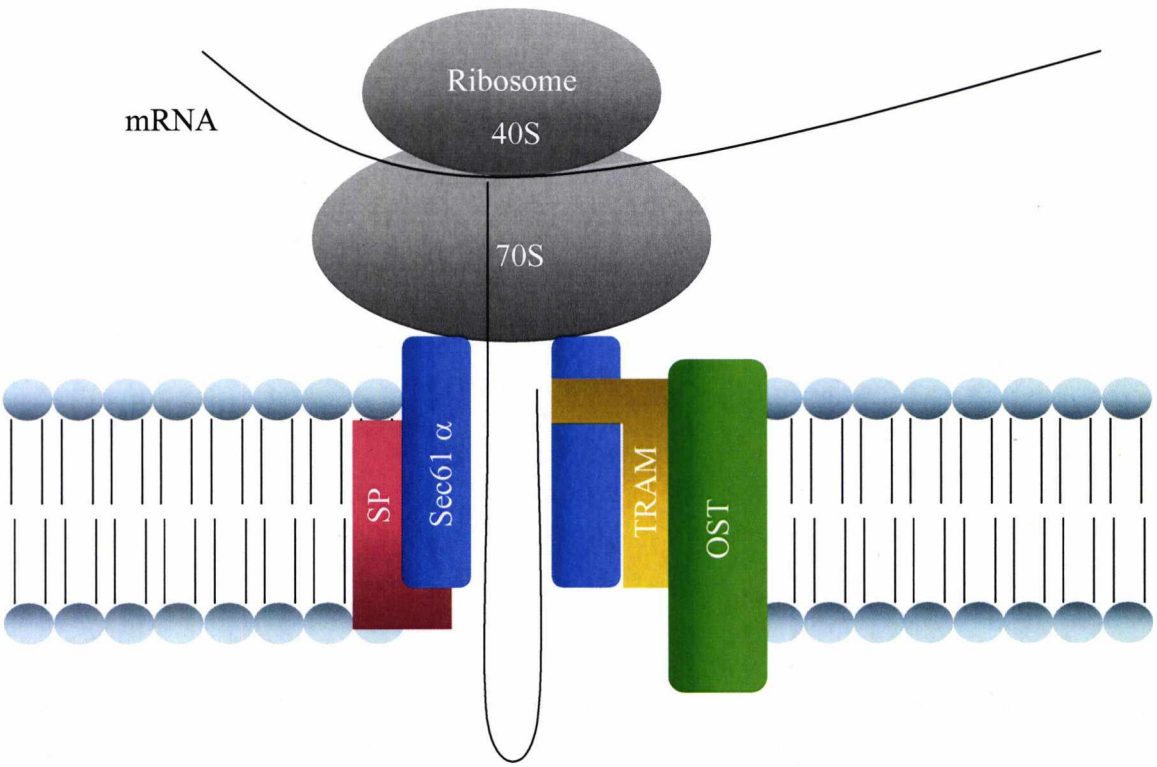

Adapted from Gilmore, 1993

Figure 1.2. A schematic representation of the translocon. A preassembled translocon site comprised of Sec61 α, TRAM, Signal peptidase (SP) and oligosaccharyltransferase (OST). Polypeptides traversing the channel contact TRAM and Sec61 α.

1.1.3 Protein folding and modification within the ER

The maturation, folding and post-translational modifications of proteins is undertaken in the lumen of the ER which provides both the oxidising environment required and houses the numerous enzymes and chaperones required for these processes. As the polypeptide chain emerges from the translocon into the lumen of the ER, it is immediately bound by the resident ER chaperone GRP78 (also know as Bip or Immunoglobulin binding protein), a member of the HSP70 family of molecular chaperones. GRP78 binds to hydrophobic segments of polypeptides, preventing protein aggregation and denaturation (Gething, 1999). GRP78 is also thought to function as part of the translocation machinery by actively facilitating transport into the ER lumen (Gilmore, 1993). After binding and hydrolyzing ATP, GRP78 releases the bound polypeptide. If the polypeptide remains in the unfolded state with its hydrophobic segment exposed, it rebinds GRP78. This cycle of binding and release continues until the protein has acquired the desired and final conformational state (Gething, 1999; Stevens and Argon, 1999).

Other chaperones present in the ER include GRP170, another member of the HSP70 family, which has been reported to be associated with Immunoglobulins in B cells (Stevens and Argon, 1999), but whose role is not yet defined. GRP94, a member of the HSP90 family, also recognises peptides but apparently a different subset than GRP78 (Stevens and Argon, 1999). This distinction is thought to enable GRP94 to associate with later folding intermediates than GRP78, thus chaperoning different phases of the folding process (Stevens and Argon, 1999).

As well as protein chaperones, the ER contains a complement of enzymes that catalyse a variety of reactions that contribute to the proper folding and modification of secretory proteins. A general property distinguishing proteins that fold in the ER from cytosolic proteins is the presence of disulphide bonds. Cysteine residues in newly synthesised secretory polypeptides tend to oxidize in the ER lumen because of its high oxidative redox potential (Gething and Sambrook, 1992). This oxidation of cysteines to form disulphide bonds is catalysed by the resident ER enzyme protein disulphide isomerase (PDI). PDI is a 58 kDa protein that catalyses thiol/disulphide interchange reactions, and depending on the nature of the polypeptide substrate and the imposed redox

potential, promotes disulphide bond formation, isomerization or reduction (Freedman, 1995). PDI does not determine the polypeptide's folding pathway, but rather facilitates formation of the correct set of disulphide bonds by promoting rapid reshuffling of incorrect disulphide pairings (Gething and Sambrook, 1992). Furthermore, a report by Mayer et al. demonstrated that GRP78 and PDI act synergistically during the *in vitro* folding of a denatured and reduced Fab fragment (Mayer et al., 2000). Their data suggest that in the absence of GRP78, unfolded antibody chains collapse rapidly upon refolding, rendering cysteine side chains inaccessible to PDI. GRP78 binds the unfolded polypeptide chains, keeping them in a conformation in which the cysteine residues are accessible to PDI (Mayer et al., 2000).

Additional studies have identified ER proteins containing thioredoxin units homologous to PDI. ERp59, ERp61, and ERp72 are three members of the thioredoxin class of proteins whose synthesis is induced upon the onset of immunoglobulin secretion in murine B cells (Gething and Sambrook, 1992). Peptidyl prolyl *cis-trans* isomerases are another class of enzyme that contribute to the modification of proteins within the ER. These proteins catalyse the otherwise slow isomerization of peptide bonds between proline residues from the *cis* to the *trans* orientation. These enzymes fall into two classes, the FK506 binding proteins (FKBP's, of which FKBP-13 is an ER resident) and the cyclophilins (Rothblatt et al., 1994).

1.1.4 Quality control within the ER

Within the ER there is an extremely well characterised quality control system which checks the integrity of secreted glycoproteins during production. This control system involves two homologous lectins; calnexin, an integral membrane chaperone, and its soluble counterpart calreticulin (Schrag et al., 2003). The process of N-linked glycosylation occurs through the transfer of a triglucosylated core oligosaccharide (Glc_3-Man_9-$GluNac_2$) to the polypeptide chain as it emerges from the translocon by the OST complex. Soon after this transfer, trimming of the core oligosaccharide is undertaken by the successive action of ER glucosidase I and II to give the monoglycosylated form (Glc_1-Man_9-$GlcNAc_2$). It is this glycopeptide form that is recognised by, and interacts with calnexin and calreticulin (Ellgaard and Helenius, 2001). The resulting interaction leads to

the interaction of the folding glycoprotein with the chaperone ERp57, a member of the PDI family (Oliver et al., 1997). Studies using reducing agents have shown that unpaired disulphide bonds prevent protein exit from the ER (Lodish and Kong, 1993). Furthermore, free thiols have been shown to mediate retention of monomeric, unassembled IgM-chains (Sitia et al., 1990). The association between calnexin/careticulin and the protein polypeptide is terminated by glucosidase II, which removes the remaining glucose from the glycan. If, at this point, the glycoprotein has reached its native conformation, it is no longer retained within the ER and is transported to the golgi complex. If not, a glucose molecule is re-added to the glycan chain, this reaction being catalysed by UDP-glucose:glycoprotein glucosyltransferase (UGGT). The calnexin/calreticulin cycle then re-starts (Ellgaard and Helenius, 2001). Failing this, the N-glycan is hydrolysed by α-mannosidase I, which then targets the protein for re-translocation through the Sec61α channel and degradation by the proteasome (Schrag et al., 2003). Together, calnexin/careticulin, UGGT, glucosidase II and ER α-mannosidase I function in order to allow incorrectly folded proteins multiple chances to acquire their correct conformation..

1.1.5 Regulation of protein expression by the ER

The folding and modification of secretory proteins within the ER requires the coordinated efforts of a multitude of chaperones and enzymes. In the context of industrial scale protein production in mammalian cells, the ER may be exposed to increased stress, due to greatly enhanced protein synthesis resulting from the use of powerful expression systems. In order to modulate ER stress, the ER has the capacity to regulate protein expression by two distinct mechanisms; the unfolded protein response (UPR), and the ER overload response (EOR) (Chevet et al., 2001).

It is difficult to distinguish between the UPR and EOR in terms of defining the triggering factor as both responses result from the excess accumulation of proteins in the ER. The EOR is believed to result from the over-accumulation of proteins in the ER membrane, which results in an increase in calcium permeability, whereas the UPR is activated by the over-accumulation of unfolded, misfolded, or aggregated proteins in the ER lumen (Kozutsumi et al., 1988; Pahl and Baeuerle, 1997). The primary function of the UPR and EOR seems to be decongestion of the ER and restoration of its normal function.

Both responses require a range of signalling mechanisms involving protein kinases and transcription factors and lead to alterations in gene expression (Cudna and Dickson, 2003). The UPR and EOR use distinct mediators in signalling, that target different genes to generate different responses. The EOR is mediated by activation of IKK (inhibitor of κB kinase) in response to EOR signals (i.e increased calcium permeability), which in turn activates the transcription factor NF-κB (nuclear factor-κB), which induces the expression of genes encoding several proteins involved in death/survival decisions and inflammatory responses (Cudna and Dickson, 2003). UPR is initiated by activation of ER transmembrane kinases IRE1 (high inositol-requiring) in response to the binding of unfolded proteins to the luminal surface of IRE1. This leads to oligomerisation with PERK (PKR-like ER kinase) (Chevet et al., 2001). These kinases act through the regulation of various transcription factors to decongest the ER by activating ER stress genes such as GRP78, GRP94, calreticulin and the growth arrest and DNA damage gene, gadd153. Additionally, IRE1 and PERK signal a global inhibition of protein translation (Cudna and Dickson, 2003). Consequently, the outcomes of UPR or EOR may range from complete cell regeneration and survival to elimination by apoptosis (Cudna and Dickson, 2003; Pahl and Baeuerle, 1997).

1.1.6 Protein transport from the ER to Golgi

Export of protein from the ER involves the sequential formation (budding), targeting and fusion of carrier vesicles to the *cis*-golgi network, the first compartment of the golgi apparatus (figure 1.1). Newly synthesised secretory proteins that have passed the quality control system in the ER are transported out by a vesicular transport mechanism. Proteins targeted for export are concentrated at specific sites at the ER membrane termed transitional elements (TE's). TE's are ribosome free areas up to 350 nm long with omega-shaped budding profiles (Klumperman, 2000). The buds on the TE's are coated with COPII. The COPII coat consists of three proteins (Sar1, Sec23-Sec24 complex, and Sec13-Sec31 complex) that are sequentially recruited to the ER membrane surface. Sar1 is a small 21 kDa GTPase, whereas Sec23-Sec24 and Sec13-Sec31 are large heteromeric protein complexes (Barlowe, 2003). To assemble the COPII coat, and consequently initiate vesicle budding, membrane bound Sar1-GTP binds Sec23-Sec24, which in turn recruits Sec13-Sec31. Activation of Sar1 to Sar1-GTP is catalysed by a membrane bound GDP-GTP

exchange factor, Sec12 that is localised to the ER membrane. Thus, COPII assembly is restricted to the ER through localised production of Sar1-GTP (Barlowe, 2003).

The transport of cargo from the ER in COPII coated vesicles is a selective event. Protein cargo must first be sorted from resident ER prior to vesicle budding. It is thought that secretory cargo contains built in signals that facilitate their export (Wieland, 1996). An example of such a signal is the di-acidic sequence (DXE) which was shown to be required for the efficient packaging of various membrane proteins into transport vesicles (Nishimura and Balch, 1997). Furthermore, COPII vesicles also contain 24 kDa membrane proteins (members of the p24 family) that selectively bind soluble ER proteins destined for transport to the golgi, and are thought to act as cargo receptors (Kaiser, 2000).

Once budding and formation of COPII coated vesicles has occurred, they are transported along micotubules a short distance to the ER-Golgi-Intermediate-Compartment (ERGIC)(Figure 1.3) where fusion takes place with the target membrane. Targeting requires receptors on the vesicle membrane that specifically interact with receptors on the target membrane (i.e. ER receptor that engages a ERGIC receptor). The specific paring of the vesicle-associated receptors (v-SNAREs; SNARE stands for soluble NSF attachment protein receptor) with target associated receptors (t-SNAREs) is referred to as the 'SNARE hypothesis'(Allan, 2000; Söllner et al., 1993). Specific paring of a v-SNARE to a t-SNARE targets a transport vesicle to the appropriate membrane and forms a scaffold for the binding of the membrane trafficking factors NSF (N-ethylmaleimide sensitive fusion protein) and SNAP (soluble NSF-attachment protein), to form a complex of four proteins linking the vesicle to the target membrane (Wieland, 1996). Hydrolysis of ATP by NSF leads to the disassociation of the COPII coat components, disassembly of the SNARE complex and fusion to the target membrane (figure 1.3) (Hong, 1998). A family of small GTP binding proteins termed rab's are also thought to participate in vesicular traffic in eukaryotic cells. These proteins are thought to function as timers for vesicular fusion by activating v-SNARE's. However, their precise role in regulating vesicular traffic has yet to be elucidated (Novick and Brennwald, 1993). The final stage of transport between the ER and golgi involves larger components of the ERGIC being transported in a microtubule dependent manner to the *cis*-golgi, where membrane fusion takes place and these compartments integrate themselves with the *cis*-golgi (Lodish, 1995).

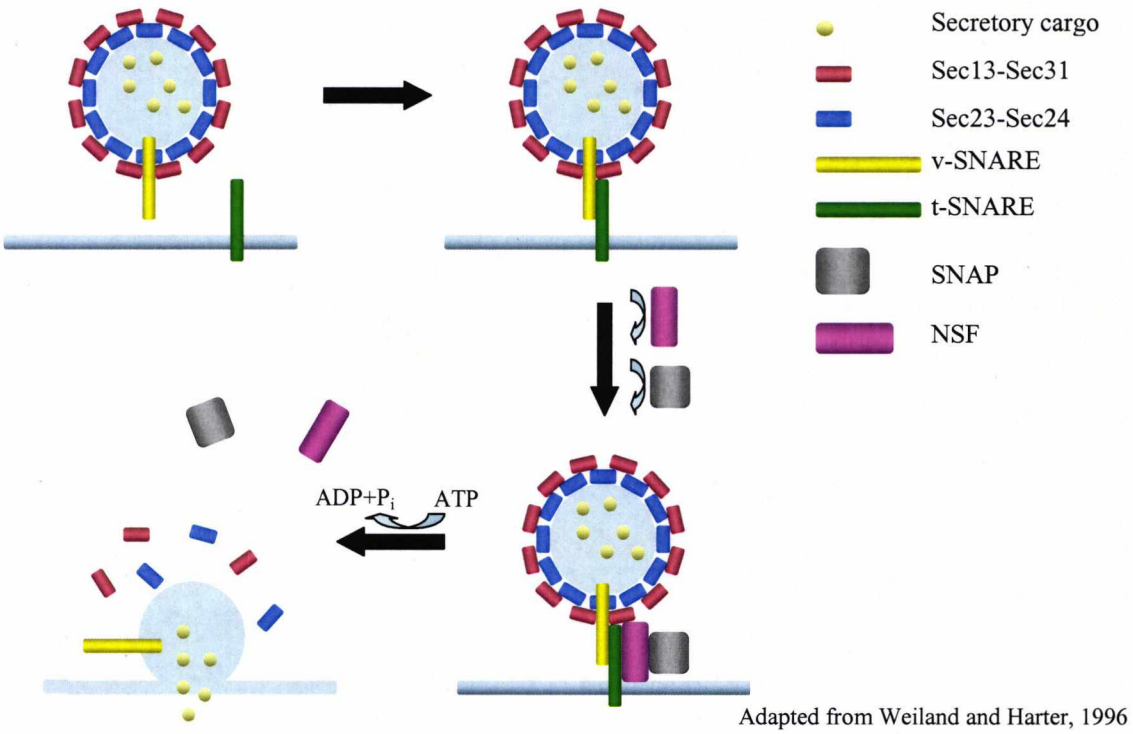

Figure 1.3 Targeting and fusion during COPII coated vesicle transport. Specific paring of a v-SNARE with a t-SNARE targets a transport vesicle to the appropriate membrane and forms the scaffold for the binding of the general membrane trafficking factors NSF and SNAP. ATP hydrolysis leads to disassembly of the SNARE complex and fusion to the target membrane.

1.1.7 Protein modification in the golgi complex

Newly synthesized secretory and membrane proteins enter the golgi complex on its *cis*-face, via fusion with compartments of the ERGIC. The golgi complex is mainly involved in trimming of N-linked glycans on proteins, and the addition of carbohydrates on proteoglycans (Varki, 1998). Resident within the compartments of the golgi complex are a host of enzymes involved in this process. These enzymes, which catalyse the steps involved in the glycan trimming process, are located to specific golgi compartments (Munro, 1998). While N-glycosylation is initiated co-translationally in the ER (section

1.1.3), trimming and rebuilding of the N-linked glycans occurs while proteins traverse across the golgi compartments (Varki, 1998). Although pre-golgi compartments have been suggested to be involved in the initiation of O-linked glycosylation, other enzymes that participate in this modification are restricted to the golgi complex (Munro, 1998). Further carbohydrate modifications such as sulfation of proteoglycans as well as the stepwise generation of the mannose-6-phosphate targeting signal of lysosomal enzymes also occur in the golgi complex (Lodish, 1995). Proteins destined for secretion move through the golgi by cisternal progression/maturation, in which the cisternae themselves are the carriers of the cargo (Storrie et al., 2000). As the cisternae of the golgi progress, the resident golgi compartments continually transport/recycle resident golgi components in the retrograde (backward) direction. This transport is carried out by vesicles with a second type of coat complex termed COPI (Schekmam, 1996). COPI transport vesicles consists of two types of proteins; the coatomer complex with 7 subunits (COP proteins) and ADP ribosylation factor (ARF) a small GTP binding protein, a homologue of Sar1.

Budding from the golgi cisternae is initiated by ARF protein exchange of GDP for GTP, a reaction catalysed by an enzyme in the golgi membrane. ARF-GTP then binds to the golgi cisternae, which is followed by recruitment of coatomers from the cytosol that bind to the cytosolic face of the golgi cisternae and polymerise into a fibrous coat that induces vesicle budding (Rothman and Orci, 1992). Soluble proteins in the lumen are selected for entry into these vesicles, by binding to specific membrane receptor proteins (Schekmam, 1996). Also incorporated into the vesicle membrane is a v-SNARE. The hydrolysis of GTP bound to ARF is required to depolymerise the coat at the target membrane, after which the NSF dependent fusion pathway is triggered (Glick, 2000; Wieland, 1996). COPI coated vesicles also mediate transport between the ERGIC and ER in order to retrieve escaped ER proteins and compensate for membrane removal from the ER (Klumperman, 2000). Vesicle movements within the secretory pathway are depicted in figure 1.4.

1.1.8 Transport of proteins out of the cell

Upon arrival of proteins at the *trans*-golgi compartment, and after all modifications have been completed, proteins destined for secretion out of the cell are concentrated at the

trans-face of the *trans*-golgi compartment. They are then packaged into secretory vesicles and transported to the plasma membrane and finally secreted from the cell. The process of exocytosis by the constitutive secretory pathway is poorly understood, but it is thought to be similar to the membrane fusion mechanisms described earlier, involving the membrane trafficking factors NSF and SNAP, GTP-binding proteins similar to ARF and Sar1, SNARE's and a number of Rab proteins. Furthermore, it is not known if the secretory vesicles that ferry proteins from the *trans*-golgi to the plasma membrane possess a distinct set of coat proteins such as COPI and COPII.

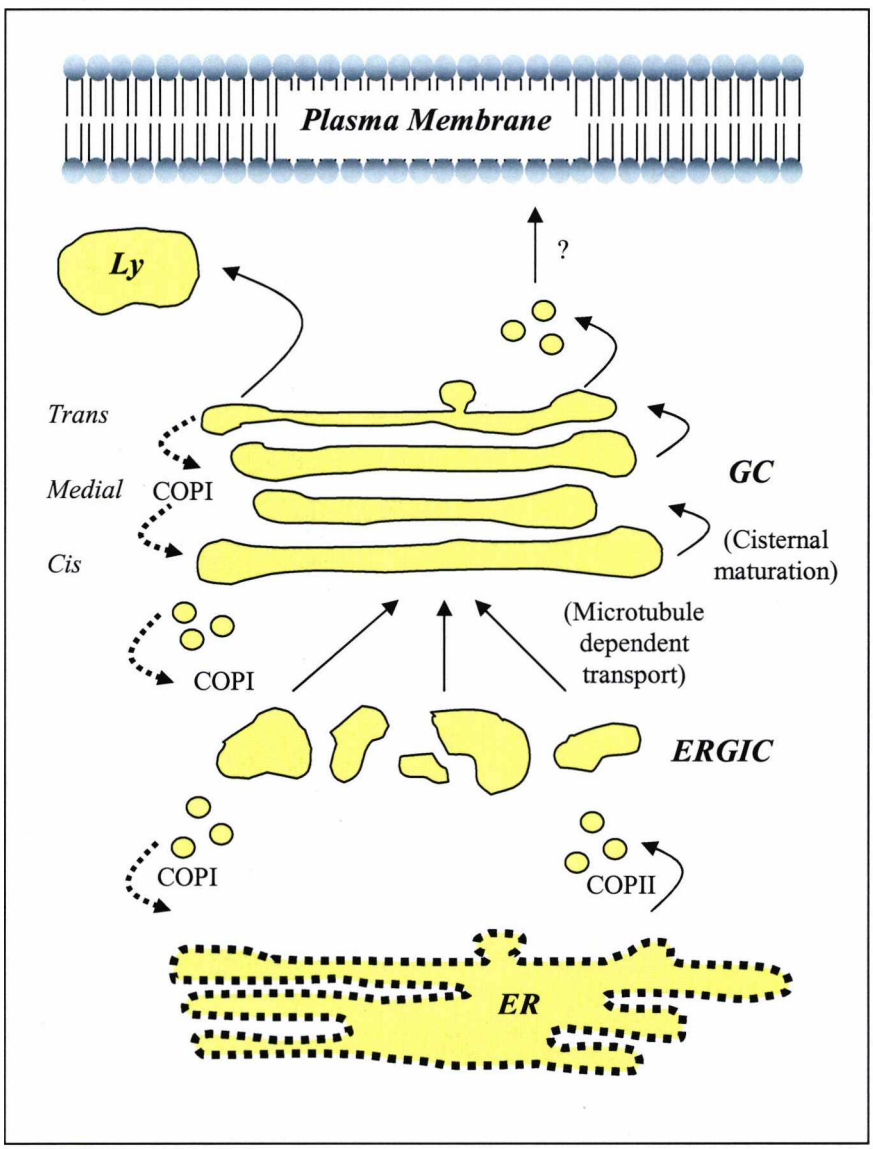

Figure 1.4 Vesicular transport between secretory pathway components. Transport between the ER and ERGIC is mediated by COPII coated vesicles. Retrograde transport between golgi complex cisternae, ERGIC and the ER is mediated by COPI coated vesicles.

1.2 Cell types for use in the large scale production of recombinant proteins

Mammalian cells can be distinguished by their requirement to grow attached to a surface (anchorage dependence) or in free suspension. The ability to grow in suspension is frequently associated with cell lines that demonstrate an 'immortal' or infinite lifespan phenotype. Suspension culture systems are preferred for most large-scale manufacturing processes because scale-up is more straightforward. Relatively homogeneous conditions can be achieved in a bioreactor, allowing efficient monitoring and control of key process parameters. A wide range of cell types can be grown in suspension cultures. The most frequently used cells (and hence important) for industrial processes are Chinese hamster ovary (CHO), baby hamster kidney (BHK), hybridomas and mouse myelomas, the most common of which is the NS0. This study involves the investigation of CHO and NS0 cell lines and as such these cell lines are discussed in more detail below.

1.2.1 Chinese hamster ovary (CHO) cells

CHO cells were originally derived from a partially inbred female adult Chinese hamster from which CHCOC1 clones were isolated (Puck et al., 1958). Mutagenesis of these original clones led to the development of the CHO K1 sub-line that showed enhanced stability (Kao and Puck, 1968). CHO cells have since been used to produce a wide range of therapeutic proteins (Table 1.1) and the choice of the CHO cell is based on several factors; compatibility with efficient gene expression systems leading to good reproducibility, ability to carry out important post-translational modifications and freedom from detectable pathogenic agents (Birch, 1999). CHO cells grow as attached cultures, and for growth in suspension CHO cells generally require a period of adaptation/selection after the production cell line has been created. This requirement for adaptation can take several weeks or even months and is one disadvantage of using the CHO cell line (Birch, 1999). CHO cells are commonly used today in combination with the DHFR system for gene amplification (see section 3.1.1 for detailed description of this system).

1.2.2 Murine myeloma non-secreting cells (NS0)

NS0 cells were derived from a plasmacytoma induced in a BALB/c mouse by peritoneal injection of mineral oil in 1962 (Potter and Boyce, 1962). Tumours induced by this procedure were investigated and one such tumour was found to secrete IgG, which was then used to establish a continuous culture named MOPC21 (Horibata and Harris, 1970). This heterogeneous population of cells were maintained in stationary culture for a period of three years after which they were renamed P3K cells. The P3K cells were then cloned to give rise to P3-X27, a clone that secreted IgG_2 (Ramasamy et al., 1974). Subsequent re-cloning gave rise to two cells lines 289-16 and P3-X63, which were developed separately. The 289-16 cell line did not secrete IgG_2 synthesizing the light chain but no heavy chain. This cell line was then renamed NSI/1 and after two more subsequent cloning steps, a subline which did not secrete or synthesize any heavy or light chains of IgG was isolated and named NS0/1 (non-secreting) cells (Galfre and Milstein, 1981).

Myeloma cells are known to be efficient fusion partners for the production of hybrids, and as a consequence NS0 cells have been used for a number of years as fusion partners for the production of hybridoma cells producing monoclonal antibodies (Barnes et al., 2000). However, NS0 cells are now an important host cell for the engineered production of recombinant proteins in their own right, particularly in combination with the glutamine sythetase (GS) system (section 3.1.1)(Birch, 1999).

1.3 Current strategies for the production and selection of cell lines for high level recombinant protein productivity

Currently there is no standard protocol for producing cell lines expressing recombinant protein at high yield. A number of different approaches are used to generate high yielding cell lines following stable transfection of the foreign gene(s) of interest. Such approaches include plasmid amplification, which involves increasing the copy number of the gene of interest in the cell and hence increasing the level of gene transcription. This is usually achieved by use of a marker gene present on the plasmid (upstream of the gene of interest) that allows cell survival in selective media. Therefore, in situations where the desired variant is present with low frequency (i.e. a clone with a high plasmid copy

number) it is advantageous to grow the cells under selective conditions to enrich the desired variant population (Birch and Froud, 1994). Example of such systems are the dihydrofolate reductase (DHFR) and the glutamine synthase (GS) system (section 3.1.1) (Barnes, 2000). Other methods for over expressing a foreign gene of interest involve using vectors containing powerful promoters such as the CMV and non-viral Elongation factor-1 promotor (Wurm and Bernard, 1999). However, in order to identify stable, productive transfectants, industry still relies on labour intensive rounds of cloning, screening and selection. Such procedures often require gradual increases in selective pressure, are lengthy, frequently result in unstable cell lines and require the continual presence of selective agents to maintain the amplified state (Barnes et al., 2003)

The yield of recombinant protein from cells generated from rounds of cloning and selection can further be improved by the optimisation of process development. The production of protein during batch culture is limited by nutrient depletion and subsequent increases in metabolite concentration (Ibarra et al., 2003). The use of fed batch culture or perfusion culture, where selected nutrients are fed to the culture during the growth cycle (or in the case of perfusion culture where fresh medium is continuously added to the reactor and spent culture removed), can increase recombinant protein yield by increasing the productive life time of cells in culture (Birch and Froud, 1994).

Increased secreted protein yields have also been accomplished by improvements in media formulations. Lambert & Merten (Lambert and Merten, 1997) reported that serum-free culture media led to higher mab production rates than when media containing serum was used. These results indicated that the composition of serum-free media positively influenced mab production. Furthermore, the presence of serum, even when added to serum-free media, had a pronounced inhibitory effect on cell specific mab productivity. The use of peptones such as primatone, or the enrichment of culture media with amino acid concentrates, is also known to increase cell growth and mab productivity and to prolong culture due to better nutrition of cells (Jan et al., 1994). Due to the limited understanding of how cells in culture adapt and respond to their environment, this optimisation of the cell culture environment has largely been accomplished by lengthy trial and error procedures. Other strategies utilised to increase productivity have focused on increasing the productive life time of a cell by either arresting the cell in the G_1 phase of the growth cycle (figure 3.4) or, over expressing anti-apoptotic genes such as Bcl-2 (Singh et al., 1996). The former

aims to increase yield by channelling energy into antibody synthesis rather than synthesising more biomass (Ibarra et al., 2003), while the latter aims to prevent cells entering the apoptotic pathway.

The strategies mentioned above such as plasmid amplification for increasing protein yield allow a high level of gene transcription, however the levels of secreted proteins are not always correlated with the level of mRNA produced (Anderson, 1998; Bibila and Flickinger, 1991). In the case of monoclonal antibody production by mouse hybridoma cell lines, it has been shown that the steady state levels of mRNAs coding for heavy and light chains of IgG do not correlate with the production rate (Lambert and Merten, 1997). It is currently hypothesised that a major rate-limiting step in the production of recombinant proteins occurs in the ER and involves retention of unfolded protein and the transport of nascent polypeptides from the ER to the golgi complex (Downham, 1996). The potential therefore to alleviate this rate-limiting step by over-expressing protein components of the ER is at present open to question.

1.3.1 Metabolic engineering as a tool to increase recombinant protein production in cultured mammalian cells

The identification of a rate-limiting step(s) in a pathway, and alleviating the 'bottleneck' by protein over-expression is described as metabolic engineering (Bailey, 1991). Metabolic engineering involves knowledge of the metabolic system of interest, in which the engineer proposes a genetic manipulation which is postulated to be beneficial in some way (i.e. an increase/decrease in enzyme expression) based on expected responses within the known biochemical network. However, in many cases the metabolic consequence of the genetic change based on the above strategy differs substantially from that desired (Bailey, 1991). Reasons for this, and consequently the inherent limitations of this strategy, are the current limited *a priori* understanding of the particular cellular mechanisms which control phenotypic function. Any pathway or network targeted for manipulation is always a sub-network of a much larger, more complex global metabolic network. The sub-network is usually associated with the global network through common co-factors, metabolites and complicated interactions that may influence levels of proteins active in the sub-network (Bailey et al., 1996). It is usually these control

connections/interactions to the sub-network from the global network, which are either unknown or not considered using conventional metabolic engineering strategies.

1.3.2 The concept of inverse metabolic engineering

The limited success of metabolic engineering approaches, has prompted the development of a new strategy termed inverse metabolic engineering. This approach involves the identification of a desired phenotype in a heterologous organism or in a related model system. Based on an inverse genetic strategy, the genetic basis for this desired phenotype are designed or hypothesised. In theory the genetic basis can then be transferred to the chosen industrial organism in order to achieve the goal of interest (Bailey et al., 1996). A schematic diagram of this approach is figure 1.5.

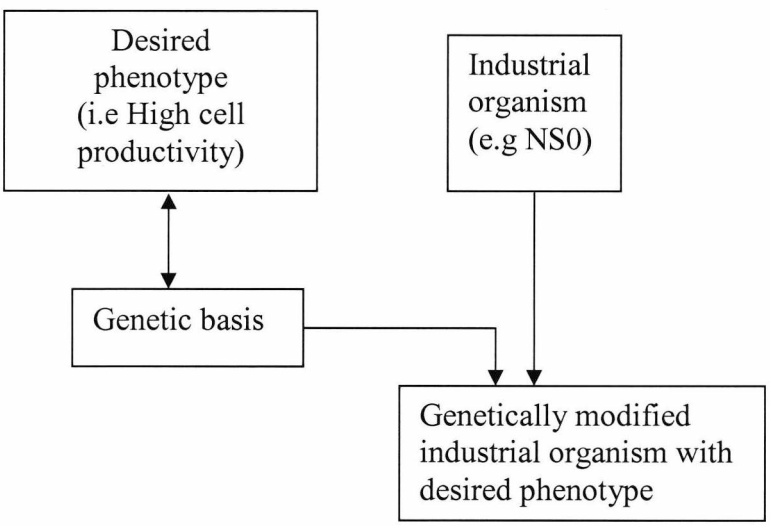

Figure 1.5 Schematic diagram of information flow in inverse metabolic engineering. The critical step is identifying the genetic basis for a desired phenotypic characteristic.

Renner et al. have shown the effectiveness of this strategy (Renner et al., 1995). An inverse metabolic engineering approach was used to achieve mammalian cell proliferation in culture without the presence of mitogens in the medium. Renner et al. compared wild type CHO K1 cells stimulated to proliferate with basic fibroblast growth factor (bFGF) and CHO K1 cells stimulated only with insulin. They found that in wild type cells exhibiting

the desired phenotype, levels of cyclin E were significantly elevated. CHO K1 cells were therefore transfected with a cyclin E expression containing vector. The result was CHO K1 transfectants grew rapidly in the absence of mitogens. This example of inverse metabolic engineering was accomplished using an area of technology that has recently emerged that allows the effective implementation of an inverse metabolic strategy. This technology enables the simultaneous monitoring of the expression of many genes within an organism in order to identify gene expression patterns characteristic of a known or observed phenotype. The technology utilised in this study is termed 'proteomics' and monitors the expression of genes at the protein level.

1.4 Proteomics

The proteome can be defined as the protein complement expressed by a genome, tissue or differentiated cell, under a given set of conditions (Haynes et al., 1998). Proteome analysis (proteomics) allows, on a large scale, a global integrated view of cellular processes and networks at the protein level (Blackstock, 1999). Proteomic data have a number of advantages over genomic data generated by serial analysis of gene expression (SAGE) or DNA microarray technology. Firstly, there is often a poor correlation between mRNA and protein expression levels. Secondly, mRNA is subjected to post transcriptional control in the form of alternative splicing, polyadenylation and mRNA editing, and as such many different protein isoforms can be generated from a single gene. Thirdly, proteins having been sythesised are subject to a range of post-translational modifications (described earlier) which cannot be accurately predicted by mRNA or DNA analysis (Graves and Haystead, 2002). Finally, the average number of protein forms per gene is predicted to be one or two in bacteria, three in yeast, and three or more in humans (Wilkins et al., 1996). Therefore it is clear that the tenet of "one gene, one protein" is an over simplification.

There are a number of steps involved in a proteomics based study. These are; (1) the high resolution separation of total protein content, (2) visualisation of separated proteins, and (3) identification and characterisation of proteins of interest. The application of proteomics, at its most basic level, is to confirm open reading frames and patterns of protein expression during different phases of a life cycle of an organism or cell. Its application with respect to inverse metabolic engineering in the production of recombinant

proteins, is the identification of potential targets for manipulation using proteomic analysis of high and low yielding cell lines. Potential targets can be defined in this case as those proteins whose expression levels can be correlated with observed changes in phenotype.

1.4.1 High resolution separation of proteins using two-dimensional gel electrophoresis (2DE)

Although the term proteomics was first used in 1995, the primary tool utilised to monitor genome-wide protein expression was first published in 1975. O'Farrel (O'Farrell, 1975) first described two-dimensional gel electrophoresis, which separates proteins on the basis of two physical properties, the iso-electric point of a protein (the first dimension) and the molecular weight of a protein (the second dimension). In the original technique, the first dimension was carried out in carrier ampholyte-containing polyacrylamide gels. Under the influence of an electric current, the carrier ampholytes would form a pH gradient. This is a critical part of iso-electric focusing (IEF). In this pH gradient (under the influence of an electric field) a protein will move to the position in the gradient where its net charge is zero. A protein with a positive net charge for example, will migrate toward the cathode, becoming progressively less positively charged as it moves through the pH gradient until it reaches its pI (iso-electric point). If the protein should diffuse away from its pI, it immediately re-gains charge, and migrates back (Fichmann, 1999b). This is the focusing effect of IEF, which concentrates proteins at their pI's and allows proteins to be separated on the basis of very small charge differences. The sample was usually applied to one end of the rod shaped carrier ampholyte containing gel, and separated at high voltage. The degree of resolution is determined by the slope of the pH gradient and the strength of the electric field (usually greater than 1000 V). However, when all proteins have reached their final zero charge position, there is very little ionic movement, resulting in a very low final current (usually below 1mA). After separation, the gel rods were equilibrated in a buffer containing a reducing agent (DDT) and an alkalyating agent (Idoacetamide) and placed on vertical SDS-polyacrylamide gels for the second dimension (Berkelman, 1998).

The use of carrier ampholytes has limitations, which until recently prevented the widespread application of 2D gel electrophoresis. Carrier ampholytes are mixed polymers that are not well characterised and suffer from batch-to-batch manufacturing variations,

reducing the reproducibility of the first dimension separation. Furthermore, the pH gradients produced using carrier ampholytes are unstable and have a tendency to drift toward the cathode over time. This adversely effects reproducibility and also causes flattening of the pH gradient at each end, rendering the 2-D technique less useful at pH extremes (Berkelman, 1998). Under these conditions part of the acidic, and almost the entire basic end, of the gradient is lost.

The development of immobilised pH gradients (IPG), has overcome many of the problems associated with carrier ampholytes. Dried gel strips containing immobilised pH gradients were commercially introduced in 1991 (Pharmacia Biotech, Immobiline® dry strip gels). The pH gradient is immobilised by covalently incorporating acrylamido buffers into the acrylamide matrix during polymerisation. Since the acrylamido buffers consist of discrete, relatively simple molecules, they can be manufactured very reproducibly, eliminating batch to batch effects and markedly increasing reproducibility. Furthermore, using these strips pI resolution to 0.01 pH unit can be achieved. The acrylamido matrix containing acrylamido buffers is cast onto a backing sheet, polymerized, washed (to remove catalysts and un-polymerized monomers, which could otherwise modify proteins and interfere with separation) and dried. The backing sheet therefore gives strips stability and simplifies handling (Fichmann, 1999a; Görg, 2000). IPG strips also improve basic protein loading capacity without affecting the shape of the gradient.

The most important pre-requisite for any successful 2-D electrophoresis experiment is sample preparation. As proteome projects develop, it has become more and more evident that some proteins cannot be properly solubilised by the lysis solution originally developed by O'Farrell (O'Farrell, 1975). In order to fully characterise the proteome of a given cell, tissue or organism, it is important that all the translated products are represented in the sample that is applied to any subsequent separation protocol or the profile generated will be non-representative. To establish this, the sample preparation procedure must, (i) stably solubilize all proteins, including hydrophobic species, (ii) prevent protein aggregation and hydrophobic interactions, (iii) remove or thoroughly digest any RNA or DNA, and (iv) prevent artifactual oxidation, carbamylation, proteolytic degradation, or conformational alteration (Fichmann, 1999b). This issue of disproportionate solubilisation is critical in studies involving the comparison of proteins isolated from, for example, healthy and

diseased tissue or cells adapted to different growth conditions. Disproportionate solubilisation may result in misleading information.

Currently, most cell lysis buffers consist of several general elements. These are 8-9.8 M urea, a non-ionic detergent, carrier ampholytes (pH range 3-10), dithiothreitol (DTT), and depending on the nature of the sample, protease inhibitors and protease-free nucleases (Fichmann, 1999b). However, there is no universal protocol for sample preparation, and the protocol devised is dependent on the nature of the sample. For example, Rabilloud et al., (Rabilloud et al., 1997) solubilised membrane proteins for 2D-electrophoresis by using a combination of thiourea, CHAPS and sulphobetain surfactants in addition to the standard lysis solution containing urea. This combination resulted in improved solubilisation and transfer of proteins to the second dimension SDS-gel. Meanwhile for nuclear proteins Görg et al. improved significantly the separation of very basic proteins by first precipitating the sample with acetone prior to solubilisation in the lysis solution (Görg et al., 2000). At present the separation efficiency and resolution of complex protein mixtures remains unparalleled with a resolution of up to 11,000 proteins from a single mixture possible (Dutt and Lee, 2000). However, the capacity of 2D-gel electrophoresis to resolve proteins still falls below the expected total number of proteins expressed by a eukaryotic cell.

1.4.2 Protein visualisation in 2D gels

There are many techniques that can be used for the visualisation of protein spots on a 2D-gel. The most sensitive among these are autoradiography and fluorography. These techniques involve radio-labelling proteins with either ^{35}S, ^{14}C, ^{3}H, or ^{32}P, and detecting with X-ray film (Berkelman, 1998). More commonly used however are the non-radioactive methods, of which the most popular are coomassie staining, silver staining and fluorescent staining.

Coomassie staining of proteins is based on binding of the dye coomassie brilliant blue G-250, which binds non-specifically to virtually all proteins. Coomassie G-250 complexes with basic amino acids, such as arginine, tyrosine, lysine and histidine, and at the same time produces very low background staining (Matsui, 1999). Although coomassie

staining is approximately 50 times less sensitive than silver staining (50 ng detection limit vs 5 ng detection limit), its main advantage is that it is an end point stain because the dye binds stoichiometrically to the protein, and therefore the relative amounts of a given protein can be determined accurately by densitometry. Furthermore, coomassie staining is compatible with mass spectrometric analysis and N-terminal sequencing.

Silver staining of polyacrylamide gels was first reported in 1979 (Rabilloud, 1999). This method was found to be around 100 times more sensitive than coomassie staining with a detection limit as low as 5 ng of protein per spot/band (Shevchenko et al., 1996), however this may vary depending upon the protocol used. Due to the high sensitivity of silver staining methods, they are ideal for the detection of trace components within a protein sample and for the analysis of protein samples available in only limited quantity. Silver staining does however have several disadvantages. Silver staining has lower reproducibility than coomassie staining, a limited dynamic range (i.e. level of staining is not always proportional to quantity), and it is not an end point stain which means the operator must choose when to stop the staining procedure. Furthermore, certain proteins are stained either poorly, negatively or not at all (Görg, 2000). Due to these limitations, silver staining cannot be considered to be 'truly' quantitative in the way that coomassie staining can be considered quantitative. Therefore one must take into account this limitation when undertaking a silver stained based quantitative analysis.

Fluorescent staining involves labelling protein with fluorescent dye molecules after the electrophoretic separation has been completed. SYPRO Orange, SYPRO Red, and SYPRO Rugy are all examples of fluorescent dyes that differ in their excitation maxima. These dyes stain non-covalently and bind to the SDS surrounding the proteins (Steinburg et al., 1996), thus, staining is not selective for particular polypeptides. The detection limit of these dyes is in the range of 1-2 ng of protein/spot (Görg, 2000). The advantage of fluorescent staining over silver staining is the protein gels do not require a fixation step prior to incubation with the dyes, and staining is complete 30 to 60 minutes following electrophoresis, with no de-staining required (Steinburg et al., 1996). These stains are also end point stains. The disadvantage of fluorescent staining is that photography or electronic image acquisition is required to document the result.

1.4.3 Alternatives to electrophoretic separation

The limitations of 2DE have inspired investigations into a number of alternative approaches to bypass protein gel electrophoresis. One such approach is to convert an entire protein mixture to peptides (usually by digestion with trypsin) and then purify the peptides using a variety of techniques such as reverse phase and cation-exchange chromatography, before subjecting them to analysis by ms (a technique termed 'Mudpit') (Graves and Haystead, 2002). The advantage of this method is that because a 2D gel is avoided, a greater number of proteins in the mixture can be represented. The disadvantage is that it requires an immense amount of time and computing power to deconvolute the data obtained (Graves and Haystead, 2002).

Recently, another technique has emerged as an alternative to protein electrophoresis, isotope-coded affinity tags (ICAT). Cell extract from two different samples is reacted with one of two forms of the ICAT reagent, an isotopically light form in which the linker contains eight hydrogen's or a heavy form in which the linker contains eight deuterium atoms (Han et al., 2001). The ICAT reagent reacts with cysteine residues in proteins via a thiol-reactive group and contains a biotin moiety to facilitate purification. Peptides are then recovered by avidin affinity chromatography and are analysed by mass spectrometry. The difference in peak heights between heavy and light peptide ions directly correlates with the difference in protein abundance in the cells. Thus, if a protein is present at threefold higher level in one sample, this will be reflected in a threefold difference in the peak heights. Following quantitation of the peptides, they can be fragmented in a mass spectrometer and the amino acid sequence deduced. Therefore using this approach, proteins can be identified and their expression levels compared in the same analysis (Aebersold and Mann, 2003; Graves and Haystead, 2002).

1.4.4 Identification and characterisation of proteins

Identification of proteins separated by 2-D gel electrophoresis, was until recently, the step which prohibited 2DE proteomics based projects. Estimates of a protein molecular

weight and pI obtained from a gel, coupled with a subsequent search of databases which contain known protein sequences, where masses and pI's have either been previously measured or calculated from putative open reading frames, often do not yield positive unambiguous identification. Immunological methods of identification decreased the detection limits of proteins, but have only provided modest increases in information and require a specific antibody. This type of approach is usually only used to confirm a suspected identity and only where a specific antibody is available (Dutt and Lee, 2000; Michalski and Shiell, 1999).

Amino acid analysis from 2D-gels blotted onto membranes and subsequent N-terminal sequencing by Edman degradation has allowed the unambiguous identification of proteins. This involves the cleavage of the N-terminal amino acid, followed by derivatisation and separation by HPLC to identify amino acids (Michalski and Shiell, 1999). Although automated, this process is still rather slow and time consuming and further limited by N-terminal blockage and insufficient quantities of protein.

More recently, 2-D gels subjected to in-gel enzymatic/chemical digestion to yield peptides, can be characterised by mass spectrometry (ms). The advent of two 'soft ionisation' mass spectrometric techniques, matrix assisted laser desorption ionisation (MALDI) and electrospray ionisation (ESI) have allowed accurate, rapid and sensitive detection of biomolecules at picomolar and femtomolar concentrations. Briefly, MALDI-ms was introduced in 1987 and is now widely used for the determination of protein and peptide molecular weights. The sample is initially dissolved in a matrix (usually an aromatic acid) and irradiated with a pulsed nitrogen laser (typically at 337nm). The sample and matrix are desorbed by pulses from the laser and the gas phase ions are electrostatically directed (most commonly into a time-of-flight (TOF) mass analyser). The time between the initial laser pulse and ion detection is directly proportional to the square root of the ions mass/charge (m/z) ratio (Aebersold and Mann, 2003). MALDI-ms has a mass range which covers over 250 kDa and mass accuracy of $\pm$ 0.1% . MALDI-ms is the method of choice for obtaining molecular weights of mixtures of peptides, such as those produced by proteolytic in-gel digestion of proteins, due to its tolerance of salts, buffers and detergents.

In contrast, electrospray mass spectrometry (ES-MS) is a process that takes the molecules directly from the liquid phase into the gas phase in an ionised state. A solution of analyte molecules (i.e proteins) is passed through a needle that is kept at high electrical potential. At the end of the needle, the solution disperses into a mist of small highly charged droplets containing protein molecules. The small droplets evaporate rapidly (by being subjected to a drying gas) and, by a process of either field desorption or residual solvent evaporation, protonated protein molecules are released into the gas phase. Once the protein ions are in the gas phase, they are leaked into the vacuum of the mass spectrometer, where they are separated and detected according to their m/z ratio by a quadrapole mass analyser (Mann and Wilm, 1994). Ionisation of biopolymers results in the production of multiply charged molecular ions (average one proton per kDa). This resulting mass spectrum of multiply charged molecular ions, is then deconvoluted to yield a single charge peak. ES-MS may be coupled with liquid chromatography systems (LC-MS) to analyse complex samples, and is capable of determining molecular weights up to 100 kDa, with a mass accuracy of $\pm$0.01%. However, it is generally intolerant of salts and detergents, which suppress ionisation (Aebersold and Mann, 2003).

Currently the most common methods for protein identification utilising the mass spectrometry technology described are peptide mass fingerprinting (PMF) and peptide sequence tags (PST). PMF has become the method of choice (since the introduction of MS in protein chemistry) for high throughput protein identification. The technique involves the protein of interest being cleaved enzymatically or chemically by in-gel digestion. An aliquot of the peptide mixture can then be analysed by mass spectrometry (usually MALDI-ms) to yield a mass spectrum of peptides produced by cleavage with a specific enzyme or chemical reagent. In other words a 'peptide mass fingerprint' of the protein is produced. The PMF is subsequently compared to 'virtual' fingerprints obtained by theoretical cleavage of protein sequences stored in a database, and the top scoring proteins are retrieved as possible candidate proteins (Gevaert and Vandekerckhove, 2000). Only a small number of accurately measured peptide masses are required for unambiguous protein identification, and low picomole to high femtomole amounts of gel separated proteins can be identified using this technique.

PST's are short stretches of amino acid sequence data, usually >3 residues, which can be generated either by Edman degradation (described earlier) or by tandem mass

spectrometry techniques. There are several versions of tandem mass spectrometry, but the most commonly used in proteomics are ms/ms (by analogy with GC/MS, as this type is performed using an ESI-ms or MALDI system) and post source decay (PSD, performed in a time-of-flight mass analyser). Both these methods rely on collision induced decomposition (CID). CID involves a peptide ion (generated from initial ionisation of an enzymatically/chemically cleaved protein) colliding with an inert gas such as argon. Collision of the peptide ion and the gas results in fragment ions being formed (Siuzdak, 1994). Fragmentation occurs mainly in the amide bonds of the peptide backbone, resulting in a nested set of peaks (CID spectrum) differing by amino acid residue masses (Mann and Wilm, 1994).

In the case of ESI-ms/ms the CID spectrum is generated by trapping an ion of interest in a quadrapole analyser (the 1^{st} ms), colliding the ion with the gas in a collision cell, and then analysing the fragment ions in another quadrapole analyser (the 2^{nd} ms) (Siuzdak, 1994). The CID spectrum in a MALDI-ms system utilising a time-of-flight analyser is can be produced in a similar way to an ESI-ms using a quadrapole system but, can also be accomplished using a method known as Post Source Decay (PSD). Fragmented ions, following collision in the flight tube, continue with the same velocity as the precursor ion, and therefore will arrive at the detector at the same time as an un-fragmented precursor ion. Therefore, an electrostatic mirror is placed in front of the first detector, which will reflect only the fragmented ions to a second detector which can measure the mass of the fragment ions (Gevaert and Vandekerckhove, 2000).

The fragments produced by tandem mass spectrometry have charges that may reside at either end of the peptide. Charge retention on the C-terminus results in the production of Y ions, and charge retention on the N-terminus results in B ions. By constructing (with the help of computer programs) a series of amino acid residue masses that fit the fragmentation pattern, an amino acid sequence match can be deduced (Mann and Wilm, 1994). Recently the MALDI-qTOF, a new mass spectrometer has been developed to permit both PMF and amino acid analysis. It is based on the combination of a MALDI ion source with a qTOF mass analyser. Thus if the sample is not identified by PMF in the first step, the amino acid sequence can then be obtained without having to use a different mass spectrometer (Graves and Haystead, 2002).

The identification techniques outlined above, rely on annotated protein databases to interpret the results that are generated (i.e PMF, PST's). A variety of web-based bioinformatic tools utilizing molecular parameters such as intact protein mass, PMFs, and PST's (or combinations thereof) are now available for routine searching of protein databases. An excellent example of such a database is the Expert Protein Analysis System (ExPASy) which is available online at http://www.expasy.ch/ and includes a suite of proteomic tools (Dutt and Lee, 2000). Also publicly available is the MASCOT search programme available online at www.matrixscience.com. This search programme is useful as it provides statistical analysis as to the probability of a match being significant (described further in section 5.3.1).

1.5 Aims of this study

The potential for manipulating cellular secretion by altering the intracellular complement of chaperone/foldase proteins that constitute the secretory pathway using an inverse metabolic engineering strategy are as yet open to question. In order to understand in molecular detail those processes which result in high level antibody secretion and select potential inverse metabolic engineering targets, we must simultaneously consider a range of different processes catalysed by a variety of proteins within the secretory pathway. This study set out to use proteome analysis to create a detailed map of known functional protein components of the secretory pathway for comparative semi-quantitative analysis in order to answer the following biological questions;

1. Do cell lines selected for high level recombinant protein secretion have altered expression of secretory pathway components?

2. For cell lines exhibiting high-level secretion, are specific cellular processes up or down regulated (e.g. unfolded protein degradation by the proteasome, ER to *cis*-golgi transport.)?

3. Are changes in protein expression conserved for different cell types producing the same protein (i.e. CHO vs NS0)?

4. Are changes in protein expression conserved for the same cell type producing a different recombinant protein product (i.e. IgG vs TIMP-1)?

The following discourse describes in detail the experiments and approaches undertaken in an effort to answer these questions. The implications of these investigations in terms of engineering the secretory pathway to improve cellular recombinant protein production is discussed.

Chapter 2 Cell Line Characterisation

2.1 Introduction

In any study that investigates mammalian cells producing recombinant proteins in culture, it is important to characterise in detail the growth and productivity of each cell line investigated. This is of particular importance when embarking on a proteomic based study to allow valid conclusions to be drawn with regard to the biological significance of any findings or changes in gene (protein) expression.

Before the functional significance of any difference can be assigned, basic information must be obtained on the growth and metabolism of cells under the defined culture conditions. This is required to ascertain if any changes in growth conditions have developed that contradict the historical information available on that particular cell line. It is also important to establish and ensure that the desired recombinant product of interest is expressed stably and secreted in the correct conformation. Therefore, some sort of quality assurance analysis must be put in place.

This chapter describes the growth and productivity characteristics of three different cell lines, a GS-NS0 cB72.3, a GS-CHO cB72.3 and a GS-NS0 TIMP-1 (see chapter 1 for

a detailed overview of the history/provenance of the cell lines). This characterisation is not only important for the reasons stated above but will also aid in the establishment of a robust comparison strategy between cell lines (i.e. deciding upon which GS-NS0 cB72.3 clone will be compared to the GS-NS0 TIMP-1 to assess product specific changes in the secretory pathway proteome) and to determine an appropriate time point for the harvest of cells for further analysis. Furthermore, the suitability of cell lines for the comparative analysis of factors that influence increased productivity in the secretory pathway was also assessed.

2.2 Materials and Methods

2.2.1 Cell Lines and Media

GS-NS0 cB72.3

GS-NS0 cell lines producing a range of cB72.3 recombinant IgG concentrations and a mock transfectant blank (transfected with GS vector lacking Mab genes) were generated and prepared specifically for this study by Dr Andrew Racher (Lonza Biologics, Slough, UK). Parental NS0 cells were transfected with a glutamine synthetase (GS) expression vector containing the cB72.3 (IgG4 monoclonal antibody) heavy (H) and light (L) chain genes (dual gene construct) by electroporation (using a Bio-Rad Gene Pulser II) in protein free medium. Primary transfectants were identified by transferring the cells into medium containing 10% dFCS and 2 mM glutamine before distribution into 96-well microtiter plates. After 24 hours the cB72.3 and GS genes were selected by inclusion of 10 μM methionine sulphoximine (MSX) and the exclusion of glutamine. The plates were then left for 3 weeks before being screened for colonies. From this point onwards the medium did not contain glutamine or MSX. Selected colonies were then moved into 24 well plates. Transfected GS-NSO cells were routinely cultured in Dulbecco's Modified Eagles Medium (DMEM) F-12, in the absence of glutamine. To the basic medium was added glutamic acid and asparagine to final concentrations of 350 μM and 400 μM respectively; 30 μM each of adenosine, guanosine, cytidine, uridine, and 10 μM thymidine. Additionally, 1% of 100× MEM non-essential amino acids (Gibco) and fetal bovine serum (PAA) to a concentration of 10% were added. The GS-NS0 parental cell line was cultured in the above media with the addition of glutamine to a final concentration of 6 mM.

GS-NS0 TIMP-1

A GS-NS0 cell line producing the metalloproteinase inhibitor TIMP-1 was provided by Celltech (Slough, UK). Cells were cultured in the same glutamine free media described for the GS-NS0 cB72.3 cells.

GS-CHO cB72.3

GS-CHO cells lines producing cB72.3 recombinant IgG were provided by Dr Andrew Racher (Lonza Biologics, Slough, UK). The cells were cultured in CD-CHO protein free, serum free media (Gibco, Paisley, UK) supplemented with L-methionine sulphoximine (MSX) to a final concentration of 25 μM.

2.2.2 Growth curves and productivity cultures

All cultures were inoculated into 100 mL of the appropriate medium to give an initial viable cell concentration of 2×10^5 cells mL^{-1} in 500 mL shaker flasks (Corning). The flasks were placed in a shaker incubator (103 rpm), and cultured at 37^0C in a 5% CO_2 humidified atmosphere. Cultures were sampled (1 mL) every 24 h for analysis. The culture sample (50 μL) was diluted 1:1 with trypan blue and counted on a hemacytometer; non-viable cells stained blue. A minimum of four hemacytometer fields were counted per determination. The remainder of the sample was centrifuged to remove cells, preserved with sodium azide (0.05%) and stored at -20^0C for later analysis.

2.2.3 Colormetric assay to determine glucose concentration in cell culture supernatants

A glucose kit from Sigma (Poole, Dorset, UK) was used to determine glucose concentration in cell free supernatants. The principle of the assay is as follows:

$$\text{Glucose + ATP} \xleftrightarrow{\text{hexokinase}} \text{Glucose-6-phosphate + ATP}$$

$$\text{Glucose-6-phosphate + NAD} \xleftrightarrow{\text{G-6-P dehydrogenase}} \text{6-phosphogluconate + NADH}$$

Cell supernatant (2 μL) was added to 198 μL glucose (HK) assay reagent (Sigma) in a 96 well microtitre plate. A blank, and a set of standards ranging from 0-30 μg of glucose was also prepared to a final volume of 200 μL per well. The plate was then incubated at 37^0C for 10 minutes and read using a MRX™ plate reader (Dynex Laboratories, Middlesex, UK.) at an absorbance of 340 nm. The glucose concentration of

the cell supernatant was calculated from the standard curve of [glucose] vs A_{340}nm, using standard linear regression analysis ($y = mx + c$).

2.2.4 Colorimetric assay to determine lactate concentration in cell culture supernatants

The principle of the lactate assay is as follows:

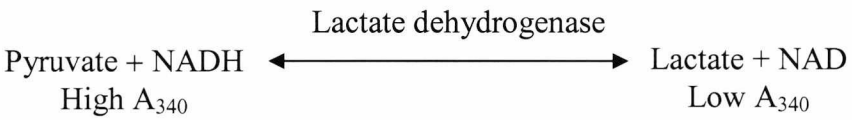

Lactate assay standard reagent was prepared using 10 mg β-Nicotinimide adenine dinulcleotide (NAD), 2 mL glycine buffer (Sigma), 0.23 mL ddH_2O and 0.1 mL lactate dehydrogenase enzyme (LDH) (Sigma). Sample reagent mix was prepared using 10 mg NAD, 2 mL glycine buffer, 4 mL ddH_2O and 0.1 mL LDH. Cell supernatant (5 µL) was added to 195 µL sample reagent mix in a 96 well microtitre plate. A blank containing only standard reagent mix and a set of standards ranging from 0 – 0.267 µg μL^{-1} were also prepared in standard reagent mix to a final volume of 200 µL per well. The plate was incubated and read as described in section 2.2.3. The lactate concentration of the cell supernatant was calculated from the standard curve of [lactate] vs A_{340}nm.

2.2.5 ELISA assay for the determination of antibody concentration.

A 96 well ELISA plate (Dynatech, UK) was coated with 100 µL/well $F(ab)_2$ Fragment Goat Anti-Human IgG, Fcγ Specific antibody (Jackson ImmunoResearch Laboratories, Pittsburg, US) diluted 1 in 500 in Coating buffer (15 mM Na_2CO_3, 35 mM $NaHCO_3$, pH 9.7) overnight at 4^0C in the dark. The plate was then washed twice using wash buffer (100 mM NaCl, 8 mM Na_2HPO_4, 2 mM NaH_2PO_4, 10 mM EDTA, 0.02% (v/v) Tween-20, 0.1% (v/v) L-Butanol, adjust to pH 7.2 with NaOH) and blocked with 200 µL/well of Block solution (15 mM Na_2CO_3, 35 mM $NaHCO_3$, 0.5% (w/v) Casein, allow to dissolve at 37^0C) and incubated for 1 hr at RT. Human IgG standards (Sigma) were prepared with a dilution range of 625 ng/mL to 9.8 ng/mL in sample buffer (100 mM

Tris pH 7.0, 100 mM NaCl, 0.02% (v/v) Tween-20) to a final volume of 100 µL/well. The plate was then washed twice as described previously. Cell culture supernatant samples were diluted 1 in 3000 with wash buffer. 100 µL of sample/standard was then added to the appropriate well and incubated for 1 hr at RT. Secondary antibody (Goat anti-human kappa light chain (bound & free) HRP conjugate, Sigma, UK.) was diluted 1 in 10000 in wash buffer following incubation with sample/standard. Plates were washed as previously described and 100 µL of secondary antibody per well added, and incubated for 1 hr at RT. The plates were then washed again as described previously. Developing agent was then prepared by adding 10 mL of substrate buffer (0.1 M Acetate, adjusted to pH 5 using 1.0 M Citric acid) 100 µL of 3,3'5,5'-tetramethylbenzidine base (TMB) solution (1% w/v TMB in DMSO) and 100 µL H_2O_2 was added. To each well 100 µL of developing reagent was added, and the resulting colour change followed visually. After sufficient colour development (judged from the standards 'colour curve') the reaction was stopped using 2.5 M H_2SO_4 (50 µL/well) and the absorbance determined at 450 nm using a Dynatech MRX microplate reader. Unknowns were calculated from the standard curve using standard linear regression analysis.

2.2.6 Quantitation of TIMP-1 from cell culture supernatant using affinity chromatography

Coupling MAC015 antibody to CnBr activated sepharose 4B

1 g of CnBr activated sepharose 4B (Amersham Biosciences) was sprinkled onto a sintered glass filter (Porosity G3) with a 5 mL of 1 mM HCL, stirred gently and allowed to swell for 15 mins. The gel was then washed with 200 mL of 1 mM HCL under gravity, and then 30 mL of coupling buffer (0.1M $NaHCO_3$ pH 8.3, 0.5 M NaCl) was added. The gel was transferred to a 15 mL falcon tube and spun at 2000 rpm for 2 mins. The supernatant was removed and discarded. Approximately 3 mg of MAC015 antibody (Celltech, Slough, UK), was resuspended in 4 mL of coupling buffer and mixed with the re-swollen gel on a rotor overnight at 4^0C. The mixture was then spun down as before, the antibody solution removed and the absorbance measured at 280 nm to assess the degree of coupling. Uncoupled sites in the gel were then blocked by adding 15 mL of 1M ethanolamine (pH 8.0) and mixing for 2 hours at RT. The gel and blocking solution was then poured onto a

sintered glass funnel and washed with 30 mL 0.1 M sodium acetate, 0.5 M NaCl (pH 4.0) for 5 mins before draining. The coupling buffer (30 mL) was then added and allowed to stand, and drained as before. The sodium acetate and coupling buffer washes were then repeated twice more. The gel was stored at 4^0C as a 50% slurry in coupling buffer containing 0.1% sodium azide.

Purification of TIMP-1 from culture supernatant

1 mL of CnBr activated sepharose coupled to MAC015 antibody (as described above) was packed into a 1mL Fast Protein Liquid Chromatography (FPLC) column (Amersham Biosciences). Purification of TIMP-1 was carried out on an AKTA FPLC system (Amersham Biosciences). The MAC015 column was equilibrated using 5 column volumes of 0.05 M Tris, 0.5 M NaCl (pH 8.0) at a flow rate of 1 mL min^{-1} and flow through absorbances measured at 280 nm. 60 mL of cultured NS0 TIMP-1 cells (section 2.2.1) was centrifuged at 1000 rpm for 5 mins, the supernatant recovered and loaded onto the column. The column was then washed with 5 column volumes of the equilibration buffer to remove unbound components. The column was then eluted using 0.05 M glycine, 0.5 M NaCl, pH 2.7. Fractions (1 mL) were collected directly into tubes containing 50 µL of a 1.0 M Tris-HCL pH 9.0 solution. The purified TIMP-1 fractions (determined by the absorbance at 280nm) were pooled and concentrated to 1 mL in a vacuum centrifuge. The amount of TIMP-1 purified was determined by Bradford assay (section 3.2.3). The purity of TIMP-1 recovered in this way was determined by standard SDS-PAGE analysis as described in section 3.2.4.

Quantitation of TIMP-1 productivity

A standard curve was generated by spiking 1 mL of fresh NS0 TIMP-1 media with 2.5, 5, 7.5, 10, 20, and 30 µg of purified TIMP-1. The MAC015 column was equilibrated as previously described and 1 mL standard curve samples applied to a sample loop and flushed through the column with 3 mL of equilibration buffer. The column was then washed as before, and bound TIMP-1 eluted using 0.05 M glycine 0.5 M NaCl pH 2.7 and the absorbance of the fractions recorded at 280 nm. Absorbance peaks were integrated automatically and peak areas determined using the Unicorn™ software (Amersham Biosciences) provided with the FPLC instrument. In this way a standard curve of

concentration *vs* area under the eluted peak was generated and the concentration of TIMP-1 in culture samples determined using standard linear regression (Y = Mx + C).

2.2.7 Purification of recombinant IgG from cell culture supernatant by affinity chromatography

5 mL of protein A was packed into a 5 mL Fast Protein Liquid Chromatography (FPLC) column (Amersham Biosciences). Purification of IgG was carried out on an AKTA FPLC system (Amersham Biosciences) controlled by Unicorn^{TM} software. The purification was undertaken using the equilibration and elution conditions as described in section 2.2.6 using 50 mL of cultured GS-NS0 cB72.3 and GS-CHO cB72.3 supernatant (section 2.2.1) and a flow rate of 4 mL min^{-1}.

2.2.8 Generation number, doubling time, growth rate and specific productivity/consumption

The generation number, doubling time and specific productivity of individual cell lines was calculated using the following formulas at mid exponetial growth phase.

Generations (*g*)

$$g = \frac{\log_{10} N - \log_{10} No}{\log 2}$$

where No = Initial cell density

N = Final cell density

Doubling Time (*Td*)

$$Td = \frac{T}{g}$$

where T = Time elapsed

Specific growth rate (μ)

$$\mu = \frac{1}{Td / \ln 2} \quad \text{(expressed } h^{-1}\text{)}$$

Specific productivity (*qMab*)

$$qMab = \frac{\Delta C}{T}\left(\frac{\ln N - \ln No}{N - No}\right) \text{ (expressed as pg cell}^{-1}\text{ h}^{-1}\text{)}$$

where C = Concentration of substrate or product

2.3 Results and Discussion

2.3.1 Growth characteristics, metabolism and recombinant protein production – Analysis of clonal variation in GS-NS0.

Tranfection of NS0 cells to produce a range of cell lines producing and secreting recombinant protein (cB72.3 monoclonal IgG antibody) led to the isolation of 6 transfectants that were examined in further detail. An untransfected parental NS0 cell line and a transfectant blank were also examined as controls. Growth and viability data was generated as described in section 2.2.2 and the results are presented in figure 2.1. Productivity of the selected transfectants was measured by ELISA as described in section 2.2.5 and the data throughout culture has been plotted and is shown in figure 2.2. Cell specific productivity, growth rate, and doubling time were calculated as described in section 2.2.8. A summary of this data is presented in table 2.1. Concurrently, glucose utilisation and lactate production was measured as stated in sections 2.2.3 and 2.2.4 and results are shown in figure 2.3.

Table 2.1 Growth and productivity data for GS-NS0 cell lines

Cell Line	μ (h^{-1})*	T_d (h)*	Max. VCC ($\times 10^5$ cells $mL^{-1} \pm$ SE)	Max.Mab Titre (mg L^{-1})	qMab (pg $cell^{-1}$ $h^{-1} \pm$ SE)*
Parental	0.037	18.5	48.8 ± 9.4	-	-
Trans Blank	0.028	24.5	22.3 ± 0.5	-	-
4O	0.024	29.3	13.3 ± 4.5	3.1	0.05 ± 0.02
4R	0.023	30.6	12.2 ± 3.2	38	0.24 ± 0.03
2X	0.026	27.1	15.3 ± 1.4	163	1.45 ± 0.57
2P	0.025	28.0	12.9 ± 3.9	177	1.46 ± 0.37
2N2	0.031	22.5	20.4 ± 0.4	210	1.40 ± 0.22

* Calculate at mid-exponential growth phase

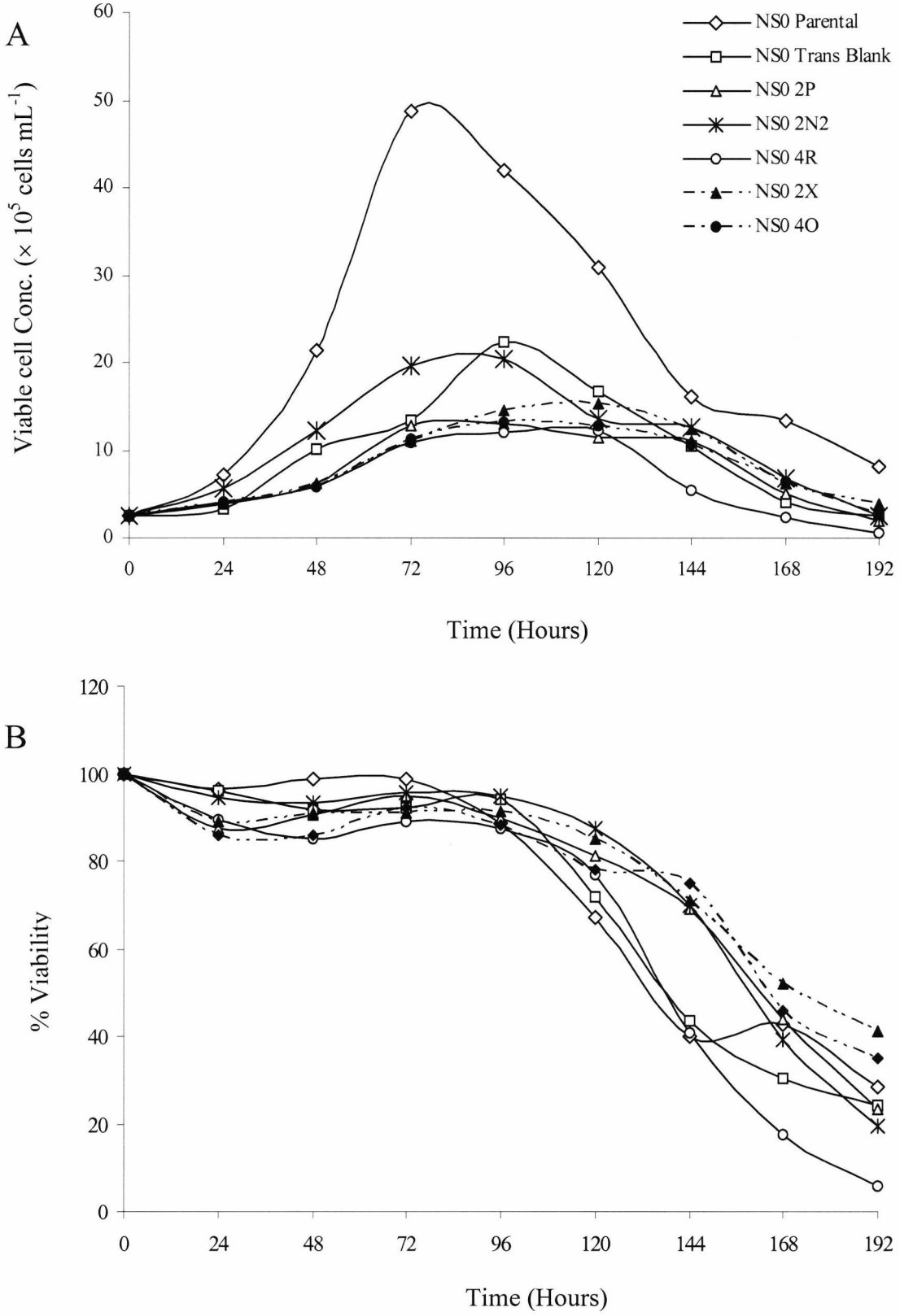

Figure 2.1. Batch culture of GS-NS0 cell lines (A) Growth kinetics of transfectants in batch culture. Transfectants consisted of NS0 cells transfected with DNA encoding cB72.3 monoclonal antibody. Growth curves were performed in 500 mL shaker flasks at 37^0C with 5% CO_2. Cells were grown in DMEM F12 supplemented as stated in section 3.2.1. **(B)** Cell viability *vs* culture time.

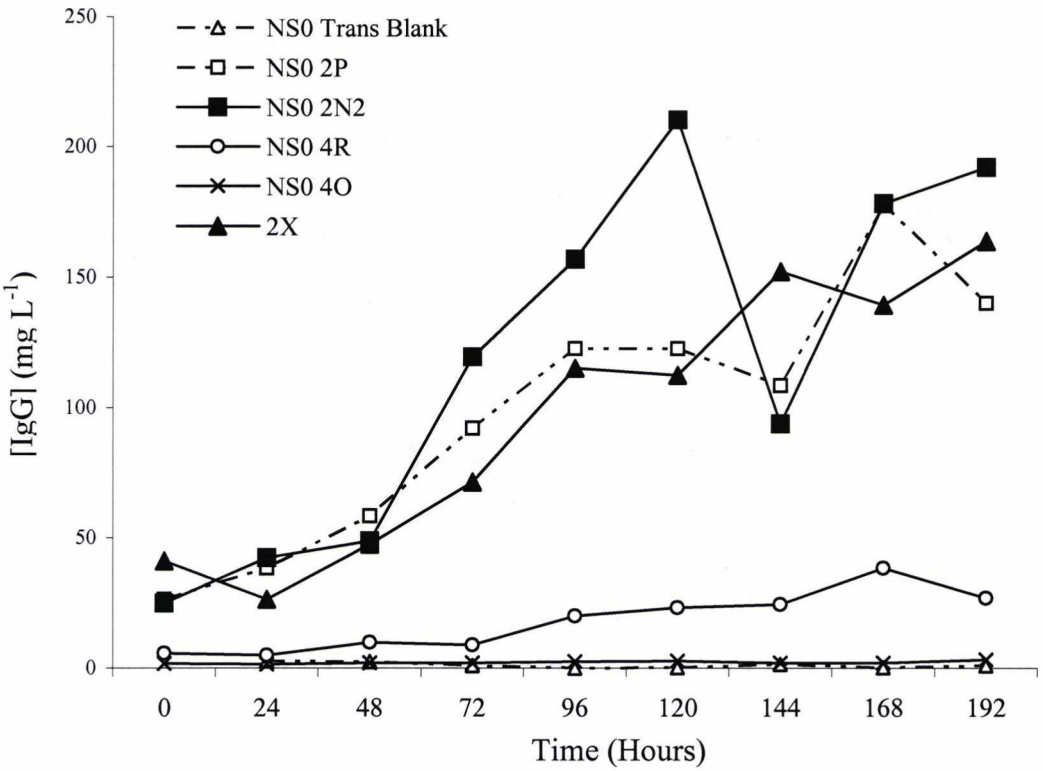

Figure 2.2. NS0 cell line productivity vs culture time. Cultures were grown in 500 mL shaker flasks at 37^{0}C in a 5% CO_2 humidified atmosphere.

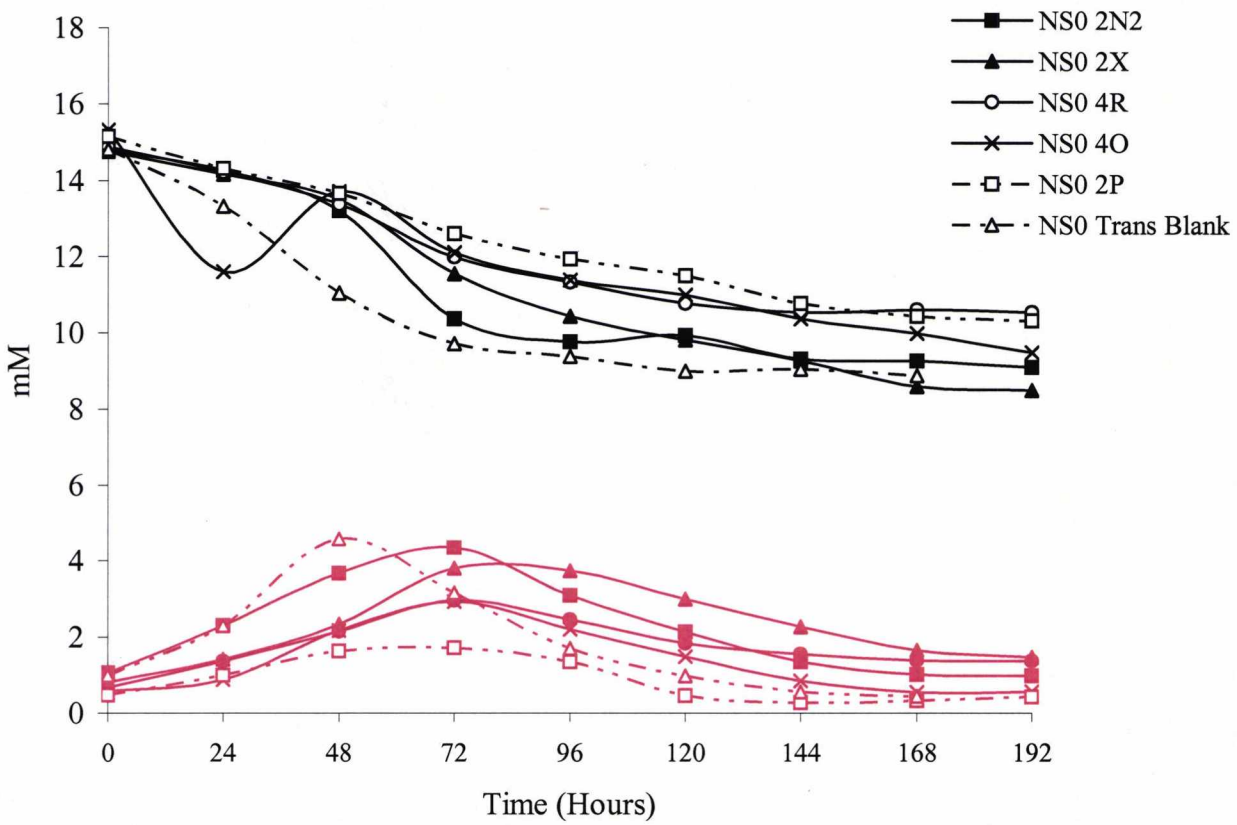

Figure 2.3. Glucose and lactate concentration of culture medium *vs* culture time. Data in black refers to glucose concentration, data in red refers to lactate concentration.

The transfectants vary in terms of growth, but all exhibited a similar pattern in their viability (figure 2.1). After an initial lag phase, all clones grew exponentially up until 100 hours after inoculation attaining the maximal cell densities shown in table 2.1. Viability of all cell lines remained more or less constant, between 80 and 100%, for this first 100 hours of culture after which a decline in cell viability was observed. A general trend was observed between cell viability and productivity. The non-productive cell lines (NS0 Parantal and GS-NS0 Transfectant Blank) showed the sharpest decline in viability (figure 2.1 B) over the last 100 hours of culture. The most productive cell lines, NS0-2N2 and NS0-2P, over the same period of time showed a slower decline in viability. This data may suggests that either the higher producers are maintained longer in the stationary phase of the growth cycle at which cells are at their most productive, or the non-productive cell lines grew more, depleting essential nutrients more quickly, thus triggering apoptosis earlier.

From the data presented in figure 2.1 similar growth characteristics are observed in the transfected cell lines. An inverse correlation between growth and productivity is not observed. Such a correlation has been previously reported by Barnes et al., (Barnes et al., 2001), but this is not the case here. The data shows that the transfectant blank cell line achieved only 46% of the maximum viable cell density achieved by the parental cell line (table 2.1). This suggests that transfection with the vector adversely affects growth rate. There are two possible reasons this. Firstly, the parental NS0 cell line was derived from an IgG secreting plasma cell from BALB/c mouse which was exposed to several rounds of cloning and selection to generate a subline which did not secrete or synthesize IgG (see chapter 1 for a detailed history of the NS0 cell line). Therefore one could speculate that as the parental cell line is not being directed to synthesize and secrete any product, the cell is under less metabolic stress and there is more energy available within the cell for growth. However, this cannot explain the difference in growth rate as the transfectant blank is not required to undertake this task either.

The second explanation is that the transfected cells have not been supplemented with glutamine in the media. Glutamine is a non-essential amino acid and is synthesised by a large variety of cells and its role within the cell is considerable. Glutamine provides a

source of nitrogen for various biosynthetic pathways and is involved in protein synthesis, purine and pyrimidine biosynthesis, ammonia formation, amino acid biosynthesis and processes such as phenylacetyl-glutamine formation (Meister, 1980). The enzymatic synthesis of glutamine is reversible and requires the hydrolysis of ATP. This reaction is catalysed by the enzyme glutamine synthetase (GS) (Barnes, 2000). The importance of glutamine to cell survival and the very low levels of endogenous GS expression within NS0 cells (Bebbington et al., 1992) means these cells have an absolute requirement for exogenous glutamine. The transfected cells depend on a glutamine synthetase gene (contained within the expression vector) to survive in the glutamine-free medium. The parental, lacking the ability to synthesise glutamine cannot survive in a glutamine free environment and rapidly died. It was therefore necessary to supplement the parental medium with glutamine. These extra metabolic steps that are carried out by the transfected cells to synthesis glutamine may therefore account for the detrimental effect on growth rate. Furthermore, the rate at which these cells synthesise glutamine was not determined but is also likely to be rate limiting in terms of growth.

The cells all utilised glucose during exponential growth (first 100 hours of culture, figure 2.3) displaying similar rates of glucose uptake. The end of exponential phase coincided with a decline in the rate of glucose uptake. No correlation was observed between glucose uptake and productivity in the clones investigated. This finding coincides with earlier reports by Miller et al., who demonstrated that specific growth rate and specific antibody production rate are independent of glucose concentration (Miller et al., 2000). The slow glucose uptake with the onset of a decline in cell viability, despite its availability, has been reported previously and for other mammalian cells in culture (Downham, 1996; Zhou, 1997). Very little lactate accumulated in the medium, with all cells exhibiting a similar rate of lactate production which did not correlate with productivity. A peak in lactate production occured between 50 and 100 hours of culture after which a small but steady decline was observed. It has been previously reported that this shift from lactate production to consumption coincides with the onset of death phase (Zhou, 1997). It cannot be confirmed that this was the case in the cells lines under investigation, however this shift from production to consumption does coincide with a slowing of growth and a reduction in cell viability.

In terms of productivity the clones can be divided into three groups; High producers (2N2, 2P, and 2X) a mid range producer (4R) and a low producer (4O) (Figure 2.2). Productivity of the high producers increased significantly between 48 and 120 hours of culture (figure 2.2) after which IgG production slowed. This slowing coincides with a decrease in glucose utilisation observed at the same time point, and as previously mentioned a decline in cell viability, which may account for this observation. The high producers exhibit significant differences in maximum monoclonal antibody (Mab) concentration with 2N2 reaching a final concentration of 210 mg L^{-1}, 2P 177 mg L^{-1}, and 2X 163 mg L^{-1}. However, if one calculates the cell specific productivities (section 2.2.6) no difference is observed 1.4 (2N2), 1.46 (2P) and 1.45 (2X) (Table 2.1). This data shows that the differences in final Mab concentration are as a result of differing growth characteristics (i.e. the final, maximum cell concentration reached for each cell line).

The mid producer (4R) has a significantly lower cell specific productivity than the high producers (0.24) and only produced 38 mg L^{-1} of recombinant protein. 4R was considered a mid range producer despite exhibiting the poorest growth with the longest doubling time of all the clones (30.6 hours) (Table 2.1). Productivity increased slowly but steadily throughout culture peaking after 168 hours.

4O produces around 70 times less Mab than the top producer, with a maximum concentration of 3.1 mg L^{-1} and a cell specific productivity measured at 0.009 pg $cell^{-1}$ h^{-1}. This cell line maintained one of the highest culture viability. This may be due to a reduction in the draining effect that results from increased rMab production (figure 2.1 B). However, this is unlikely as the transfectant blank exhibits a lower viability. No significant change in productivity was observed throughout culture, with Mab concentration levels remaining at approximately the same low level.

2.3.2 Growth characteristics, metabolism and recombinant protein production – Analysis of clonal variation GS-CHO

Four transfected GS-CHO cell lines producing cB72.3 monoclonal antibody were examined in detail. Growth and viability data throught batch culture were generated as

described for the GS-NS0 cell lines (section 2.3.1) and this data is presented in figure 2.4. Glucose utilisation and lactate accumulation were also measured as described previously for the GS-NS0 cell lines and this data is presented in figure 2.5. Growth and productivity figures for cell specific productivity, growth rate, generation number and doubling time were also calculated as described earlier. A summary of this data is presented in table 2.2.

All of the GS-CHO cell lines, with the exception of the 22H11 cell line, grew exponentially for the first 150 hours of culture (figure 2.4 A). The 30B5 cell line exhibited the highest and most rapid growth reaching a maximum viable cell density of 9.06×10^6 cells mL^{-1} after 168 hours in culture, followed by 34C10 which reached 6.46×10^6 cells mL^{-1} after 192 hours of culture, 63E4 (4.96×10^6 cells mL^{-1} after 216 hours) and finally 22H11 which reached 1.56×10^6 cells mL^{-1} after 120 hours. In general an inverse correlation was observed between cell growth and productivity in the GS-NS0 cell lines, with transfection adversely affecting growth (section 2.3.1). Such a correlation between growth and productivity was not observed in the GS-CHO cell lines. Productivity charts for the GS-CHO cell lines (figure 2.4 A) show 30B5 to be the highest producer, followed by 63E4, 34C10, and finally 22H11. This data suggests that transfection of the CHO cell lines with the GS and cB72.3 genes, does not adversely affect growth rate as the highest producer is also exhibiting the highest growth. However, this hypothesis is not conclusive as there is no data present for a parental or transfectant blank CHO cell line, as these cell lines were not available at the time of this study. Furthermore, although the number of gene copies per cell was not measured for the GS-NS0 or the GS-CHO cell lines, the number of copies in the GS-NS0 cells investigated here is <10 while in GS-CHO cells is very high (usually more >100 and possibly 1000's)(Dickinson, 2003)). Coupled to this CHO cell lines possess and endogenous GS gene, and as such to maintain selection in culture the presence of a selection agent (MSX) is required in the medium at low levels in addition to the absence of glutamine (Cockett et al., 1991). As a result the GS-CHO cells have many more copies of the GS gene and therefore should be able to synthesise much more glutamine. Hence, this suggests that the GS-CHO cell lines are not growth limited by the amount of glutamine synthesised, unlike the GS-NS0 equivalents.

Table 2.2 shows the GS-CHO growth and productivity data. This data clearly shows that the cell specific productivities (qMab) correlate with the maximum Mab

concentration (i.e. a cell possessing a high max Mab concentration also exhibits a high qMab). Its should be noted that the qMab values for the GS-CHO cell lines are generally lower than those values calculated for the GS-NS0 cells (table 2.1). Therefore, the top GS-NS0 cB72.3 secreting cell line actually produces more antibody per cell per unit of time than the highest GS-CHO producer. This discrepancy can be accounted for by the maximum viable cell densities that are achieved by both cell types. The differences are due to the GS-CHO cells ability to achieve and sustain very high cell densities (as stated earlier) for a prolonged period during stationary phase (figure 2.4 A) (i.e. a lower cell specific productivity produced by a much higher number of cells gives a much higher overall yield than a higher specific productivity by fewer cells). Coupled to this the GS-CHO cell lines (with the exception of 22H11) exhibit greater than 90% viability for the first 240 hours of culture (figure 2.5 B, C, and D).

We can postulate that this sustained high viability of the GS-CHO cell lines for prolonged periods may be due to the cells ability to utilise lactate as an energy source once glucose present in the media has been depleted. The breakdown and oxidation of glucose leads to the formation of the three carbon carboxylic acid pyruvate (Flick and Konieczny, 2002). Pyruvate is generally converted to acetyl CoA which enters into the tricarboxylic acid (TCA) cycle for complete oxidation, to lactate for the oxidation of NADH generated by glycolysis, and to alanine via the transamination pathway in which glutamate in converted to α-ketoglutarate (Zhou, 1997). Increases in lactate accumulation in the media can become toxic to mammalian cells in culture (Miller et al., 2000), often coinciding with the onset of death phase (Zhou et al., 1997). In the initial stage of culture (0-150 hours) there is an increase in viable cell density (proliferation), of the three top GS-CHO cell lines, with a concurrent increase in the Mab titre (production) (figure 2.4). During this time, a high rate of lactate accumulation is observed (figure 2.5). This indicates that this phase of culture is an energy expensive process as high lactate levels are indicative of the use of an energetically less efficient metabolic pathway (Fu and Barford, 1994). After this initial phase, proliferation and production halts, although viability is not affected (figure 2.5). At the same time, glucose is almost depleted and there is a shift to lactate metabolism. This shift to lactate metabolism suggests that it provides only enough energy to maintain cell survival but not enough to facilitate recombinant protein production. There are two

possible mechanisms by which these cells may be controlling and utilising accumulated lactate.

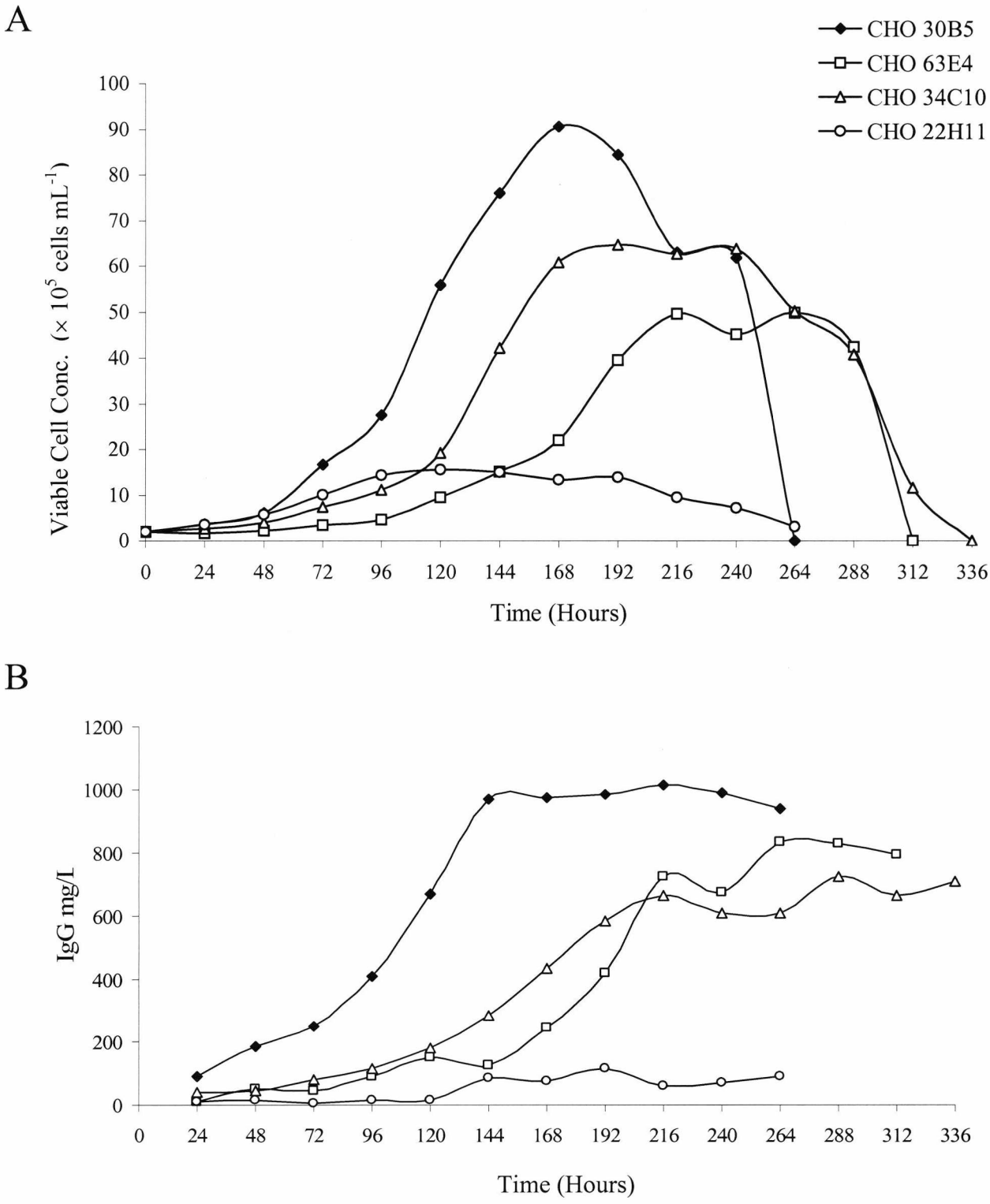

Figure 2.4 Growth and productivity of GS-CHO cB72.3 in batch culture. (**A**) Typical batch culture of GS-CHO cB72.3. Growth curve was performed in 500 mL shaker flasks and samples taken at the time points indicated throughout batch culture to determine viable cell concentration. (**B**) Productivity of GS-CHO cB72.3 cell lines during batch culture.

Firstly, lactate can be converted to pyruvate by lactate dehydrogenase, and ultimately through a series of reactions catalysed by a number of enzymes in the mitochondria, cytosol and ER, to glucose although this pathway is very energy inefficient using up more molecules of ATP that can be produced (Campbell and Farrell, 2003)

Secondly, the lactate to pyruvate conversion may be used to generate NADH for use as an alternative method of generating ATP (Berg et al., 2003; Zhou, 1997). Alternatively, rather than the cell controlling lactate utilisation intracellularly, it has been reported that CHO cell lines secrete active lactate dehydrogenase (Ducommun et al., 2002). This would allow the conversion of extracellular lactate to pyruvate that can then be utilised in the manner described earlier.

The apparent ability to utilise lactate appears greater in the GS-CHO cells than in the GS-NS0 cells, and is particularly pronounced in the 30B5 cell line. Figure 2.5 D shows that there is a peak in lactate concentration after 120 hours of culture at 14.2 mM. This drops slightly over the next 72 hours to 12.2 mM. Concurrently glucose levels have almost been depleted and dropped to less than 1 mM at the same time point. It is at this point (192 hours of culture) that a shift to the metabolism of lactate is observed with levels dropping from 12.2 mM to 0.87 mM in the space of 48 hours, with little or no effect on cell viability or productivity at the same time point. Furthermore, unlike the GS-NS0 cell lines, there appears to be a general trend between the ability to utilise accumulated lactate and productivity (figure 2.5). The least productive of the GS-CHO cells (22H11 figure 2.5 A) shows no major drop in lactate accumulation over culture. The 34C10 cell line (figure 2.5 B), exhibits a slight reduction in lactate over culture from a peak of 14 mM at 120 hours, to a low of 7.87 mM at 336 hours of culture. The 63E4 cell line (figure 2.5 C), shows a peak in lactate accumulation of 15 mM at 192 hours of culture. This is followed by a dramatic decline in the lactate levels similar to that observed for the 30B5 cell line described earlier, however this decline takes place at a much slower rate over a period of 120 hours. All the GS-CHO cell lines exhibit the same pattern in glucose metabolism, with the depletion of glucose occurring at the same rate. As mentioned previously (section 2.3.1), like the GS-NS0 cells no correlation between the rate of glucose consumption and productivity is observed.

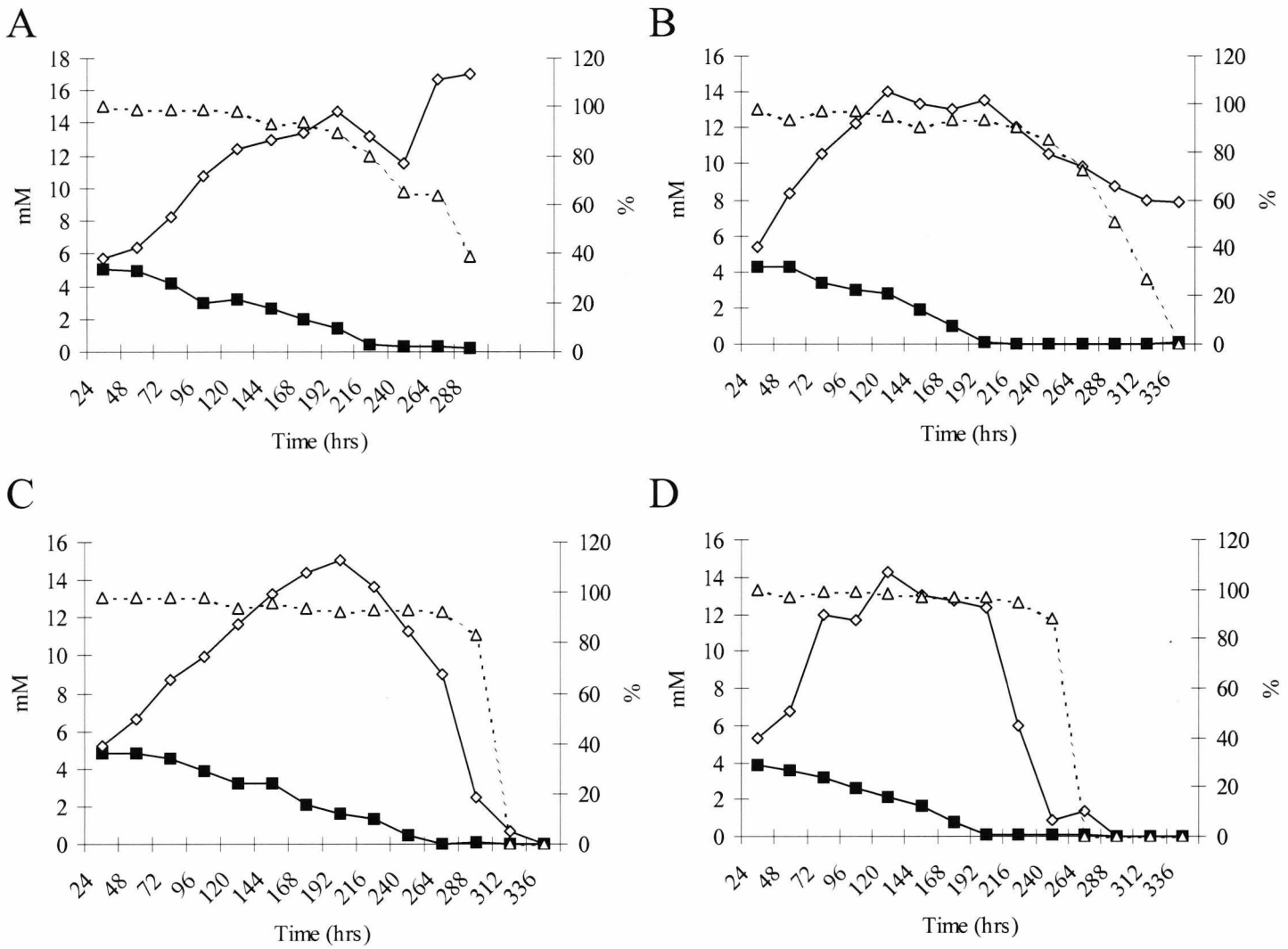

Figure 2.5 Glucose metabolism, lactate accumulation and cell viability over time. (**A**) CHO 22H11 (**B**) CHO 34C10 (**C**) CHO 63E4 and (**D**) CHO 30B5. Data was collected at the time points indicated throughout batch culture in 500 mL shaker flasks. [△] % Cell viability, [◊] Lactate (mM), [■] Glucose (mM)

Table 2.2 Growth and productivity data for GS-CHO cell lines

Cell Line	μ (h^{-1})*	T_d (h)*	Max. VCC ($\times 10^5$ cells $mL^{-1} \pm$ SE)	Max.Mab Titre (mg L^{-1})	qMab (pg $cell^{-1}$ $h^{-1} \pm$ SE)*
CHO 22H11	0.024	29.1	15.6 ± 0.96	117.0	0.10 ± 0.06
CHO 34C10	0.028	33.3	64.6 ± 1.2	725.3	0.93 ± 0.11
CHO 63E4	0.024	52.4	49.8 ± 1.7	837.5	1.20 ± 0.09
CHO 30B5	0.023	27.8	90.6 ± 2.1	1014.2	1.31 ± 0.19

*Calculated at mid-exponential growth phase

2.3.3 Characterisation of the growth and productivity of a GS-NS0 TIMP-1 cell line.

A GS-NS0 cell line expressing the metalloproteinase inhibitor TIMP-1 was obtained from CellTech (Slough, UK). Growth and viability data was obtained as described in section 2.2.2 and the results are presented in figure 2.6. TIMP-1 productivity was measured using affinity chromatography on a Fast Protein Liquid Chromatography (FPLC) system as described in section 2.2.6. FPLC chromatograms of the standard amounts of TIMP-1 used to generate the standard curve are shown in figure 2.7. Peak areas calculated from the chromatograms were used to generate the standard curve (Figure 2.8).

Samples of cell culture supernatant (1 mL, previously clarified by centrifugation at 1500 rpm) at each time point of the growth curve (figure 2.6) were applied to the column as described in section 2.2.6. The sample peak areas were then calculated as previously described and used to determine the TIMP-1 concentration by linear regression analysis. The resulting data is presented in figure 2.9.

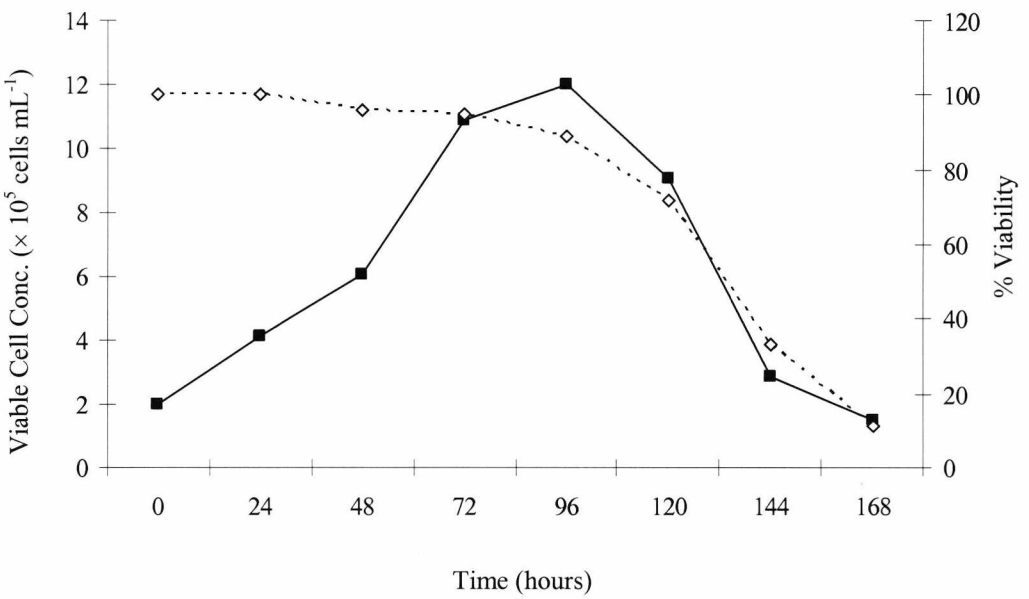

Figure 2.6 Batch culture of GS-NS0 TIMP-1 cell line. Typical batch culture growth of NS0 TIMP-1. Growth curves were performed in 500 mL shaker flasks using a working culture volume of 100 mL. Samples were taken at the times indicated to determine cell concentration (■) and viability (◊) during the course of culture.

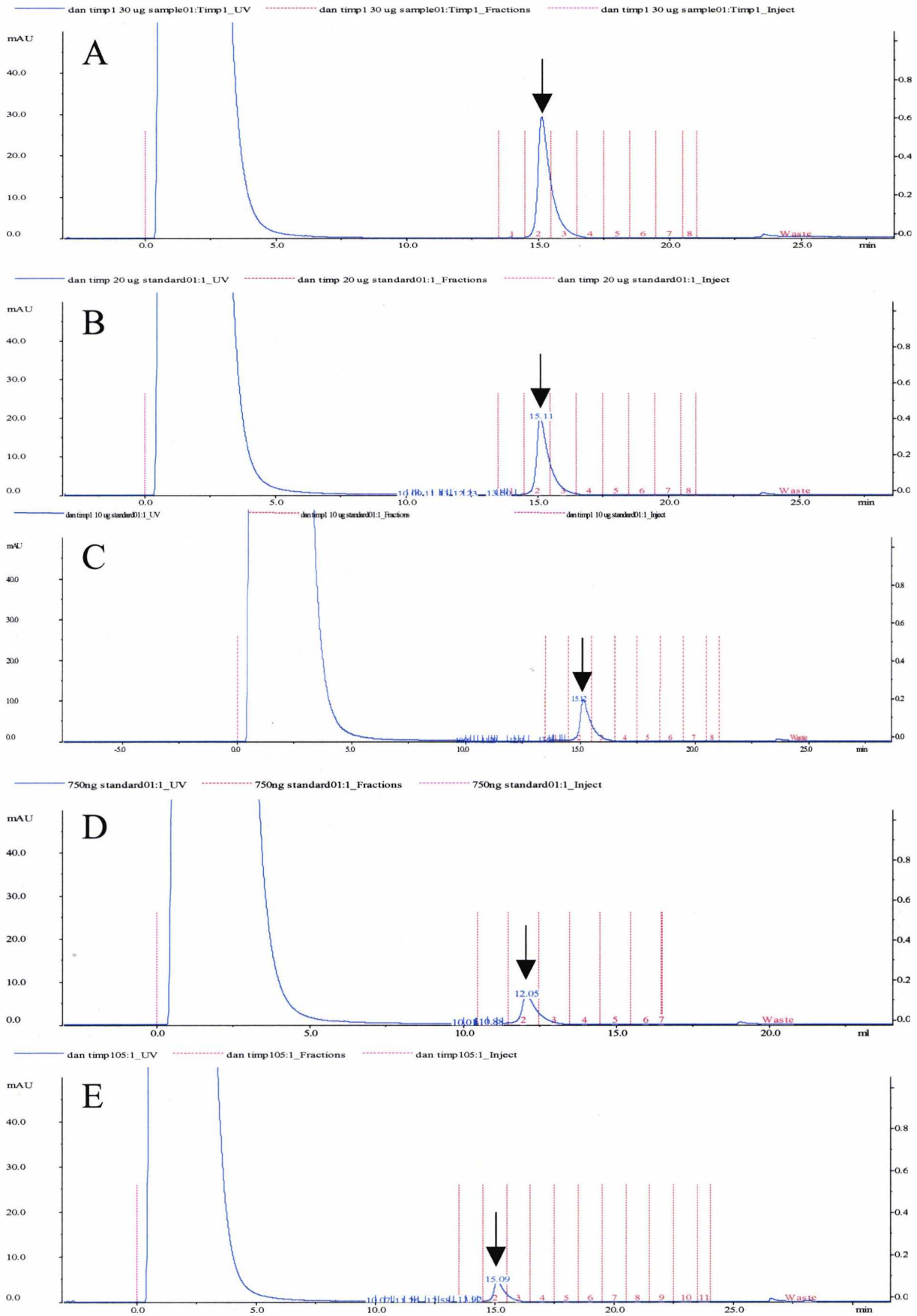

Figure 2.7 FPLC traces of standard amounts of TIMP-1 for quantitation by affinity chromatography. Absorbance was measured at 280 nm (Blue) and TIMP-1 peaks are indicated.(**A**) 30 µg TIMP-1 (**B**) 20 µg (**C**) 10 µg (**D**) 7.5 µg and (**E**) 5 µg.

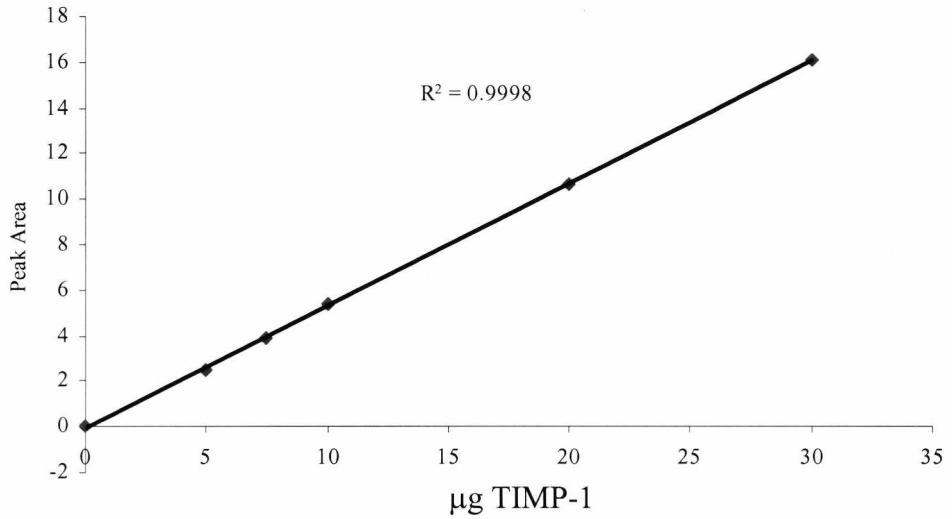

Figure 2.8 Standard curve for TIMP-1. Data was calculated from figure 2.7 and is based on peak area. A line of best fit was calculated using linear regression.

GS-NS0 TIMP-1 cells show a similar growth pattern to the GS-NS0 cB72.3 producing cells (figure 2.1 A), growing exponentially for the first 100 hours of culture. After the peak in viable cell density (1.2×10^6 cells mL^{-1}), the onset of death phase occurred, with viability dropping from 90% to 11% in the space of 72 hours (figure 2.6). This decline in cellular viability is reflected by a slowing in the production rate of TIMP-1, during the same culture period (figure 2.9).

The quantitation of TIMP-1 was carried out by affinity chromatography. An ELISA assay similar to that used to quantify the cB72.3 antibody could not be performed in this case as two antibodies specific to different epitopes on the TIMP-1 molecule were not available. Figure 2.8 shows the standard curve generated from the chromatogram traces (figure 2.7).

The standard curve exhibits an R^2 value of 0.9998 indicating the estimation of TIMP-1 in the samples analysed to be accurate to $\geq$ 99% confidence. Therefore, the quantitation of TIMP-1 by this method was considered a viable alternative in the absence of an ELISA assay.

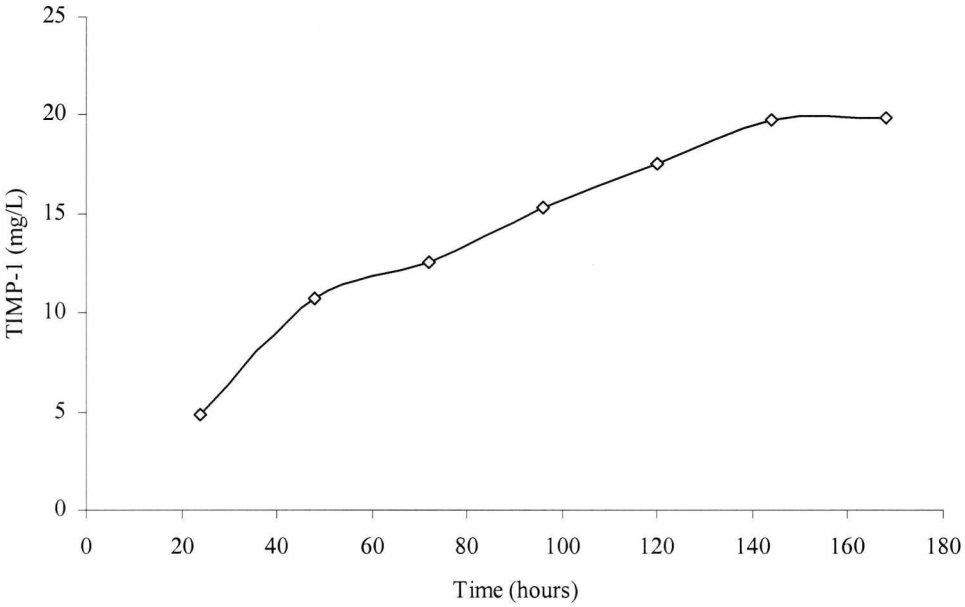

Figure 2.9 Productivity of TIMP-1 by GS-NS0 cells throughout culture. Values were calculated using regression analysis from the data shown in figure 3.9. Peak areas and corresponding TIMP-1 concentrations are also shown.

Table 2.3 Growth and productivity data for GS-NS0 TIMP-1 cell line

μ (h^{-1})*	T_d (h)*	Max. VCC ($\times 10^5$ cells mL^{-1})	Max.TIMP Conc.(mg L^{-1})	qTIMP (pg $cell^{-1}$ h^{-1})*
0.032	21.8	12	19.87	0.02

* Calculated at mid-exponential growth phase

The main thrust of the investigation reported herein is to undertake a proteomic comparison of cell lines that differ in cell specific secretory productivity. The aim of this investigation is to determine whether changes in the cellular proteome of individual cell lines are correlated with productivity and/or the product produced. Therefore, it would be prudent where possible when comparing cell lines producing different products, for the cell lines selected to display similar growth and productivity characteristics. Table 2.3 shows the growth and productivity data for the TIMP-1 cell line. Comparison of this data with the data for the GS-NS0 cB72.3 cell lines (table 2.1) shows that the most similar cell line in growth and productivity to the NS0 TIMP-1 is the NS0 4R cell line. This cell line reaches a similar maximum viable cell density (1.2×10^6 cells mL^{-1} for GS-NS0 TIMP-1 and 1.22×10^6 cells mL^{-1} for GS-NS0 4R), indicating similar growth characteristics. In terms of

productivity, 4R produces more recombinant protein in weight, however the productivity of these cell lines are more similar if we take into account the molecular weight of the protein being produced. IgG has a MW of 150,000 Da, whereas TIMP-1 has a molecular weight of 25,000 Da (Baker et al., 2002). Therefore if the specific productivities are calculated in terms of mols $cell^{-1}$ h^{-1} the productivities are 16×10^{-19} mol $cell^{-1}$ h^{-1} (GS-NS0 4R) and 8×10^{-19} mol $cell^{-1}$ h^{-1} (GS-NS0 TIMP-1). However, it is difficult to directly compare the cell specific productivities of the IgG and TIMP-1 producing cell lines due to the nature of these proteins. TIMP-1 is a single domain protein while IgG is a multi-domain protein requiring a much more complex set of folding reactions and cellular machinery. With these constraints in mind we have chosen the GS-NS0 cB72.3 producing cell line 4R as that exhibiting a cell specific productivity closest to the TIMP-1 producing cell line from those in the panel of cell lines available.

2.3.4 Evaluation of the molecular integrity of recombinant protein products by SDS-PAGE

Recombinant TIMP-1 and recombinant IgG were purified by affinity chromatography using an FPLC system as described in sections 2.2.6 and 2.2.7. Aliquots of each sample (10 μg) was diluted into 20 μL of Lamelli buffer (ommiting the β - mercaptoethanol for the non-reduced sample) and run on 12.5% tris-glycine gel as described in section 4.2.4. After electrophoresis the gels were washed briefly in ddH_20 and stained with coomassie blue solution (0.1% coomassie G250, 50% methanol, 10% acetic acid) for 60 minutes at room temperature. The gels were then de-stained using 12% methanol, 7% acetic acid. Gel images were captured as described in section 4.2.4 and the results are shown in figure 2.10.

Figure 2.10A shows the results of the purification of TIMP-1 from the cell culture supernatant. One band is observed at approximately 25 kDa which is concurs with the reported molecular weight of TIMP-1 (Baker et al., 2002; Ikenaka et al., 2003). This confirms the authenticity of the recombinant protein product produced by the GS-NS0 TIMP-1 cell line. Figure 2.10B and C confirms the production of immunoglobulin G by the GS-NS0 and GS-CHO cell lines. Two bands are observed in the lanes run under reducing conditions which correspond to heavy (~65 kDa) and light (~30 kDa) chains. In the lanes

run under non-reducing conditions, only one band was observed at approximately 150 kDa. These molecular weights correspond to those reported in the literature for Immunoglobulin G (Lodish, 1995).

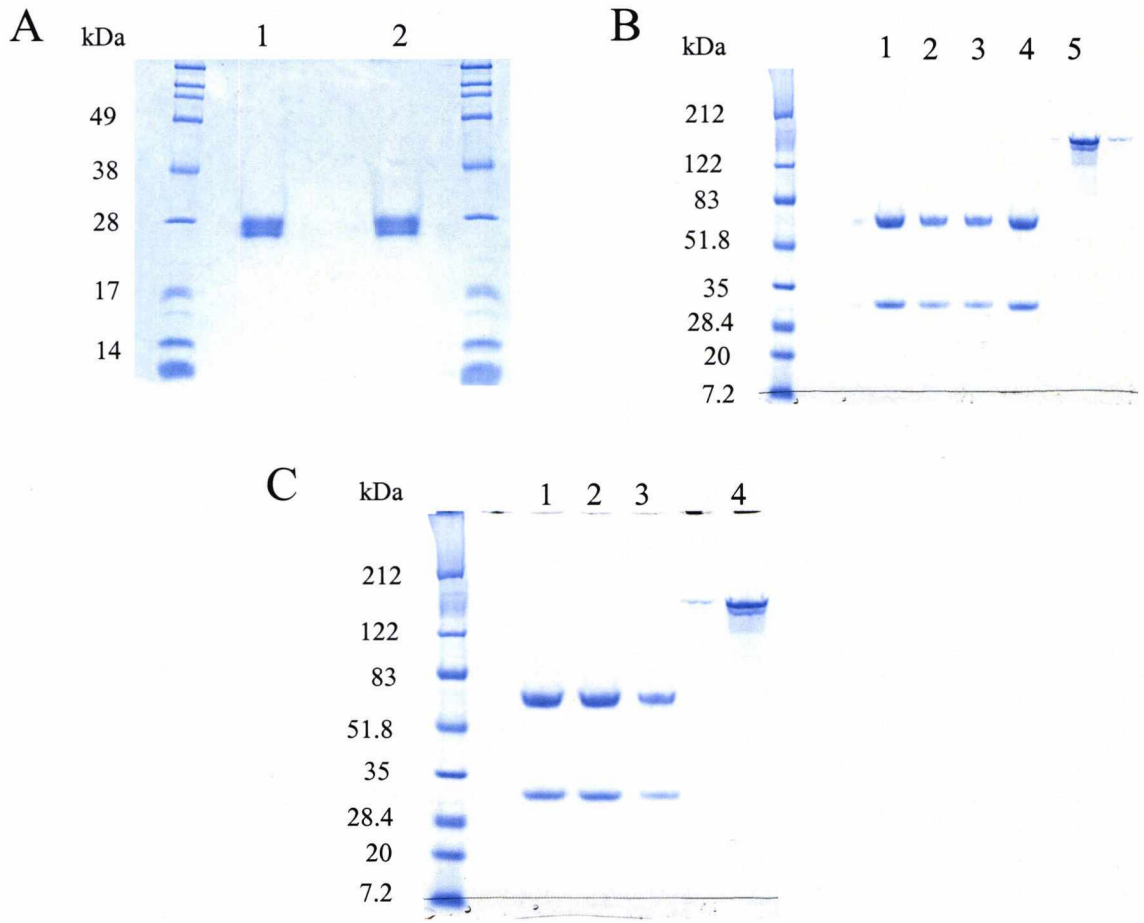

Figure 2.10 SDS-PAGE analysis of recombinant protein product. (**A**) Lanes 1 & 2 show TIMP-1 purified from cell culture supernatant. (**B**) Purified IgG run in the presence of β - mercaptoethanol from GS-NS0 cell culture supernatants Lane (1) NS0 4R, (2) NS0 2X, (3) NS0 2P, (4) NS0 2N2. Lane 5, purified IgG run in the absence of β - mercaptoethanol. (**C**) Purified IgG run in the presence of β - mercaptoethanol from GS-CHO cell culture supernatants. Lane (1) 30B5, (2) 63E4, (3) 34C10. Lane 4, purified IgG run in the absence of β - mercaptoethanol.

2.3 Conclusions

The data presented here for the GS-NS0 cell lines confirm a panel of cell lines that are observed to have similar growth characteristics but exhibit a variation in cell specific productivity. This spread of productivities observed under the same growth conditions is ideal for undertaking a proteomic investigation into cellular factors that influence the productivity of recombinant proteins by mammalian cells in culture. Meanwhile the GS-CHO cell lines characterised here exhibit good variation in productivity of the cB72.3 antibody and produce significantly larger amounts of protein product then the GS-NS0 cells however this is mainly due to an increased ability to maintain a high viable cell density and not due to increased cell specific productivity. Despite this, the GS-CHO cell lines were still considered suitable to investigate if changes observed in the GS-NS0 proteome which correlate with productivity are conserved with the GS-CHO cell line (i.e. between mammalian cell line species). Furthermore characterisation of the GS-NS0 TIMP-1 cell line showed that in terms of growth and productivity it best matched the GS-NS0 4R cell line, and therefore these two cell lines will be used to compare the cellular machinery utilised by the same cell type to produce two different protein products.

Chapter 3 Measurement of mRNA levels and gene copy number in GS-NS0 and GS-CHO

3.1 Introduction

3.1.1 Gene amplification

The process of developing a mammalian cell line to express a recombinant protein begins with the introduction of the gene of interest into the cell. The instructions for the desired product (in the form of DNA) must first be transcribed into messenger RNA (mRNA) which is then translated into the protein product. To obtain a cell line producing high levels of the desired product, clones are often selected that possess high numbers of recombinant DNA copies, which in turn should produce high levels of mRNA to be translated into recombinant protein. This can be achieved by (i) efficient introduction of DNA into mammalian cells (Keown et al., 1990), and (ii) by co-amplification of the DNA sequence using a selectable marker system. Two such selectable systems in common use are the dihydrofolate reductase (DHFR) system and the Glutamine synthetase system (GS).

The DHFR system is most commonly employed in CHO cell lines. This system was first described by Alt et al, (1978) and has been in use for foreign gene co-amplification since 1980 (Strutzenberger et al., 1999). In this system the genes for heavy and light chain are transfected on plasmids bearing the neomycin resistance gene. A

plasmid containing the *dhfr* gene is co-transfected and cells are first selected by resistance to neomycin, after which the gene copy number can be amplified by culturing the cells in increasing concentrations of methotrexate (MTX). Only cells that produce increased amounts of DHFR will survive this treatment (Strutzenberger et al., 1999; Urlaub and Chasin, 1980). As the *dhfr* genes are amplified other neighbouring genes are often co-amplified, and so after each round of amplification cells are subcloned to search for clones with increased production rates (Grillari et al., 2001).

The second system (the GS system), involves transfection of a plasmid vector containing the recombinant gene of interest together with the gene for glutamine synthetase (GS)(figure 3.1). Cells are then selected by culture in glutamine free media (Bebbington et al., 1992). Amplification of the recombinant genes is achieved by the addition of increasing concentrations of methylsulphoxamine (MSX) that is a specific inhibitor of GS activity (Barnes, 2000). As discussed previously in chapter 2 (section 2.3.1), glutamine is essential to cell survival, therefore in the absence of glutamine in the media, and the suppression of the GS gene using MSX, the cell is forced to amplify the GS gene to survive. Any gene co-transfected with the GS gene (such as a recombinant protein) will be amplified simultaneously. The GS coding sequence is usually under the control of a weak promoter (e.g. SV40), however the recombinant protein coding sequence is often under the control of a powerful hCMV promoter (Keen and Hale, 1996). This is designed to ensure that successful transfectants, surviving in glutamine-free media using the weakly transcribed GS gene, should produce reasonable levels of recombinant protein mRNA due to the powerful hCMV promotor (Brown et al., 1992). The GS system has been used in both CHO cells and NS0 cells, however NS0 cells unlike CHO cells are phenotypically GS-deficient and hence this allows easier selection of successful transfectants (Bebbington et al., 1992). In comparison to the DHFR system, the GS system, especially when used with NS0 cells, offers a large advantage in terms of the time to develop a 'new' cell line and requires fewer copies per cell (Brown et al., 1992).

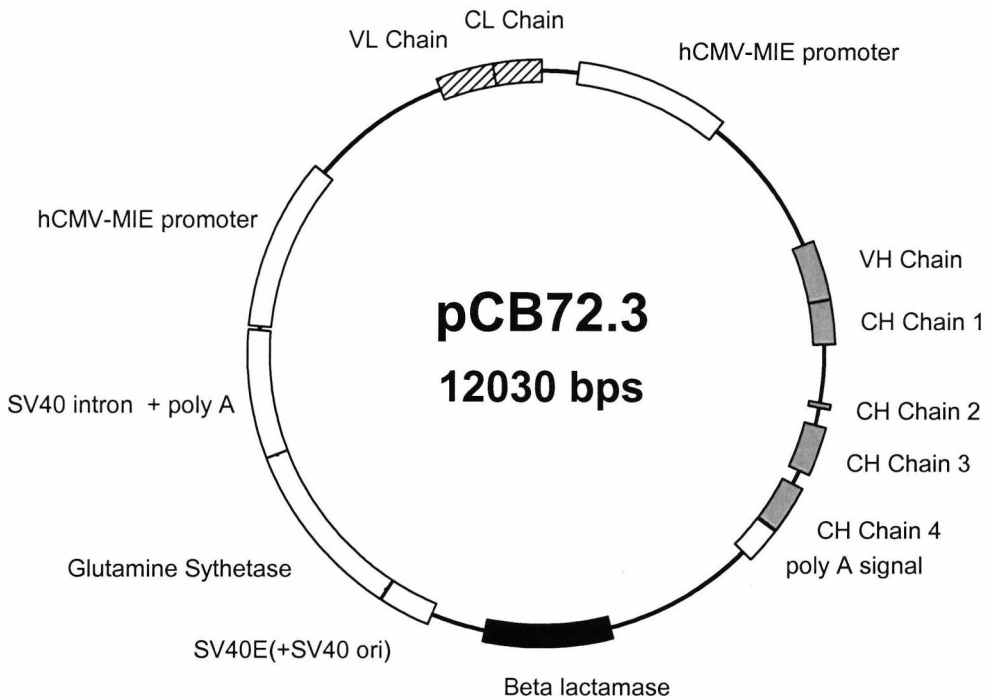

Figure 3.1 A plasmid vector containing genes for the IgG heavy and light chain utilising the GS system.

3.1.2 mRNA levels and recombinant protein production

Presently, the use of highly efficient expression systems (GS and DHFR) to amplify gene copy number has led to high levels of mRNA being produced by mammalian cell lines in culture. However, it is still a point of contention as to whether a direct correlation exists between mRNA level and productivity of mammalian cells in culture. Schröder et al., demonstrated that ATIII mRNA increased proportionally with ATIII cDNA copies, and intracellular ATIII increased proportionally with ATIII mRNA (Schröder et al., 1999). A study by Fann et al., investigating the relationship between recombinant activated protein C (APC) secretion rates and mRNA levels in baby hamster kidney cells reported a linear increase in APC secretion rate with increasing mRNA level, and concluded that mRNA levels limited the rate of APC secretion (Fann et al., 1999). Furthermore, this was also reported for the secretion of recombinant human protein C by HEK293 cells (Walls et al., 1989).

However, there have now been several published studies that show no correlation between mRNA levels and increased levels of recombinant protein production. For example Merten et al., investigated the production kinetics of monoclonal antibodies by murine hybridoma cells (Merten et al., 1994) and reported that there was no correlation between mRNA levels and the specific productivity of the I1317-DC hybridoma cell line. Furthermore, although mRNA levels increased with increasing growth rate, there was either a decrease or no modification of mab production rates during batch culture. These findings concur with a report by Bilbila and Flickinger (1991) who also found no correlation between mRNA levels coding for heavy and light chain IgG and production rate. This study also noted that mRNA levels followed specific growth rates during batch culture (Bibila and Flickinger, 1991). In a review by Anderson and Anderson (1998) they describe a multi-gene comparison plot of mRNA vs protein abundances for cellular gene products. The results of this plot showed a low correlation coefficient between mRNA and protein product levels, with as much as 10 fold variations observed in either mRNA or protein concentration at constant values of the other parameter (Anderson, 1998).

It has been postulated by various groups (Bibila and Flickinger, 1991; Merten et al., 1994; Strutzenberger et al., 1999) that the rate limiting steps in the production of recombinant proteins from mammalian cells in culture, stem from the assembly process within the post-translational pathway. In other words the so called "bottle neck" is thought to occur downstream of transcription. Therefore, before undertaking rigorous proteomic analysis of the cell lines investigated in this study, this chapter aims to measure the specific mRNA levels for both the heavy and light chain of the cB72.3 antibody produced in GS-NS0 and GS-CHO cell lines that differ in productivity in batch culture (Chapter 2). Concurrently, we will attempt to quantitate the gene copy number of the cB72.3 genes within these cell lines. Furthermore, the relationship between cellular RNA, mRNA and cell size will be investigated.

3.2 Materials and Methods

3.2.1 Genomic DNA extraction from cultured cells

After harvesting extractions of genomic DNA were carried out on 1×10^7 GS-NS0 or GS-CHO cells harvested at mid exponential phase of growth during batch culture. Cells were cultured as previously described in chapter 2 (section 2.2.1). The cells were washed twice in 1 mL of PBS. The final wash supernatant was then removed and 1 mL of lysis buffer consisting of 9.7 mL TNE (10mM Tris, 100 mM NaCl, 1 mM EDTA), 0.2 mL SDS (10% w/v stock), and 0.1 mL Proteinase K (100 μg mL^{-1} Roche Diagnostics, Lewes, UK) made up to 10 mL with ddH_20 was added and mixed by inverting several times. The mixture was then incubated for 5 hours or overnight at 37^0C. RNase (Roche Diagnostics) was then added to the mixture to give a final concentration of 10 μg mL^{-1} and the solution incubated for a further 30 – 60 minutes at 37^0C. An equal volume of phenol:chloroform:IsoAmyle alcohol (25:24:1 pH 8.0, BDH, Poole UK) was then added to the mixture, inverted and then centrifuged at 3000 rpm for 10 minutes. The top (aqueous) layer was transferred to a fresh tube and the phenol:chloroform extraction repeated. Traces of phenol were removed by adding an equal volume of chloroform, mixing and then centrifuging as before. The aqueous layer was transferred to a fresh tube and the chloroform extraction repeated. The aqueous layer was then transferred again to a fresh tube and 1 volume of ice cold isopropanol was added, the tube was covered in parafilm, mixed several times and then incubated overnight at -20^0C to precipitate the DNA. The resulting DNA precipitate was pelleted by centrifuging at 16000 rpm for 30 minutes. The supernatant was discarded and the pellet carefully washed with 70% ethanol. The ethanol was then decanted and the pellet left to air dry in air. Finally, the pellet was resuspended in 100 μL of TE buffer (1.0 M Tris, pH 7.4 0.5 M EDTA) and stored at 4^0C.

3.2.2 Total RNA extraction from cultured cells

RNA extractions were carried out on 1×10^7 cells harvested at mid exponential phase using an RNeasy™ Kit (Qiagen, Crawley UK) as per the manufactures instructions. Briefly, the samples were disrupted and lysed using a 21 gauge needle in a buffer containing guanidine isothiocyanate. Ethanol was then added and the sample was applied

to an RNeasy spin column for adsorption of RNA to the membrane. Contaminants were then removed with three washes using the buffers providedin the kit (RW1 and RPE). Finally, the RNA is eluted in RNase free water.

3.2.3 Spectrophotometric measurement of DNA and RNA concentration

Purity of the extracts were assessed by determining the A_{260}:A_{280} ratio. Good quality DNA results in a ratio of between 1.7 & 1.8. Good quality RNA results in a ratio of between 1.9 and 2.0 (Maniatis et al., 1982). The concentration of double stranded DNA (dsDNA) and RNA in extracts prepared as described above was calculated using the following equations.

Concentration of dsDNA ($\mu g\ mL^{-1}$) = $50 \times A_{260} \times$ Dilution factor

Concentration of RNA ($\mu g\ mL^{-1}$) = $40 \times A_{260} \times$ Dilution factor

3.2.4 Agarose gel electrophoresis of DNA

DNA preparations and their integrity were determined by analysis on agarose gels. A 1% agarose gel was prepared using 0.6g of agarose dissolved in 60 mL of TBE (89 mM Tris, 89 mM Boric acid, 2 mM EDTA, pH 8.0). The solution was heated to 100^0C and then allowed to cool to approximately 50^0C. Ethidium bromide (5 μL of a 10 mg mL^{-1} stock) was added to the mixture prior to pouring. Samples (1μg) were mixed with 6 × sample buffer (0.25% bromophenol blue, 0.25% xylene cyanol FF, 15% Ficoll) prior to loading. Gels were run in TBE at 60V until the dye front was at least 7 or 8 cm from the wells. DNA bands were visualised using a UV illuminator and images were recorded using a Gel Doc™ system (BioRad).

3.2.5 Formaldehyde gel electrophoresis of RNA

RNA integrity was determined by formaldehyde agarose gel electrophoresis. A 1% agarose gel mix was prepared to a final volume of 250 mL, consisting of 2.5 g agarose, 155 mL diethyl pyrocarbonate (DEPC) treated water (0.1% v/v DEPC to de-ionised water, incubate overnight and sterilize by autoclaving), 50 mL 5× MOPS (0.2 M MOPS, 0.05 M sodium acetate, 0.005 M EDTA, pH 8.0 made using DEPC treated water and autoclaved). The solution was heated to 100^0C and allowed to cool until the temperature was

approximately 55^{0}C. Formaldehyde (45 mL of a 37% w/v molecular biology grade solution, Sigma, UK) was added prior to pouring. The mixture was poured into the gel casting apparatus that had been pre-cleaned using RNase Zap^{TM} (Ambion, Cambridge UK). Samples (10 μg) were mixed with 6 × sample buffer (section 3.2.4) prior to loading. Gels were run using 1 × MOPS buffer at 80V for approximately 2 – 5 hours or until the dye front had migrated at least 10 cm from the wells. To visualise RNA bands the gels were stained using ethidium bromide (0.5 μg mL^{-1} in 1.0 M ammonium acetate) for 30 – 45 minutes with agitation and visualised using a UV illuminator and recorded using a GelDoc^{TM} system.

3.2.6 Northern transfer of RNA to a nylon membrane

After gel electrophoresis, RNA was transferred to nylon membranes by capillary transfer. All solutions used were prepared using DEPC treated water. All plastic and glassware was pre-treated using RNase Zap^{TM} before use. After electrophoresis (section 3.2.5) all areas of the gel which did not contain RNA were trimmed using a razorblade. The gel was then rinsed in several changes of DEPC treated water and then soaked for 20 minutes in 0.05 M NaOH. The gel was then washed as before and soaked for 45 minutes in 20 × SSC (3.0 M NaCl, 0.3 M sodium citrate, adjust to pH 7.2 using 10M NaOH). A piece of Whatman 3MM paper the same width as the gel was placed on a piece of glass on top of a solid support in a large glass dish. The dish was filled with 20 × SSC until the level of the liquid reached almost to the top of the support ensuring that the 3MM paper made contact with the liquid (see figure 3.2). Once the 3MM paper was thoroughly wet, place the gel on the support in an inverted position so that it is centred on the 3MM paper ensuring that there were no air bubbles between the paper and the gel. A piece of nitrocellulose membrane (Amersham Biosciences) cut to the size of the gel was then floated on a dish of deionised water until wet, then soaked in 20× SSC for 5 minutes. The membrane was then placed on top of the gel making sure all the edges were aligned and ensuring there were no air bubbles between the membrane and the gel. A dry piece of 3MM paper was then placed on top on the membrane followed by a stack of paper towels around 5 – 8 cm high. A glass plate was then placed on top of the towels and weighed down with a 500 g weight. Transfer was allowed to proceed for 10-16 hours. After transfer the membrane was rinsed in 5 × SSC for 5 minutes. The membrane was then laid flat on 3MM paper and allowed to air dry for 30 minutes. The RNA was then UV cross-linked to the membrane at 120

mJoules using a UVP CL-100 ultra violet cross-linker. Cross-linked membranes were wrapped in foil and stored at –20^{0}C.

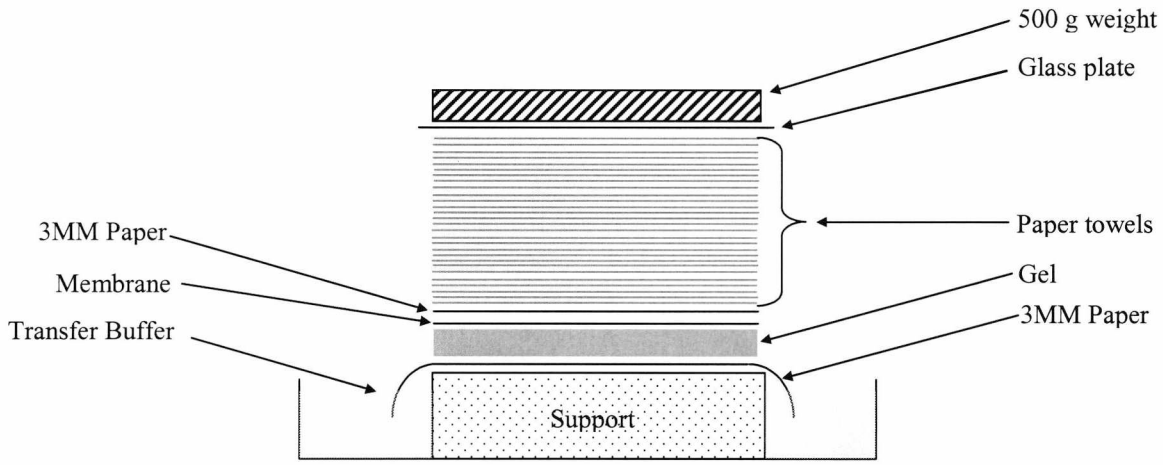

Figure 3.2 Capillary transfer of nucleic acids from agarose gels to solid supports. Buffer is drawn from a reservoir and passes through the gel into a stack of paper towels. The nucleic acid is eluted from the gel by the moving steam of buffer and is deposited onto the membrane. (REF: adapted from Sambrook et al., 1989).

3.2.7 Southern transfer of DNA to nylon membranes

A restriction digest of the extracted genomic DNA was carried out using *HINDIII* (Promega, Southampton, UK) as per the manufacturers instructions. Digested samples were then run on agarose gels as described in section 3.2.4. After electrophoresis the gels were trimmed with a razor blade and soaked in several changes of 1.5 M NaCl 0.5 M NaOH for 45 minutes with agitation. The gel was then rinsed briefly in ddH_2O and then soaked in 1 M Tris 1.5 M NaCl (pH 7.4) with agitation. The blot was carried out as described in section 3.2.6 using 10 × SSC as the transfer buffer. After transfer was complete the apparatus was disassembled and the membrane washed for 2 minutes in 2 × SSC, allowed to air dry and then UV crosslinked as described in section 3.2.6. The blots were stored at –20^{0}C between two pieces of 3MM paper.

3.2.8 Radio labelling of DNA with ^{32}P using T4 polynucleotide kinase

DNA oligonuceotide probes to B72.3 variable heavy and light chain mRNA's were obtained from Qiagen Operon (Germany). The nuceotide sequences are listed below.

Southern Blot sequences:

Variable heavy chain $^{3'}$ TGCAGACAAATCCTCCAGCACTGCC $^{5'}$

Variable light chain $^{3'}$ TGGCAGTGGATCGGGCACACA $^{5'}$

Northern blot sequences:

Variable heavy chain $^{3'}$ACGTCTGTTTAGGAGGTCGTGACGG $^{5'}$

Variable light chain $^{3'}$ ACCGTCACCTAGCCCGTGTGT $^{5'}$

Oligonuceotide probes were labelled using [γ-^{32}P]ATP (ICN, Basingstoke, UK) with the DNA 5' End-labeling System^{TM} (Promega, Southampton, UK) as described in the manufactures instructions (Promega technical bulletin #096).

3.2.9 Hybridisation and autoradiography of ^{32}P labelled oligonucleotide probes to northern blots

Blot membranes were pre-hybridised using 30 mL of ULTRAhyb^{TM}-oligo hybridisation buffer (Ambion, Cambridge, UK) for 1 hour at 42^{0}C. The buffer was then poured into a separate container and 320 ng of radio-labelled heavy and light chain probe was added to the buffer, which was then incubated with the blots overnight at 42^{0}C. Following hybridisation, the buffer was discarded and the blots washed for 3 × 30 minutes using 50 mL of 2 × SSC containing 0.5% SDS at 42^{0}C. The blots were then wrapped in clingfilm, and exposed to autoradiography film (Amersham Biosciences) with an intensifying screen for 4 hours at -70^{0}C. The developed autoradiograph image was captured using a powerlook III^{TM} prepress colour scanner (Amersham Biosciences).

3.2.10 Hybridisation and autoradiography of ^{32}P labelled oligonucleotide probes to southern blots

Prior to hybridisation and autoradiography of the DNA blots, the membranes were pre-hybridised in 30 mL of pre-hybridisation solution (5× Denhart's solution (Maniatis et al., 1982), 6× SSC, 0.5% (w/v) SDS, 100 μg mL^{-1} denatured fragmented salmon sperm

DNA (Sigma), 50% Formamide) for 1 hour at 42^0C. Following pre-hybridisation, 30 mL of hybridisation solution (as described for pre-hybridisation with the exception of Denhart's solution) containing 300 ng of radio labelled (section 3.2.8) heavy and light chain probe was added to cover the membrane and incubated overnight at 42^0C. After hybridisation the blots were washed as described in section 3.2.9. The blots were then wrapped in clingfilm, and exposed to autoradiography film (Amersham Biosciences) with an intensifying screen for 24 hours at -70^0C. The developed autoradiograph image was captured using a powerlook III^{TM} prepress colour scanner (Amersham Biosciences).

3.2.11 Cell size measurements

Extracts of cell culture sample (100 μL) were diluted into 5 mL of Casytone buffer and measured on a CASY instrument set up for cell size measurements, carried out at Lonza Biologics (Slough, Berkshire. UK). Results were recorded as mean cell diameter and mean cell volume.

3.3 Results and Discussion

3.3.1 Extraction and quantitation of DNA and RNA from GS-NS0 and GS-CHO cell lines

Genomic DNA and total RNA extractions were carried out on GS-NS0 and GS-CHO cell lines as described in section 3.2.1 and 3.2.2. Extracted DNA and RNA was quantified by spectrophotometry as described in section 3.2.3. Three extractions per cell line were carried out and the data plotted as pg of DNA/RNA $cell^{-1}$ (Figure 3.3). Generally no correlation was observed between the amount of DNA extracted and the productivity of the cell in either cell line (CHO or NS0). This was also the case for the total RNA content. However, this contradicts a study carried out by Dalili and Ollis, who reported a correlation between the total cellular RNA content and the antibody secretion rate (Dalili and Ollis, 1990). One would not expect there to be a correlation between total RNA and productivity of the cB72.3 antibody. This is because the total RNA extracted consists not only of the mRNA's for every expressed protein (which are expressed at different levels), but also ribosomal RNA and transfer RNA's. The variation in cellular RNA content observed between the cell lines is most likely due to the presence of cells at various stages of the cell cycle. Generally, the cellular RNA content increases as the cells proceed through various phases of the life cycle (Dalili and Ollis, 1990). Furthermore, no correlation is observed between the levels of DNA and the levels of RNA present per cell. This suggests that the amount of RNA is not purely a consequence of the amount of DNA present within a cell but rather is indicative of the various factors such as the metabolic state of the cell and the phase of the cell cycle it currently occupies, which affects the protein complement of the cell.

A comparison of the specific growth rate (μ) (table 2.1 and 2.2) with the total cellular RNA (figure 3.3 B) also shows no observable trend. This also contradicts findings by Bibila and Flickinger, who reported that total cellular RNA appears to decrease almost linearly with decreasing specific growth rate (Bibila and Flickenger, 1991). However, it should be noted that the reported decrease in cellular RNA was as a function of time as the cells proceed from exponential into stationary phase of growth. The data reported here for total cellular RNA was collected at the same time point (i.e. mid exponential phase of growth), and as such may account for this discrepancy.

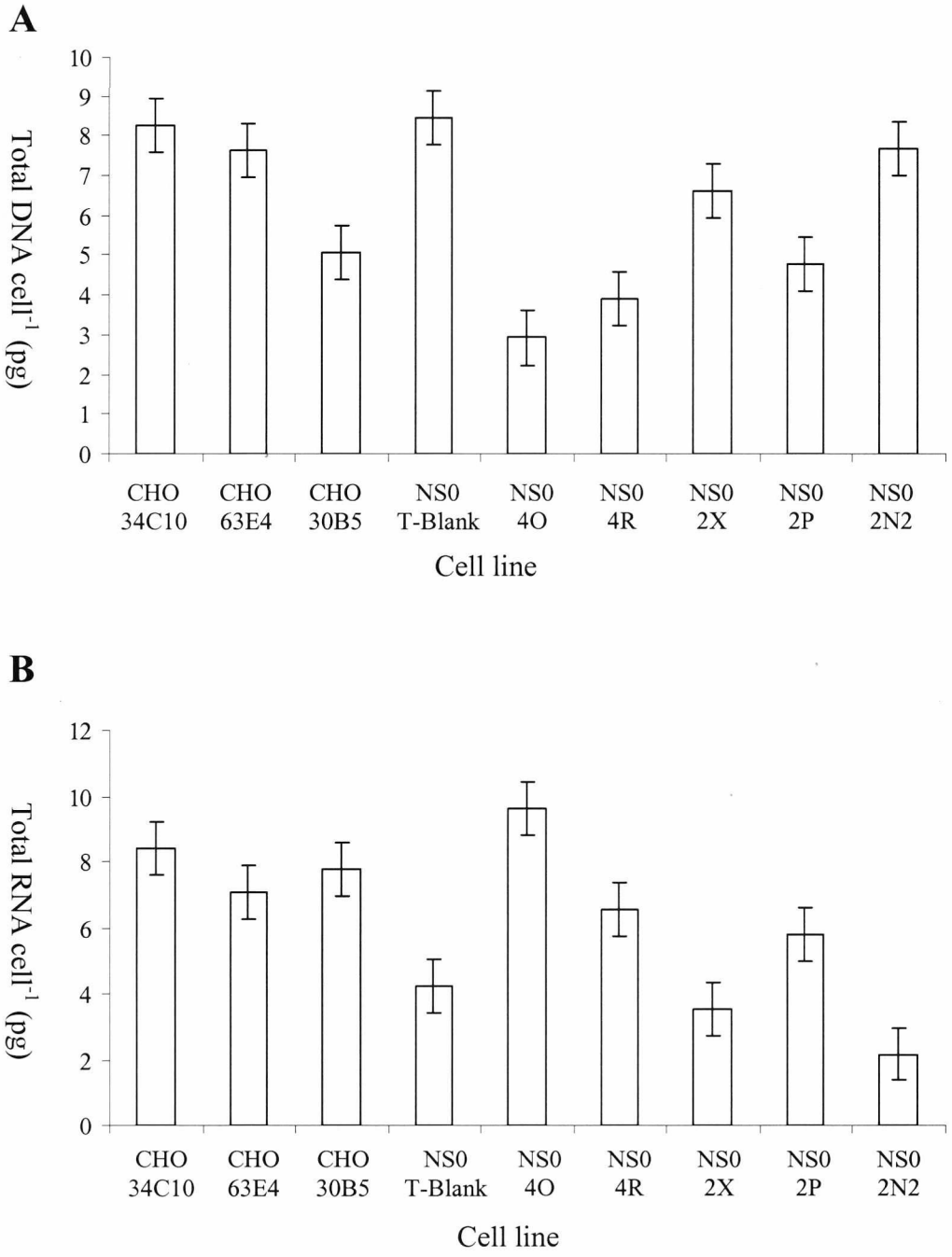

Figure 3.3 DNA and RNA content of GS-NS0 and GS-CHO cell lines. (**A**) Estimation of genomic DNA content of cell lines expressed as mean pg of DNA cell^{-1} (**B**) Estimation of total RNA content of cell lines expressed as mean pg of RNA cell^{-1}. All estimations were carried out in triplicate and standard errors are shown accordingly.

A general trend however was observed in the productive cell lines (excluding the parental and transfectant blank) between specific growth rate and cellular DNA content in both the GS-NS0 and the GS-CHO. From the data in figure 3.3A and tables 2.1 and 2.2, it appears that the cell lines with the highest specific growth rates also exhibit the highest levels of cellular DNA. It is possible that this correlation is entirely coincidental, caused by a non uniform loss in the extraction procedure used to isolate genomic DNA. If this is not the case, one could hypothesise that the cells that exhibit the highest specific growth rates, may have a larger percentage of the cell population in the S phase of the growth cycle. During this phase of growth DNA synthesis occurs and the DNA content within a cell doubles as the cell enters the G_2 phase and prepares to undergo mitosis (figure 3.4) (Lodish, 1995).

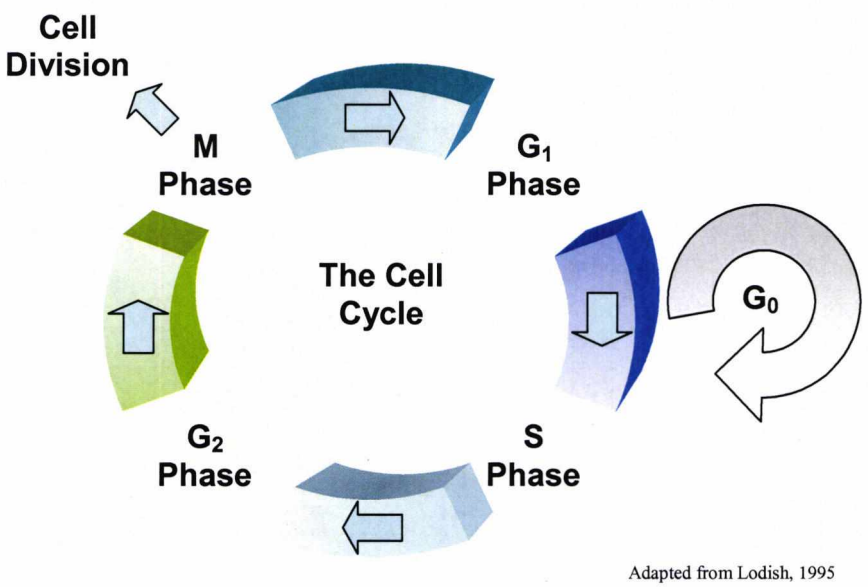

Figure 3.4 The eukaryotic cell cycle. The cell cycle comprises the G_1, S, G_2, and M phases. DNA is synthesised in the S phase and, and other macromolecules are synthesised throughout interphase (G_1, S, G_2 phases), so the cell roughly doubles its mass. During G_2 the cell is prepared for the mitotic (M) phase, when genetic material is evenly partitioned and the cell divides. Non-dividing cells exit the normal cycle, entering into the quiescent G_0 state (Lodish, 1995).

3.3.2 Cell size measurements in GS-NS0 and GS-CHO cell lines

In order to examine whether any correlation exists between cell size and specific productivity, cell size measurements (cell volume and cell diameter) were carried out as described in section 3.2.11. Three measurements were taken per cell line and the results are presented in figure 3.5. The results presented here show that cell diameter and cell volume was fairly constant between the clones of the GS-NS0 and GS-CHO cell lines. It has been proposed that mammalian cell size does fluctuate in the early stages of growth, but usually the cell size returns to a constant (Conlon and Raff, 2003; Wells, 2002). However, as far as we are aware there are no reports which investigate variations in cell size between clonal variations derived from the same parental cell line. This constant cell size may also be indicative of the fact that cells were harvested at the same stage of growth (mid-exponential phase). Neither cell diameter or cell volume shows a correlation with cell specific productivities, in either of the cell types (NS0 and CHO) investigated. This data suggests that the hypothesis that bigger cells produce more recombinant protein (due in part to the abundance of more secretory pathway machinery), is not the case in these cell lines. In a study of cell growth, division and size using 3T3 cells in culture, Brooks and Shields found that large 3T3 cells actually grew more slowly that their smaller counterparts (Brooks and Shields, 1985). No such relationship was observed in the GS-NS0 cells investigated here. Furthermore, the opposite was observed in the GS-CHO cell line. The 30B5 cell line has the highest specific growth rate (table 2.5) but is the smallest of the CHO cell lines investigated. This data suggests that any correlation observed between growth rate and cell size is most likely to be cell line specific.

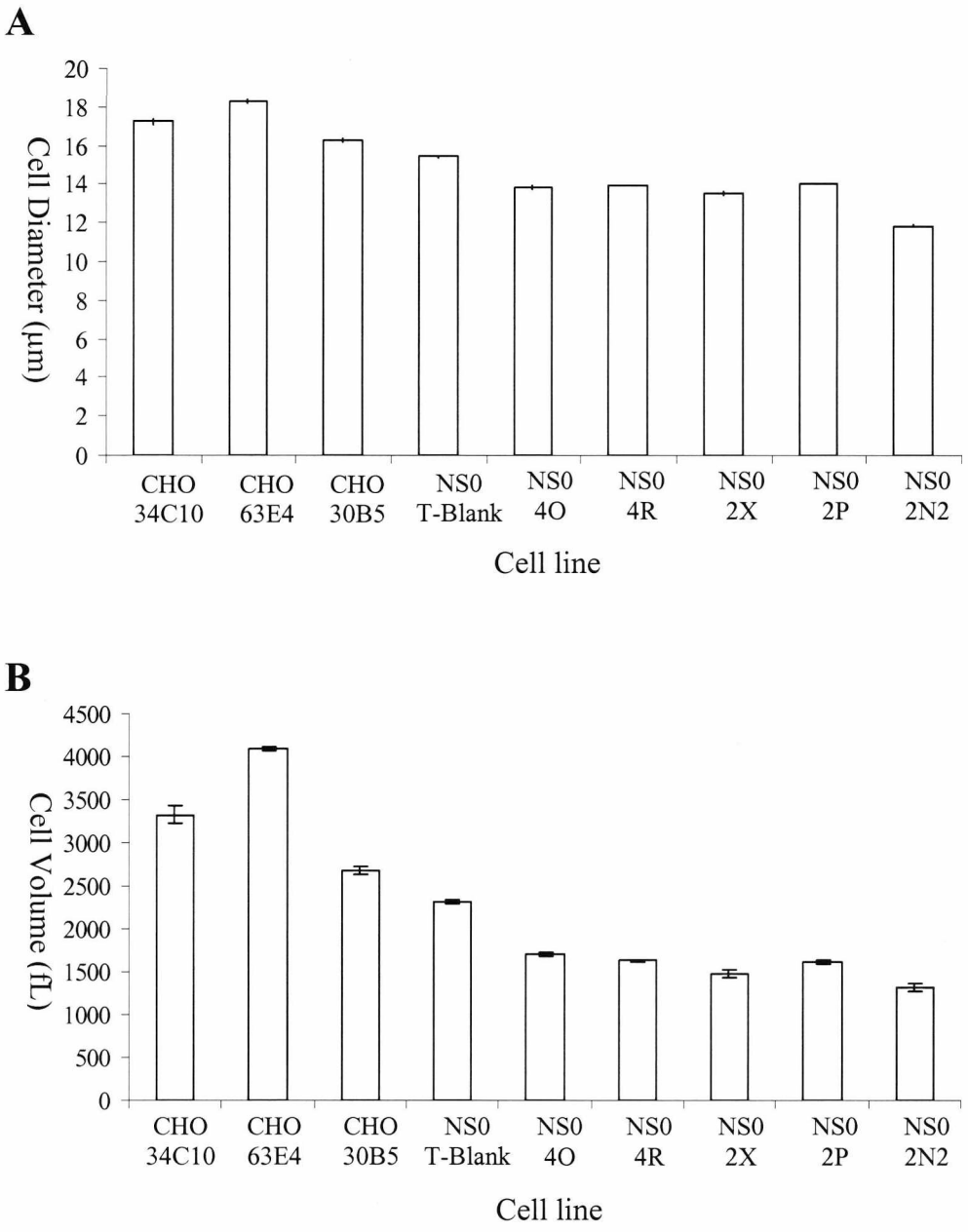

Figure 3.5 Cell size measurements of GS-NS0 and GS-CHO cell line. (A) Cell diameter measurements (B) Cell volume measurements. Values represent the mean values from three separate measurements of >2000 cells per cell line, and standard deviations are shown accordingly.

3.3.3 Formaldehyde gel electrophoresis of RNA extracts and measurement of messenger RNA levels

After total RNA extraction and gel electrophoresis, two major bands were observed which correlate to the 28S and 18S ribosomal subunits (figure 3.6). Several other lighter bands were also present which may correspond to degradation products. The banding patterns between the clones of each cell line were very similar. This suggests consistency in the quality of the RNA prepared. Slightly different banding patterns were observed between the GS-NS0 cell lines (figure 3.6B) and the GS-CHO cell lines (figure 3.6A). This may be due to differences in the cellular RNA between the cell species. These electrophoresis results indicate that the integrity of the RNA was sufficient (i.e. the RNA was not degraded) to perform northern blot analysis to determine the specific mRNA levels of the heavy and light chain in the cell lines under investigation.

Northern blot analysis of total cellular RNA hybridised with cB72.3 specific heavy and light chain probes labelled with ^{32}P (section 3.2.8) was carried out on the GS-CHO and GS-NS0 cell lines as detailed in sections 3.2.6 and 3.2.9. The resulting northern blots were analysed by densitometry using the Image Master™ 1D software (Amersham Biosciences). The autoradiograph of the northern blot is shown in figure 3.7A. Two distinct bands are observed in lanes 1 to 8. The higher band corresponds to the cB72.3 heavy chain mRNA and the lower band corresponds to the light chain mRNA. As the probes used were directed against the variable region of both the heavy and light chain, it is unlikely that these bands correspond to additional/other RNA's. Furthermore, no bands were detected in the transfectant blank (negative control) which would not be the case if these RNA's were present endogenously.

The densitometry data for the heavy and light chain mRNA levels were plotted against cell the specific productivities (qMab)(sections 2.3.1 and 2.3.2) and the resulting data is shown in figure 3.7B. It should be noted that the analytical procedure used for the measurement of mRNA levels aimed to establish differences in the cellular levels of mRNA relative to each other. As such the analysis carried out here cannot be considered

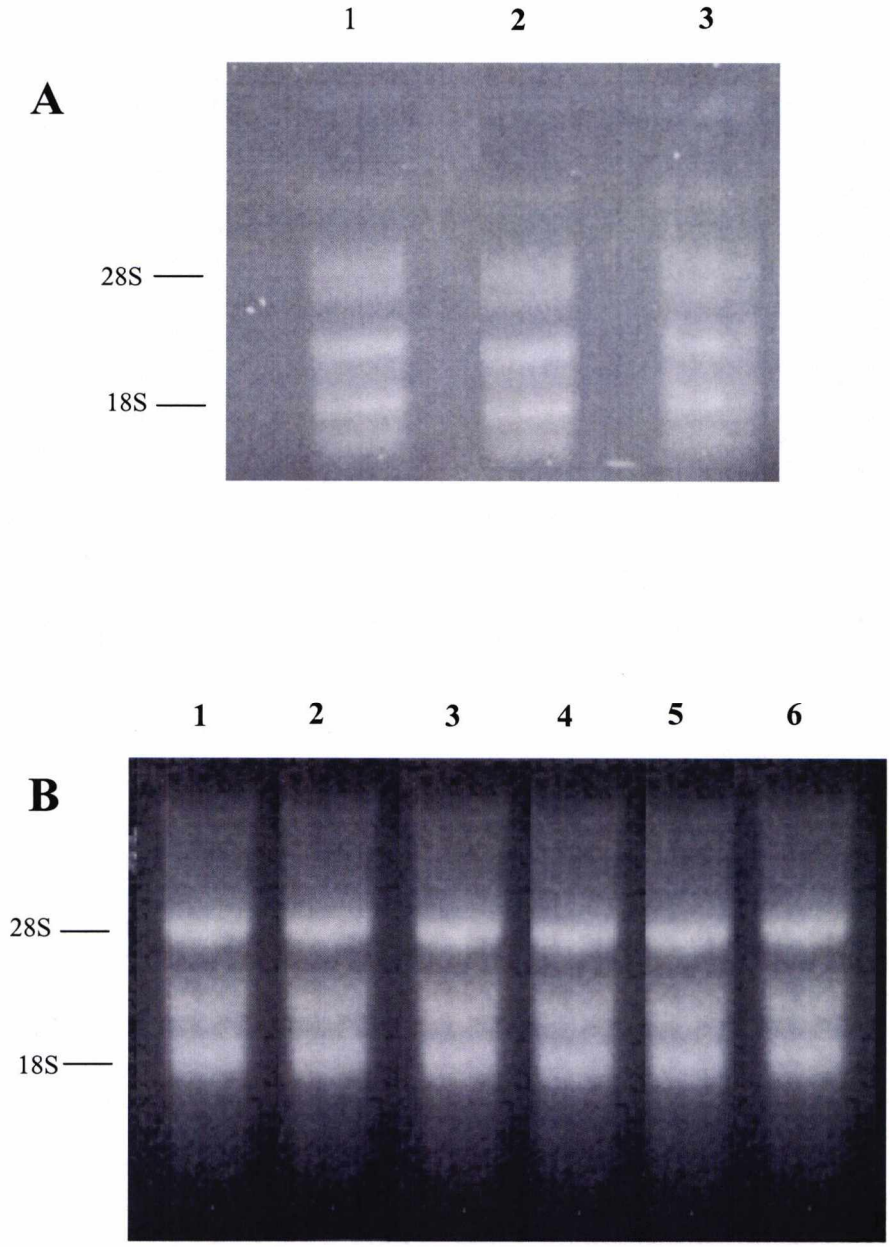

Figure 3.6 Formaldehyde gel electrophoresis of RNA. 10 μg of total RNA was loaded per lane. Positions of the 28S and 18S ribosomal bands are indicated. (**A**) RNA extracted from GS-CHO cells. CHO 30B5 (lane 1) CHO 63E4 (lane 2) CHO 34C10 (lane 3). (**B**) RNA extracted from GS-NS0 cells. NS0-T-Blank (lane 1) NS0-2N2 (lane 2) NS0-4O (lane 3) NS0-4R (lane 4) NS0-2P (lane 5) and NS0-2X (lane 6)

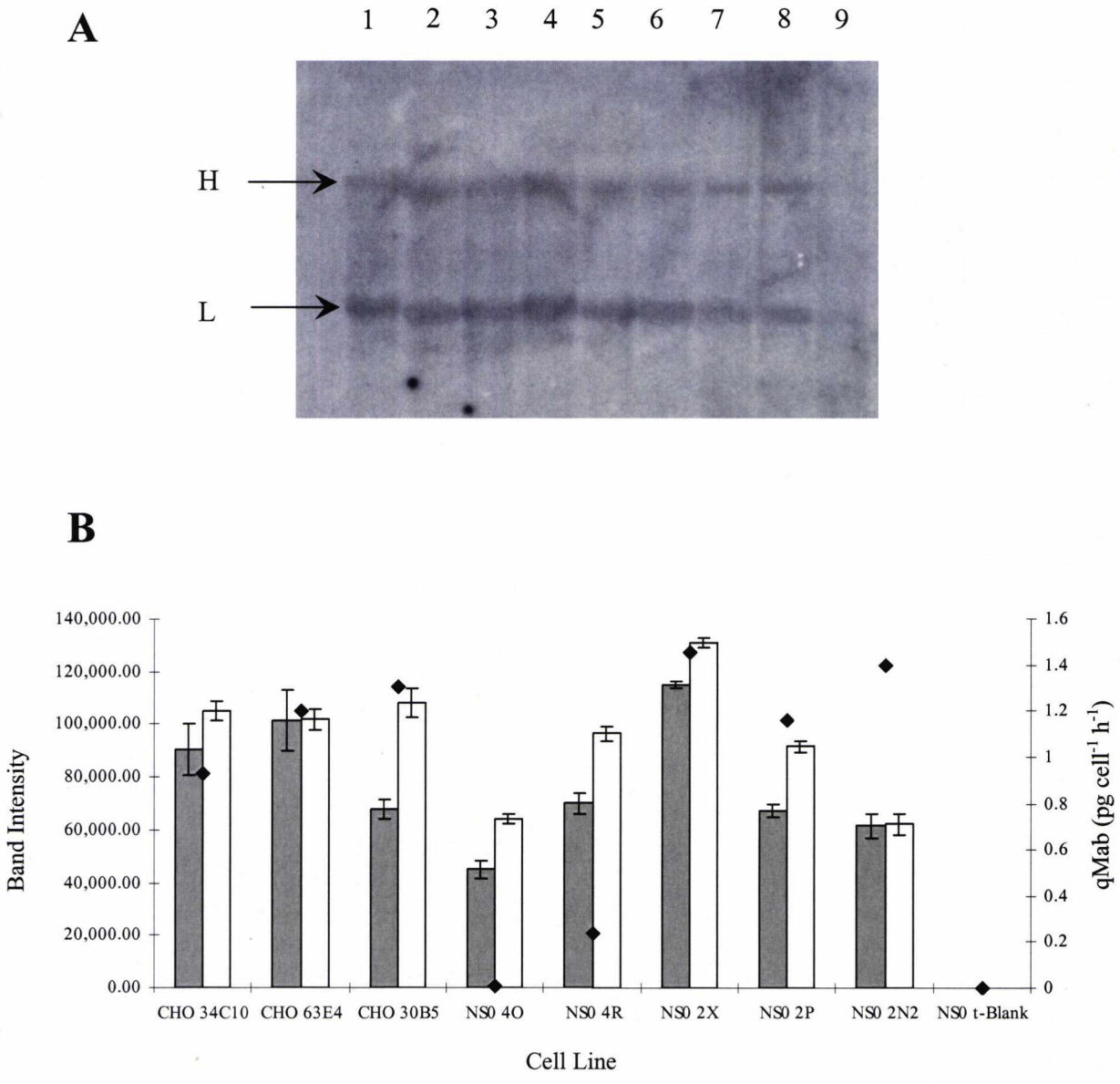

Figure 3.7 Northern blot analysis of heavy and light chain mab mRNA isolated from GS-CHO and GS-NS0 cell lines. (A) Autoradiograph of GS-CHO and GS-NS0 cell lines. Heavy and light chain specific mRNA's are indicated. Lane 1: CHO 30B5, Lane 2: CHO 63E4, Lane 3: CHO 34C10, Lane 4: NS0 2X, Lane 5: NS0 2P, Lane 6: NS0 4R, Lane 7: NS0 4O, Lane 8: NS0 2N2, Lane 9: NS0 Transfectant Blank. **(B)** Relative mRNA levels measured by densitometry plotted against cell specific productivity(♦). Values are based on three separate blots, and standard errors are shown accordingly. Open bars refer to the light chain and closed bars refer to the heavy chain.

fully quantitative as the detection and saturation limits of the assay were not established. Generally there appears to be a greater abundance of light chain mRNA than heavy chain mRNA in all the clones. This observation contradicts a study by Borth et al., who found a greater abundance of heavy chain mRNA (Borth et al., 1999). However, Merten et al., compared the mRNA levels of two hybridoma cell lines, the original (I1317-DC) and a subclone (I1317-SF11). I1317-DC showed significantly higher light chain mRNA levels than heavy chain mRNA levels (~2 fold). In contrast the sub-clone (I1317-SF11) showed an inverse relationship with double the levels of heavy chain mRNA to light chain mRNA (Merten et al., 1994).

However, the difference in the levels of IgG heavy and light chains shown by the GS-NS0 cell line correlates with a study by Kromenaker and Srienc, in which they investigated the kinetics of IgG heavy and light chain accumulation in mouse hybridoma cell lines. They found that there was an unbalanced synthesis of IgG heavy and light chain, with the relative mean rate of heavy chain accumulation approximately half the relative mean of light chain accumulation (Kromenaker and Srienc, 1994). Furthermore, this data supports a model proposed by Lee et al., for IgG folding *in vivo*. Their model states that firstly, Immunoglobulin binding protein (GRP78) interacts with the C_H1 domain of unfolded free heavy chains. In the second step of this model, a light chain either 'catches' the heavy chain when GRP78 has cycled off thereby preventing GRP78 from rebinding, or associates with the GRP78 heavy chain complex and 'triggers' GRP78 release. Finally, the C_H1 domain is able to fold and assemble stably with the light chain. In order for this to take place there needs to be an excess of IgG light chain, that aids folding by preventing the C_H1 domain from re-associating with GRP78 (Lee et al., 1999).

Overall the data presented here shows that there is no correlation between the cell specific productivities of the GS-NS0 cell lines (qMab) and IgG heavy and light chain mRNA. However, there is a linear increase observed in the mRNA levels (heavy and light chain) with an increase in qMab in cell lines 4O, 4R, and 2X. The mRNA level of the top two clones 2P and 2N2 is significantly lower, but this does not affect the productivity of these clones with 2N2 exhibiting the highest productivity. Fann et al., reported that in baby hamster kidney cells secreting activated protein C (APC) there was a linear relationship observed between APC secretion rate and mRNA level up to 2.2 $\mu g/10^6$ cells/day. After this point they concluded that a saturation in APC secretion had been reached (Fann et al.,

1999). It is worth noting however that this study was carried out on only two clones over batch culture. From the data presented here, it is clear that the GS-NS0 cell populations do not exhibit growth characteristics or recombinant heavy or light chain mRNA levels that correlate with mab productivity. Whilst intracellular recombinant mRNA levels may be expected to be proportionately related to productivity for monomeric proteins the same does not hold true for recombinant mab expression. In the case of mab's that require the coordinated expression, folding and assembly of both heavy and light chains, a number of studies using clonally derived cell lines or hybridomas all demonstrated that mab productivity does not correlate with the cellular availability of heavy or light chain mRNA (Flickinger et al., 1992; Kim et al., 1998; Leno et al., 1992a; Leno et al., 1992b). Thus, intracellular mab mRNA content may well be a poor indicator of mab productivity, however intracellular mab protein content is likely to be positively correlated with mab productivity as mab assembly and secretion is likely to be regulated post-translationally.

The data presented for the GS-CHO cell lines (figure 3.7B) shows no correlation between mRNA level and productivity in both heavy and light chain as for the GS-NS0 cell lines. Similar levels of light chain mRNA were observed between the clones indicating similar rates of light chain gene transcription and/or similar gene copy numbers. This is not the case with the heavy chain mRNA, with the highest levels exhibited by clone 63E4, followed by 34C10 and finally the highest producer 30B5. As stated earlier, an excess of light chain is required for efficient folding of monoclonal antibodies. It is possible that highly productive cell lines limit their production of heavy chains as production of heavy chains is energy expensive and in theory takes twice the amount of time to produce relative to light chain (Smales, 2003). Furthermore, excess expression of heavy chain, which interacts extensively with Bip, would be retained in the ER in constant association with Bip where it can induce ER chaperone synthesis. In this case unassembled heavy chain would be trafficked to the proteosome for degradation. This is supported by the data presented here for both GS-CHO and GS-NSO with the top producers of the respective cell lines exhibiting limited levels of heavy chain mRNA (figure 3.7B). It may also be the case that heavy chain mRNA levels above the levels exhibited by the top producers of each cell line will lead to a saturation effect and therefore any increase in heavy chain mRNA will not increase the intracellular levels of heavy chain. This is also supported by additional work completed within this laboratory on these cell lines that has shown that intracellular

levels of light chain correlate with productivity whilst intracellular levels of heavy chain are much lower.

3.3.4 Agarose gel electrophoresis of genomic DNA and determination of gene copy number

Genomic DNA extractions were performed on GS-NS0 and GS-CHO cell lines harvested at mid-exponential phase as described in section 3.2.1. The quality of the extracted DNA was determined by agarose gel electrophoresis as described in section 3.2.4 and the results are shown in figure 3.8. The integrity of the genomic DNA was clearly maintained post-extraction, with band sizes of all clone samples above 1Kb in length. DNA of this length is deemed suitable to undertake southern analysis.

A restriction digest, and southern blot of the extracted genomic DNA was carried out on all clone samples as described in section 3.2.7. DNA oligonucleotide probes specific to the variable heavy and variable light genes, were labelled using ^{32}P as described in section 3.2.8 and hybridised to the blots as described in section 3.2.10.

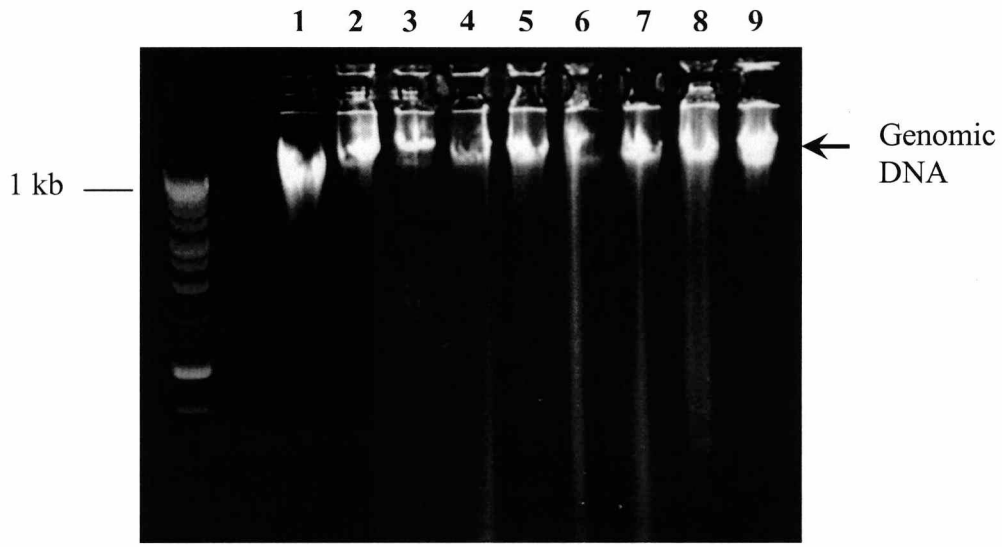

Figure 3.8 Agarose gel electrophoresis of DNA. 1 μg of genomic DNA was loaded per lane. DNA extracted from GS-CHO and GS-NS0 cells. Lane 1:CHO 30B5, Lane 2: CHO 63E4, Lane 3: CHO 34C10, Lane 4: NS0-T-Blank, Lane 5: NS0-2N2, Lane 6: NS0-4O, Lane 7: NS0-4R, Lane 8: NS0-2P, Lane 9: NS0-2X.

Results of the blots (not shown) were inconclusive with no distinct bands observed in either the GS-NS0 or GS-CHO samples. There are several reasons that may account for this. Firstly, as previously stated (Chapter 2) NS0 cells possess very low copy numbers (<10) therefore it may be the case that any signal was too weak to be detected above the background or there was not sufficient DNA present on the membrane, although the former is unlikely to be the case for the CHO cell lines. Secondly, there may have been inefficient digestion of the genomic DNA to allow adequate access of the probes to the gene sequence. Finally, the probes may have a poor affinity for the target. It is known that the affinity of RNA for DNA is greater than the affinity of DNA for DNA (Maniatis et al., 1982). Studies by Guarna et al., using 12 BHK clones expressing rAPC found that at lower cDNA copy numbers (i.e <240 copies), a non-linear cooperative relationship between increasing cDNA copy numbers and increasing APC production rates was observed, but at copy numbers greater than 240, both secretion rates per cDNA and per cell were decreased. They concluded that additional copies above the range tested would not result in higher recombinant protein production rates (Guarna et al., 1995).

3.4 Conclusions

The data presented in this chapter has demonstrated that there is no correlation between cellular quantities of genomic DNA or total RNA and cellular productivity for GS-CHO and GS-NS0 cells producing recombinant mab. However, a relationship between DNA content and specific growth rate was observed in the producing GS-NS0 cell lines although the reason for this is unclear. We have also reported that there was no correlation between cell size and cellular productivity between these cell lines. Our data suggests that any fluctuation in cell size is a consequence of other factors such as growth characteristics, rather than productivity. We have demonstrated based on a semi quantitative analysis that heavy and light chain mRNA levels do not correlate with mab productivity in GS-NS0 or GS-CHO cell lines. Furthermore due to the need for a coordinated expression and folding of both heavy and light chains it is more likely that intracellular mab protein content is positively correlated with mab productivity. We can therefore conclude that higher production rates are not a consequence of increased mRNA and it is likely that other intracellular factors downstream of transcription are rate limiting. We were unable to determine the gene copy numbers of the cell lines used in this investigation. It therefore remains unclear whether the differences in mRNA levels exhibited between the clones of both species (NS0 & CHO) are as a result of higher gene copies or a more efficient transcription rate due to amongst other variables, a more favourable gene locus. Taken together the data reported here clearly shows that the regulation of productivity is post-transcriptional/post-translational and as such a proteomic approach is needed to focus on protein production in the cell lines under investigation down stream of transcription/translation.

Chapter 4 Development of analytical methodology

4.1 Introduction

The secretory pathway consists of a complex system of endomembranes which include the endoplasmic reticulum (ER), ER to golgi intermediate compartment (ERGIC), the golgi apparatus, lysosomes, the endosome and various secretory and transport vesicles (Orci, 1992; Wieland, 1996). After initial disruption of the cell, small vesicles result from the fragmentation of the intracellular membranes (figure 4.1). These vesicles are collectively referred to as microsomes (Hinton, 1997).

In this chapter, the development of a differential centrifugation method for the isolation of whole microsome fractions from NS0 cells is described, together with the optimisation of protein recovery and solubilizing conditions complementary to current 2D electrophoresis technology. This is necessary as although 2D electrophoresis is a powerful, mature and sensitive technique, its ability to characterise elements of the proteome is specific to the characteristics of the sample (quantity of membrane and hydrophobic proteins), therefore the technique must be optimised to account for these differences.

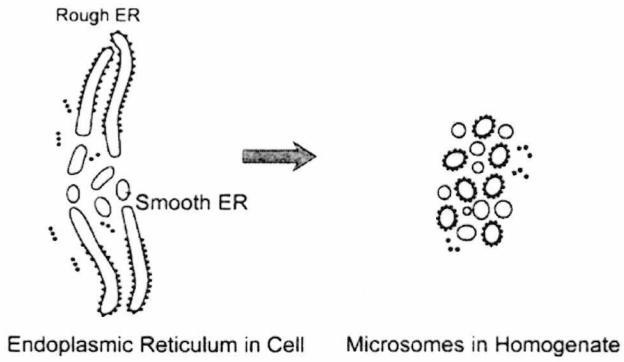

Figure 4.1. Example of the fragmentation of membrane systems during homogenisation. The sheets and tubules present *in vivo* fragment into small vesicles with almost perfect preservation of contents.

4.1.1 Cell Disruption

The final method used for the disruption of cells depends on the nature of the cells (i.e, solid tissues or cultured cells). Any disruption method must stress the cells sufficiently to cause disruption of the surface membrane and so release the cytosol and any internal organelles. Ideally, one would achieve reproducibility and maximum cell breakage, with the minimum amount of disruptive force, while causing no damage to any of the organelles of interest.

There are various methods of cell disruption, some rely on shear forces while others use the properties of the cells themselves. These include; chemical methods (Cull, 1990; Jazwinski, 1990) sonication (Cull, 1990), osmotic lysis (Dignam, 1990), and freeze-thaw lysis (Lenstra, 1983). By far the most widely applied methods of cell disruption are those that use mechanical or liquid shear forces. For soft tissues and mammalian cells the shear force is usually applied using a Dounce (or all-glass) homogeniser, which consists of a glass containing vessel and a pestle with a smooth glass ball. It should be noted however, that different types of cultured cells respond individually to liquid shear technique in their susceptibility to the shearing conditions. A useful method of disruption method involves the use of an abrasive (e.g glass beads). Cells in this case are suspended in an appropriate buffer and vortexed in the presence of glass beads. The abrasive action of the vortexed beads result in the breakage of cell

walls, liberating the cellular contents (Cull, 1990; Jazwinski, 1990). For the purposes of this investigation, only disruption methods involving liquid shear, osmotic or freeze-thaw lysis, and glass beads are relevant.

The choice of buffer components in which cell disruption takes place is also important but, perhaps surprisingly, often little consideration is given to this point. The standard isotonic medium generally used for the isolation of all organelles from mammalian cells usually includes sucrose (0.25 – 0.5 M) and EDTA (1 – 2 mM). EDTA is a chelating agent that is useful in protecting enzymes from inactivation by heavy metals and proteolysis by metalloproteases. However, when EDTA is included in the medium, the nuclei are particularly fragile and prone to leak DNA, therefore it is prudent to include $MgCl_2$ as this is beneficial to nuclear integrity (Dignam, 1990). An organic buffer such Tris, Hepes, Tricine or Triethanolamine (TEA) is commonly added at pH 7.0 – 7.6. TEA is more favourable than Tris, due to metal contamination associated with Tris. TEA also appears to promote a high percent cell lysis, especially for cultured cells, however the reasons for this are unclear (Graham, 1997). Thiol compounds are also frequently added to protect protein thiols from oxidation. Dithiothreitol (DTT) is usually the reagent of choice. An alternative reducing agent, mercaptoethanol is very aggressive and tends to denature proteins (Dignam, 1990).

Finally, to protect organelles from the potentially damaging effects of proteases that may be released, for example from lysosomes during disruption, it is common to include a cocktail of protease inhibitors into the buffer. Phenylmethyl sulfonyl fluoride (PMSF), leupeptin, antipain, and aprotinin are commonly used with mammalian cells (Dignam, 1990; Graham, 1997).

4.1.2 Cell Fractionation by Differential Centrifugation.

The aim of subcellular fractionation is to separate cell organelles with as little damage as possible to the resulting preparations. However, it is never be possible to separate organelles completely undamaged, as most organelles are attached to cytoskeletal elements. Separation of cell organelles by centrifugation depends on differences in size and density. Two distinct and complementary methods are used for the separation of particles on the basis of their size, simple differential pelleting and

rate-zonal sedimentation. In this study only differential pelleting is relevant. Differential centrifugation involves centrifuging a suspension of particles for sufficient time to sediment the largest group of particles. The supernatant is then poured off and re-centrifuged to collect the next fraction and so on. The components of a homogenate may be divided broadly into three class sizes; relatively large intact organelles (e.g the nucleus), the microsomes, and the soluble proportion of the cell, the cytosol.

As these components differ significantly in size, their rate of sedimentation is also different and they can thus be separated by centrifugation. Subcellular fractionation procedures to isolate microsomes usually produce four fractions (figure 4.2). The first of these fractions (low speed pellet 3000 rpm) contains the unbroken and partially broken cells together with nuclei, large sheets of plasma membrane and a proportion of other larger cell organelles and is commonly referred to as the nuclear fraction. This low speed pellet is usually 'washed' by resuspension in the homogenisation medium and recentrifuged under the same conditions (to minimise the loss of the smaller organelles) and the supernatant is then combined with the original. The combined supernatants are then recentrifuged at high speed (9000 rpm) to give the large particulate fraction that contains the majority of intact cell organelles. This fraction is often termed the mitochondrial fraction. This fraction will inevitably be contaminated by the larger microsomal fragments, for these overlap in size with the smaller cell organelles, but this contamination can be minimized by washing. Finally microsomes are sedimented by ultracentrifugation at around 100,000 – 150,000 × g (50,000 rpm), with the resultant supernatant containing the soluble or cytosolic fraction (Hinton, 1997; Storrie, 1990).

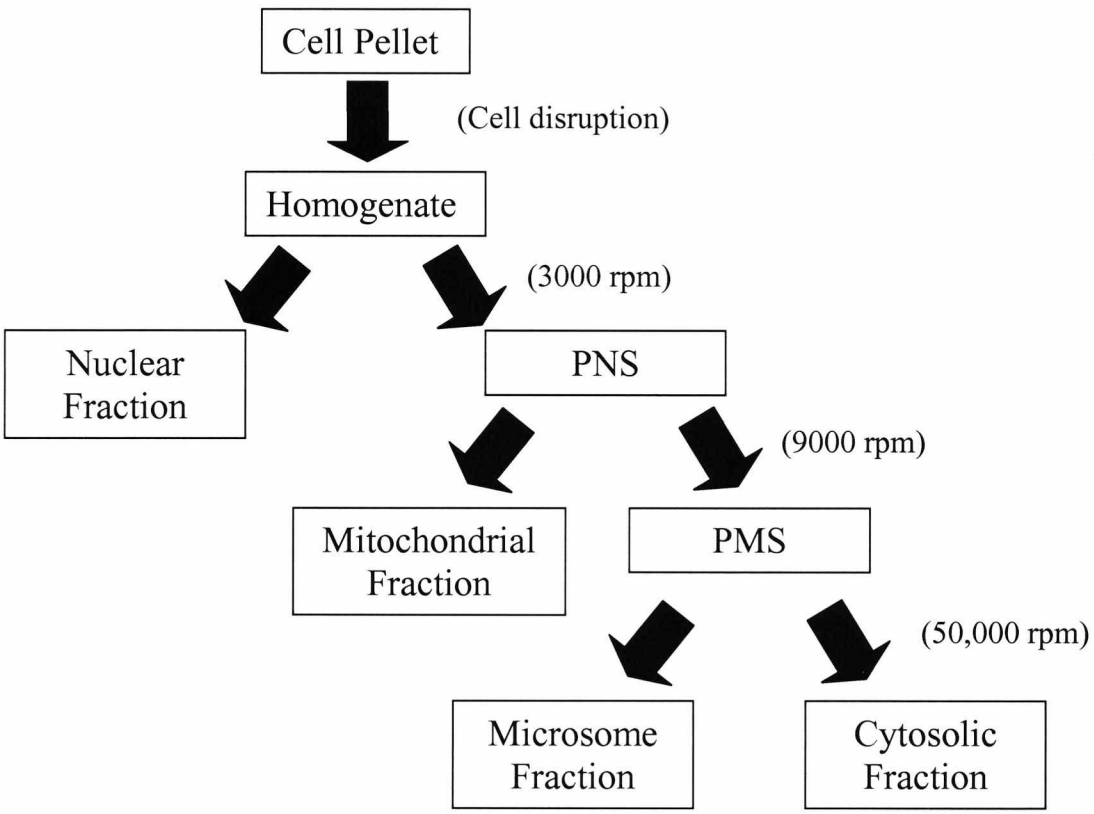

Figure 4.2. Schematic diagram showing fractions generated by a differential centrifugation cell fractionation procedure of cultured mammalian cells.
PNS – Post Nuclear Supernatant, **PMS** – Post Mitochondrial Supernatant.

4.1.3 Detergents and Solubilisation

The analysis of any protein sample requires effective solubilization. This is especially true for protein samples that are to be subjected to 2D-PAGE separation. The ideal solubilizing procedure for 2D-PAGE would result in the disruption of all covalently bound protein complexes and aggregates into a solution of individual polypeptides. Failure to achieve this may result in persistent protein complexes in the sample that are likely to result in new spots in the 2D profile, with a concomitant reduction in the intensity of those spots representing single polypeptides (Dunn and Görg, 2001). The majority of solubilization buffers used for 2D-PAGE, are based on that originally described by O'Farrell (O'Farrell, 1975). This contained 8 – 9.5 M urea (a neutral chaotrope, used as a denaturant), a non-ionic detergent (e.g Nonident P-40) and a reducing agent such as DTT. While this method works well for many samples, it is not universally applicable, particularly in the solubilization and separation of insoluble samples such as membrane-associated proteins or those from tissues that are highly resistant to denaturation (Dunn, 2001; Herbert, 1997). Good solubility of the sample is fundamental in achieving a successful reproducible 2D-PAGE separation. Essential to this, is the choice and concentration of detergent in the solubilizing buffer.

Detergents are used to mimic a lipid-like environment on the inside of micelles, but the quality and quantity of this mimickry is highly variable from one detergent to another, such that solubilization performance varies widely (Santoni et al., 2000). When choosing a detergent its compatibility with the specific preparative and analytical method of choice must be considered. In the case of this investigation the principal analytical procedure is 2D-PAGE, therefore the detergent selected must not contribute to the net charge of the molecule to which it is bound as this would alter the native pI of specific proteins. Both non-ionic and zwitterionic detergents in which the pK values of the two functional groups are widely separated, behave essentially as uncharged molecules and therefore are suitable for 2D-PAGE, specifically for iso-electric focusing (IEF) (Hjelmeland, 1990). Traditionally either of two similar non-ionic detergents, Nonident P-40 (NP-40) or Triton X-100, have been used (Berkelman, 1998; Hjelmeland, 1990; O'Farrell, 1975). Subsequent studies have demonstrated that the zwitterionic detergent CHAPS, and the non-ionic detergent Triton X-114 are far more

effective at solubilizing membrane proteins at concentrations up to 4% (Dunn, 2001; Wu et al., 2000).

When difficulties are encountered in achieving full solubilization using these detergents, sodium dodecyl sulfate (SDS) can be used as an alternative agent. SDS disrupts most non-covalent protein interactions and is very effective at solubilizing membrane proteins (Ames and Nikaido, 1976). However, SDS is highly negatively charged and forms complexes with proteins and can only be used as a pre-solubilization procedure for samples prior to IEF. Using this approach the sample is initially solubilized in SDS and then diluted into a normal solubilizing solution containing an excess of non-ionic or zwitterionic detergent. The aim is to displace the SDS from the proteins and replace it with a non-ionic or zwitterionic detergent, thereby maintaining the proteins in a soluble state (Berkelman, 1998; Dunn, 2001). This method requires careful control of the ratio of protein to non-ionic detergent and the ratio of SDS to non-ionic detergent for effective solublization. Failure to achieve this results in deleterious effects during IEF and poor resolution upon separation in the second dimension (Ames and Nikaido, 1976; Dunn, 2001). Figure 4.3 shows the chemical structures of some commonly used non-ionic and zwitterionic detergents

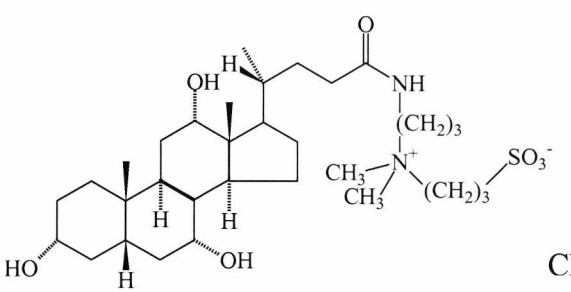

CHAPS

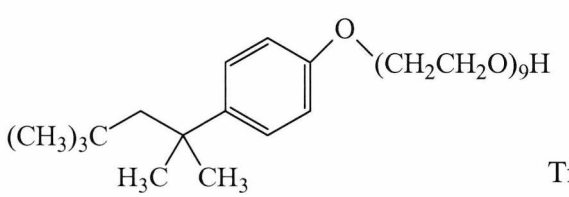

Triton X-100

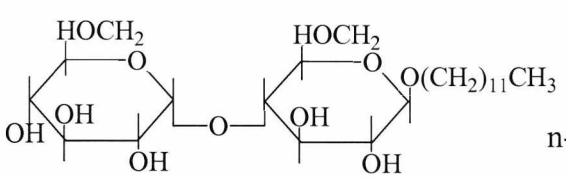

n-Dodecyl β-D-Maltoside

Figure 4.3. Chemical structures of detergents commonly used in protein purification and separation. Triton X-100 and n-Dodecyl β-D-Maltoside are non-ionic detergents. CHAPS is a zwitterionic detergent.

4.1.4 Experimental

A reproducible, robust method for the preparation of microsome fractions from NS0 cells, which is complementary to current 2D technology and adequately represented the protein complement of the secretory pathway was developed and optimised. This methodology was developed in three stages.

1. Qualitative analysis and immunological verification of the cell fractionation protocol of choice using markers of the secretory pathway, Mitochondria, and Cytosol.

2. Mini 2D gel (7 × 7 cm) analysis to assess differences in resolution and protein spot number under selected conditions to improve visualisation of membrane bound proteins.

3. The quantitative analysis of protein recovery at each stage of the cell fractionation procedure, using selected detergents and cell numbers in order to optimise solubilisation and recovery conditions.

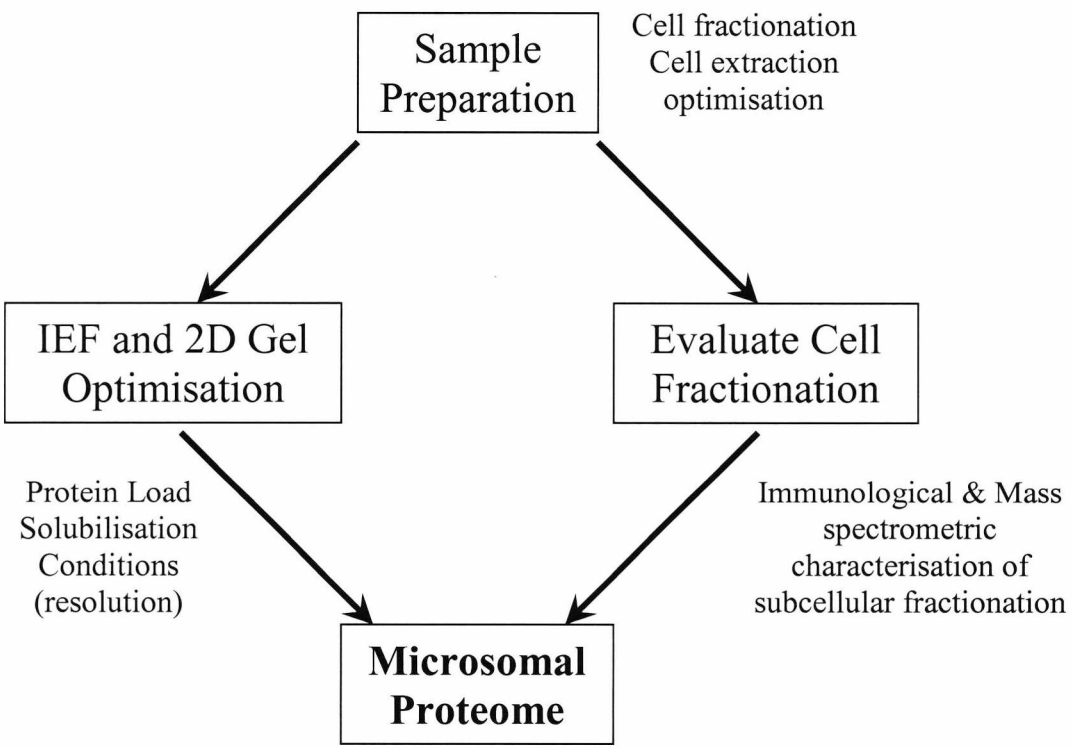

Figure 4.4. Experimental overview for microsomal proteome analysis method development and optimisation

4.2 Materials and Methods

Unless otherwise stated all chemicals and regents used in this investigation were of analytical grade and were obtained from BDH (Poole, UK), Sigma (Poole, UK), Fisher Scientific (Loughborough, UK), Fisons (Loughborough, UK), or BioRad (Hertfordshire, UK). All tissue culture grade chemicals and reagents, unless otherwise stated were obtained from Gibco Life Sciences (Paisley, UK) or Sigma (Poole, UK). Tissue culture grade plastic-ware was obtained from Falcon (New Jersey, USA) or Sarstedt (France).

4.2.1 Cell Culture

All operations were performed under sterile airflow, in Gelaine Flow hoods (Gelaine Flow Laboratories, Milan, Italy). All reagents and plastic-ware were sterile and pre-warmed to 37^0C prior to use. GS-NS0 cells producing IgG were grown in Iscoves Modified Dulbecco's Medium (IMDM) prepared without glutamine. To the basic medium was added glutamic acid and asparagine to final concentrations of 350 μM and 400 μM respectively; 30 μM each of adenosine, guanosine, cytidine, uridine, and 10 μM thymadine. Additionally, Insulin Transferin Selenium-X (ITXS) (1%, v/v); lipid concentrate (0.1%, v/v); β-Cyclodextrin to a final concentration of 45 μM and Bovine Serum Albumin (BSA) (5%, w/v) were added. All cultures were performed in 250 or 500 mL shaker flasks and stirred at 103 rpm. Batch culture were grown at 37^0C and in a 5% CO_2 humidified atmosphere.

4.2.2 Cell Fractionation

All operations were carried out at on ice. Microsome fractions were prepared from GS-NS0 IgG cells harvested at exponential phase, washed in PBS, then resuspended in 3 mL of a 0.5 M sucrose, 100 mM triethanolamine (TEA) pH 7.5, 100 mM KOAc, 12 mM $MgCl_2$, 4 mM dithiothreitol (DTT), protease inhibitor cocktail solution (Amersham Biosciences).

The cells were then subjected to two rounds of freeze-thaw lysis using liquid N_2. Glass beads (1 g) were then added to the homogenate which was then votexed for 5 mins. The homogenate was cooled on ice for 5 mins and then vortexed as before. The homogenate was made up to 10 mL with buffer and centrifuged at 3000 rpm (1000 g) for 10 mins using a Beckman JA-20 108.0 rotor. The supernatant was recovered and the pellet re-suspended in an equal volume of buffer and re-centrifuged as before. Both supernatants were then combined and centrifuged at 9000 rpm (10,000 g) for a further 10 mins. The supernatant was recovered and subjected to ultra-centrifugation at 50,000 rpm (100,000 g) for 150 mins using a Sorvall T-865 rotor. The resultant pellet was washed in PBS and solubilized in the appropriate buffer.

4.2.3 Protein Quantification

Protein quantification was carried out using a modified Bradford assay, as described by Ramagli (Ramagli, 1999). Briefly, a standard curve was prepared as described below using BSA (5 mg mL^{-1}) in dd H_20 as the standard protein:

Table 4.1. Modified Bradford assay standard curve preparation

μg Protein	50	100	200	400	500
μL BSA Stock Solution	1	2	4	8	10
μL Lysis Buffer	9	8	6	2	0
μL 0.1 M HCL	10	10	10	10	10
μL dd H_20	80	80	80	80	80

Samples were diluted in lysis buffer and made up to a volume of 10 μL, to which 10 μL of 0.1 M HCL and 80 μL of dd H_20 were added. BIO-RAD protein assay solution (3.5 mL), diluted 1 in 4, was then added to each standard and sample. Absorbances were read at 595 nm, and unknown protein concentrations determined using linear regression analysis.

4.2.4 SDS-Polyacrylamide Gel Electrophoresis (SDS-PAGE)

Soluble cellular proteins were analysed using sodium dodecyl sulphate polyacrylamide gel electrophoresis (SDS-PAGE). A 12.5% acrylamide solution,

sufficient for 2-4 1.0 mm mini gels was prepared using 4.2 mL of 30% Bis-acrylamide, 3.7 mL of dd H_2O, 2 mL of 1.875 M tris-HCL pH 8.85, 10% SDS (100 µL), APS (50 µL, 15% w/v). To this was added 10 µL of TEMED and the mixture then poured quickly into 1.0 mm mini gel cassettes (Invitrogen, Paisley, UK). Sufficient space was left to overlay the stacking gel. Each gel was then overlaid with water-saturated butanol and allowed to polymerise for 20 min. A 5% stacking gel was then prepared using 0.88 mL of 30% Bis-acrylamide, 3.6 mL of dd H_2O, 0.3 mL of 1.0 M tris-HCL pH 6.8, 50 µL of 10% SDS, 40 µL of 15% (w/v) APS and 7 µL of TEMED. The butanol was poured off the separation gel, stacking gel solution placed over each set separation gel, and well combs immediately placed in position. The gel was left to polymerise for 45 min. When running the gels the inner chamber of a Xcell^{TM} Mini-cell was filled with TGS-running buffer (25 mM Tris-HCL, 192 mM glycine, 0.1% SDS) and buffer then poured into the outer chamber until approximately half of the gel was immersed. Samples were prepared by dilution (as appropriate) into 1X Laemmli buffer (5X stock; 11.6 g glycerol, 6 mL 1.0 M tris-HCL pH 6.8, 1 g SDS, 2 mL β-mercaptoethanol, a few grains of bromophenol blue and pyronin G, made upto 20 mL with dd H_2O). Samples were heated to 100^{0}C for 2 min prior to loading into the gel wells. Gels were run at 125 V, 35 mA for approximately 90 min or until the loading dye front had reached the base of the resolving gel. Gel Images were captutered at 200 dpi using a powerlook III prepress colour scanner (Amersham Biosciences). 1D image analysis was carried out using Image Master® 1D software (Amersham Biosciences).

4.2.5 Mini 2-D Polyacrylamide Gel Electrophoresis (2-D PAGE)

Fractionated proteins were solubilized in 9.5 M Urea, 0.8% Pharmalytes pH 3-10 (Amersham Biosciences), 1% DTT, and either 4% Triton-X100, 2% n-Dodecyl b-D-Maltoside (DDM), or 2 or 4% CHAPS. Protein samples (10 µg) were then subjected to isoelectric focusing on 7 cm non-linear pH 3-10 Immobiline dry strips (Amersham Biosciences). The strips were rehydrated by in-gel reswelling and then subjected to electrophoresis for 17.5 h at 20^{0}C using an IPGphor Isoelectric focusing system (Amersham Biosciences). The second dimension was run on a 12.5% tris-glycine polyacrylamide SDS gel using a Novex Xcell II™. Silver staining visualisation was performed as described by Shevchenko *et al.* (Shevchenko et al., 1996). Briefly, this involved fixing the gel overnight in 50% methanol, 5% acetic acid in dd H_20. The gel

was then washed for 10 min with 50% methanol in dd H_20 followed by an additional 30 min in water to remove any remaining acetic acid. The gel was sensitised by incubation for 1 min in 0.03% sodium thiosulphate and then rinsed with two changes of distilled water for 1 min each. After rinsing the gel was submerged in 0.1% silver nitrate solution and incubated at RT for 20 mins. Following incubation the silver nitrate was discarded, and the gel was rinsed twice with dd H_20 for 1 min before developement with 0.04% formaldehyde (stock formaldehyde solution 38% w/w), 2% sodium carbonate with intensive shaking. Once the developer turned yellow it was discarded and replaced with fresh developer. When the desired intensity of staining was achieved the development was terminated with 5% acetic acid. Silver-stained gels were stored in 1% acetic acid at 4^0C until analysed. Resulting gel images were captured at 200 dpi using a powerlook III prepress colour scanner (Amersham Biosciences).

4.2.6 Western Transfer and Immunoblots

Following separation of proteins by SDS-PAGE, proteins were transferred to Hybond-P polyvinylidene difluoride (PVDF) membranes (Amersham Biosciences) using the Novex™ X-Cell II™ Wet Blot Module. The gel and membrane were sandwiched in the module as outlined in figure 4.5. The blot module was filled with transfer buffer (25 mM Tris, 192 mM glycine, pH 8.3, 20% (v/v) methanol) until the gel/membrane sandwich was just covered. The outer buffer chamber was filled with de-ionised water to approximately 2 cm from the top of the chamber. The gels were blotted at 25 V for 90 min.

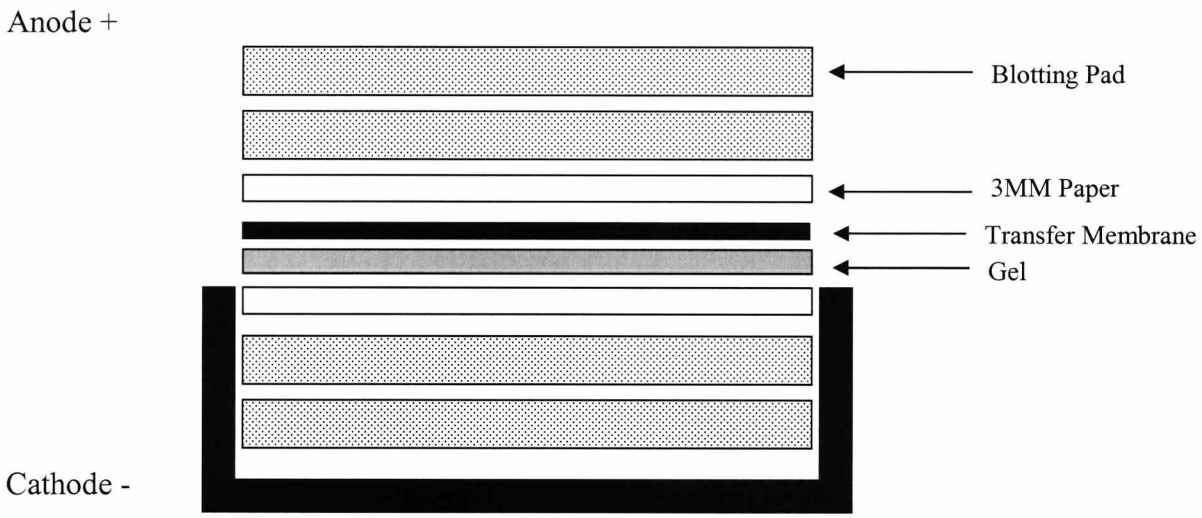

Figure 4.5. Electroblot apparatus for transfer of proteins from SDS-PAGE gels to PVDF membranes

Unoccupied binding sites on the PVDF membrane were blocked by incubation in 10% dried milk powder in TBS, 0.05% Tween-20 for 1 h at room temperature. Primary antibody was diluted as required in 5% milk in TBS, 0.05% Tween-20 and incubated with the membrane overnight at 4^0C. The membrane was then washed three times for 5 min using T-TBS (TBS, 0.05% Tween-20). Peroxidase conjugated secondary antibody (Sigma) was diluted 1:1000 in 5% milk in TBS, 0.05% Tween-20 and incubated with the membrane for 1 h at room temperature. The membrane was then washed three times as above and once with TBS. Protein on the blots was then detected using an enhanced

chemiluminescence kit (ECL) (Amersham Biosciences) as per the manufacturer's instructions.

4.2.7 Generation of polyclonal antibodies against KDEL and KEEL peptide sequence.

Synthesis of Peptide antigens

Peptide sequences KDEL and KEEL were prepared in house. Each peptide was synthesised with an N-terminal cystein residue linked to the peptide via aminocaprioic acid as shown below:

KDEL Cys-AA1-Lys-Asp-Glu-Leu-OH

KEEL Cys-AA1-Lys-Glu-Glu-Leu-OH

Activation of Keyhole Limpet Heamocynin (KLH)

KLH (30 mg) (Calbiochem, Nottingham, UK), was dialysed overnight against 1 L of 50 mM phosphate pH 7.2 at 4^0C. Maleimidobe acid N-hydroxy-succinamid ester (MBS) (8 mg) was dissolved in 100 µL dry Dimethyl formide (DMF) and added dropwise to stirred KLH solution at RT. The reaction was stirred in a stoppered vial for 30 mins after which 100 µL glycyl glycine solution (50 mg/mL in phosphate buffer adjusted to pH 7 using 1 M NaOH) was added. The solution was microfuged at 13000 rpm for 10 mins and the supernatant recovered. The recovered supernatant was desalted over a Pharmacia FPLC fast desalting column equilibrated and eluted using 50 mM phosphate buffer pH 7.5. Protein concentration was determined as described in section 4.2.3 and then stored as 3-4 mg aliquots at -80^0C.

Coupling of peptides to activated KLH

KDEL and KEEL peptides were dissolved in 100 µL of 50 mM phosphate buffer pH 7.4. The peptide solution was then mixed with activated KLH and stirred for 3 h in the dark. The solution was then dialysed overnight against PBS at 4^0C. The protein concentration was then determined as previously described and stored as 400 µg aliquots.

Production of poyclonal anti-sera - Rabbit imunisations

Two New Zealand White rabbits were immunised with 400 μg coupled KDEL or KEEL peptide antigen administered subcutaneously with 100 μg Titre Max Gold adjuvant. Injections were performed as detailed in table 4.2.

Table 4.2 Rabbit Immunisation schedule

Week	Imunisation/Booster	Antigen Dose
0	Primary Imunisation	400 μg
4	Booster Injection	400 μg
8	Test Bleed	NA
10	Booster Injection	400 μg
14	Test Bleed	NA
18	Terminal Bleed	NA

All Test bleeds and the terminal bleed were carried out under sedation with Hypnorm.

Serum preparation

After each test and final bleed, the blood was allowed to clot for 60 mins at RT. The clot was separated from the collection vessel and placed at 4^0C overnight to contract. Serum was removed and centrifuged at 10 000 g for 10 mins at 4^0C to remove any insoluble matter then stored at 4^0C.

4.3 Results and Discussion

4.3.1 Verification of Cell Fractionation Protocol

Qualitative analysis was performed on the fractions collected from the cell fractionation procedure using SDS-PAGE and Immunoblots to validate the procedure. Following the fractionation of 1×10^8 NS0 IgG cells (section 4.2.2), and determination of the protein concentration in these fractions (section 4.2.3), SDS-PAGE was performed on all fractions and stained with silver as described in sections 3.2.4 and 4.2.5 (Figure 4.6). The pelleted fractions were then subjected to SDS-PAGE, Western Transfer and Immunoblot (sections 4.2.4 and 4.2.6). All pellet fractions were probed using antibodies against GRP78, PDI (Stressgen, York. UK), HSP60 (Santa Cruz Biotech, Calf. USA), and Tubulin (A kind gift from Dr. A Roobol, University of Kent, Kent, UK) (Figure 4.7).

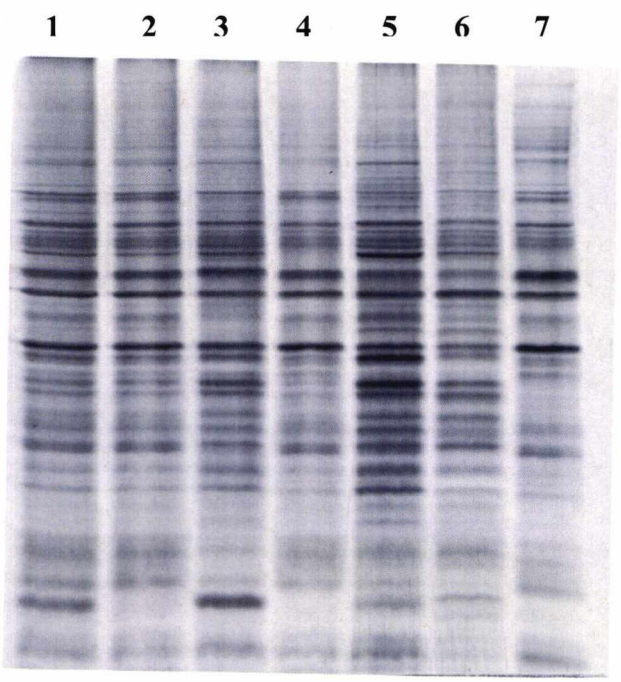

Figure 4.6. SDS-PAGE analysis of the subcellular fractionation procedure. **1** Whole Cell (WC), **2** Post Nuclear Supernatant (PNS), **3** Nuclear Fraction (NF), **4** Post Mitochondrial Supernatant (PMS), **5** Mitochondrial Fraction (MF), **6** Microsomal Fraction (McF), **7** Soluble Fraction (SF). 5 μg of each sample, solubilised in 20 μL 1 X Laemmli buffer was loaded onto a 12.5% gel and silver stained (section 4.2.5).

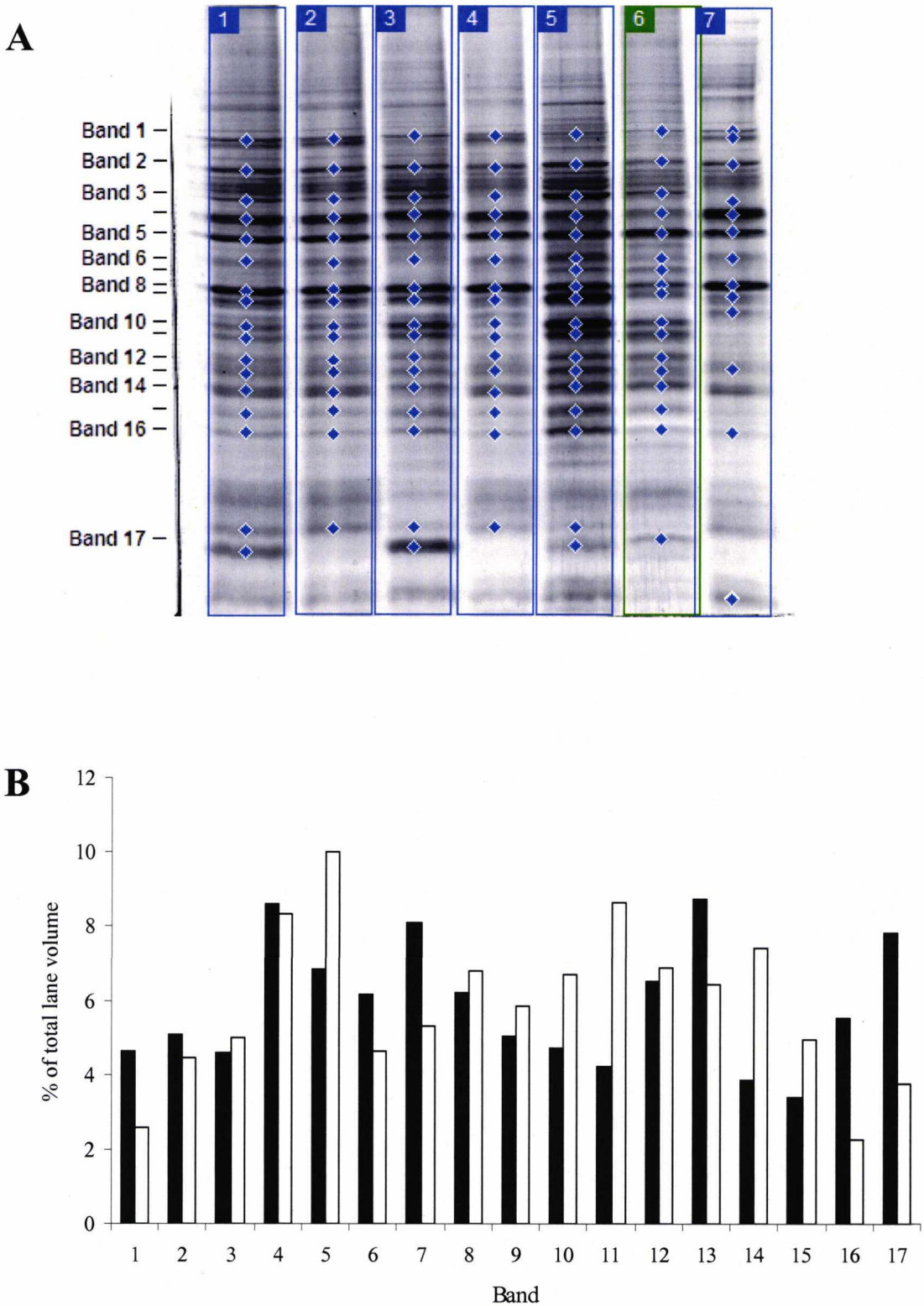

Figure 4.7 (A) 1D Image analysis of the subcellular fractionation procedure. Lane numbers correspond to those described in figure 4.6. 17 bands present in all fractions were highlighted for analysis. (**B**) Comparison of protein band volumes expressed as a percentage of the total lane volume. Open bars refer to the microsome fraction (lane 6), closed bars refer to the whole cell homogenate (Lane 1).

Figure 4.6 shows clear differences observed in banding patterns between fractions. This is particularly evident in fractions 4 to 7. Using image analysis of the separated fractions, a comparison of bands in the whole cell fraction (WC) and microsome fraction (McF) was carried out (Section 4.2.4, figure 4.7 A & B). Significant enrichment is observed in the microsome fraction of bands 5 (10% of the McF fraction vs 6.8% of the WC fraction), band 10 (7% McF fraction vs 4.7% WC fraction), band 11 (8.7% McF fraction vs 4.2% WC fraction), and band 14 (7.4% McF fraction vs 3.8% WC fraction) (figure 4.7 B). Conversely there is also reduction in the intensity of some bands between the whole cell and microsome fraction. Reductions are observed in bands 1 (4.6% vs 2.5%), 7 (8.1% vs 5.2%), 16 (5.5% vs 2.2%), and 17 (7.8% vs 3.7%) (figure 4.7 B). Together the qualitative and quantitative data suggests that a fractionation has taken place rather than just a dilution of the starting material by the fractionation procedure. If the latter had taken place, one would expect the all bands in both fractions to account for the same percentage of the total lane volume (i.e. the sum of the intensities of all the bands in that given lane).

Western analysis showed that enrichment of the ER proteins GRP78 (78-82 kDa) (Takemoto et al., 1992) and PDI (51 kDa) (Noiva, 1999) was observed in the microsome fraction in relation to the whole cell homogenate (Figure 4.8 A & D) These proteins are were present in lower concentrations in the other fractions. To some extent this loss of protein into non-microsomal fractions is unavoidable due to non-uniform cell lysis and aggregation that may cause some proteins to be pulled down in the nuclear and mitochondrial fractions. Tubulin (55 kDa) and HSP60 (60 kDa) are also found in the microsome fraction, however the presence of these contaminants is minimal with enrichment of tubulin and HSP60 in the whole cell homogenate and mitochondrial fraction respectively (figure 4.8 B & C). The presence of non-secretory pathway proteins in the microsome fraction is not unexpected and is not without precedent. A recent study characterising 491 microsomal proteins confirmed the prevalence of transmembrane, regulatory, and membrane associated proteins (Han et al., 2001).

Furthermore, it was estimated that known ER/Golgi proteins accounted for only 4.7 % of the total protein complement (Han et al., 2001). The results presented here confirm that the protocol used in this study results in an enrichment of resident ER proteins. In view of this result and the minimal contamination of cytosolic and

mitochondrial proteins in the microsomal fraction, the post ultracentrifugation fraction isolated in this study can be considered a microsomal preparation.

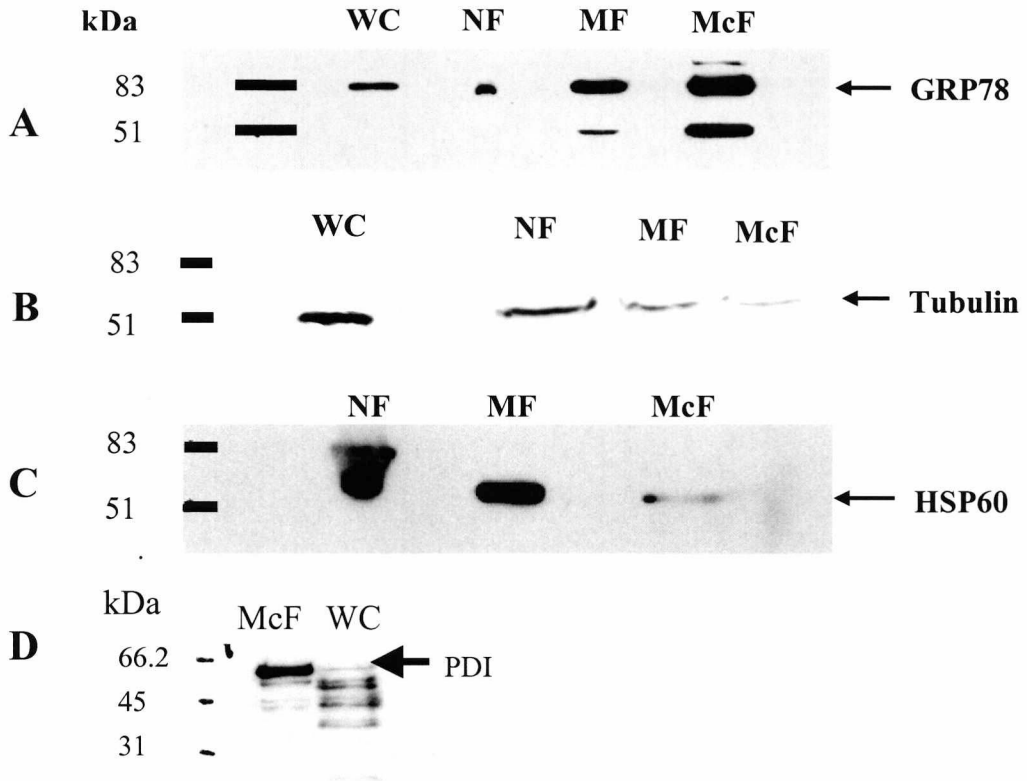

Figure 4.8. Immunological verification of microsome cell fractionation procedure. Immunoblots of GRP78 (**A**), Tubulin (**B**), HSP60 (**C**) and PDI (**D**), in pellets obtained from a microsome fractionation protocol using NS0 IgG cells. **WC** – Whole Cell, **NF** – Nuclear Fraction, **MF** – Mitochondrial Fraction, **McF** – Microsomal Fraction.

4.3.2 Quantitative Analysis of Protein Recovery from Cell Fractionation Procedure

Quantitative analysis of the protein recovered from each stage of the cell fractionation procedure was undertaken in order to optimise cell disruption and the cell number to detergent volume ratio. Cell disruption was optimised using Microsome fractions prepared as described in section 4.2.2 using 1×10^8 cells. Cells were disrupted by either three rounds of freeze-thaw lysis using liquid N_2, liquid shear with a glass

homogeniser, or by vortexing with glass beads as described in section 4.2.2. Final pellets (microsome fraction) were solubilised in 500 µL of lysis buffer containing 9.5 M Urea, 0.8% Pharmalytes pH 3-10 (Amersham Biosciences), 1% DTT and 4% CHAPS for 1 h at RT with agitation. Protein concentration was determined using the modified Bradford assay as described in section 4.2.3 (figure 4.9). Microsome preparations were also carried out using 1×10^8, 5×10^7, 1×10^7, and 5×10^6 cells as described in section 4.2.2. The nuclear fractions (NF) were solubilised as described above in 500 µL of lysis buffer. The mitochondrial and microsomal fractions were solubilised in 300 µL of lysis buffer. Samples (100 µL) of the whole cell homogenate, and all subsequent supernatants were taken and solubilised in 100 µL of lysis buffer as above, except twice the amount of detergent was used (i.e 8% CHAPS) to give a final concentration of 4%. Protein concentrations were determined for each fraction of each cell number as described above (Figure 4.10). This procedure was repeated for all cell numbers using lysis buffers containing 2% CHAPS and 4% Triton X-100.

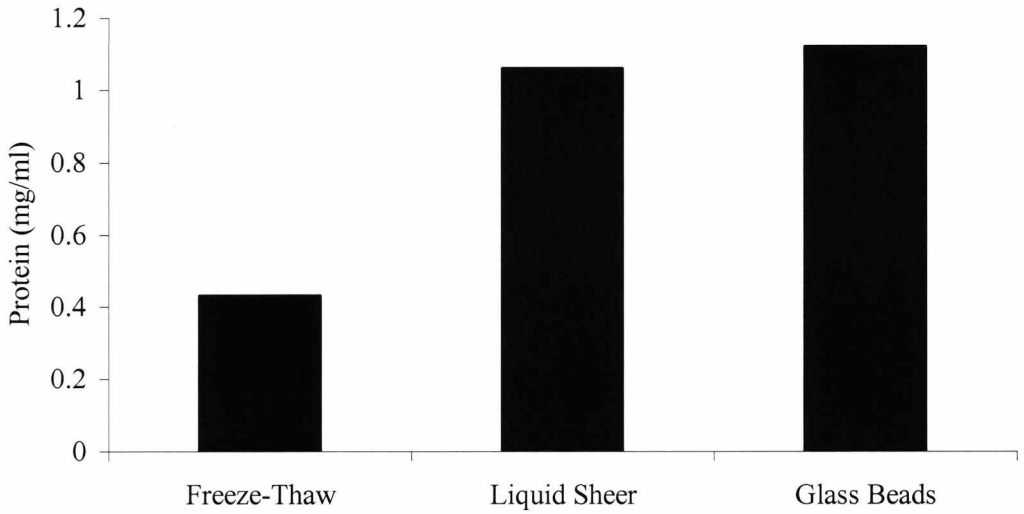

Figure 4.9. Comparison of cell disruption methods. Protein recovery and quantitation of Microsome fractions prepared from 1×10^8 NS0 cells disrupted, either by freeze-thaw, liquid sheer or vortexing in the presence of glass beads.

Freeze-thaw lysis was shown to be the least effective disruption method when preparing microsome fractions, recovering 0.43 mg mL^{-1} of protein. Disruption using liquid shear and glass beads gave similar recovery with concentrations of 1.06 mg mL^{-1} and 1.12 mg mL^{-1} respectively (Fig 4.9). Lysis using glass beads was preferable to lysis by liquid sheer due to the reproducibility of the procedure. The intensity and time of the vortex can be controlled precisely, whereas the magnitude of the shear force generated when using liquid shear is dependent on the clearance between the pestle and the contained vessel and the thrust of the pestle. The latter (thrust of the pestle) is impossible to quantify and reproduce as it is solely operator dependant.

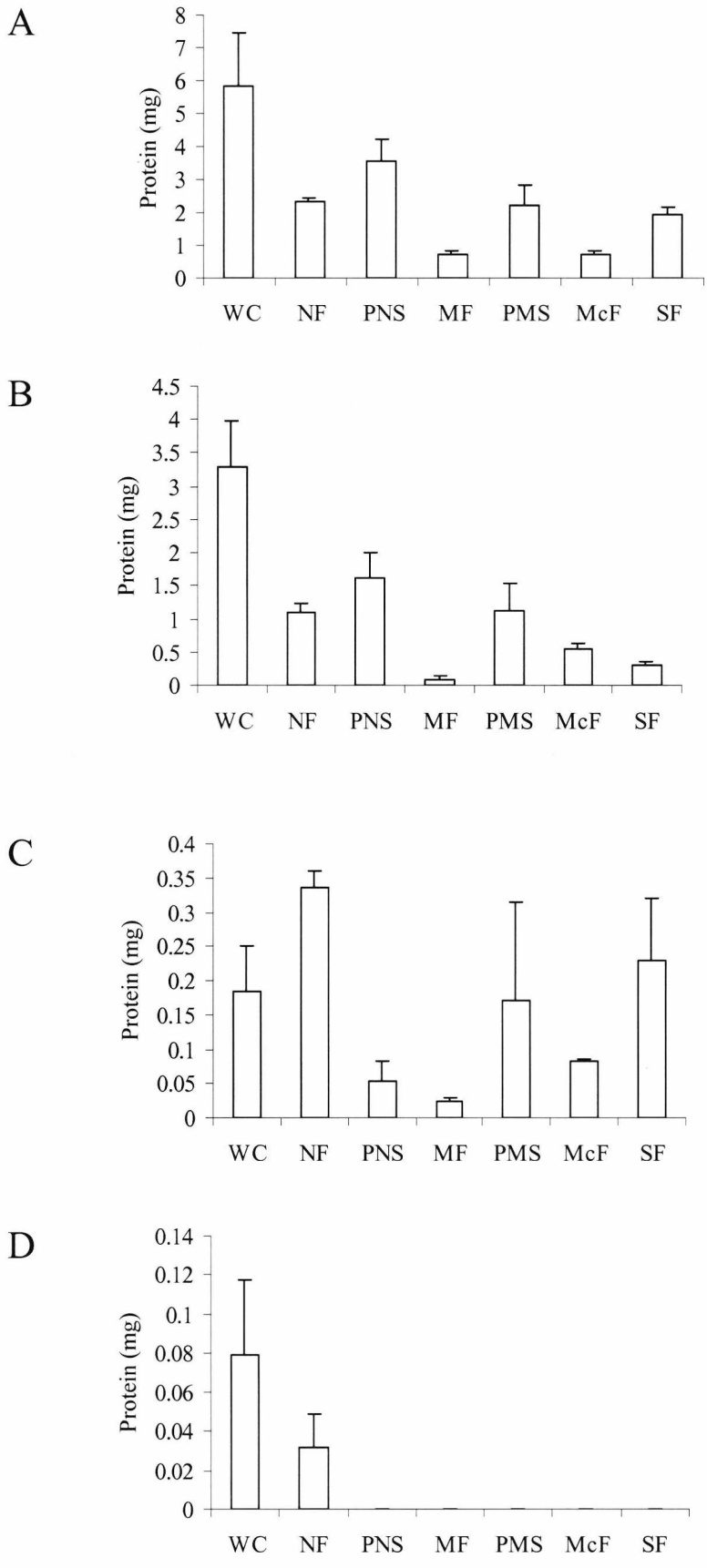

Figure 4.10. Protein quantitation at each stage of the cell fractionation procedure. Total protein estimation of each fraction using 1×10^8 (**A**), 5×10^7 (**B**), 1×10^7 (**C**), and 5×10^6 cells (**D**). Data shown above derives from fractions solubilised in lysis buffer containing 4% CHAPS (section 4.3.2). Protein estimations are based on the mean of three separate repeat preparations, and the standard errors are shown accordingly.

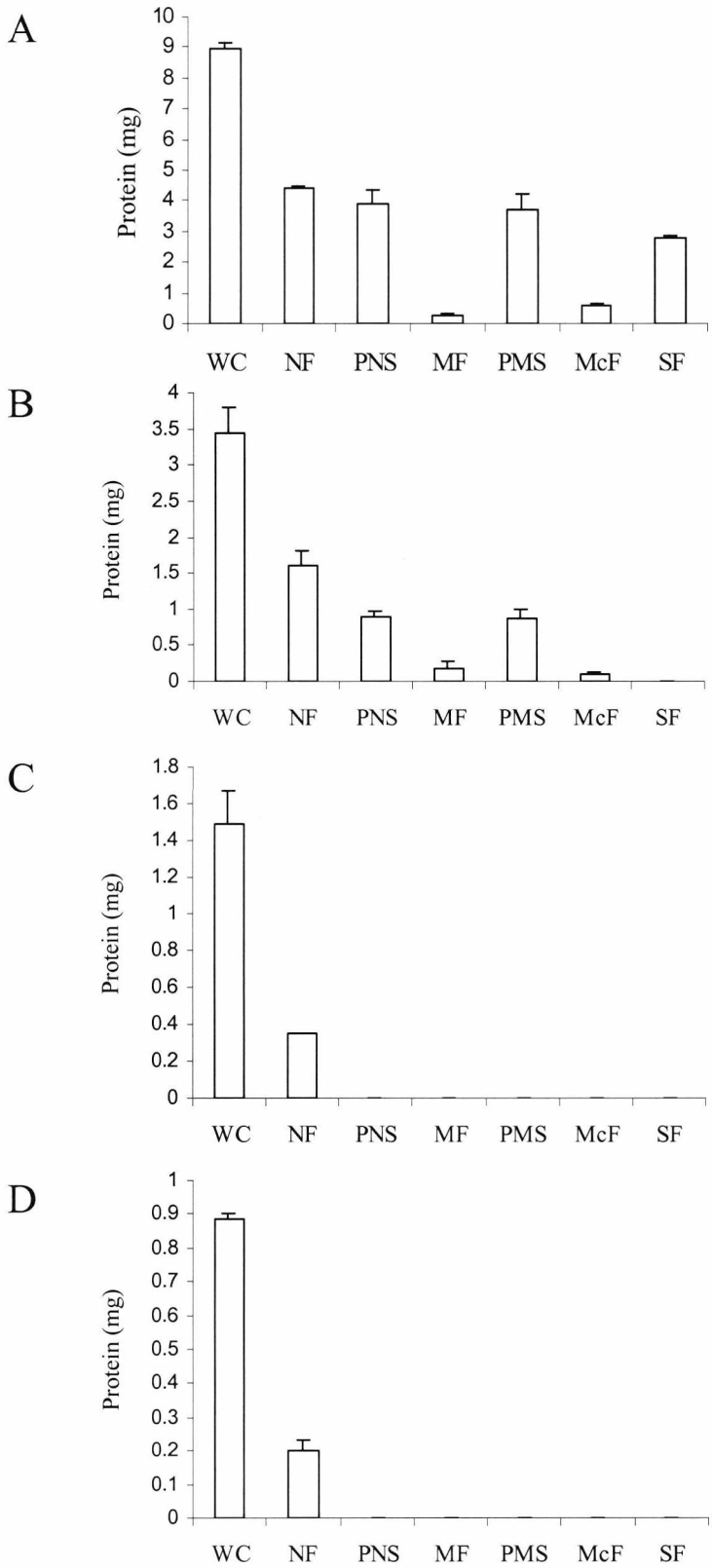

Figure 4.11. Protein quantitation at each stage of the cell fractionation procedure. Total protein estimation of each fraction using 1×10^8 (**A**), 5×10^7 (**B**), 1×10^7 (**C**), and 5×10^6 cells (**D**). Data shown above derives from fractions solubilised in lysis buffer containing 2% CHAPS (section 4.3.2). Protein estimations are based on the mean of three separate repeat preparations, and the standard errors are shown accordingly.

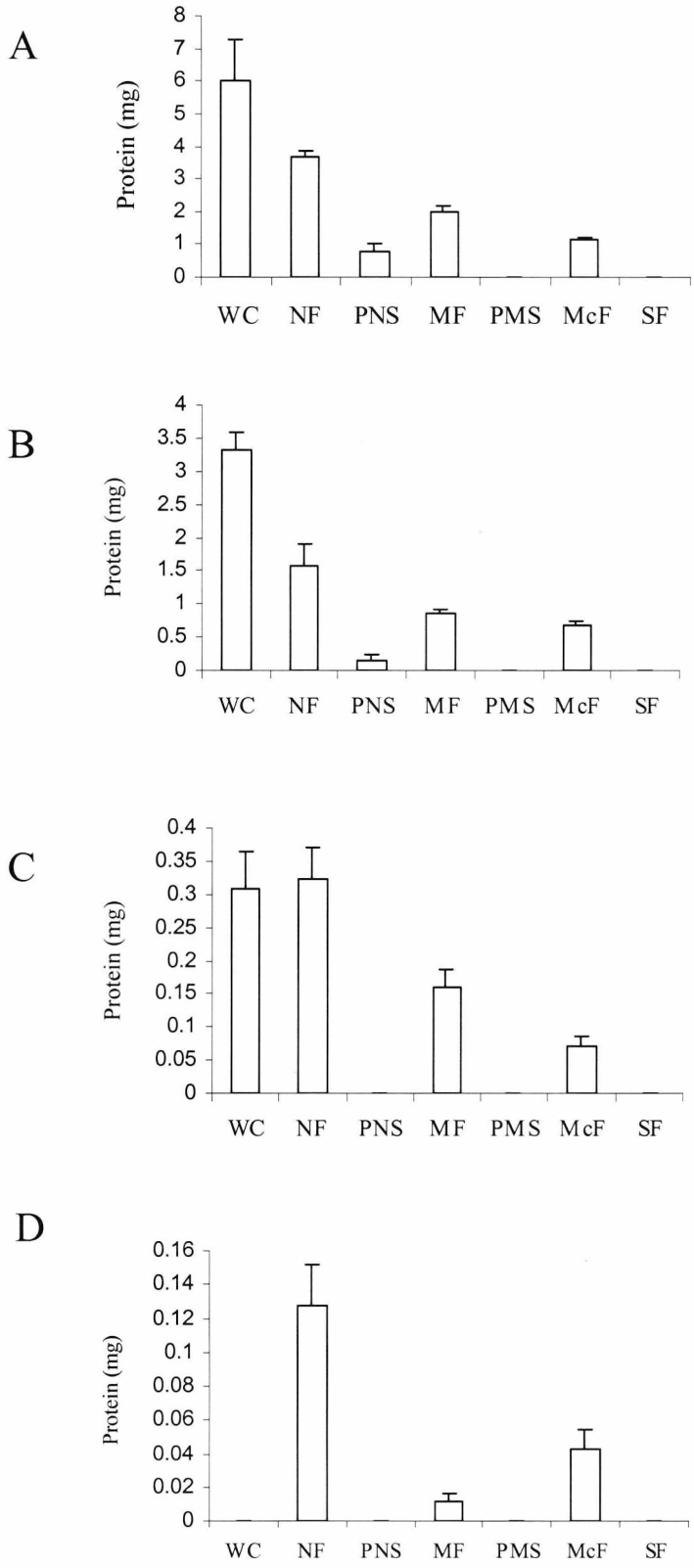

Figure 4.12. Protein quantitation at each stage of the cell fractionation procedure. Total protein estimation of each fraction using 1×10^8 (**A**), 5×10^7 (**B**), 1×10^7 (**C**), and 5×10^6 cells (**D**). Data shown above derives from fractions solubilised in lysis buffer containing 4% Triton X-100 (section 4.3.2). Protein estimations are based on the mean of three separate repeat preparations, and the standard errors are shown accordingly.

The pattern of protein loss observed using cell numbers of 1×10^8 and 5×10^7, solubilised in 4% CHAPS (figure 4.10, A & B) was similar as one would expect. The total protein present in the nuclear fraction (NF) and post nuclear supernatant (PNS) was approximately equal (taking into account standard error values) to that of the whole cell (WC) from which the fractions derive. This pattern was also observed in all subsequent fractions with the total protein of the resultant pellet (MF and McF) and supernatant fractions (PMS and SF) being equal to the previous supernatant to which the fractions were derived, suggesting that under these detergent conditions, and at these cell numbers, protein loss is minimal throughout the fractionation protocol. At cell numbers below 5×10^7 (i.e 1×10^7 & 5×10^6) the pattern of protein loss does not conform to that described above, with large standard errors observed between repeats (figure 4.10 C & D).

Similar patterns of protein loss were observed using cell numbers of 1×10^8 and 5×10^7, when solubilised in lysis buffer containing 2% CHAPS, however lower protein yields were obtained than fractions solubilised using 4% CHAPS (figure 4.11). Protein could not be detected in the majority of fractions with the exception of the whole cell and nuclear fraction at 1×10^7 and 5×10^6 cells when solubilised using 2% CHAPS (figure 4.11 C & D). At cell numbers below 5×10^7, under both solubilising conditions, the values detected did not correspond to a uniform loss of protein throughout the procedure. Furthermore, the absence of detectable protein in some fractions and the high standard errors as mentioned above, suggest that either the accuracy of the assay at very low protein levels is limited or at low cell numbers the protein loss that occurs as a result of the fractionation procedure is of greater significance.

Protein quantitation was also carried out using fractions solubilised in lysis buffer containing the detergent Triton X-100 at 4% (v/v) concentration (figure 4.12). The protein extraction values again exhibited the expected pattern as described for 4% CHAPS for 1×10^8 and 5×10^7 cells, although the protein yield seen in the pellet fractions was higher than all previous detergent conditions (figure 4.12 A & B). Protein content of the supernatant fractions using Triton was the lowest of the three detergent conditions. Furthermore, no protein was detected in any supernatant fractions at cell numbers below 5×10^7 (figure 4.12 C & D). Triton detergents are more hydrophobic than the zwitterionic detergents such as CHAPS (Neugebauer, 1990), therefore it may

be the case that poor interactions take place between Triton and less hydrophobic extrinsic proteins, such as those found in the supernatant fractions. This may limit the effectiveness of the detergent and provide a plausible explanation as to the values observed, although this has not been confirmed experimentally.

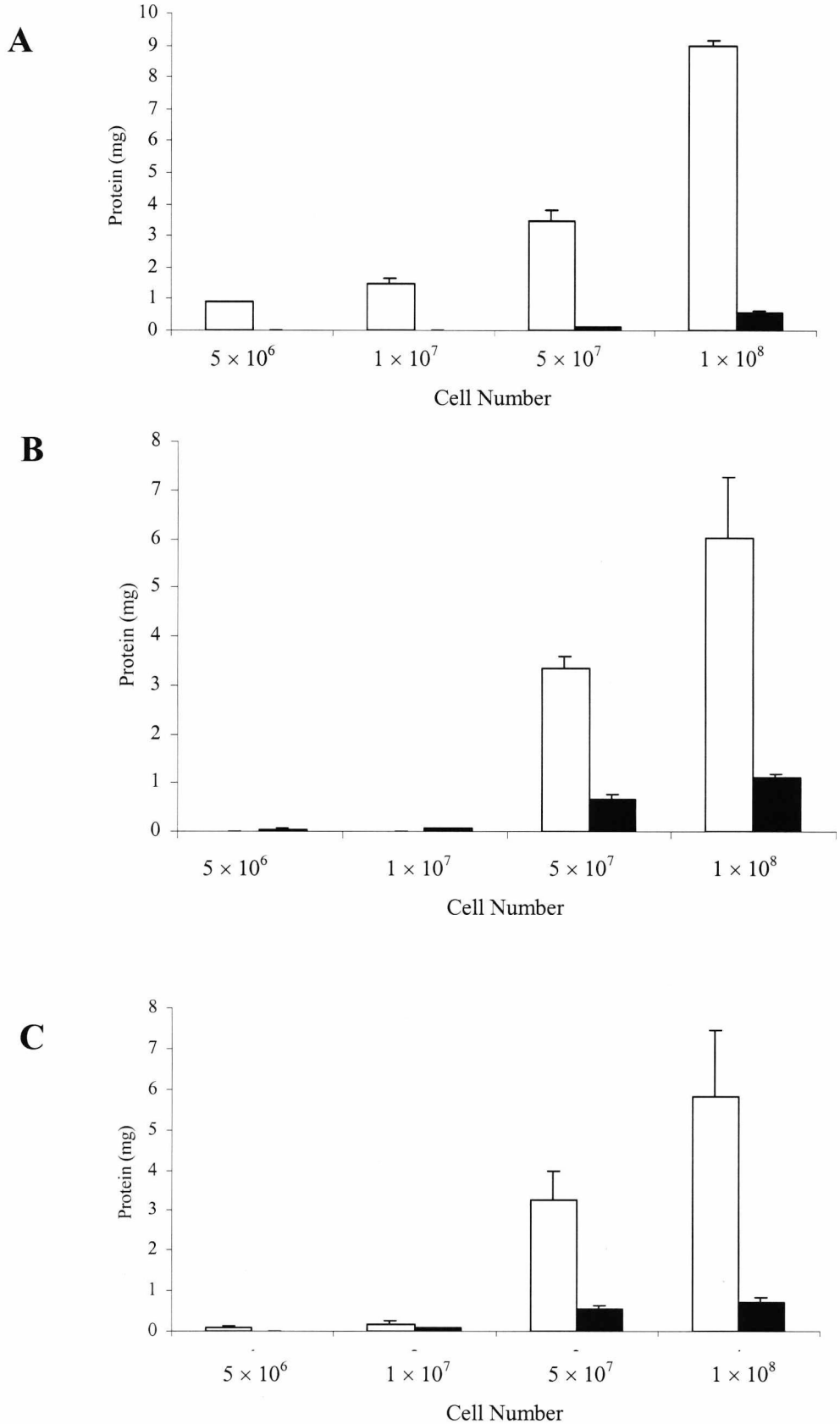

Figure 4.13. Comparison of whole cell homogenate protein recovery against final microsome protein recovery. (**A**) Cell homogenate and microsome pellet solubilised in lysis buffer containing 2% CHAPS. (**B**) as **A** except using lysis buffer containing 4% Triton X-100. (**C**) as **A** except using lysis buffer containing 4% CHAPS. Open bars refer to the whole cell homogenate, closed bars refer to the microsome pellet. Protein estimations are based on the mean of three separate repeat preparations, and standard errors are shown accordingly.

Figure 4.13 shows a summary of protein recovery under all three detergent conditions (2% CHAPS, 4% Triton X-100, and 4% CHAPS). Whole cell protein values increase linearly with an increase in cell number. Protein values between 1×10^8 and 5×10^7 cells gave a ratio of approximately 2:1 under all conditions (taking into account standard error values), correlating to the difference in cell number. Furthermore, ratios of approximately 10:1 were observed between 1×10^8 and 1×10^7 cells solubilised using 2% and 4% CHAPS. Clear differences in solubilising capacity of the selected detergents for whole cell and membrane proteins can be seen. Maximum whole cell protein recovery values were 8.95 mg, 6.03 mg, and 5.84 mg for cells solubilised using 2% CHAPS, 4% Triton X-100, and 4% CHAPS respectively. From this data the detergent CHAPS at a concentration of 2% is the most effective for the solubilisation of whole cell homogenate proteins. This is not the case for the microsomal fraction, which mainly consists of membrane bound proteins. Maximum microsome protein recovery values were 1.12 mg, 0.71 mg, and 0.56 mg when solubilised in 4% Triton X-100, 4% CHAPS and 2% CHAPS respectively (figure 4.14). Hence, for membrane proteins lysis, conditions using 4% Triton X-100 are optimal. This observation is as expected for Triton X-100 or derivatives thereof, as these are commonly the detergents of choice for the solubilisation of membrane proteins (Hjelmeland, 1990; Taylor et al., 2000). The difference in solubilising efficiency between the detergents used here may be due to the hydrophobic character (as mentioned previously) of the detergent Triton X-100. As such, there is greater hydrophobic interaction between the membrane proteins (which are usually highly hydrophobic) and the detergent promoting more efficient solubilisation.

Microsomal protein recovery increases proportionally with an increase in cell number under conditions using Triton X-100. This is not the case however when CHAPS was used. Under conditions using 4% CHAPS an increase of approximately 5 fold is present between 1×10^7 and 5×10^7 cells (figure 4.14). This proportional increase is not observed between 5×10^7 and 1×10^8 cells, suggesting that at cell numbers greater than 5×10^7 the maximum solubilising capacity has been reached for that mass of detergent in that volume (300 µL). Therefore solubilisation at 1×10^8 cells is now favouring proteins in the fraction which are the most soluble. Furthermore, such a bias in solubilisation would ultimately lead to an inaccurate representation of the

protein complement of the microsome fraction when subjected to two-dimensional separation.

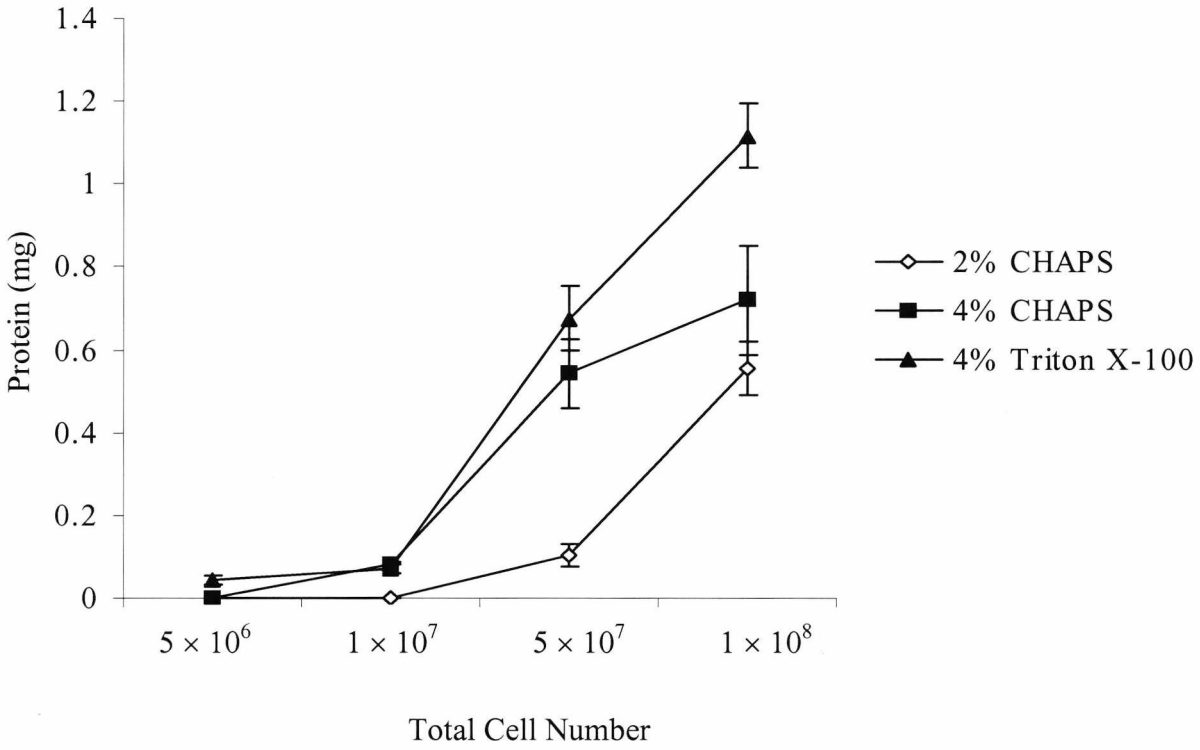

Figure 4.14. Comparison of the protein recovery of microsome fractions prepared from 5×10^6, 1×10^7, 5×10^7 and 1×10^8 cells. Fractions were solubilised in 300 μL lysis buffer containing either 4% Triton X-100, 2% or 4% CHAPS. Protein estimations are base on the mean of three separate repeat preparations, and the standard errors are shown accordingly.

4.3.3 Qualitative analysis of protein solubilisation using Mini 2D PAGE

The resolution performance of four different detergent conditions used to solubilise microsome fractions was investigated using mini-2D PAGE. Microsome preparations were carried out as described in section 4.2.2 using NS0 IgG cells. The final microsome pellet was solubilised in 500 μL of lysis buffer as described in section 4.2.5. Protein estimations were then carried using the modified Bradford assay (section 4.2.3). Samples were then subjected to mini 2D PAGE as described in section 4.2.5.

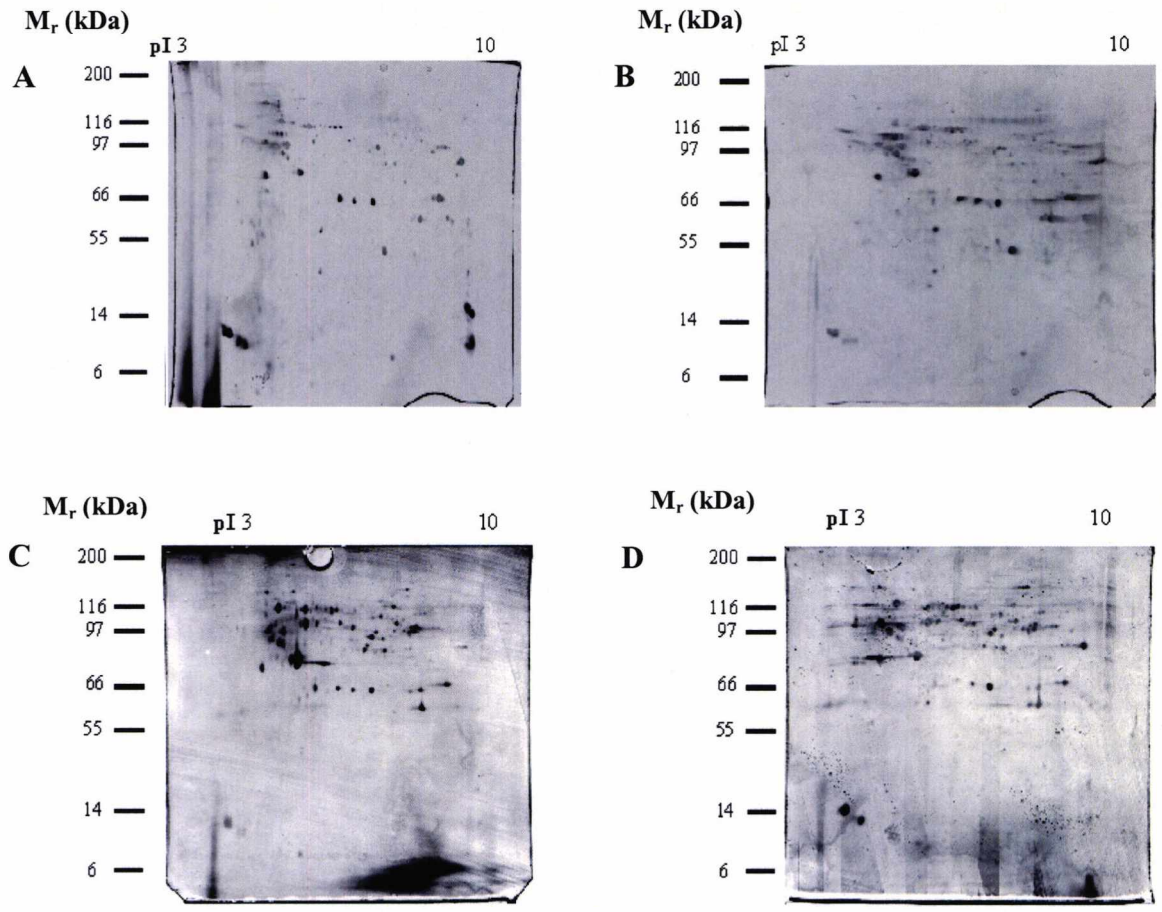

Figure 4.15. 2D polyacrylamide gel electrophoresis separation of microsome fractions solubilised under different conditions. Microsome fraction solubilised under the following conditions; Lysis buffer containing (A) 2% n-Dodecyle β-D-Maltoside, (B) 4% Triton X-100, (C) 4% CHAPS, and (D) 2% CHAPS.

Good reproducibility was observed between all gels with similar spot patterns produced (figure 4.15). n-Dodecyl β-D-Maltoside (DDM) was shown to produce the best resolution, with sharp protein spots and low background staining (figure 4.15 A). However, there was poor resolution of low abundance proteins with only 106 protein spots visualised compared with 158, 147 and 122 protein spots using 4% Triton, 4% CHAPS and 2% CHAPS respectively. This finding suggests this detergent may have a bias toward the solubilisation of certain proteins, or may cause the proteins to be stained poorly. Furthermore, the use of DDM was problematic as the detergent readily adopted an insoluble crystalline state in the presence of urea.

Samples solubilised using Triton X-100 produced the best representation of low abundance proteins, an observation that correlates with results shown in figure 4.14. Resolution as a whole was poor using Triton, particularly in the basic region. Furthermore there was high background staining (figure 4.15 B). Although Triton X-100 is clearly most effective at solubilising membrane bound proteins, its use in isoelectric focusing (IEF) and other electrophoretic techniques is somewhat problematic. Detergents such as Triton have a characteristic change of micelle molecular weight with temperature. IEF is associated with non-uniform thermal patterns across pH gradients, which is caused by the change in conductance of carrier ampholytes at various pH values. As such, the local areas of heat generated by IEF may change the properties of such detergents that may cause undesirable results (Hjelmeland, 1990; Neugebauer, 1990).

2D-PAGE separation results using CHAPS yielded the best results overall, combining good representation of low abundance protein spots with good resolution and low background staining. Separation using CHAPS at 4% was slightly better than at 2% as there was an increase in the abundance of most proteins (figure 4.15 C & D). This indicates more efficient solubilisaton at this concentration (4%), again correlating with the results shown in figure 4.14. Furthermore, Zwitterionic detergents such as CHAPS are commonly used in sample preparation prior to IEF (Dunn and Görg, 2001; Görg, 2000). These detergents offer the combined properties of ionic and non-ionic detergents. Like non-ionic detergents they possess no net charge and lack conductivity and electrophoretic mobility. However, like ionic detergents they are efficient at breaking

protein-protein interactions and are less denaturing than detergents such as Triton X-100 (Chevallet et al., 1998; Neugebauer, 1990).

4.3.4 Investigation into the use of KDEL and KEEL retention sequences as a means to separate resident ER proteins

The use of the ER retention sequences Lys-Asp-Glu-Leu (KDEL) and Lys-Glu-Glu-Leu (KEEL) (see Chapter 1) as an alternative to a cell fractionation procedure for the separation of specific resident ER proteins was investigated. Antibodies to the retention sequences were generated as described in section 4.2.7, with the aim of constructing an affinity column. The generated antibodies were assessed for their reactivity using different mouse tissues that were separated by SDS-PAGE as described in section 4.2.4 (figure 4.16).

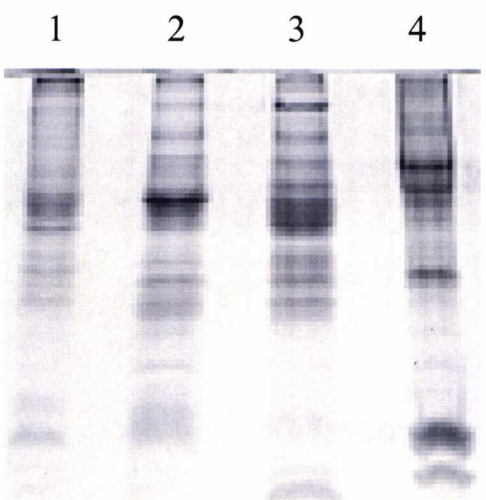

Figure 4.16. SDS-PAGE separation of mouse tissue lysates. **1** Brain tissue lysate, **2** Pancreas tissue lysate, **3** Liver tissue lysate, **4** NS0 whole cell lysate. Mouse tissues were collected from a balb C mouse and homogenized in 250 mM sucrose, 20 mM HEPES-NaOH pH 7.2, 0.5 M EDTA, protease inhibitor cocktail (Roche, Germany). Tissues were diluted 1 in 4 in laemmli buffer prior to loading. 1 $\times 10^7$ NS0 cell pellet was homogenised in above buffer and diluted 1 in 2 in laemmli buffer prior to loading.

Immunoblots using both antibodies were performed (section 4.2.6) and are shown in figure 4.17. Figure 4.17 B shows the result of the blot probed using the anti-KDEL antibody. In three of the tissues only one band is observed at approximately 100 kDa in the NS0 whole cell lysate and 51 kDa in the pancreas and liver tissue. A likely candidate for the 51 kDa band is Protein disulphide isomerase (PDI), this protein is abundant in both liver and pancreas, furthermore PDI is known to have a C-terminal KDEL retention sequence (Frand et al., 2000; Wieland, 1996). The results of the blot probed using anti-KEEL antibody (figure 4.17 A) shows only one band at approximately 35 kDa and 75 kDa observed in the NS0 whole cell lysate and liver tissue respectively. The expression of this latter band at high levels in the liver together with its apparent molecular weight correlates with that of the protein Erp72. This is a calcium binding protein that possesses a KEEL retention sequence at its C-terminus (Frand et al., 2000), however protein identification of the bands observed have not been confirmed experimentally. Both antibodies showed no reaction to the brain tissue which is as expected. Although ER resident proteins are expressed ubiquitously, any expression in brain tissue would be minimal and therefore it would act as a negative control.

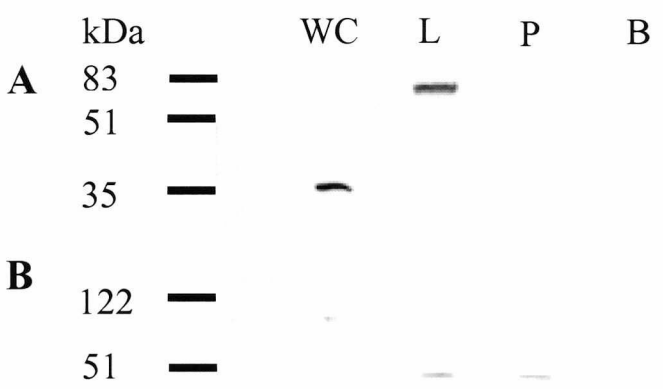

Figure 4.17. Assessment of anti-KDEL and anti-KEEL antibody. (A) Immunoblot using KEEL antibody and (B) immunoblot using KDEL antibody. **WC** – NS0 whole cell, **L** – liver tissue, **P** – pancreas tissue, **B** – brain tissue.

The reactivity of both antibodies was disappointing as the detection of more bands was expected, particularly in the liver and pancreas tissues. Table 4.3 shows ER proteins known (to date) to possess either a KDEL or KEEL C-terminal retention sequence.It was expected that the antibodies generated here would recognise at least the proteins listed in table 4.3. The reasons for this limited reactivity are unclear. It is unlikely that the retention sequences are inaccessible to the antibody as these residues are hydrophilic, furthermore the tertiary structure of the protein will be disrupted by the reducing agent present in the SDS-PAGE running buffer. The presence of some proteins in much higher abundance than others may limit the amounts of antibody available to react with the lower abundant proteins, however high concentrations of soluble ER proteins are present in both the liver and pancreas tissues. Regardless of the reason(s) for this limited reactivity it is clear that this approach cannot be used as an alternative to centrifuge based subcellular fractionation procedures for enriching ER and Golgi resident proteins.

Table 4.3. Resident ER proteins and their respective retention sequence

Protein	ER retention sequence	Reference
PDI	KDEL	(Edman et al., 1985; Frand et al., 2000)
GRP94	KDEL	(Pelham, 1990)
GRP78	KDEL	(Pelham, 1990)
Calreticulin	KDEL	(Pelham, 1990)
P5	KDEL	(Ferrari and Soling, 1999)
PDIp	KEEL	(Desilva et al., 1997)
Erp72	KEEL	(Mazzarella et al., 1990)

4.4 Conclusions

The presence of microsomal marker proteins PDI and GRP78 in the post-ultracentrifugation fraction confirming the presence of microsomal proteins, hence validating the protocol used. Cell lysis using an abrasive agent was preferred to liquid shear for the preparation of microsomes. Optimal detergent to cell number ratio for the solubilisation of the microsomal fraction was found to be 1.7×10^5 cells/ μL of detergent (5×10^7 cells/ 300 μL). Although Triton X-100 was the most effective at solubilising the microsomal fraction, CHAPS at a concentration of 4% was favoured due to its greater compatibility and resolution for 2D-PAGE separation. The assessment of the reactivity of the anti-KDEL and anti-KEEL antibody has been shown to be poor. Therefore, it is unlikely that any affinity separation strategy based on these antibodies prior to 2D electrophoresis will yield a 'better' cell fractionation procedure than that optimised by ultracentrifugation as outlined in this chapter.

Chapter 5 Comparative analysis of the GS-NS0 microsome proteome

5.1 Introduction

Previously results and experiments reported in chapter 3 of this thesis have clearly demonstrated that the specific mRNA levels of the heavy and light chain of the cB72.3 antibody do not correlate with productivity within the selected NS0 cell lines utilised in this study. This is thought to be due most likely to cellular factors down stream of transcription (Strutzenberger et al., 1999). It has been suggested by various groups that a major rate limiting step in the production of recombinant proteins occurs in the endoplasmic reticulum (ER). These rate limiting steps are thought to involve the retention of unfolded proteins and limitations in the transport rate of newly sythesized polypeptides from the ER to the Golgi (Downham, 1996). These dynamic processes are mediated by a range of ER-lumenal protein folding factors, and the trafficking of secretory vesicles between distinct subcellular compartments (Gething and Sambrook, 1992; Hauri et al., 2000). Furthermore, it has previously been established that a correlation exists between the cellular levels of the ER resident proteins, protein disulphide isomerase (PDI) and glucose regulating protein 94 (GRP94), and the levels of monoclonal antibody expression (Lambert, 1997). However, due to our limited *a priori* understanding of these cellular mechanisms (i.e. folding and trafficking) which influence the function and performance of

animal cells in culture, investigations to date have been unable to manipulate cells such that these processes are optimised.

As such, improvements in large-scale production of recombinant proteins, although considerable, has been the result of systematic empirical optimisation of the cell culture environment and improvements in expression vectors (Birch and Froud, 1994). The process of intensive screening and adaptation in order to identify stable high yielding transfectants is often lengthy and labour intensive, and proceeds mainly by trial and error (Barnes, 2000). The possibility of engineering a cell line for increased productivity by manipulating and/or altering the complement of secretory pathway components is largely unknown and open to question. However, complex biological functions (such as recombinant protein production) involve multiple gene products, presumably because this affords greater efficiency or higher quality control (Fussenegger, 1998). Therefore, in order to understand the processes at work during recombinant protein production in mammalian cells it requires a system that can simultaneously monitor the changes of a multitude of proteins in order to identify targets for genetic manipulation.

The aim of this chapter is to investigate the microsome proteome of GS-NS0 cell lines in order to identify any cellular change(s) that may lead to high-level productivity in culture. The proteomic analysis platform and cellular fractionation procedure previously optimised (Chapter 4) were therefore utilised to undertake this study. We have also fully characterised a range of GS-NS0 cell lines that differ in their ability to produce recombinant monoclonal antibody (Chapter 2). Microsomal proteomes generated from these cell lines were subjected to comparative analysis and used to identify proteins of significance. Semi-quantitative analysis was then utilised to examine expression patterns.

5.2 Materials and Methods

5.2.1 Large format two-dimensional gel electrophoresis

Cellular proteins post-fractionation (section 4.2.2) solubilised in lysis buffer containing 4% CHAPS (section 4.2.5) were focused on a 24 cm precast non-linear immobilised pH gradient 3-10 strip (Amersham Biosciences) for 75,000 Vh in the first dimension using a horizontal electrophoresis IPGphor system (Amersham Biosciences). Aliquots of the fractionated cellular extract that equated to 100 μg total protein (as determined by the modified Bradford assay, section 4.2.3) were made up in additional lysis buffer to bring the total volume to 450 μL. Following the addition of a few grains of bromophenol blue the resulting protein solution was loaded into an IPGphor strip holder (for 24 cm strips), an immobiline DryStrip (non-linear immobilised pH gradient 3-10, 240 × 3 × 0.5 mm) was placed over the sample, and the strip was overlaid with mineral oil (Amersham Biosciences). Isoelectric focussing was undertaken using the following conditions: instrument temperature 20^0C; maximum 50 μA/strip; rehydration step 1, 30 V for 12 h; step 2, step-n-hold at 500 V for 1 h; step 3, step-n-hold at 1000 V for 1 h; step 4, step-n-hold at 8000 V until the total volt-hours reached 75,000. After focussing strips were rinsed in ddH_20 and stored at -80^0C until the second dimension.

Second dimension SDS-PAGE was performed on 12.5% self-cast tris-glycine gels (26 × 20 × 0.1 cm) using an Ettan DALT II apparatus from Amersham Biosciences. Protein(s) on the IPG strips were reduced and alkylated prior to electrophoresis by equilibrating the strip at room temperature for 15 minutes in 10 mL of SDS equilibration buffer (50 mM Tris-HCl, pH 8.8, 6 M Urea, 30% (v/v) glycerol, 2% (w/v) SDS and a few grains of bromophenol blue), containing 65 mM dithiothreitol (DTT) followed by incubation for a further 15 minutes in SDS equilibration buffer containing 130 mM idoacetamide. IPG strip were then sealed on top of SDS-PAGE gels with agarose and run at 20^0C using a tris-glycine-SDS buffer system (Biorad) and the following programme: step 1, 5 W per gel for 35 minutes; step 2, 100 W until the bromophenol blue tracking dye reached the base of the gel.

5.2.2 Protein visualisation by silver stain

Protein gels were visualised using an adapted version of the silver stain plusone protocol (Amersham Biosciences). Gels were fixed overnight in 40% ethanol, 10% acetic acid in dd H_20. The gels were sensitised by incubation for 30 min in 30% ethanol, 0.2% (w/v) sodium thiosulphate and 7% (w/v) sodium acetate and then rinsed with two changes of distilled water for 10 min each. After rinsing the gels were submerged in silver solution (0.1% silver nitrate, 0.04% stock formaldehyde solution (38% w/v)) and incubated at RT for 20 mins. Following incubation the silver nitrate was discarded, and the gels were rinsed twice with dd H_20 for 1 min before development with 0.02% formaldehyde (stock formaldehyde solution 38% w/v), 2.5% sodium carbonate, with intensive shaking. Once the developer turned yellow it was discarded and replaced with fresh developer. When the desired intensity of staining was achieved the development was terminated with 1.5% (w/v) EDTA. Silver-stained gels were stored in ddH_20 at 4^0C until analysed. The resulting gel images were captured at 200 dpi using a powerlook III prepress colour scanner (Amersham Biosciences).

5.2.3 Protein visualisation by coomassie stain

Post electrophoresis, protein gels were rinsed briefly in dd H_20 and incubated for at least 1 h in coomassie stain (0.1% (w/v) coomassie G250, 50% methanol, 10% acetic acid). Gels were then de-stained using 12% methanol, 7% acetic acid until protein spots were visible. Gels were digitally recorded as described in section 5.2.2, and stored at 4^0C in dd H_20.

5.2.4 Image analysis

Gel images were analysed using ImageMaster 2D Elite software (version 4.01; Amersham Biosciences). Spot detection was performed automatically using the spot detection wizard and the final parameters were as follows: sensitivity 8475; noise factor 5; operator size 31 and background 1. Following automatic detection spot filtering was carried out using the following clauses: circularity >= 0.3, and Volume >= 2100. Manual splitting of non-split spots and deletion of noise was then undertaken. Following spot

detection, background subtraction was achieved using the mode of non-spot option and a margin of 45. One gel (usually the one with the most spots) was selected as a reference gel and all other gels were matched to it automatically after the placement of at least 300 user seeds across the gel to account for gel warping during running. Once the gels had been successfully matched, the reference gel was modified to include unmatched spots from gels being matched to it, and then all gels were then re-matched to the modified reference gel. The spot volumes were finally normalised automatically using the total spot volume method in the analysis software.

5.2.5 In-gel proteolytic digestion of protein spots

Spots of interest were excised from the gel using a clean scalpel blade. Gel pieces were then placed into 1.5 mL eppendorf tubes. The gel pieces were washed and de-stained by washing in three changes of a 50% acetonitrile (ACN) solution (for silver stained gels, gel pieces were first de-stained in 1% v/v H_2O_2). The gel pieces were then dried for 30 minutes in a vacuum centrifuge. The gel pieces were then reduced by incubation in 10 mM DTT, 5 mM ammonium bicarbonate (pH 8) for 45 minutes at 50^0C. After reduction, the proteins were then alkylated by incubation with 50 mM idoacetamide, 5 mM ammonium bicarbonate (pH 8) for 1 hour in the dark at room temperature. The gel pieces were then washed in two changes of 50% ACN and dried as before. After drying just enough 5 mM ammonium bicarbonate containing 50 ng trypsin to be absorbed by the gel pieces was added (typically ~5 μL). The gel pieces were then incubated on ice for 30 mins, after which sufficient 5 mM ammonium bicarbonate was added to ensure the gel pieces remained moist (covered) overnight. The gel pieces were then incubated overnight at 37^0C. The next day the gel pieces were centrifuged briefly, and 10 μL of a 50% ACN, 5% trifloracetic acid (TFA) solution was then added to the tube and the supernatant removed to a fresh tube. This procedure was repeated twice. The samples were then concentrated in a vacuum centrifuge until dry. Samples were stored at -20^0C until analysed. Prior to analysis by mass spectrometry samples were re-suspended in 0.1% formic acid.

5.2.6 Sample preparation for peptide mass fingerprinting and peptide sequence identification by MALDI-MS and MALDI-MS/MS

A matrix solution consisting of a saturated solution of 2,5-dihydroxybenzoic acid (DHB) in dd H_20 was prepared. Matrix solution (1 μL) then was spotted onto a MALDI target plate and 0.5 μL of sample was spotted on top of the matrix before it was allowed to air dry.

5.2.7 Identification of peptide fragments by MALDI-TOF-MS

Mass spectra were obtained using a Brucker Ultraflex^{TM} Matrix Assisted Laser Desorption Ionisation time of flight (MALDI-TOF) mass spectrometer (Brucker GmBH, Germany) in reflectron mode. Calibration was performed using peptide calibration standards (part Number 20 16 95, Brucker GmBH) adjacent to the samples. MS/MS analysis was performed at the University of Queeensland (Brisbane, Australia) using a QSTAR^{TM} MALDI-TOF-TOF mass spectrometer. Peptide masses were used to prosecute the SwissProt mouse database via www.matrixscience.com.

5.3 Results and Disscusion

5.3.1 Characterisation of the GS-NS0 microsome proteome

GS-NS0 (1×10^8 cells total) were harvested and subjected to the cell fractionation procedure described and optimised in section 4.2.2. The resulting microsome fraction was separated by 2D-PAGE as described in section 5.2.1. Protein spots in the gel were visualised using the silver staining protocol previously described (section 5.2.2). Concurrently, GS-NS0 (1×10^7) cells were washed using 0.35 M sucrose and solubilised in lysis buffer containing 4% CHAPS (section 4.2.5) for 1 hr. The resulting sample was then separated by 2D-PAGE and stained in the same manner as previously described. A comparison of the NS0 microsome proteome and the NS0 whole cell proteome is shown in figure 5.1. Despite the membranous environment and lipid-rich nature of the microsomes, protein spots separated well within the isoelectric range of pH 3-10 (figure 5.1A). Some horizontal streaking is observed on both gel images with proteins possessing an isoelectric point (pI) greater than 8, but this phenomenon is common with proteins focusing in the basic range. The masses of the proteins detected in the microsome fraction ranged from 10 to 100 kDa. An enrichment of major spots within the microsome proteome (figure 5.1A) was clearly observed relative to these same spots that were present in the whole cell proteome (figure 5.1B). This clearly demonstrates that a fractionation has been achieved, rather than a dilution of the protein complement.

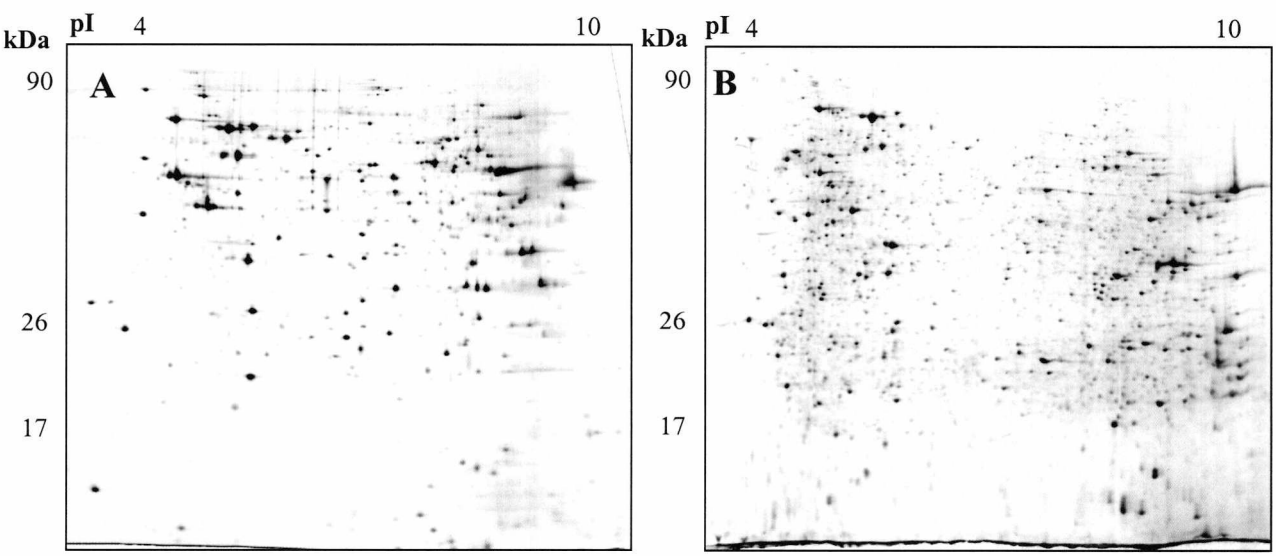

Figure 5.1 Large format 2D-PAGE of GS-NS0 2X cell extracts. (A) 2D separation of the GS-NS0 microsomal fraction Prepared using the cell line 2X.(B) 2D separation of the GS-NS0 whole cell fraction prepared using the cell line 2X.

The protein complement of the microsome proteome yielded between 700 and 1000 discrete protein spots (mean of 813 spots ± 135, based on 7 gels), compared to between 2000 and 2500 (mean 2525 spots ± 79 based on 7 gels) discrete spots generated by the whole cell separation (Smales et al., 2003). This data shows the consistency in the number of spots detected is greater in the whole cell separation than in the microsome fraction. This is not unexpected as the process of cellular fractionation (described in detail in chapter 4) will inevitably introduce some element of variability and will therefore result in a reduction in the consistency observed in the microsome fraction with respect to protein spot numbers. The greatest variability occurs in the spots of lowest abundance as expected.

In order to characterise the microsome proteome further, 2D-PAGE gels were run as described in section 5.2.1 with a protein load of 500 μg/350 μL of lysis buffer and focussed for a total of 150,000 Vhrs. Protein spots within the gels were then visualised using coomassie stain as described in section 5.2.3. Major protein spots were excised from the gel and subjected to in-gel proteolytic digestion and MALDI-TOF mass spectrometric analysis as described in sections 5.2.5 and 5.2.6. Peptide mass fingerprints (PMF) were generated for each protein spot excised. An example of a PMF is shown in figure 5.2A. The peptide masses generated were used to search the SwissProt database via the mascot internet search program (section 5.2.7). Figure 5.2B shows a probability histogram constructed using the molecular weight search (Mowse) algorithm developed by Pappin and co-workers (Pappin et al., 1993). The histogram is a probability based Mowse score distribution of the top 50 matching proteins. Essentially, the Mowse score is a measure of the statistical significance of a match between experimental data and data derived from a sequence database such as SwissProt. The region in which random matches may be expected is shaded green (figure 5.2B). This region extends up to a significance threshold which has a default setting of 5% (i.e. an event is significant if it would be expected to occur at random with a frequency of less than 5%). Therefore, if a score falls in the green shaded area, there is greater that 5% probability that the match was a random event, and of no significance. Conversely, a match in the unshaded region of the histogram (figure 5.2B) has a less than 5% proberbility of being a random event. In this investigation a match was only considered achieved if the Mowse score generated was greater than the significance threshold.

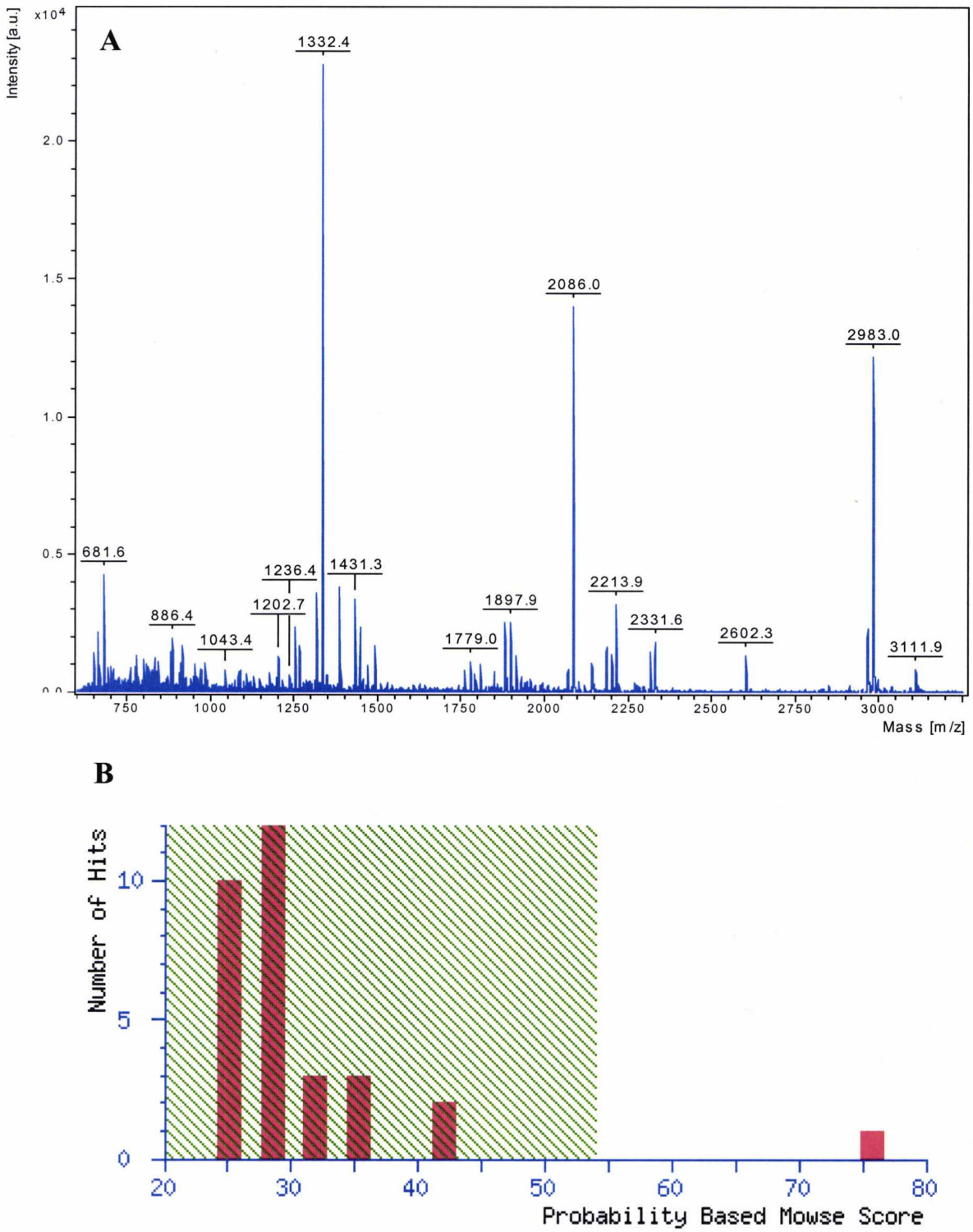

Figure 5.2 Protein identification by Peptide Mass Fingerprinting (PMF). (**A**) Example of a mass spectrum generated by MALDI-TOF analysis after in-gel tryptic digestion of protein spot 20.(**B**) Mascot probability based mowse score chart. The score is $-10 \times \text{Log}(P)$ where P is the probability that the observed peptide match is a random event. Scores greater than 53 are significant. The score depicted shows a match for protein spot 20 to proteome subunit α type 1.

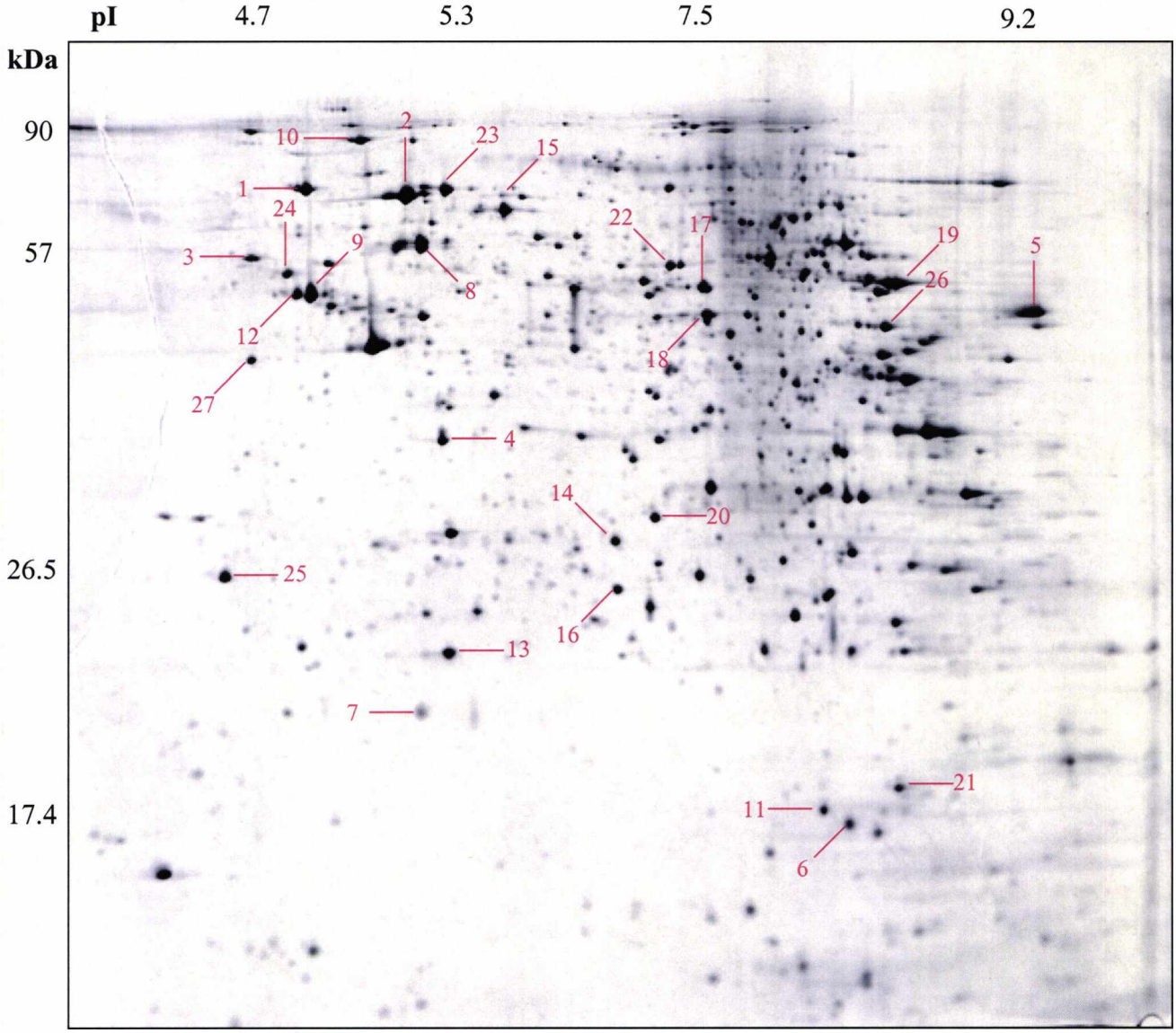

Figure 5.3 Identifications in the GS-NS0 microsome proteome map. All protein spot identifications shown were identified by peptide mass fingerprinting generated by MALDI-TOF mass spectrometry.

In total 70 major protein spots were excised from the gels and subjected to digestion and MALDI-MS analysis. Of these 70 spots, identifications were positively made on 27. A list of the identified proteins including their corresponding SwissProt accession numbers and Mowse proberbility based scores is presented in table 5.1. The positions of the identified spots on the GS-NS0 proteome map are shown in figure 5.3.

The identified proteins can be placed into three catagories according to subcellular location. These are; microsomal, cytoplasmic, and mitochondrial. 8 of the proteins identified fall into the microsomal category (spot No. 1, 3, 5, 6, 9, 10, 15, and 27) (figure 5.3). A further 12 proteins are categorised as cytosolic (spot No. 2, 4, 7, 10, 14, 16, 18, 20, 21, 23, 24, and 25). Finally, 7 proteins fall into the mitochondrial category (spot No, 8, 12, 13, 17, 19, 22, and 26). Proteins identified as microsomal are involved in protein folding (GRP78 and GRP75), protein modification (PDI, and PPIase), translocation (Elongation factor 1α) and protein transport between the ER and Golgi apparatus (TER ATPase). The cytoplasmic proteins identified are mainly structural (β-actin and tubulin) and involved in the ubiquitin mediated degradation pathway (proteosome subunits). The proteins identified as located/associated with the mitochondria are mainly involved in energy metabolism (ATP synthase and fumarate hydratase). Also identified were proteins with multiple functions induced by heat shock such as HSC70 and HSP60. This variety of proteins within the microsomal fraction (i.e. a large component of non-microsomal proteins) has also been previously reported by Galeva and Altermann, who compared the separation of rat liver microsomes by one and two-dimensional electrophoresis. In this study it was reported that one third of all proteins detected on the 2D gels represented microsomal proteins (Galeva, 2002)(i.e. one thirds were not microsomal). Furthermore, a study by Han et al., identified 491 proteins from microsome fractions using isotope-coded affinity tags and found that only 4.7% corresponded to ER/golgi proteins, 5.1% to mitochondrial proteins, and 4.5% to cytosolic proteins. By far the largest majority of identified proteins corresponded to functionally uncharacterised proteins (Han et al., 2001). It is clear from this evidence and that reported in this study that microsome fractions represent a more heterogenous mixture of proteins with diverse functions which do not neccesarily fall into the category of secretory pathway proteins. This is ultimately the result of the fractionation procedures which generate the microsome fractions. As such these fractions should be considered 'enriched' microsomal fractions but not as microsome fractions per se.

In this study an approximate 30% success rate was achieved in the identification of excised protein spots by peptide mass fingerprinting (PMF). This low success rate in protein identification is mainly due to ambiguity caused by peptide mass redundancy. Peptide mass redundancy occurs as a result of peptides which contain the same amino acids in a different sequence order exhibiting the same mass or a combination of different

amino acids which give the same mass. For example, a peptide of 5 amino acids can have the same mass by simple re-arrangement of its constitutive amino acids, e.g., peptide VAGSE has the same mass as AVGSE or AEVGS and so on. In order for peptide mass fingerprinting to be successful, the masses of a large number of peptides must be obtained to provide enough specificity in the search, and this is not always possible. Mass redundancy occurs with greater frequency in large genomes. Moreover, peptide mass fingerprinting is at its most effective only in the analysis of proteins from organisms whose genome is small, completely sequenced and well annotated (Graves and Haystead, 2002). This is not the case with the mouse genome at present. Furthermore, it is estimated that using peptide mass fingerprint data alone, one can only cover around 10-15% of the mouse proteome (Haystead, 2003). One more limiting factor of peptide mass fingerprinting is mass accuracy. It is critical to obtain an accurate measurement of the masses of multiple peptides and as such, factors that alter the masses of those peptides can reduce the success of the method. One such example is the post-translational modification of proteins. If the unknown protein is extensively modified, the peptides produced from that protein will not match the unmodified protein in the database (Graves and Haystead, 2002)

Table 5.1 Identifications of protein spots excised from the GS-NS0 microsome proteome map

Protein No.	SwissProt Accession No.	Identification	Protein Mass (Da)	Protein pI (theoretical)	Peptide matches	Mascot Score	Reference
1	P20029	GRP78	72493	5.07	8	82	(Kozutsumi et al., 1989)
2	P08109	HSC71	71059	5.37	11	77	(O'Malley et al., 1985)
3*	P09103	PDI	57143	4.79	N/A	N/A	(Edman et al., 1985)
4	P48975	β-Actin	41711	5.22	8	84	(Chik et al., 1996)
5	P10126	Elongation factor 1 α	50163	9.10	12	96	(Whiteheart et al., 1989)
6	P17742	PPIase A	17829	7.88	9	101	
7	P24142	B-Cell receptor associated protein 32	29859	5.57	10	100	(Terashima et al., 1994)
8	P19226	HSP60	61091	5.91	11	92	(Venner and Gupta, 1990)
9	P27773	PDI	56621	5.99	13	97	(Edman et al., 1985)
10	Q01853	TER ATPase	89948	5.14	9	59	(Zhang et al., 2000)
11	Q01768	Nucleotide diphosphate kinase B	17468	6.97	7	69	(Urano et al., 1992)

Table 5.1 continued

Protein No.	SwissProt Accession No.	Identification	Protein Mass (Da)	Protein pI (theoretical)	Peptide matches	Mascot Score	Reference
12	P56480	ATP synthase β chain	56256	5.19	11	116	(Andersson et al., 2000)
13	Q9DCX2	ATP synthase δ chain	18665	5.53	8	70	(Strausberg et al., 2002)
14	P70195	Proteasome subunit β type 7	30220	8.14	10	73	(Kasahara et al., 1996)
15	P38647	GRP75	73773	5.91	11	83	(Domanico et al., 1993)
16	O08807	Peroxiredoxin	31265	6.67	7	68	(Wong et al., 2000)
17	P47738	Aldehyde dehydrogenase	57024	7.53	8	54	(Chang and Yoshida, 1994)
18	P17182	Alpha enolase	47328	6.36	10	86	(Kaghad et al., 1990)
19	Q03265	ATP synthase α chain	59832	9.22	10	71	(Yotov and St-Arnaud, 1993)
20	Q9R1P4	Proteasome subunit α type 1	29818	6.00	8	74	(Hopitzan et al., 2000)
21	P18760	Cofilin	18780	8.22	7	66	(Moriyama et al., 1990)

Table 5.1 continued

Protein No.	SwissProt Accession No.	Identification	Protein Mass (Da)	Protein pI (theoretical)	Peptide matches	Mascot Score	Reference
22	Q61753	D-3-phosphoglycerate dehydrogenase	36665	6.51	8	67	(Miller and Bieker, 1993)
23	P08109	HSC71	71059	5.37	11	77	(O'Malley et al., 1985)
24	P05218	Tubulin β-5 chain	50103	4.87	11	83	(Lewis et al., 1985)
25	Q9Z2U1	Proteasome subunit α type 5	26568	4.74	6	54	(Strausberg et al., 2002)
26	P97807	Fumarate hydratase	54568	9.12	7	66	(Strausberg et al., 2002)
27	P14206	40S Ribosomal protein SA	32933		6	53	(Rao et al., 1989)

* Identified by MS/MS sequence tag analysis. See table 5.3 protein 1 for sequence tag information.

5.3.2 Image analysis of GS-NS0 cell lines differing in monoclonal antibody productivity.

In order to undertake a proteomic analysis of the GS-NS0 cell lines large format two dimensional gels were run using 1×10^8 GS-NS0 cells (parental, transfectand blank, 4O, 4R, 2X, 2P, and 2N2) harvested at mid-exponential phase of growth (figure 2.1A). Microsome fractions were prepared from these cell lines as detailed in section 4.2.2. Gels were run, proteins visualised (silver), and recorded as described in section 5.2.1.

Figure 5.4 shows the detections of protein spots using the image analysis software and the parameters outlined in section 5.2.4. Figure 5.4A shows the image captured after visualisation by silver stain, and figure 5.4B is an image master produced digital image of the spots detected from the gel depicted in figure 5.4A. Good spot detection was observed with the software generated image exhibiting very silmilar spot paterns to the original image. The average spot numbers detected across the gels is presented in section 5.3.1 and the total number of spots detected in each gel is presented in table 5.2. After the completion of spot detection, background values were subtracted from the gel images. This is used to account for the background intensity of the gel material on the image. The 'mode of non-spot' method in the image analysis software was used to do this. The software examines a set number of pixels surrounding each spot. The most frequently occuring pixel intensity in this area is deemed to be the background value for that spot. This is then repeated for each spot on the gel.

In order to match the gel images of each cell line to one another and ultimately investigate changes in protein expression, it is necessary to construct a reference gel. The chioce of gel to act as the reference gel is arbitrary but it is usually prudent to select the gel with the most detected spots. Each gel in the experiment is then matched to the reference gel. User seeding was used to match like spots to the reference gel. The user seeding method has been shown to reduce mismatching of spots, and hence reducing error, when compared to the automatic matching mode built into the software package. This is mainly due to the variation in 2D gels. In an ideal world the same protein (present on a different gel) would migrate to the same position on a 2D gel every time (providing the gel has been run under the same conditions). However, in reality this is not the case due to variation

arising from sample preparation or perhaps local fluctuations in the acrylamide concentration which may have occurred during the preparation of the gel leading to slight distorting when the gel is run. Once all gels in the experiment have been matched to the reference gel, the reference gel is modified to produce a composite image which includes unmatched spots from the gels being matched to it. A schematic diagram showing the construction of the reference gel used is shown in figure 5.5. Table 5.2 below shows the total number of spots matched per sample gel to the reference gel, and the percentage match between the sample gel and the reference gel. All percentage match values were over 80% which shows a high degree of matching was achieved between the reference gel and the sample gels present in the image analysis experiment. This high degree of matching allows us to monitor the expression of the majority of proteins present in the microsome proteome of the GS-NS0 cell lines under investigation .

Table 5.2 Gel Statistics from image analysis of GS-NS0 2D gels

Cell Line	Total Spot Number	Total Spot Matches	% Match*
NS0-Parental	827	753	91
NS0-Trans Blank	730	649	89
NS0-40	627	546	87
NS0-4R	718	653	91
NS0-2X	919	831	90
NS0-2P**	1029	1029	100
NS0-2N2	840	686	82

* Number of spots matched to the reference gel
** This gel was selected as the reference gel

After matching was complete, a comparison of the normalised spot volumes for each spot was undertaken. This comparison was carried out between the productive cell lines (i.e. 4O, 4R, 2X, 2P, and 2N2) in the first instance, after which a comparison was carried out between the parental cell line and the transfectant blank. The analysis was carried out in this manner because a valid comparison can only be carried out with cells in the same functional state (i.e producing recombinant mab). Therefore, as the parental and transfectant blank cell line have not been engineered to produce recombinant mab they cannot be considered to be in the same functional state as the producer cell lines. Furthermore, it is unclear what level of productivity would be achieved if one were to insert a plasmid vector containing the mab genes into these cell lines due to cell specific differences as discussed later in this chapter. A comparison between the parental and

transfectant blank was also undertaken (section 5.3.4) in order to assess the effect of inserting the plasmid vector.

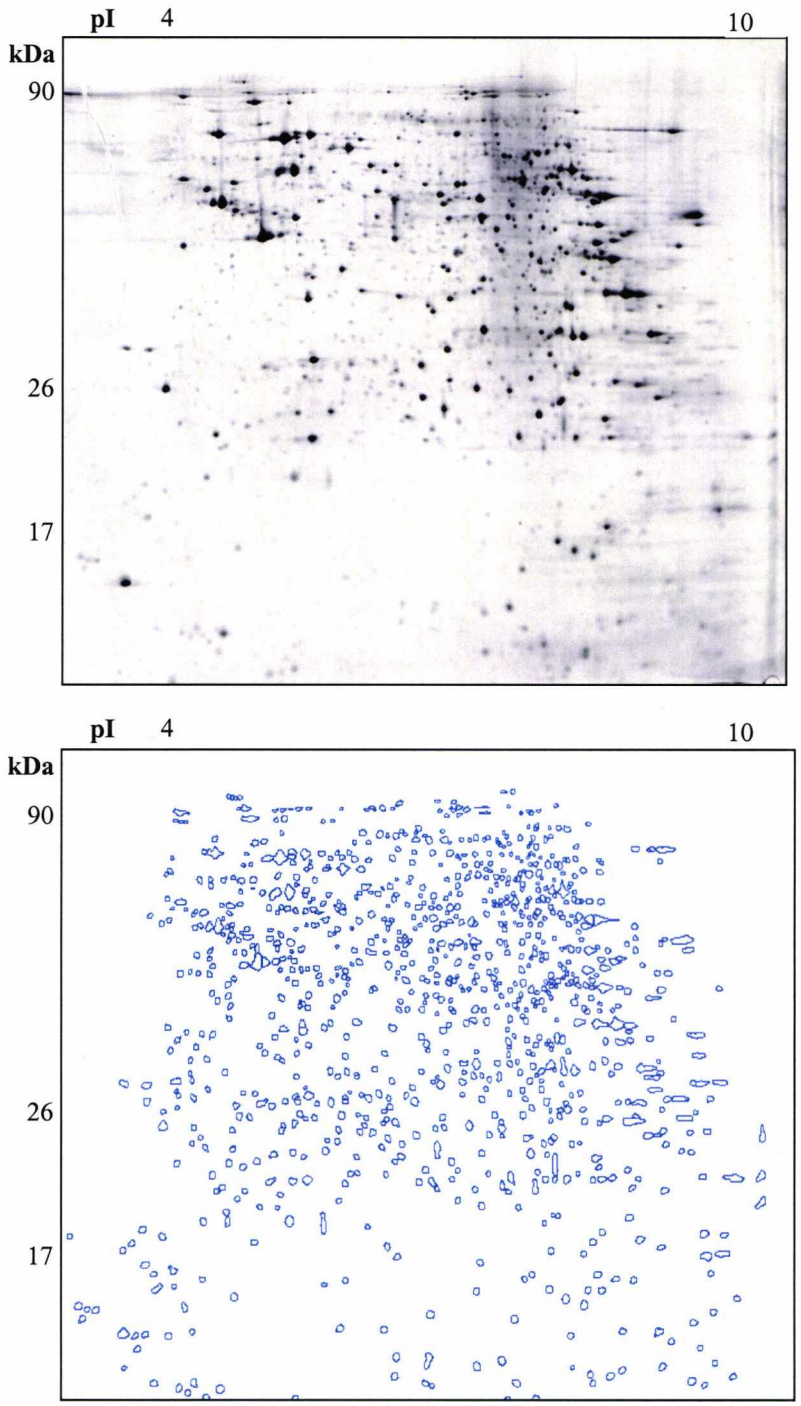

Figure 5.4 Large format 2D SDS-PAGE GS-NS0 2P microsome fraction. (**A**) A 100 µg/350 µL protein load stained with silver. (**B**) An ImageMaster produced image of (**A**) showing 1029 spots detected using the software.

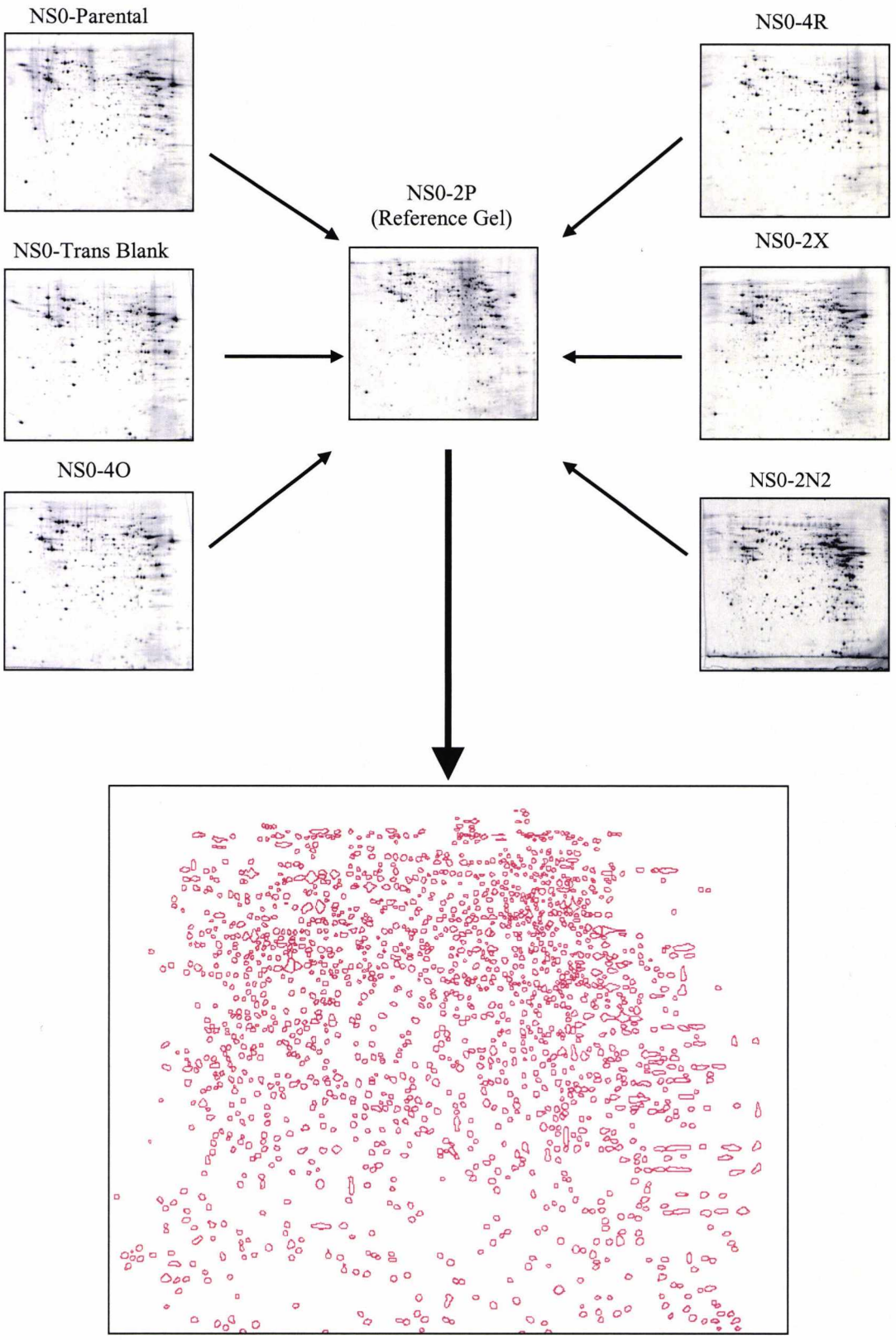

Figure 5.5 Schematic diagram for the generation of a composite reference gel. Initially all gels are matched to a gel selected as a 'reference'. After matching any unmatched spots are added to the reference gel providing a composite image of all protein spots from all gels.

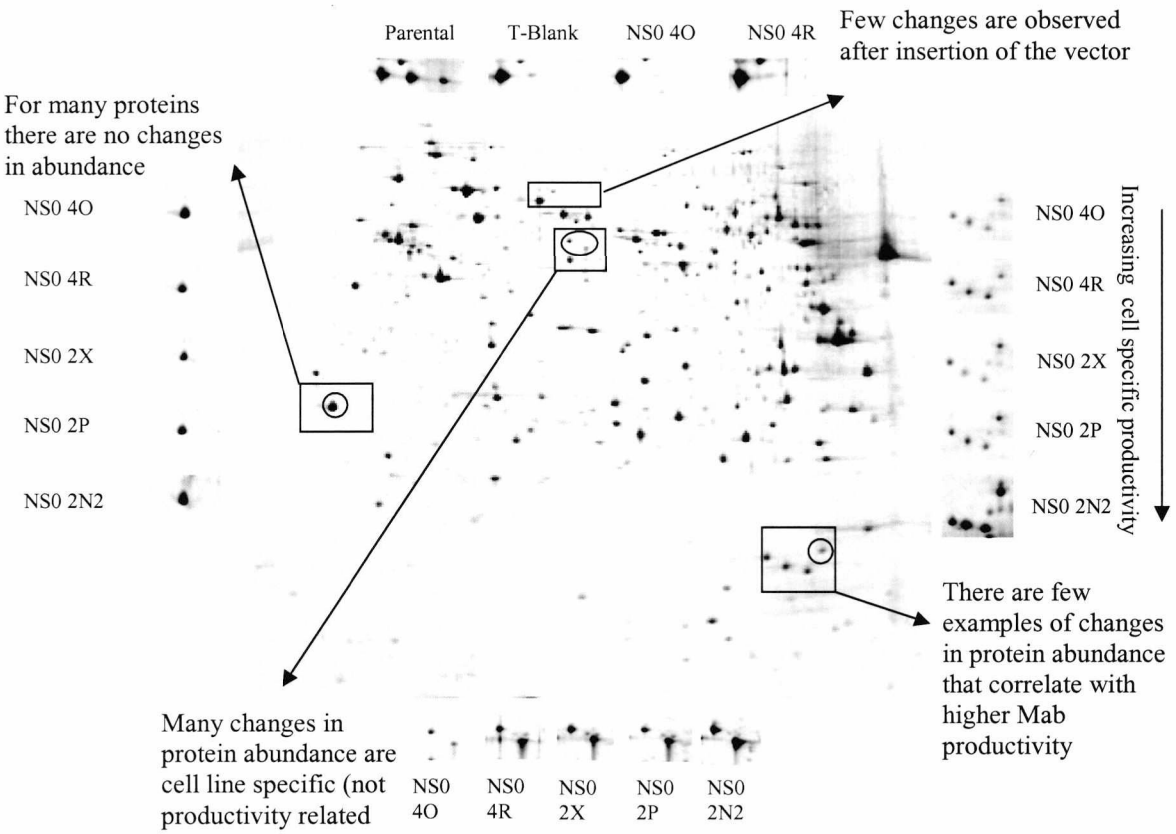

Figure 5.6 Comparative analysis of microsome fractions of GS-NS0 cell lines differing in specific productivity by 2D-PAGE. The potential changes that may be (and were) observed in gene expression are highlighted.

Changes in protein expression between cell lines can be categorised into distinct groups (figure 5.6) which allow the identification of funtionally relevant changes to the proteome. Firstly, we may observe no alterations in any given protein abundance between the different cell lines. This suggests that these proteins are either absolutely required by the NS0 cell or that changes in the expression levels of these proteins is relatively rare or even intolerable in these cell lines. As such changes in mab productivity could be the result of changes in cellular functional properties that occur by mechanisms other then changes in gene expression, such as metabolomics or post-translational protein modification.

Secondly, we may observe alterations in the abundance of specific proteins which correlate with increases in specific productivity (i.e. only changes in the expression of cellular proteins that may directly affect a functional property). Thirdly, many small alterations in protein abundance are observed, which may indicate that changes in cell

function properties occur by changing the overall 'bias' of gene expression. Lastly, we observe changes that result after the insertion of the plasmid vector itself (without heavy and light genes). Such changes are likely to be related to the glutamine limited growth conditions that these cells have to operate under.

5.3.3 Semi-quantitative analysis of GS-NS0 proteins whose expression correlates with mab productivity and identification by mass spectrometry

In section 5.3.2 the types of potential changes in protein expression identified using image analysis were discussed. The image analysis software was used to identify protein spots which showed an increase/decrease in abundance in response to an increase in mab specific productivity. In total 8 spots were identified (7 up-regulated and 1 down regulated) which fit this criteria. The expression patterns of these proteins were quantified by the ImageMaster software and the resulting data is presented in figure 5.7. This data is only semi-quantitative as it may be the case that since silver is not an endpoint stain different gels were stained to different degrees dispite every effort being made to ensure consistency when staining. Nevertheless, for the eight proteins chosen for further analysis a clear pattern in expression levels is observed (figure 5.7). It should also be noted that a criteria defining an increase in expression (i.e. a protein spot must be at least two-fold more abundant to be considered as a significant increase) was not applied. Such criteria are only useful when comparing two functional states (for example diseased tissue vs non diseased tissue). Given that we are comparing five cell lines, if such a criteria were to be applied here (i.e. two-fold difference), the minimum difference in abundance to be considered significant between the first and last cell line would be 16-fold. Therefore, a positive/negative trend in the abundance of a protein spot which correlates with productivity was considered sufficient. However, if one considers the difference between the highest and the lowest expression levels across the cell lines, in all cases there is more than a two-fold difference in expression levels (e.g. for protein 1, fig 5.7A the difference between the expression levels of this protein in 4O and 2N2 is greater than two-fold).

Generally, the majority of proteins observed do not change significantly between the productive cell lines.The changes that do occur are almost entirely cell specific changes and involve proteins that are present only in low abundance. Images of the selected protein spots 1-8 showing the change in expression as productivity of the cell lines increases is shown in figure 5.8. The position of the regulated proteins on the GS-NS0 microsome proteome map is shown in figure 5.9. The selected proteins were excised from sample gels and were then subjected to in-gel tryptic digestion and peptide mass fingerprinting/ peptide sequence tags in order to identify the protein of interest as described in section 5.2.5, 5.2.6,

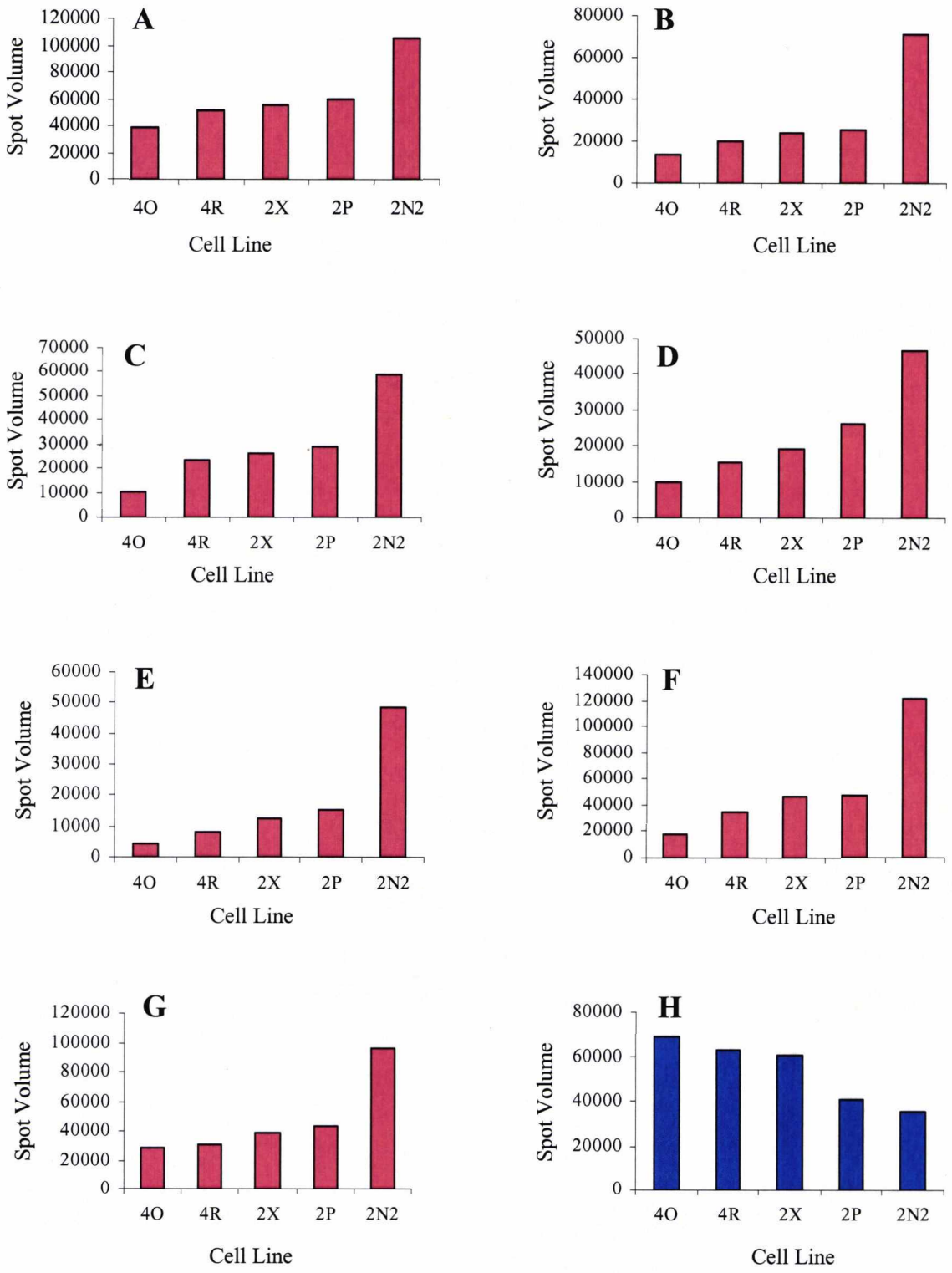

Figure 5.7 The semi-quantitative expression of protein spots 1-8 identified to change in accordance with cellular productivity . The charts show the spot volume information from GS-NS0 cell line microsome fraction proteins detailed later in table 5.3. Up-regulated protein spots are shown in red, down-regulated spots are shown in blue **(A)** Protein 1, **(B)** Protein 2, **(C)** Protein 3, **(D)** Protein 4, **(E)** Protein 5, **(F)** Protein 6, **(G)** Protein 7, **(H)** Protein 8.

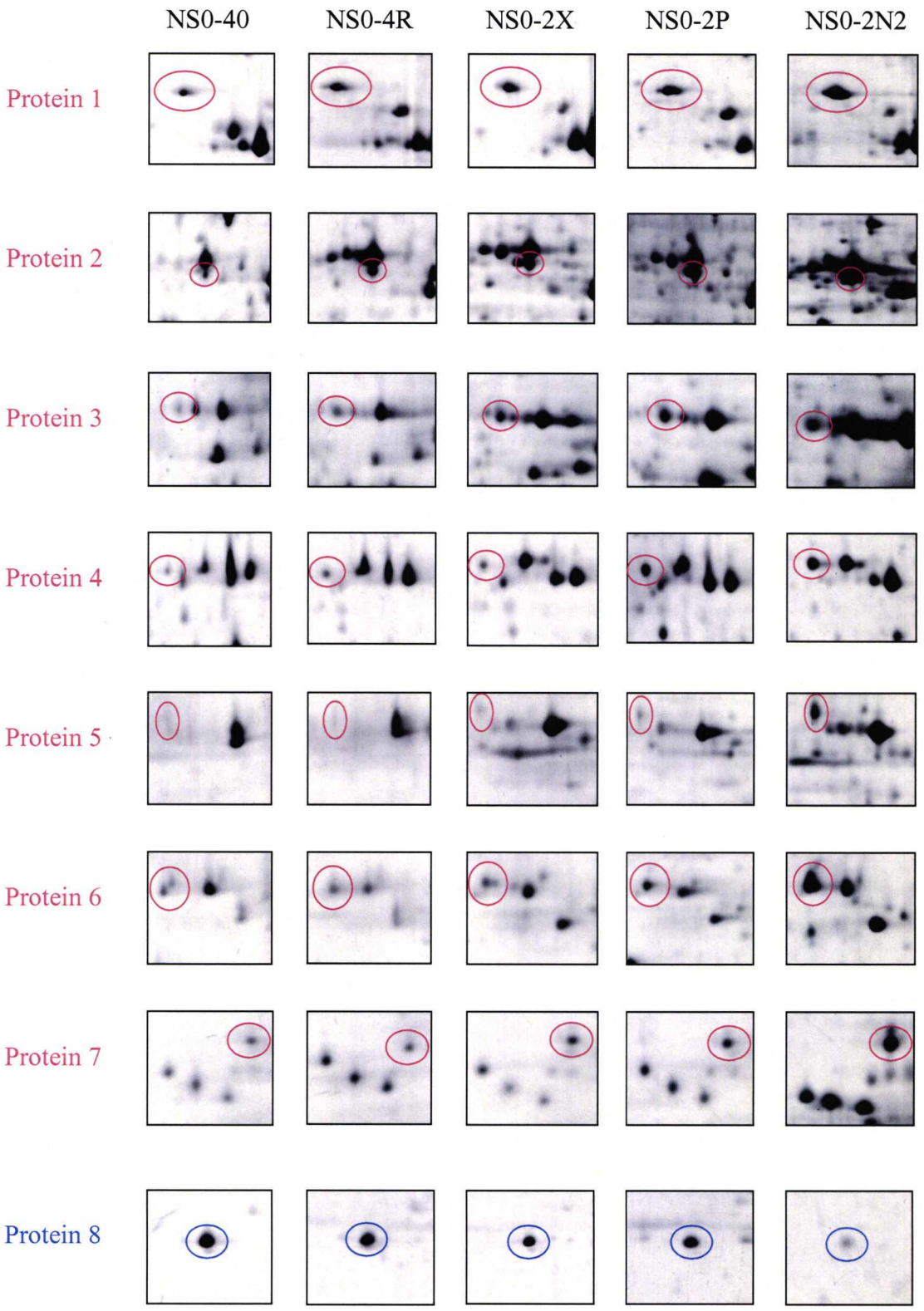

Figure 5.8 Regulated protein spots from GS-NS0 microsome fractions that correlate with cell specific productivity. Enlarged regions from each gel are shown to provide better resolution of spots selected for protein identification. All spots (except protein 7) were excised and identified by tandem mass spectrometry (MS/MS). Identifications of numbered proteins are presented in table 5.3

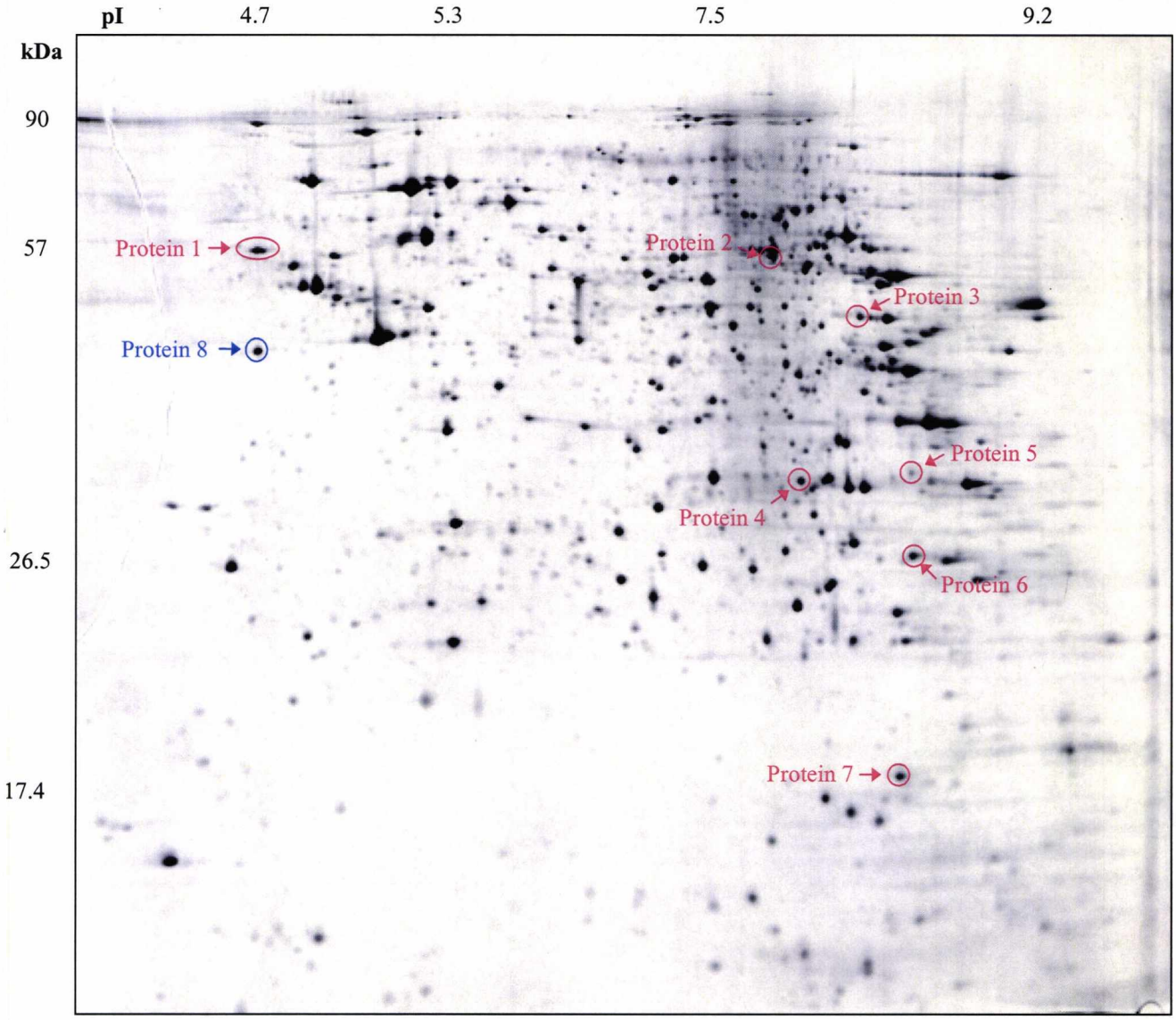

Figure 5.9 Large format 2D-PAGE separation of the GS-NS0 microsome fraction. Position of protein spots that were identified as correlating with productivity (figure 5.7 & 5.8) are highlighted. Proteins highlighted in red represent up-regulated proteins and proteins highlighted in blue represent down-regulated proteins.

Table 5.3 MS/MS Identification of GS-NS0 protein spots that change with increasing productivity.

Protein No.	SwissProt Accession No.	Identification	m/z peak(s)	Sequence Tag(s)	Protein Mass (Da)	pI (theoretical)
Protein 1	PO9103	Protein disulphide isomerase	1781.882 1666.8657 1743.9485	ATEESDLAQQYG EVAFDEK DHENIIIAK	57143	4.79
Protein 2	O08749	Dihydrolipoamide dehydrogenase	1525.8107 1566.8211	HAHPTLS EEQLKEE	54212	7.97
Protein 3	P97807	Fumarate hydratase	1763.9679 1505.7961	AAGGTAVGTGLNTR AAEVNQEYGL	54370	9.12
Protein 4	Q60930	Voltage dependent anion selective channel protein 2	1428.7721	DTTFSPNTGK	31732	7.44
Protein 5	Q60932	Voltage dependent anion selective channel protein 1	1400.735	SSFSPNTGK	32351	8.55
Protein 6	Q9CWH6	Proteosome subunit α type 7	1634.9074	EDPVTVEYITR	27865	8.81
Protein 7*	P18760	Cofilin	N/A	N/A	18780	8.22
Protein 8	P14206	40S Ribosomal protein SA	1203.762	AAATGATPIAGR	32719	4.74

* Protein identified by peptide mass fingerprint Up-regulated spots Down-regulated spots

Table 5.4 Cellular functions of proteins identified to change with productivity

Protein No.	Identification	Category	Function
1	Protein disulphide isomerase	Protein Folding	Catalyses the formation/Isomerisation of disulphide bonds within the ER
2	Dihydrolipoamide dehydrogenase	Energy Metabolism	Located in the mitochondrial matrix, it catalyses the formation of lipoamide from dihydrolipoamide reducing NAD^+ to NADH in the process (Johnson et al., 1997).
3	Fumarate Hydratase	Energy Metabolism	Catalyses the reduction of malate to fumerate as part of the TCA cycle
4	Voltage dependent anion selective channel protein 2	Energy Metabolism	Found in the mitochondrial outer membrane, and allows the diffusion of small hydrophilic molecules such as adenine nucleotides (Buettner et al., 2000).
5	Voltage dependent anion selective channel protein 1	Energy Metabolism	As Above
6	Proteosome subunit α type 7	Degradation	Involved in an ATP/Ubiquitin-dependent non-lysosomal proteolytic pathway
7	Cofilin	Structural	Controls actin polymerisation /depolymerisation and is the major component of intranuclear and cytoplasmic actin rods
8	40S Ribosomal protein SA	Cell attachment	Thought to be a laminin receptor invoved in tumour cell metastasis (Rao et al., 1989).

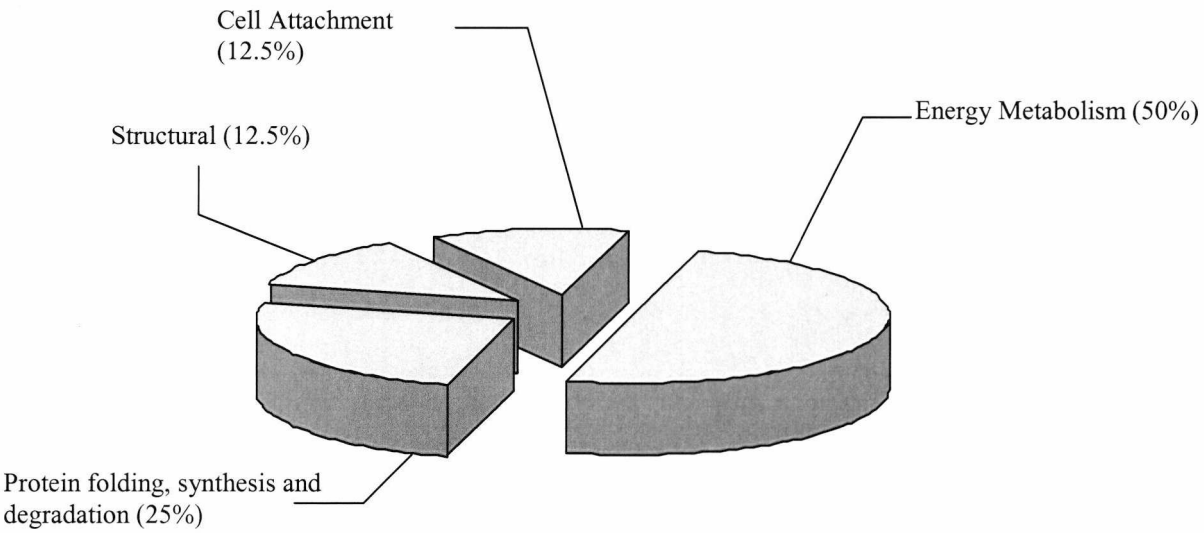

Figure 5.10 Categories of proteins identified to be up/down regulated in with productivity. The 8 proteins identified and semi-quantified were classified by broad functional criteria. The numbers in brackets indicate the percentage fraction of identified proteins represented by each category.

and 5.2.7. Subsequent protein identifications and entry details are presented in table 5.3. The functions and catagories of regulated proteins (i.e. proteins 1-8) are presented in table 5.4.

Figure 5.10 shows the regulated proteins can be grouped into four categories. The majority of the proteins regulated are involved in protein folding/degradation (25%) and energy metabolism (50%). This is unsurprising if we consider this data with reference to the growth and productivity data presented in table 2.1 (Chapter 2). The high producers exhibit lower doubling times (T_d) and as such grow at a faster rate. This increase in growth rate may require the cell to increase its energy needs, and therefore up-regulate components of the energy metabolism pathways. However this is in direct contrast to other previously published studies whereby higher producing cell lines have been reported to exhibit longer doubling times (i.e. grow slower) (Barnes et al., 2001). One must also consider that the processes involved in the increased production of recombinant proteins is likely to be closely linked to or dependent upon, increasing the cells energy needs (e.g. the release of proteins bound to GRP78 is energy dependent, (Lee et al., 1999)) which further supports the case for an increase in components of the energy metabolism pathways. However, once again this does not fit exactly with the view that cells which grow quickly

have less 'excess' energy capacity to produce recombinant protein while slower growing cells have more 'excess' energy capacity which can be funnelled towards recombinant protein production.

Of the eight proteins identified that are regulated as a result of increase mab production, protein disulphide isomerase (PDI) (protein 1) is the only protein that is known to be actively involved in the folding and modification of proteins within the ER. PDI is an abundant soluble acidic protein that catalyses thiol:protein-disulphide interchange reactions and, dependent on the redox state of the substrates and the overall applied redox potential, can catalyse net protein disulphide formation, reduction or isomerisation (Frand et al., 2000). In mammals, PDI constitutes approximately 0.4% of total extractable protein, 2% of total protein in the microsome fraction, and 10% of the soluble protein content of the ER lumen (Frand et al., 2000). PDI's cell and tissue distribution suggests that it acts as a catalyst of native disulphide bond formation during the biosynthesis of secretory and cell surface proteins. Furthermore, Roth et al., reported a specific association between PDI and newly-synthesised immunoglobulin chains within the ER (Roth and Pierce, 1987). This suggests that PDI may be up regulated in the GS-NS0 cell lines investigated here in response to increased mab production (protein 1 figure 5.8) in order to catalyse the formation or isomerisation of disulphide bonds present between the B72.3 heavy and light immunglobulin chains.

It has been reported for many years that the cellular PDI levels correlate with synthesis rates in cells producing secretory proteins (Lambert and Merten, 1997). Indeed, Hensel et al. were able to demonstrate that the sythesis of secretory proteins is preceded by an increase of the mRNA levels coding for PDI and the sysnthesis of PDI (Hensel et al., 1994). Furthermore, Robinson et al. reported that the overexpression of cellular PDI levels in recombinant yeast cells very frequently led to an increase in the secretion of foreign proteins (Robinson et al., 1994). However, a recent study by Davis et al. showed that over expression of PDI in Chinese hamster ovary (CHO) cells expressing a tumor necrosis factor receptor: fc fusion protein resulted in low levels of secreted recombinant protein and retention of the synthesised protein within the cell (Davis et al., 2000)

The increase in the levels of PDI observed within the microsomal fraction correlates with work performed in this laboratory using whole cell extracts, in which PDI was observed to increase with an increase in cellular productivity (Smales et al., unpublished). This is further corroborated by immunoblots of whole cell extracts form each cell line using an anti-PDI antibody, that clearly show an increase in PDI levels with increasing mab productivity (figure 5.11 A). This evidence demonstrates the observed increase in PDI levels, and therefore on the 2D gels is not the result of inconsistencies in gel loading, staining or quantitation. Furthermore, a report by Lambert and Merten investigating ER based proteins in various mouse hybridoma cell lines concluded that although cellular levels of PDI do not depend on mab production rate, it is likely that higher cellular PDI levels would lead to an increase in specific mab production (Lambert, 1997). These findings, together with the evidence presented here, indicate that the formation of disulfide bonds or the chaperone activities of PDI can be a rate-limiting step.

It is important when undertaking an analysis of changes that may lead to increased production of recombinant mab's that we consider what proteins do not show any change in abundance in response to increased mab production. Figure 5.12 shows the changes observed to occur in selected proteins that may play a role either directly or indirectly in pathways involved in recombinant protein sysnthesis such as folding (GRP78 & PPIase), initiation of stress responses (HSP70) and energy metabolism (HSP60). This figure demonstrates that these proteins show either no significant change in abundance (which correlate with higher productivity), or change in a cell specific manner (Figure 5.12B). One of the protein candidates hypothesised to be up-regulated with an increase in mab productivity is GRP78 (also referred to as immunoglobulin binding protein, BiP). GRP78 is a 78 kDa broad specificity molecular chaperone resident in the ER and a member of the HSP70 family of molecular chaperones. GRP78 binds transiently to newly-synthesised proteins in the ER, and more permanently to misfolded, underglycosylated or unassembled proteins whose transport from the ER is blocked (Gething, 1999). Although GRP78 has a broad substrate specificity its association with Immunoglobulin (Ig) heavy and light chains are among the best characterised. GRP78 binds transiently to nacent Ig light chains *in vivo* when the variable region is in an unfolded state, and on unassembled Ig heavy chains in the C_H1 domain (Lee et al., 1999). GRP78 is thought to play a role in the folding and assembly of newly sythesized proteins by recognising unfolded polypeptides and by intra- or intermolecular aggregation, maintaining them in a state competent for subsequent folding

and oligomerisation (Gething, 1999). Other roles for GRP78 include maintaining the permeability barrier to the ER membrane by sealing the lumenal end of the translocon pore before, and in early, translocation (Hamman et al., 1998).

As mentioned previously, it would be a valid assumption that due to the intimate nature of the association of GRP78 with Ig heavy and light chains, that the expression of GRP78 would be up-regulated in response to an increase in the production of recombinant mab's. However, figure 5.12B clearly shows that there is no increase in the abundance of GRP78 present in the microsomal fraction of the GS-NS0 cell lines under investigation. Furthermore, western blots carried out using whole cell fractions probed using an anti-GRP78 antibody (figure 5.11B) shows no increase in GRP78 levels with increasing productivity levels. This evidence further corroborates the findings presented for the microsomal fraction. An increase in GRP78 levels would indicate that the ER is under stress caused by the accumulation of misfolded protein aggregates or the reduction in the levels of free GRP78. Such increases in chaperone levels are likely to signal the initiation of the unfolded protein respons (UPR) (Gething, 1999). When unfolded proteins accumulate in the ER the cell responds by increasing its ability to fold proteins, thus alleviating the increasing demand on the existing cellular protein folding machinery. However, the initiation of the UPR usually leads to the cessation of cell growth and proliferation, and if the ER stress is too severe, cells are directed into the apoptotic pathway (Cudna and Dickson, 2003). From the growth characteristics data presented for the GS-NS0 cell lines (Chapter 2), there is no evidence of a premature cessation of growth and proliferation (when compared to the transfectant blank, which is not producing any mab) suggesting that it is unlikely the cells have initiated the UPR. This indicates that the amounts of recombinant mab synthesised by the GS-NS0 cell lines under investigation here are not sufficient to cause ER stress and initiate increased expression of GRP78. Therefore this may explain the relatively constant levels of GRP78 observed in figure 5.11. This finding agrees with a study by Lambert and Merten, who reported that it is unlikely that there is a direct relationship between mab production rate and cellular GRP78 levels (Lambert, 1997). Furthermore, the effect of GRP78 over-expression in the protein secretory pathway has previously been examined in CHO cells by Dorner et al. Dorner et al. reported that over-expressed GRP78 decreased the secretion efficiency of proteins that transiently associated with this chaperone. This report also suggests that GRP78 may be involved in selective protein retention in the ER and that its over-expression does not

enhance recombinant protein production (Dorner et al., 1992). This evidence suggests that in the GS-NS0 cell lines investigated here, the intracellular levels of GRP78 do not represent a bottleneck in the production of recombinant mab.

The identification of proteasome subunit α type 7 (Protein 6, figure 5.7 & 5.8), as a protein that exhibited an increase in abundance with increasing cell specific recombinant mab productivity suggests that protein degradation plays a role in maintaining high productivity of recombinant proteins. The proteasome subunit α type 7 is part of the 20S proteasome complex. This is the proteolytic core of several intracellular high molecular mass multi-subunit proteinase complexes. ATP-dependent assembly of the 20S proteasome and a regulatory 19S complex results in the formation of the 26S proteasome, which is involved in ubiquitin dependent protein degradation (Stohwasser et al., 1996). With regard to function, the 20S proteasome occupies a central role in intracellular protein metabolism, being involved in processes such as cell cycle, apoptosis and transcriptional regulation (Stohwasser et al., 1996). It is possible that protein degradation plays a role in the context of recombinant mab synthesis being involved in targeting misfolded intermediates rapidly to the ubiquitin-dependent proteasome pathway (Schubert et al., 2000). This should ultimately prevent protein aggregation and may delay the onset of any unfolded protein response in high producing cell lines, which as discussed earlier is detrimental to cell growth. It should be noted however, that it remains unclear whether the up or down regulation of a component of the 20S proteasome complex constitutes an up or down regulation in protein degradation within the cell.

In total 8 proteins expression levels were observed to change with increasing mab productivity. Only one of these proteins was observed to be down-regulated as a result of increased productivity (Protein 8 figure 5.7H & 5.8). This protein was identified by MS/MS (table 5.3) as 40S ribosomal protein SA. This protein was originally identified as a precursor of the high affinity metastasis associated murine laminin receptor. The laminin receptor is believed to play a role in cellular events such as adhesion, morphology, spreading, migration, differentiation and tumour cell metastasis (Rao et al., 1989). As the precise role of this protein is unclear, and due to the limited literature available, one can only speculate as to why it is down regulated in response to increasing productivity. This may be due to the protein becoming somewhat redundant within a suspension cell culture

environment. The down regulation may allow the cell to direct energy resources to pathways and mechanisms more relevant to the cells immediate environment. In other words, the cell simply does not need to synthesise this protein under the culture conditions utilised for this study.

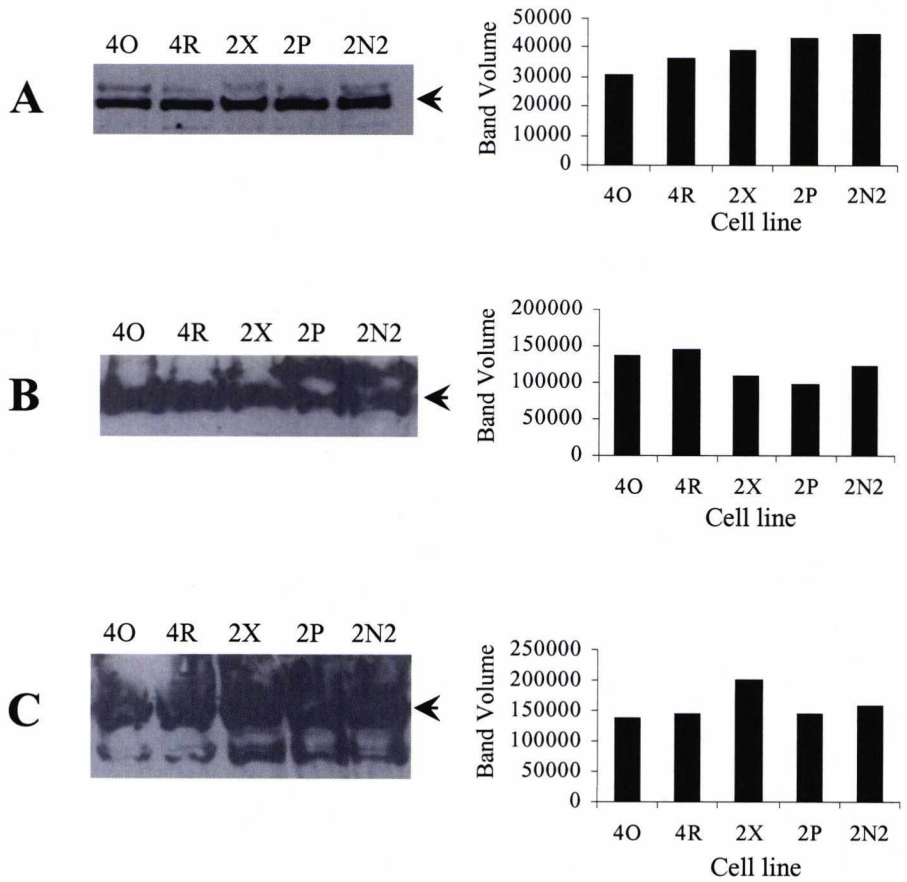

Figure 5.11 Immunoblots of whole cell extracts of GS0-NS0 cell lines. 1×10^7 cells harvested at mid-exponential phase of growth were solubilised in lysis buffer containing 4% CHAPS. Protein quantitation was carried out as described in section 4.2.3. Protein (30 μg) was separated by SDS-PAGE as described in section 4.2.4, and a Western transfer was carried out as described in section 4.2.6. Blots were probed using (**A**) anti-PDI antibody (Stressgen), (**B**) anti-GRP78 (Santa cruz), and (**C**) anti-HSP70 (Santa cruz). Images were quantified using ImageMaster 1D software (Amersham Biosciences). It should be noted that the detection and saturation limits of this approach were not determined and therefore the data must be considered to be semi-quantitative.

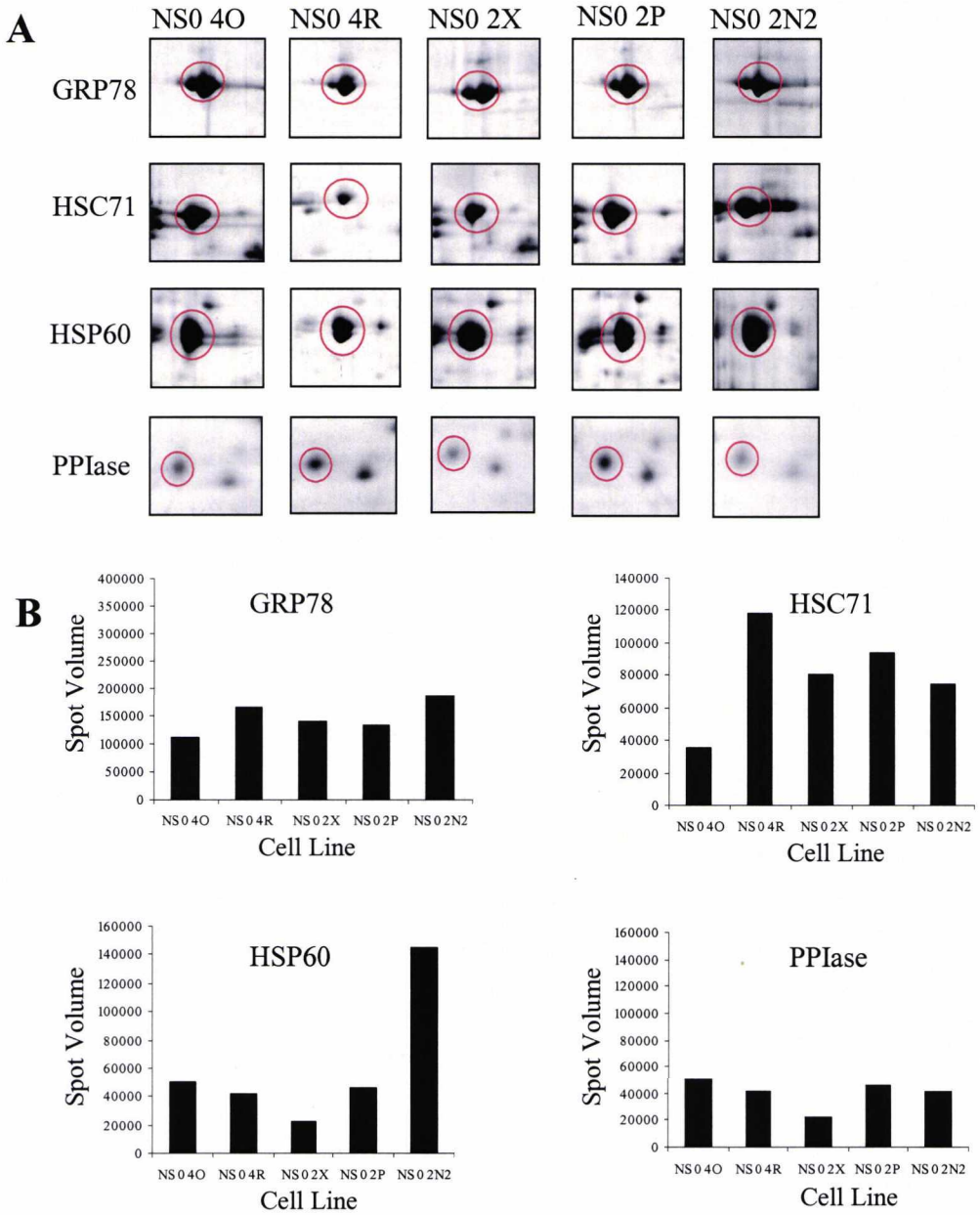

Figure 5.12 Changes in expression of proteins identified that may play a role in recombinant protein production. (**A**) Enlarged regions of GS-NS0 cell line gels showing expression of the protein spot of interest. (**B**) Semi-quantitative expression of selected proteins of interest.

5.3.4 Comparative analysis of the NS0 parental cell line and a GS-NS0 transfectant blank

Previously in this study it was clearly demonstrated that the insertion of the GS vector adversely affects the growth of the GS-NS0 cell lines (Chapter 2, figure 2.1A). This is thought to be most likely due to the need to synthesise glutamine (discussed in detail in chapter 2, section 2.3.1). In order to further assess the effects of vector insertion on the GS-NS0 microsomal proteome, a proteomic analysis was carried out between the parental cell line and the GS-NS0 transfectant blank. Sample preparation, gel running, staining and analysis were all performed as described in section 5.3.2.

In total 7 proteins in the microsome proteome were observed to have changed significantly between the parental cell and the GS-NS0 transfectant blank (figure 5.13). However, the identity of the majority of these changes elusive to date by either MALDI-TOF peptide mass fingerprinting or the generation of peptide sequence tags by MALDI-MS/MS. However, two of these proteins were identified by peptide sequence tag and are presented in table 5.5. In the absence of identifications for all the protein changes, it is difficult to assess the effects of vector insertion on the NS0 microsome proteome. Furthermore, it is also equally difficult to discern what changes might be the result of clonal variation, and what changes account for vector insertion. However, one can speculate as to likely functions of the protein changes. It is likely that the protein changes observed are as a result of the need for the transfected cell (i.e. the transfectant blank) to synthesis its own glutamine. It may also be the case that one of the protein changes represents the enzyme glutamine synthetase as this is present on the B72.3 vector (figure 3.1). Murine glutamine synthetase has a calculated molecular weight of 42 kDa (Kuo and Darnell, 1989) and a theoretical pI of 6.47 (swiss prot accessin No. P15105). It is therefore equally plausible that the GS protein is present at sub-proteomic levels (i.e. levels too low to be detected) or at very low level, due to the gene being driven by a weak promotor. Furthermore, it is unlikely that high levels of glutamine synthetase enzyme would be observed in a microsome preparation. One of the possible results of this capability to synthesise glutamine, are changes to the cells complement of proteins involved in providing energy for the demands of this extra metabolic step. This hypothesis is supported by the increase in the levels of ATP synthase γ chain observed in the transfectant blank cell line (Protein 3, figure 5.13).

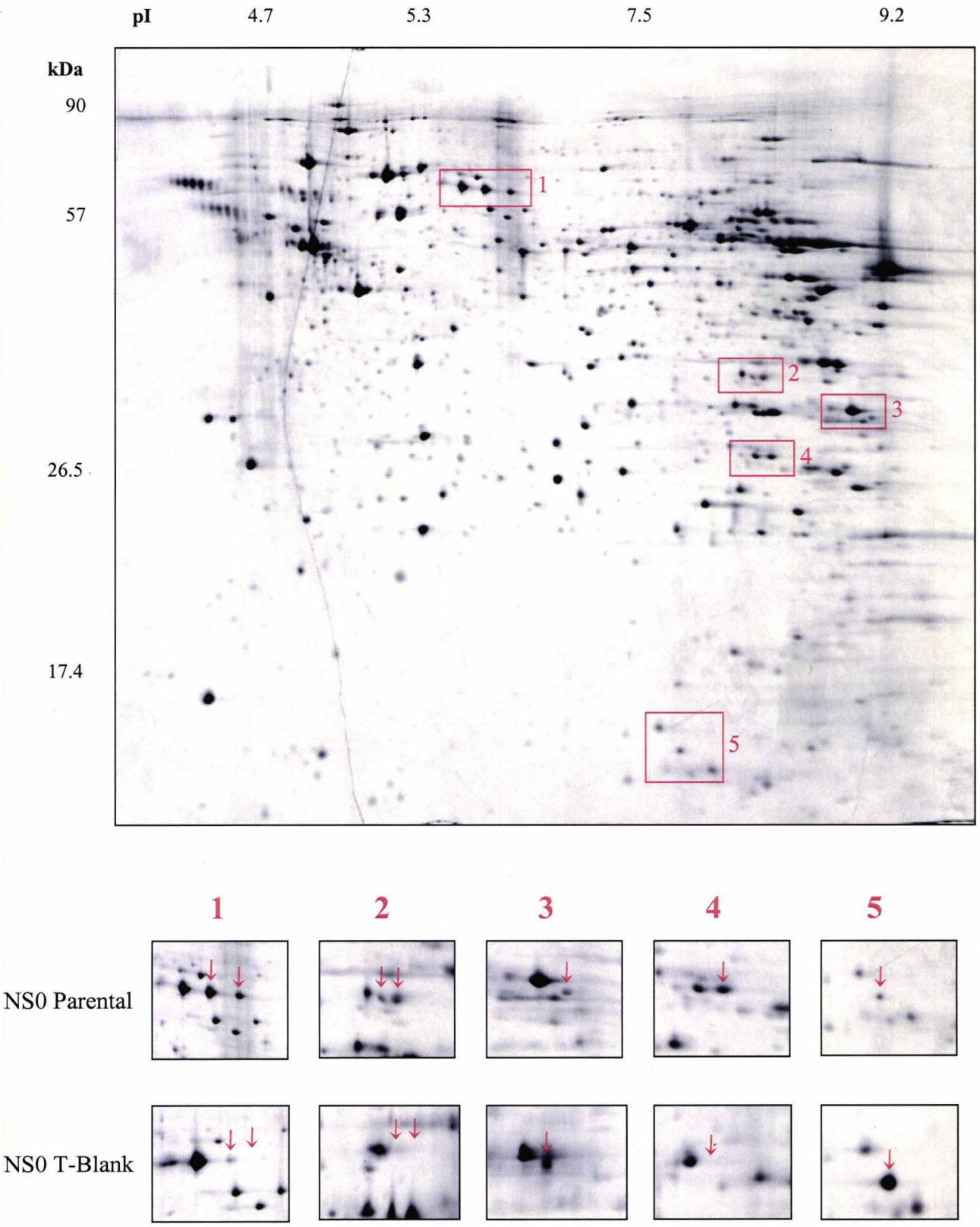

Figure 5.13 Comparison of the NS0 parental microsome proteome with the GS-NS0 transfectant blank microsome proteome. 100 µg of protein was loaded per gel, and proteins spots were visualised by silver staining. **(A)** Locations on the NS0 proteome map of differences in protein expression after insertion of the vector. **(B)** Enlarged regions of the parental and transfectant blank gels showing changes in protein expression identified as a result of transfection with the vector.

Table 5.5 Identifications by tandem mass spectrometry of protein changes after vector insertion

Protein Number	SwissProt accession No	Identification	m/z peak	Sequence tag	Mass (Da)	pI (theoretical)
Protein 3	Q91VR2	ATP synthase γ chain	1754.93	DKLTLTFNR	322885	9.06
Protein 4	Q9R1P0	Proteasome subunit α type 4	1226.72	LDEVFFS	29470	7.58

ATP synthase γ chain is part of F_1 component of the F_0F_1 ATP synthase complex involved in the synthesis of ATP from ADP and P_i. Specifically the γ chain is thought to be involved in binding of the F_1 complex to the F_0 complex located on the inner membrane of the mitochondria, to form a proton conducting channel (Lodish, 1995).

The second protein identified (protein 4) is the proteasome subunit α type 4. This protein is present in the parental cell line but is absent in the transfectant blank (figure 5.13). It is unclear why a component of the protein degradation pathway would be down regulated or absent after the insertion of the vector. Given that the transfectant blank is not producing any recombinant protein, it may be the case that the protein degradation apparatus within the cell has been down regulated to some extent. It was demonstrated earlier in this chapter that the protein degradation apparatus may be closely linked to the expression of recombinant mab, due to the increase in the levels of the proteosome subunit α type 7 with a concurrent increase in recombinant mab productivity (figure 5.7 and table 5.4). However, as stated earlier, it remains unclear whether this down regulation of a component of the proteosome complex constitutes a down regulation in protein degradation within the cell. Furthermore, it is also the case that the parental cell line is not producing any recombinant mab's, and therefore a down regulation in response to this is unlikely. Finally, it may be the case that the protein degradation apparatus is reduced or down regulated in response to the slower growth rate of the transfectant when compared to the parental cell line (Chapter 2, figure 2.1A), although this cannot be confirmed.

5.4 Conclusions

The comparative proteomic analysis presented here of GS-NS0 cell lines producing differing amounts of the recombinant monoclonal antibody cB72.3 has shown that the majority of proteins present within the microsome fraction exhibit no significant change in abundance. Among the population of proteins that do exhibit change, the majority of these are cell specific changes as a result of clonal variation. Few changes were observed (8 in total) in the microsome fraction correlating with an increase in recombinant monoclonal antibody productivity. All eight regulated proteins were identified by mass spectrometry and 50% of these were shown to be involved in energy metabolism.

The levels of the PDI in the microsome fraction were shown to increase with increasing in productivity, which suggests that the levels of this enzyme may represent a rate limiting step in the production of recombinant proteins containing disulphide bonds by GS-NS0 cells in culture. On the other hand, the levels of the immunoglobulin binding protein GRP78 remain relatively unchanged between cell lines, regardless of their cell specific productivity. This suggests that the levels of GRP78 present across the cell lines were sufficient to process the folding and oligomerisation of the increasing amounts of heavy and light chains. We can therefore conclude that within the GS-NS0 cell lines investigated here, the levels of GRP78 are unlikely to be rate limiting with respect to the production of recombinant monoclonal antibodies. It is clear that other processes such as energy production/utilisation and protein degradation play an important role in high level recombinant protein production, but to what extent remains unclear. What is clear is that due to the cell specific nature of the majority of the changes, and the small number of proteins identified that correlate with productivity, is that a productive cell exhibits a 'bias' towards its range of proteins involved in a range of integrated cellular functions such as productivity and metabolism.

This data shows that for GS-NS0 cell populations that exhibit a relatively high cell specific mab productivity, the intracellular content of the major protein machinery is not notably different to that in low producing cell populations. This implies that for cell populations selected for high productivity there is little evidence of a concerted regulation of the major secretory pathway proteins. Perhaps this is not surprising considering the

numerous coordinated cellular processes involved in recombinant protein synthesis, folding, post-translational modification, and secretion. Ultimately these results show that the cellular engineering of single components in order to improve cellular productivity is likely to fail in most cases.

Finally, from the data presented here it is difficult to assess the effects of vector insertion on the microsome proteome and formulate any concrete conclusions due to the limited number of protein identifications and the difficulty in discerning change as a result of vector insertion and change as a result of clonal variation. It is likely be the case that an analysis using whole cell fractions is needed to address the effects of vector insertion in a more comprehensive manner. We would not necessarily expect to see any major changes in the microsome component of GS-NS0 cells after vector insertion.

Chapter 6 Comparative proteomic analysis of GS-NS0 mab producing cells against GS-CHO mab producing cells and GS-NS0 cells producing recombinant TIMP-1.

6.1 Introduction

Chapter 5 reported the findings from a comparative proteomic analysis of GS-NS0 cell lines with respect to whether those cell lines that exhibited high level recombinant mab secretion have altered expression of microsome fraction components. Although GS-NS0 cells are used for the production of therapeutic proteins, Chinese hamster ovary (CHO) cell lines are extensively used for the expression of biopharmaceutical protein products. In order to ascertain if the changes in protein expression observed in the GS-NS0 cell lines that correlate with increased production of recombinant monoclonal antibodies were also prevalent in GS-CHO cell lines producing differing levels of the same monoclonal antibody (i.e. are these changes conserved between cell lines producing the same recombinant protein), a selection of GS-CHO cell lines were generated producing the cB72.3 monoclonal antibody and fully characterised (Chapter 2). These cell lines were

subjected to the same rigorous proteomic analysis as described for the GS-NS0 cB72.3 producing cell lines (Chapter 5).

Concurrently, a comparative proteomic analysis was undertaken between an NS0 cell line producing the cB72.3 monoclonal anitibody (GS-NS0 4R) and an NS0 cell line producing the homomeric metaloproteinase inhibitor TIMP-1 (GS-NS0 TIMP-1). This was investigated in order to address whether changes in protein expression as a result of recombinant protein production are product specific. In particular cell lines expressing these two recombinant proteins were chosen in order to investigate possible differences involved in the production of multi-domain, multi-gene products (mabs) as opposed to a single gene, single domain protein product (TIMP-1) We have investigated the changes in expression levels of a variety of proteins involved in different cellular functions when expressing these different recombinant proteins in the same cell system. The results of this investigation and implications are discussed herein.

6.2 Materials and Methods

All materials and methods pertaining to this chapter were as previously described for the comparative proteomic analysis of the GS-NS0 cB72.3 producing cell lines in chapter 5.

6.3 Results and Discussion

6.3.1 Separation and characterisation of the GS-CHO microsome proteome

GS-CHO cells (1×10^8 CHO 22H11) were harvested and subjected to a cell fractionation procedure as described in section 4.2.2. The resulting microsome fraction was separated by 2D-PAGE as described in section 5.2.1. The gel was visualised using silver staining (section 5.2.2). The image of the resulting silver stained gel is presented in figure 6.1. The average number of spots observed in the GS-CHO microsome proteome was 871 spots $\pm$ 44 (based on 4 gels). This compares with an average of 813 spots for the GS-NS0 cell line (section 5.3.1). However, when comparing the GS-CHO microsome proteome to that of the GS-NS0, it appears that there is less acidic proteins present in the proteome map (i.e. possessing pI's between 3 and 6). This may be due to the variation in post-translational modification of proteins observed between species.

For identification purposes (mass spectrometry), 2D-PAGE gels were run as described in section 5.2.1 with a protein load of 500 µg/350 µL lysis buffer, and focussed for a total of 150,000 Vhrs. The gels were visualised using coomassie stain as described in section 5.2.3. The major protein spots were excised from the gel and subjected to in-gel proteolytic digestion and MALDI-TOF mass spectrometric analysis as described in sections 5.2.5 and 5.2.6. Peptide mass fingerprints (PMF) were generated for each protein spot excised. The success rate of GS-CHO cell protein identification by PMF was very limited only 5% all the spots subjected to PMF identified (2 matches out of a total of 35 spots excised). This low success rate is thought to be mainly due to a loss of strigency involved in cross-species database matching, as a database of Chinese hamster proteins is not currently available. The general consensus also seems to be that the CHO protein complement and the makeup (amino acid sequence) of CHO proteins is not as close a match to the mouse protein complement as initially thought. Therefore MS/MS sequence tagging is absolutely essential for the analysis and identification of CHO proteins, however until a CHO database becomes available even this will give a low or limited number of positive protein identifications. Therefore a comparative matching approach was undertaken to tentatively identify protein spots based on their molecular weight and pI values as determined by their migration point on a 2D gel. This was undertaken using a

combination of the NS0 microsome proteome map presented in chapter 5, and publised CHO proteome maps (Champion et al., 1999; Van Dyk et al., 2003). Spots which were identified with a 'reasonable' degree of certainty are listed in table 6.1 with the respective positions on the GS-CHO microsome proteome map indicated in figure 6.1 (Champion et al., 1999; Van Dyk et al., 2003). Overall, a comparison of the GS-CHO and GS-NS0 microsome proteome maps shows that many of the major protein spots are present on both gels, suggesting the cellular machinery is similar and at roughly the same levels, and in both cases there is a small number of proteins observed that correlate with productivity.

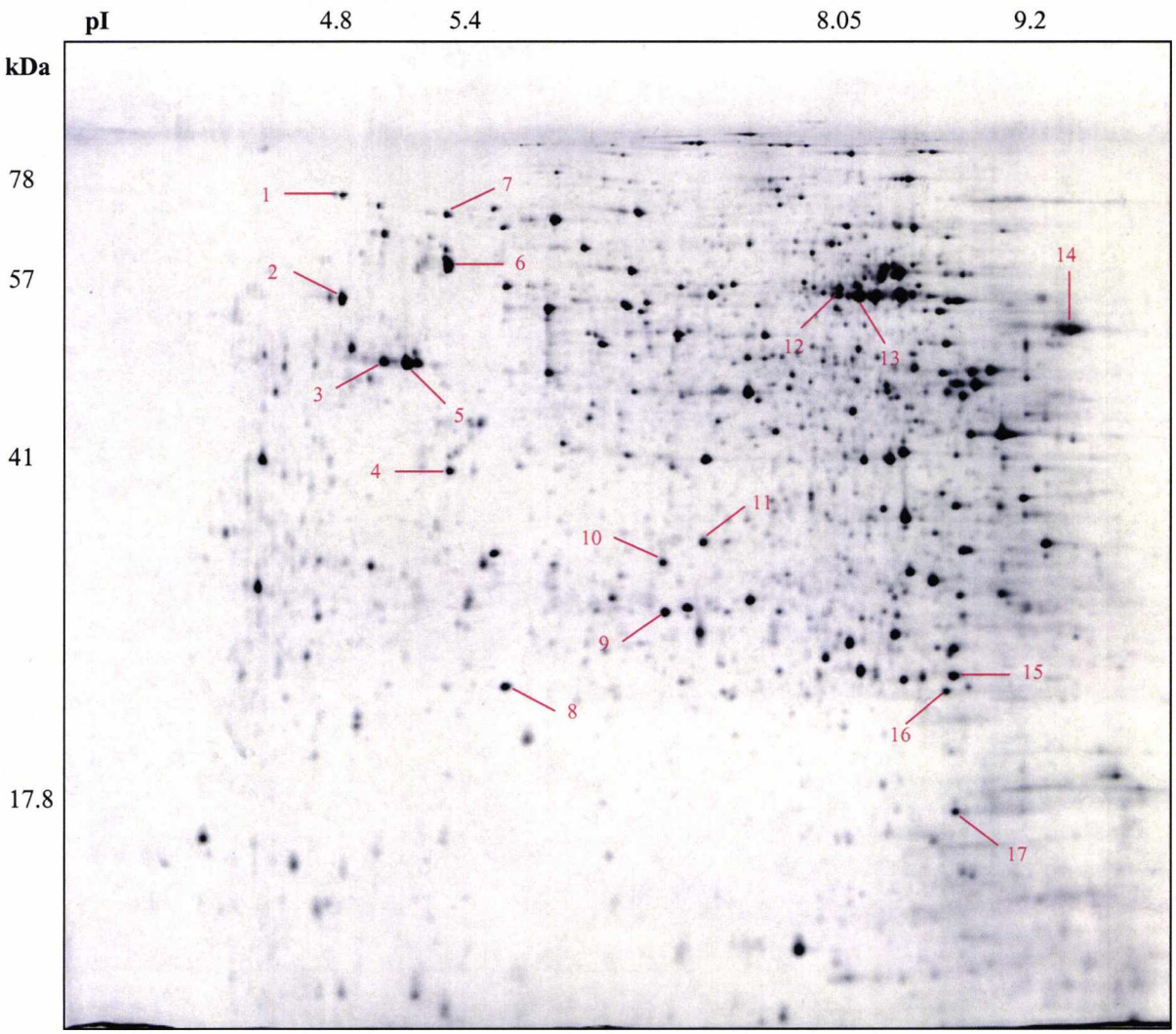

Figure 6.1 Current tentative identifications of proteins in the GS-CHO microsome proteome map. Spots were identified by a combination of comparative matching using published maps and peptide mass fingerprinting.

The majority of the proteins identified were, as in the GS-NS0 microsome proteome, those involved in protein synthesis and energy/nutrient metabolism. Two proteins identified on the GS-CHO microsome map that were not identified on the GS-NS0 microsome map are glutamate dehydrogenase (spot 12 & 13), and superoxide dismutase (spot 16). Glutamate dehydrogenase was identified by PMF. Eight of the fifteen experimentally obtained peptide masses matched the theoretical masses of this protein (mascot score of 73, scores >56 were significant). Glutamate dehydrogenase is involved in catalysing the formation of α-ketoglutarate from L-glutamate and is located within the mitochondria (Meister, 1985). On the other hand, superoxide dismutase is also located in the mitochondrial matrix and is involved in protecting the cell from free radicals generated during oxidative phosphorylation (Hearn et al., 2001).

Table 6.1 Identification of protein spots from the GS-CHO proteome map

Protein	Identification	Accession No.	MW (Da)	pI (theoretical)
1	GRP78*	P20029	72493	5.07
2	PDI*	P09103	57143	4.79
3	ATP synthase β*	P56480	56256	5.19
4	Actin*	P48975	41711	5.22
5	PDI*	P27773	56621	5.99
6	HSP60*	P19226	61091	5.91
7	HSC71*	P08109	71059	5.37
8	ATP synthase δ*	Q9DCX2	18665	5.53
9	Peroxiredoxin*	O08807	31265	6.67
10	Proteasome subunit β*	P70195	30220	8.14
11	Proteasome subunit α*	Q9R1P4	29818	6.00
12	Glutamate dehydrogenase¶	P26443	61337	8.05
13	Glutamate dehydrogenase¶	P10860	61428	8.05
14	Elongation factor 1 α*	P10126	50163	9.10
15	Glutathione S transferase§	P46424	23507	8.1
16	Superoxide dismutase§	P04179	22204	7.3
17	PPIase§	P05092	17881	8.2

* Proteins identified by comparative matching with GS-NS0 microsome proteome map (figure 5.3)
§ Proteins identified by comparative matching with a CHO map published by Champion et al. (Champion et al., 1999)
¶ Proteins identified by MALDI-MS peptide mass fingerprinting

6.3.2 Comparative proteomic analysis of GS-CHO cell lines differing in monoclonal antibody productivity

Comparative proteomic analysis of GS-CHO cell lines was undertaken using large format two dimensional gels run using 1×10^8 GS-CHO cells (22H11, 34C10, 63E4 and 30B5) harvested at mid-exponential phase of growth. Microsome fractions were prepared from these cell lines as detailed in section 4.2.2. Gels were run, visualised (silver), and recorded as described in section 5.2.1. Image analysis software was used to detect the protein spots using the detection parameters described in section 5.2.4. Background subtraction and spot matching was carried out as described in section 5.3.2. Figures for total spot numbers and total spot matches (matches made to a reference gel) are presented for the GS-CHO cell lines in table 6.2. A high degree of matching was achieved with over 80% of all gel spots matched to the reference gel.

The image analysis software was used to identify protein spots which showed an increase/decrease in abundance in response to an increase in mab productivity. In total 7 spots were identified (4 up-regulated and 3 down-regulated) which fit this criteria. The expression patterns of these proteins were quantified by ImageMaster software and the resulting semi-quantitative data is presented in figure 6.2. A visual representation of the spots identified to be up/down-regulated is shown in figure 6.3 with their corresponding positions on the GS-CHO microsome proteome map indicated in figure 6.4. In general the majority of proteins present in the GS-CHO microsome proteome showed no changes in abundance between the cell lines and the majority of those that do change, do so in a cell specific manner, similar to that observed for the GS-NS0 cell lines.

Table 6.2 Gel statistics from the image analysis of the GS-CHO 2D gels

Cell Line	Total Spot Number	Total Spot Matches	% Match*
CHO 22H11	897	839	93
CHO 34C10	830	684	82
CHO 63E4**	920	918	99
CHO 30B5	840	673	80

*Number of spots matched to the reference gel
** This gel was selected as the reference gel

The pattern of expression of regulated proteins (i.e. those proteins whose expression increases or decreases with an increase in productivity) in the GS-CHO cell line differs from that observed in the GS-NS0 cell line. Firstly, there are less regulated proteins in total, secondly, up-regulated proteins account for 57% of the total regulated proteins (as opposed to 88% observed in the GS-NS0), and finally, the number of down regulated proteins is increased in the GS-CHO cell line (43% in GS-CHO and 12.5% in GS-NS0). However, these figures may be mis-leading due to the small number of charges observed. Furthermore the range of cell specific productivities available for study in the GS-CHO range (i.e. ~10 fold change) was much smaller than in GS-NS0 cell lines (i.e. ~ 100 fold change).

However, the data presented here clearly shows that the regulation (up or down) of specific proteins which may result in high level productivity is not conserved between different cell types producing the same protein. This is not surprising if we consider that the cell lines investigated (NS0 and CHO) differ considerably in their behaviour in culture (i.e. growth and productivity), their culture conditions, and their nutritional requirements that will ultimately result in quite different protein expression patterns. Unfortunately, due to the limitations in the protein databases discussed earlier, it was not possible to identify the proteins that were shown to change in line with increasing productivity. We can therefore only speculate about the possible roles of these proteins (i.e protein folding, energy metabolism etc.) based on the growth and productivity data presented earlier in chapter 2. As discussed earlier, the GS-CHO cells lines were able to grow at a rapid rate achieving and sustaining high viable cell densities in culture. It was these high cell densities that accounted for the high maximum mab concentration observed in the GS-CHO cell lines, as the specific productivity values (qMab) were lower than those of the top producing GS-NS0 cell lines (table 2.1 & 2.2). Furthermore, high cell viability was sustained even after glucose in the media had been depleted (figure 2.5), with the onset of death phase coinciding with the utilisation of accumulated lactate. Interestingly, a trend was observed in the GS-CHO cell lines between the ability to utilise accumulated lactate and productivity. Therefore it is possible that the up-regulated proteins that are observed in the GS-CHO cell line microsome proteome may play a role in nutrient/energy metabolism (particularly lactate metabolism) in order to sustain cell viability beyond the period of glucose depletion. The up-regulation of proteins associated with metabolism in response to increased production of recombinant proteins is not without precedent. A study by Van

Dyk et al., investigating the cellular changes associated with increased production of human growth hormone in CHO cells by a proteomic approach, showed the induction of a number of cellular proteins located in the mitochondria (Van Dyk et al., 2003). These were subsequently identified as GRP75, enolase, and cytochrome C oxidase, involved in cell proliferation, glycolysis, and ATP production respectively (Van Dyk et al., 2003).

Unlike the GS-NS0 cell lines, an increase in the levels of the enzyme PDI in response to increases in recombinant mab productivity was not observed in the GS-CHO cell lines. The reasons for this are at present unclear. It is however, difficult to be sure that this is indeed the case, due to the different PDI's present within the cell, which as yet have not been identified on the GS-CHO microsome proteome map presented here. Furthermore, as described earlier, as the cell specific productivities between these GS-CHO cell lines did not cover a wide dynamic range we may not have been able to detect significant differences in this study. It is possible that in a very low GS-CHO producer mab productivity may be limited by PDI levels although this is only conjecture.

There was no up-regulation observed in expression levels of the chaperone proteins GRP78 and HSP70 either that correlated with an increase in productivity. This again concurs with findings presented by Dyk et al., who reported that the chaperone proteins GRP78, HSP90, GRP94 and HSP70 were not up-regulated in response to increased production of human growth hormone in CHO cells (Van Dyk et al., 2003). The data presented here suggests that the levels of chaperones involved in protein folding and the prevention of aggregation are not limiting factors in the production of recombinant monoclonal antibodies in GS-CHO cell lines. Furthermore, the growth and productivity data for the GS-CHO lends evidence to the suggestion that the cells investigated here have not implemented a stress response (such as the unfolded protein response), and as such the up-regulation of proteins involved in such responses (e.g. heat-shock proteins) above endogenous levels would not be expected to occur. This is entirely in agreement with the observations in the GS-NS0 cell lines. The results from the studies of both of these systems agree well in that they show, firstly, that mab productivity does not appear to be limited by components of the microsome secretory pathway in either system and, secondly, that every cell line has a bias to its components and make up of its integrated systems (Protein folding, metabolism etc.) due to cell line specific differences.

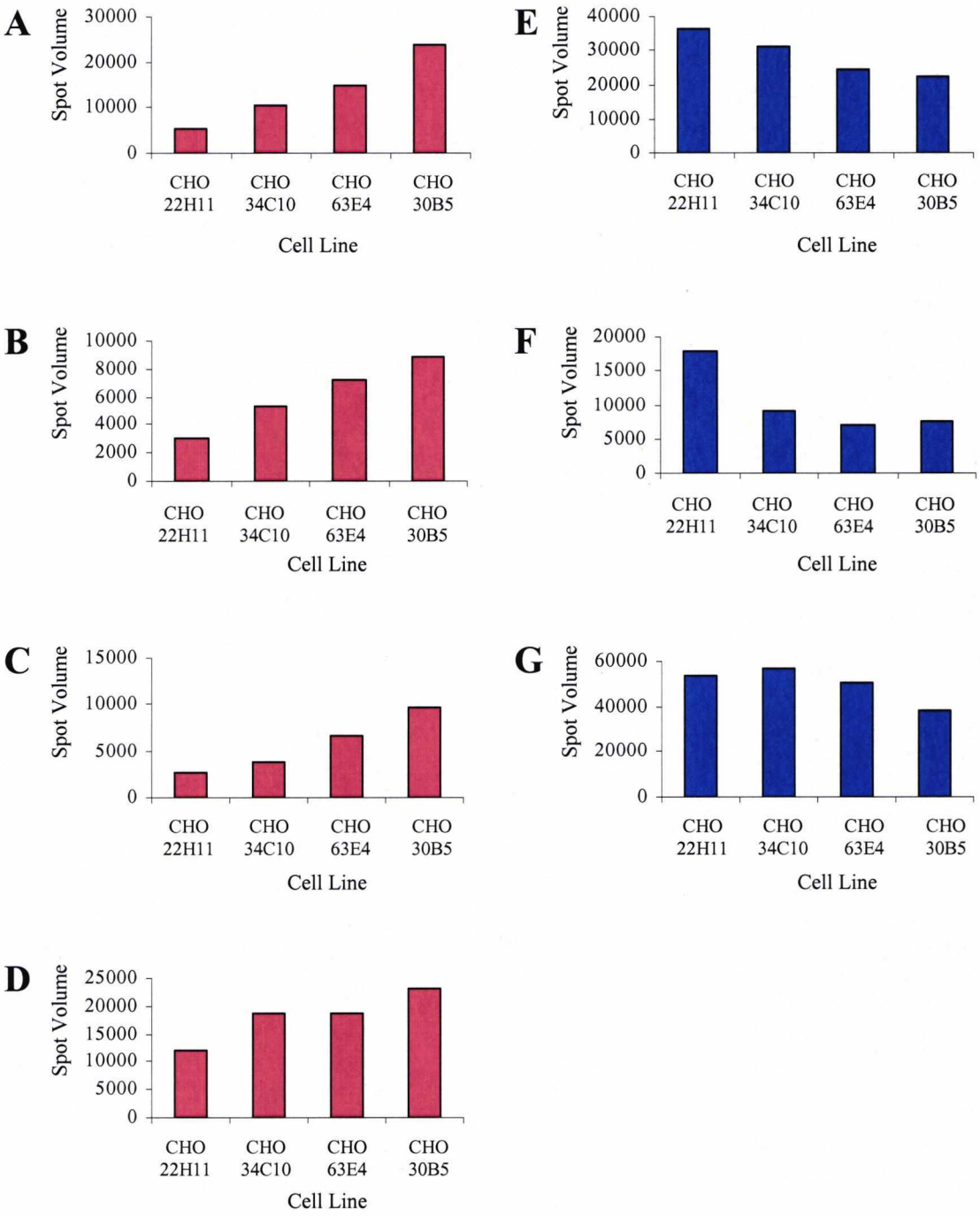

Figure 6.2. The semi-quantitative expression of protein spots that change in expression with cellular productivity. The charts show the spot volume information from GS-CHO cell line microsome fraction proteins. Up-regulated protein spots are shown in red, down regulated protein spots in blue. (A) Protein 1, (B) Protein 2, (C) Protein 3, (D) Protein 4, (E) Protein 5, (F) Proteins 6, and (G) Protein 7.

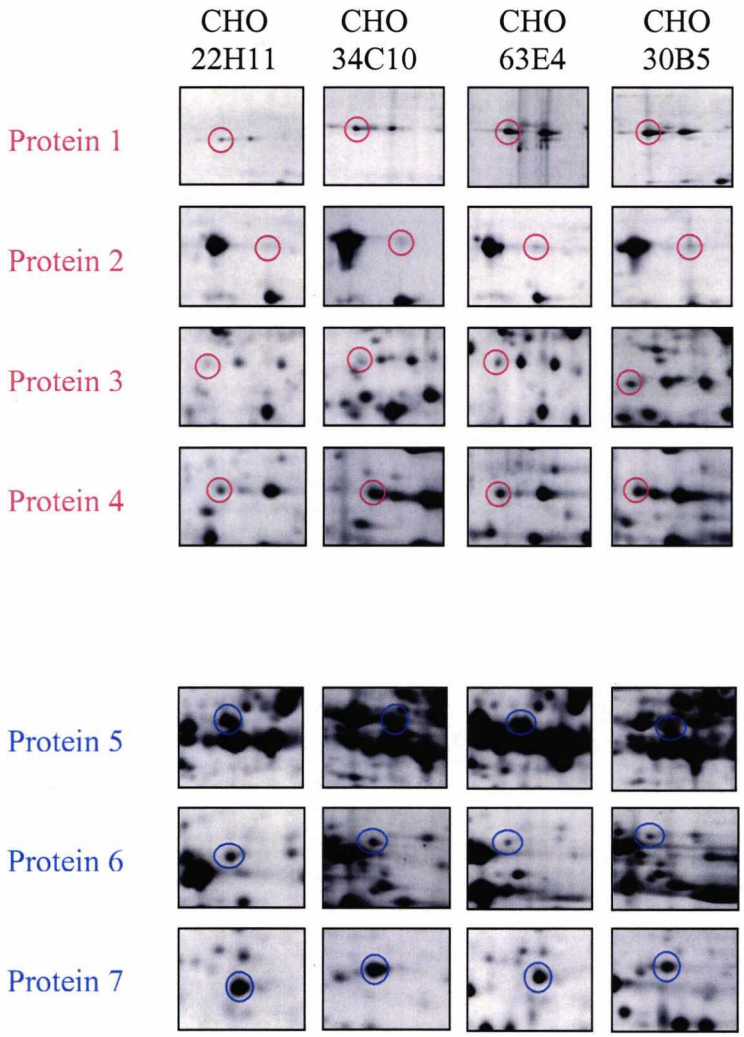

Figure 6.3 Regulated protein spots from GS-CHO microsome fractions. Enlarged regions from each gel are shown to provide better resolution of spots that are shown to increase/decrease with productivity.

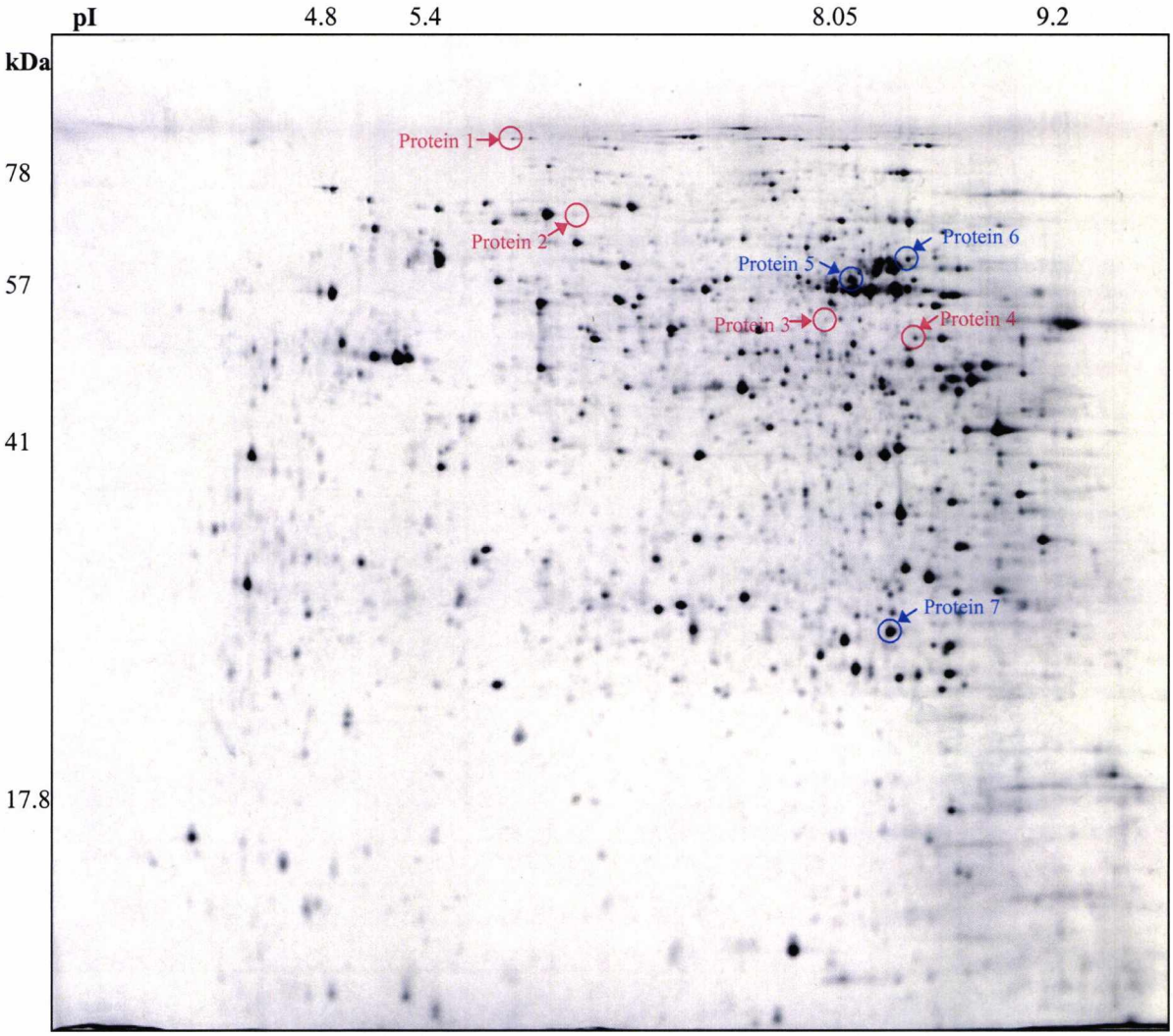

Figure 6.4 Large format 2D PAGE separation of a GS-CHO microsome fraction. The positions of protein spots that have been identified to correlate with productivity (figure 6.2 & 6.3) are highlighted. Proteins highlighted in red represent up-regulated proteins and those highlighted in blue represent down regulated proteins.

6.3.3 Comparative proteomic analysis of Mab and TIMP-1 producing GS-NS0 cell lines

In order to examine the differences in the expression of selected proteins in the same cell line type (GS-NS0 cells) producing different proteins, a proteomic analysis of the GS-NS0 4R cell line versus the GS0-NS0 TIMP-1 producing cell line was undertaken. Both of these cell lines were characterised in detail earlier (Chapter 2) and their growth and productivity characteristics deemed sufficiently similar to compare the cellular machinery utilised by the same cell type to produce two different protein products.

NS0 cells (GS-NS0 4R and GS-TIMP-1, 1×10^8) were harvested at mid-exponential phase of growth and microsome fractions were prepared from these cell lines as described in section 4.2.2. The microsome fractions were then separated by 2D-PAGE, visualised, and recorded as described in section 5.2.1. Image analysis was performed on the resultant images using the parameters detailed in section 5.2.4. Background subtraction and spot matching were carried out as stated in section 5.2.2. Data for total spot numbers and matching (shown as % match) is presented in table 6.3. Matching was carried out using the NS0 TIMP-1 gel as the reference gel. Greater than 80% of the spots present on the NS0 4R gel were matched to the reference gel (NS0 TIMP-1 gel).

A greater number of spots were observed in the NS0 TIMP-1 microsome proteome than in the NS0 4R proteome. Although this illustrates the differences in the microsome proteome that occur even with cells from the same cell line, all major protein spots were present in both gels. Differences in spot number are primarily the result of low abundance spots. The expression pattern of the 2D gels is very similar (figure 6.7), suggesting that the overall protein distribution at mid exponential phase of growth remained more-or-less the same. Figure 6.5 shows a difference map between TIMP-1 and cB72.3 producing cell lines generated using the ImageMaster software. This depicts the difference in protein abundance between the two gels. Spots that differ by more than 2-fold are highlighted. Although the TIMP-1 cell line displays a greater number of spots in the microsome proteome, it can be seen from the difference map (figure 6.5) that a higher proportion of matched spots (i.e. present on both gels) are at least 2-fold more abundant in the NS0 4R cell line. It may be the case that the NS0 4R cell possesses a larger microsome component than the NS0 TIMP-1 cell line. In other words, this data suggests that the NS0 4R cell line has more recombinant protein production machinery at its disposal than the NS0 TIMP-1 cell line. Further evidence for this hypothesis is presented in figure 6.6. Figure 6.6A shows a selection of proteins involved in various aspects of protein synthesis (i.e. polypeptide synthesis, folding and energy metabolism.). In all cases the levels of these proteins present within the microsome fraction is higher in the GS-NS0 4R cell line than in the GS-NS0 TIMP-1 cell line. The expression levels of two proteins previously identified as changing with mab productivity in the cB72.3 producing GS-NS0 cell lines investigated earlier (Chapter 5) are also presented (figure 6.6B). The levels of Proteasome subunit α were

observed to be higher in the TIMP-1 cell line than the 4R. The TIMP-1 cell line also displayed greater abundance of the only protein (40S ribosomal protein SA) to be identified as down-regulated in response to increasing mab productivity.

It is possible that despite the comparable level of secretion observed between the two cell lines, the increased abundance of many proteins involved in aspects of protein synthesis observed in the NS0 4R relative to the TIMP-1 cell line cell may be due to the makeup of the protein being produced. IgG is a multi-subunit protein that consists in its simplest form of two identical heavy chains with a mass of approximately 50 kDa, disulphide bonded to two identical light chains with a mass of approximately 25 kDa, forming an H_2L_2 molecule (Lee et al., 1999). In total IgG possesses four disulphide bonds, two between the heavy chains and two between the light chain and the heavy chain. IgG also possesses only one conserved glycosylation site at Asn-297 (Roitt, 1985). TIMP-1 is a single subunit protein with a mass of approximately 27 kDa. TIMP-1 is stabilized in its tertiary structure by 6 disulphide bonds. It also possesses two N-linked glycosylation sites at Asn-30 and Asn-78 (Huang et al., 1996). The multi-subunit nature of the IgG molecule would most likely require the cell to perform more work to carry out its synthesis than that of the single subunit smaller TIMP-1 molecule. Therefore, it is reasonable to suggest that such an increase in the complexity of the molecule being synthesised would require an expansion of the protein synthesis machinery, which may account for the data presented here.

Table 6.3 Gel statistics from image analysis of NS0 4R and TIMP-1 gels

Cell Line	Total Spot Number	Total Spot Matches	% Match*
NS0 4R	659	563	85
NS0 TIMP-1**	982	982	100

* Number of spots matched to the reference gel
** This gel was selected as the reference gel

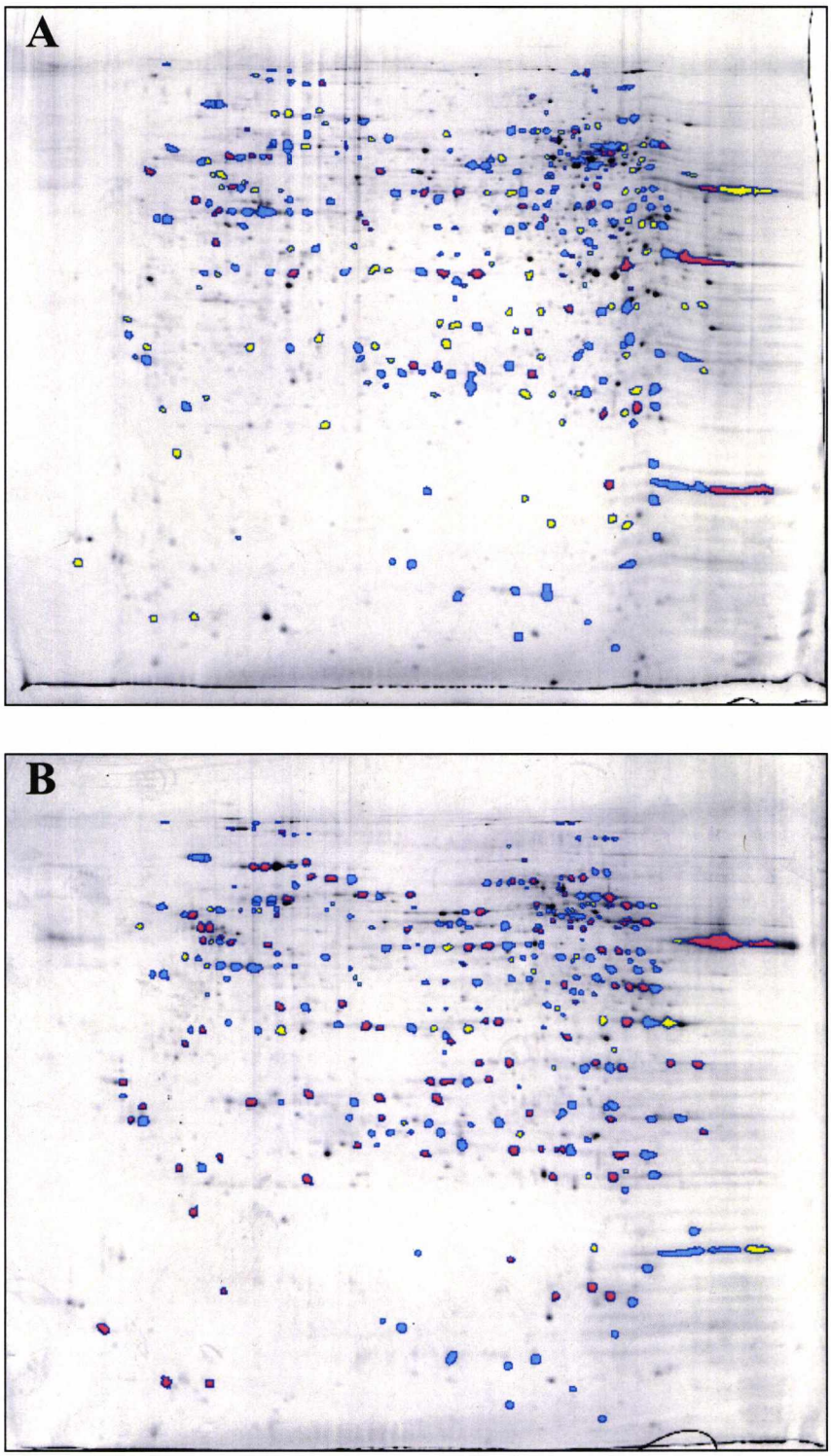

Figure 6.5 Difference maps generated using image master software of 2D separated proteins. (A) GS-NS0 TIMP-1 (B) GS-NS0 4R. Increases in protein expression by a minimum of 2-fold are represented in red. Decreases in spot abundance by a minimum of 2-fold are represented in yellow. Protein spots in blue

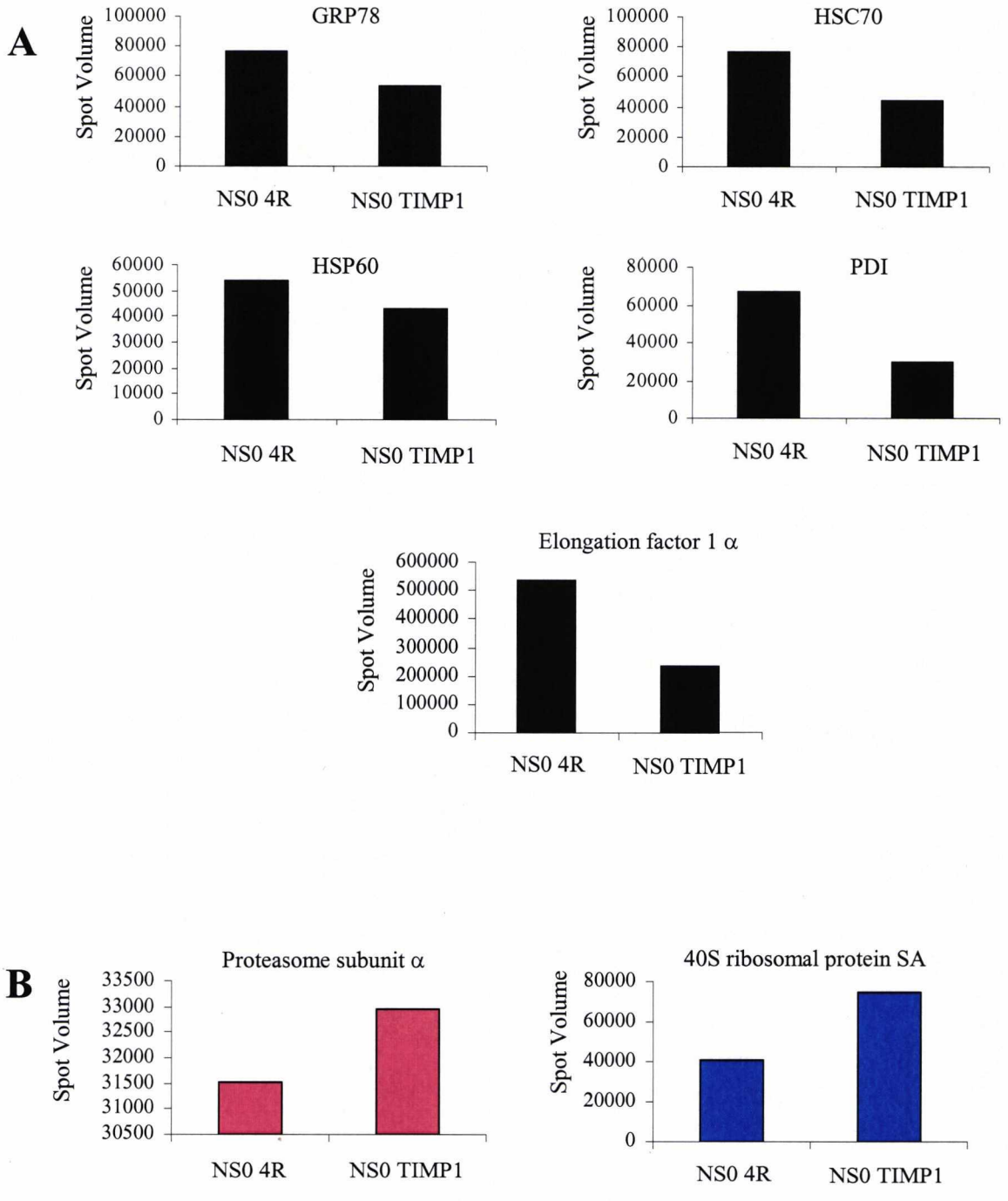

Figure 6.6 Comparison of changes in protein expression between GS-NS0 TIMP-1 and GS-NS0 4R. (**A**) Semi-quantitative expression of proteins are involved in folding, energy metabolism, and polypeptide synthesis. (**B**) Semi-quantitative expression of two proteins identified to be up/down-regulated in accordance with productivity in GS-NS0 cell lines (figure 5.7).

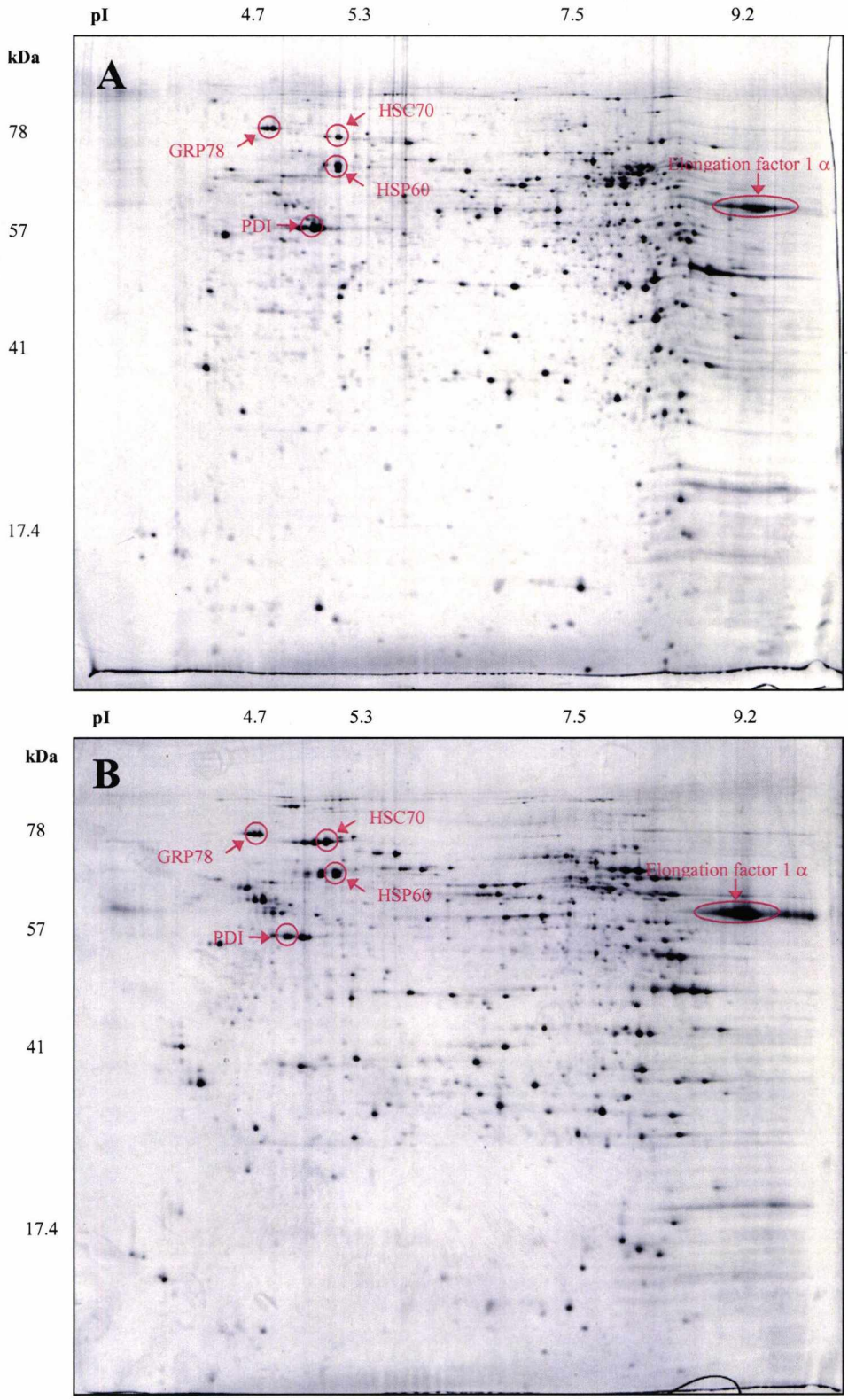

Figure 6.7 Large format 2D-PAGE separation of microsome fractions from GS-NS0 TIMP-1 and GS-NS0 4R. Positions of spots selected for comparison are highlighted. (A) Microsome proteome map of NS0 TIMP-1. (B) Microsome proteome map of NS0 4R.

6.4 Conclusions

In this chapter comparative proteomic analysis was undertaken on GS-CHO cell lines differing in the productivity of the cB72.3 monoclonal antibody. This was carried out to determine if the changes previously observed in the GS-NS0 cell lines (chapter 5) are conserved between different cell types (NS0 *vs* CHO) producing the same recombinant protein product. The data presented here has clearly shown that the specific changes in the microsome proteome that may lead to high-level productivity are not conserved. However, clustering of the proteins that have been observed to change into functional categories has revealed that while specific protein changes may not be conserved the metabolic processes up-regulated (i.e. energy metabolism) are essentially similar between the cell types. This suggestion is corroborated by a study previously published by Van Atken et al. (Van Atken et al., 2003). Van Atken et al. reported that B cells anticipate their secretory role by up-regulating processes in a defined manner. Metabolic capacity expands first, then secretory machinery to accommodate the mass production of IgM that follows (Van Atken et al., 2003).

A proteomic comparison of the microsome fraction of an GS-NS0 cell line producing the cB72.3 monoclonal antibody (4R) versus a GS-NS0 cell line producing the metalloproteinase inhibitor TIMP-1 was also investigated and the results presented in this chapter. It was difficult to assess whether the changes in protein expression observed in the GS-NS0 monoclonal antibody producing cell lines, which correlated with productivity, were conserved between the same cell type producing different protein products. This is because a range of GS-NS0 cell lines producing TIMP-1 was not available. Therefore it is currently unclear as to whether the upregulation of specific proteins is conserved with a cell type producing a different product at roughly equivalent levels. It will be important to understand this further in the future if cell engineering strategies are to succeed. The data presented here for the levels of major proteins present in the microsome proteome between the two cell types shows that there appears to be differences in the machinery available within cells dependent upon what protein product is being produced. Furthermore, it is likely that this increase or expansion in cellular machinery is due to the multi-subunit nature of the IgG molecule being produced as opposed to the single-subunit structure of TIMP-1.

In summary, the analysis presented here for the GS-NS0 and GS-CHO cell lines agree in that there is a high number of cell line specific changes that give each cell an overall bias towards its range of microsomal components. Furthermore, the cellular complement of microsomal machinery does not appear to limit secreted recombinant protein production in the systems investigated and reported here.

Chapter 7 General discussion

This project initially set out to investigate the protein complement of the microsome fraction (i.e. the secretory pathway machinery) of a range of mammalian cell lines that differ in their ability to produce recombinant monoclonal antibodies under batch culture conditions (i.e. different cell specific productivities). A panel of cell lines from two industrially relevant cell types (GS-NS0 & GS-CHO) were extensively characterised (chapter 2) and considered to be ideal for an investigation of this type. The specific aims of this investigation was to identify cellular factors (i.e. proteins) that lead to higher cell specific productivity which ultimately could provide novel targets for genetic manipulation (inverse metabolic engineering, chapter 1). This approach tests a 'conserved mechanism' hypothesis that is to say that cell populations exhibiting higher qMab achieve this by a similar conserved cellular mechanism. It is not possible, by this methodology, to test the alternative hypothesis that different mechanisms underpin functional competence (i.e. divergent mechanisms). In order to simultaneously monitor the changes that occur in the protein complement of the microsome fraction, we utilised a proteomic approach. This approach utilised high-resolution cellular protein separation technology (2D-PAGE) in combination with mass spectrometric identification.

mRNA levels do not correlate with secreted monoclonal antibody protein product

Progress in improving the productivity of mammalian cells has largely been the result of media optimisation and the development of more efficient expression systems resulting in high levels of specific mRNA. The data presented in this thesis has shown however that the amount of specific mRNA (i.e. mRNA coding for the antibody heavy and light chain) does not correlate with the levels of secreted product. While mRNA content for monomeric proteins may be expected to be proportionally related to cell specific productivity, this does not hold true for recombinant mab expression. Furthermore, in the case of mabs, these require the coordinated expression, folding and assembly of both heavy and light chains, and a number of studies have shown qMab does not correlate with available heavy and light chaim mRNA.

One could speculate that either an increase in the mRNA levels is proportional to an increase in recombinant protein productivity up to a certain threshold or saturation level, after which any further increase in mRNA does not result in an increase in productivity, or that each cell only has a certain amount of machinery to translate the mRNA and as such the levels of mRNA are not rate limiting, rather it is the apparatus required for the task that limits its translation. The evidence presented in chapter 3 suggests that combinations of both these factors are occurring. It is likely that each cell line possesses a different mRNA threshold or saturation point, due to differences in the translational machinery present or indeed the efficiency with which the cell utilises the machinery that it has available. Therefore it seems to be the case that a strategy to increase productivity by increasing specific mRNA levels would have limited success as it is dependent on and is proportional to, the efficiency translational machinery within each cell line.

There are other variables which may also affect any possible correlation between mRNA and productivity such as the gene locus. The fact that chromosomal location can affect the expression of eukaryotic genes has been known for a long time and the effect of inserting genes into areas of chromatin can lead to the "position effect", which results in differences in expression of the inserted gene at its new location, as compared with levels of expression when in its native environment (Barnes et al., 2003). However, from the data presented here it is unlikely that the chromosomal location of the genes are having a significant effect. This is due to the low producing cell lines (GS-NS0 4O and GS-NS0 4R)

exhibiting similar levels of mRNA as the high producing cell lines (GS-NS0 2P and GS-NS0 2N2). Together the evidence presented in this thesis clearly demonstrates that any rate-limiting steps or 'bottle-necks' in the production of recombinant mab's by mammalian cells are post-transcriptional.

Cell size does not influence productivity

To date (as far as we are aware) there have been no reports on the influence of cell size on the production of recombinant protein by mammalian cells in culture. Cell size measurements were made of GS-NS0 and GS-CHO cell lines (section 3.3.2). Although there appears to be an inverse correlation between cell volume and the maximum mab titre, no correlation was observed between cell volume and cell specific productivity. Fluctuations in cell size are known to occur and have been reported previously (Conlon and Raff, 2003), but this is thought to be governed in the main by the stage of the cell cycle that the cell currently occupies.

Cellular levels of PDI may be rate limiting?

It has previously been reported in the literature that the major rate limiting step in the production of recombinant proteins by mammalian cells in culture occurs within the ER and involves the folding of nascent polypeptide chains (Downham, 1996). A microsome fractionation procedure was optimised (chapter 4) which was complementary to current 2D-PAGE technology that allowed examination, in detail, of the protein complement that constituted the secretory pathway of GS-CHO and GS-NS0 cell lines. These results clearly show that there were very few changes that correlate with increased cell specific productivity in both cell types. The proteins that were identified to increase in abundance were mostly present at low levels and around half of these proteins are involved in the metabolic processes that generate energy (chapter 5). However, because of the observation that PDI does increase in abundance with increasing levels of cell specific productivity in GS-NS0 cell lines and the fact that this is corroborated by studies performed elsewhere (Smales et al., unpublished)(Lambert, 1997), it is reasonable to deduce that the cell specific productivity of mab's by GS-NS0 cell lines are limited, at least to some extent, by cellular PDI levels, and that an increase in PDI levels could lead to an increase in the cell specific production rate. However, the results obtained in this study are

inconclusive as to whether PDI levels are definitely rate limiting. Furthermore, there are a number of PDI isoforms present and only one of these appeared to increase with specific productivity. It appears unlikely that with all the coordinated processes required to produce mabs (section 1.1), upregulation of one component of the machinery prevents a bottleneck. Other proteins involved in this procedure, such as GRP78 and GRP94, did not alter.

A productive cell has a bias to its range of proteins involved in mab productivity

The majority of changes observed within the protein complement of the microsome fraction in both cell line species were cell line specific. The results presented in this thesis imply that each cell has a 'bias' (cell specific bias) to its range of proteins involved in integrated cellular functions such as productivity and metabolism. In other words, it seems that each cell line exhibits a slightly (or majorly) different pattern in protein expression which ultimately effects the productive state of the cell. Such specific changes in protein expression do not appear to be conserved between cell species or clonal populations. Furthermore, the high numbers of cell specific changes between cell lines which are high producers (i.e. GS-NS0 2X, 2P, 2N2 and GS-CHO 34C10, 63E4, 30B5) lends evidence to this hypothesis of a cell specific bias. It also appears that the levels of folding intermediates such as GRP78 and HSC70 within the microsome fraction are not rate limiting in the production of recombinant mabs as these are already present at high levels. Furthermore, an increase in the levels of ER chaperones involved in recombinant protein synthesis such as GRP78 and GRP94 would in all likelihood initiate a stress response such as the unfolded protein response (UPR) (Cudna and Dickson, 2003; Rothblatt et al., 1994) which is detrimental as UPR leads to cessation of cell growth and proliferation and ultimately the cell would be directed to the apoptotic pathway. It is therefore likely that due to the cell specific bias in protein complement described earlier and the evidence that folding intermediates are not rate limiting, an engineering strategy to improve cell specific productivity by altering specific components of the secretory pathway is unlikely to succeed.

An increase in metabolic capacity may be required for high cell specific productivity

From the data presented in this thesis of the comparative analysis of the microsome fraction of GS-NS0 and GS-CHO cell lines, we speculate that it is not the up-regulation of

specific proteins that is conserved between cell lines and clonal populations which limits cell specific productivity, but rather the up-regulation of specific processes (i.e. energy metabolism) involved in the production of recombinant mabs. Indeed, the research presented here shows that the majority of proteins up-regulated in accordance with productivity are involved in energy metabolism. This observation correlates with a report previously published by Van Atken et al. (Van Atken et al., 2003). This report used a comparative proteomic approach to investigate the changes in protein expression that occur as a B cell prepares for antibody secretion. They found that by clustering proteins according to temporal expression patterns, it appeared that B cells anticipate their secretory role in a multi-step process. The up-regulation of proteins involved in metabolism indicated that metabolic capacity expanded first followed by an expansion of secretory machinery to accommodate the mass production of antibodies that followed (Van Atken et al., 2003). From this respect it may be a more prudent strategy to direct the cell to use high-ATP–yielding metabolic pathways (i.e. complete oxidation of glucose through the tricarboxylic acid cycle rather than incomplete oxidation via glycolysis) rather than up-regulating elements of protein sysnthesis and folding. This strategy has been applied with some success in a study by Irani et al.(Irani et al., 1999). In this study, cytoplasmic pyruvate carboxylase (PYC) was introduced into host cells to reconstitute the link between glycolysis and the TCA cycle. Cells expressing PYC displayed more efficient energy production from glucose and glutamine. Consequently, the consumption of these two carbon sources was lowered and this resulted in decreased production of lactate and ammonia. As a result, the culture lifespan and productivity were extended.

Translation efficiency, and the optimisation of heavy and light chain levels within the ER. Are these valid targets for manipulation?

As previously discussed, it appears likely that a strategy based on altering protein folding components within the ER is unlikely to succeed in terms of improving cell specific productivities as these components are already present at high levels and such a strategy may indeed have a negative effect on productivity. Furthermore, growth curve data presented in this thesis (chapter 2) for the cell lines investigated suggests that a stress response (such as the UPR) is not induced. Therefore, it is plausible that the capacity of the ER to process recombinant protein has not yet been realised. It also appears to be the case that increases in mRNA levels had a limited effect on cell specific productivity, possibly due to a threshold or saturation effect. One could therefore speculate that the levels of

nascent polypeptide within the ER may be rate limiting, and as such a strategy to increase the efficiency of mRNA translation may be more likely to succeed in increasing productivity.

It is well known that control of gene expression at the translational level is mostly governed by the coding gene structure (Kim et al., 1997). Therefore one potential strategy to increase productivity is to modify the coding sequence of an individual gene without altering the amino acid sequence of the gene product. In other words, to alter the codon bias. Expressivity is a major determinant of codon usage in all species studied so far. As such, genes that are highly expressed tend to use a narrow set of codons corresponding to the most abundant species of tRNA. This minimises the risk of tRNA depletion during translation (Fuglsang, 2003). It may be the case that the codons (or tRNA availability) can be a rate limiting factor in productivity. In order to overcome this problem, the non-optimal codons in the recombinant genes can be substituted for codons that correspond to the more abundant tRNA species. A report by Kim et al. illustrates that highly expressed human and yeast genes show non-random codon usage patterns (Kim et al., 1997). Furthermore, Sueoka et al. showed that human prevalent codons usually have a cytosine (C) or guanosine (G) at their third degenerative position. This results in more stable mRNA secondary structures because of stronger GC base pairing and can protect the mRNA from rapid degradation (Sueoka and Kawanishi, 2000). This strategy has been used in the past to successfully improve expression of recombinant genes in *E.coli* (Humphreys et al., 2000) but the potential of altering the codon bias in mammalian cells is still unknown and open to question.

Recent studies carried out elsewhere (Smales et al., unpublished) have shown that the intracellular levels of IgG heavy and light chains in productive GS-NS0 cell lines do not correlate with the levels of secreted IgG molecules. This suggests that inefficiencies in the formation of this heteromeric complex may be inhibiting its transport out of the ER, and consequently, its secretion out of the cell. Furthermore, it is likely to be the case that unassembled components of the IgG are retained within the ER due to a stable association with the ER chaperone GRP78 (Mayer et al., 2000). A report by Lee et al. (Lee et al., 1999) suggests that an excess of light chain is required to facilitate proper folding and assembly of a transport competent IgG molecule. This study showed that without sufficient levels of light chain expression the constant heavy domain of the IgG heavy chain neither

fold nor forms its intra-domain disulphide bond and therefore remains a substrate for GRP78 (Lee et al., 1999). Furthermore, *in vivo* light chains are required to facilitate both the folding of the heavy chain and the release of GRP78. Therefore, a strategy to optimise the ratio of expressed light chain to heavy chain may facilitate more efficient IgG assembly and lead to an increase in the levels of transport competent IgG molecules for secretion out of the cell.

In summary this investigation has demonstrated that a strategies to improve recombinant monoclonal antibody productivity from mammalian cells based on altering the complement of secretory pathway components is unlikely to succeed. However, future strategies based on directing a productive cell to expand its metabolic capacity by more efficient use of carbon sources in the media could yield a positive outcome. We have also demonstrated that mRNA levels do not correlate with mab productivities and as such efforts to improve the amount of mRNA translated by altering the codon bias may increase the levels of nascent polypeptide within the ER. This strategy could be coupled with improving the efficiency of antibody assembly within the ER by optimising the ratio of expressed heavy to light chain. The presence of excess light chain may result in an increase in the rate of antibody assembly which in turn would increase the rate of transport and ultimately secretion.

References

Aebersold, R. and Mann, M. (2003) Mass spectrometry-based proteomics. Nature, 422, 198-207.

Allan, B.B., Weissman, J., Aridor, M., Moyer, B., Chen, C., Yoo, J., and Balch, W.E. (2000) Stage-specificb assays to study biosynthetic cargo selection and role of SNAREs in export from the endoplasmic reticulum and delivery to the golgi. Methods, 20, 411-416.

Ames, G.F. and Nikaido, K. (1976) Two-dimensional gel electrophoresis of membrane proteins. Biochemistry, 15, 616-23.

Anderson, N.L., and Anderson, N.G. (1998) Proteome and proteomics: New technologies, new concepts, and new words. Electrophoresis, 19, 1853-1861.

Andersson, U., Antonicka, H., Houstek, J. and Cannon, B. (2000) A novel principle for conferring selectivity to poly(A)-binding proteins: interdependence of two ATP synthase beta-subunit mRNA-binding proteins. Biochem J, 346, 33-39.

Bailey, J.E. (1991) Toward a science of metabolic engineering. Science, 252, 1668-1675.

Bailey, J.E., Sburlati, A., Hatzimanikatis, V., Lee, K., Renner, W.A. and Tsai, P.S. (1996) Inverse metabolic engineering: A strategy for directed genetic engineering of useful phenotype. Biotechnol Bioeng, 52, 109-121.

Baker, K.N., Rendall, M.H., Patel, A., Boyd, P., Hoare, M., Freedman, R.B. and James, D.C. (2002) Rapid monitoring of recombinant protein products: a comparison of current technologies. Trends Biotechnol, 20, 149-156.

Barlowe, C. (2003) Signals for COPII-dependent export from the ER: What's the ticket out? Trends Cell Biol, 13, 295-300.

Barnes, L.M., Bentley, C.M. and Dickinson, A.J. (2003) Stability of protein production from recombinant mammalian cells. Biotechnol Bioeng, 81, 631-639.

Barnes, L.M., Bentley, C.M. and Dickson, A.J. (2001) Characterization of the stability of recombinant protein production in the GS-NS0 expression system. Biotechnol Bioeng, 73, 261-270.

Barnes, L.M., Bently, C.M., and Dickson, A.J. (2000) Advances in animal cell recombinant protein production: GS-NS0 expression system. Cytotechnology, 32, 109-123.

Bebbington, C.R., Renner, G., Thomson, S., King, D., Abrams, D. and Yarranton, G.T. (1992) High-level expression of a recombinant antibody from myeloma cells using a glutamine synthetase gene as an amplifiable selectable marker. Biotechnology (N Y), 10, 169-175.

Bennett, M.K. and Scheller, R.H. (1993) The molecular machinery for secretion is conserved from yeast to neurons. Proc Natl Acad Sci U S A, 90, 2559-2563.

Berg, J.M., J, T. and Stryer, L. (2003) Biochemistry (5th edition). W.H.Freeman.

Berkelman, T., and Stenstedt, T. (1998) 2-D Electrophoresis using immobilised pH gradients. Principles & Methods. Amersham Pharmacia Biotech.

Bibila, T. and Flickinger, M.C. (1991) A Structured Model for Monoclonal Antibody Synthesis in Exponetially Growing and Stationary Phase Hybridoma Cells. Biotechnol Bioeng, 37, 210-226.

Birch, J.R. (1999) Suspension Culture, Animal Cells. In Flickinger, M.C. and Drew, S.W. (eds.), Encyclopedia of Bioprocess Technology: Fermentation, Biocatalysis, and Bioseparation. J Wiley & Sons, pp. 2509-2516.

Birch, J.R. and Froud, S.J. (1994) Mammalian cell culture systems for recombinant protein production. Biologicals, 22, 127-133.

Blackstock, W.P., and Weir, M.P. (1999) Proteomics: quantitative and physical mapping of cellular proteins. Trends in Biotechnology, 17, 121-127.

Borth, N., Strutzenberger, K., Kunert, R., Steinfellner, W. and Katinger, H. (1999) Analysis of changes during subclone development and ageing of human antibody-producing heterohybridoma cells by northern blot and flow cytometry. J Biotechnol, 67, 57-66.

Brooks, R.F. and Shields, R. (1985) Cell Growth, Cell Division and Size Homeostasis in Swiss 3T3 Cells. Exp.Cell Res, 156, 1-6.

Brown, M.E., Renner, G., Field, R.P. and Hassell, T. (1992) Process development for the production of recombinant antibodies using the glutamine synthetase (GS) system. Cytotechnology, 9, 231-236.

Buettner, R., Papoutsuglou, G., Scemes, E., Spray, D.C. and Dermietzel, R. (2000) Evidence for secretory pathway localization of a voltage-dependent anion channel isoform. PNAS, 97, 3201-3206.

Campbell, M.K. and Farrell, S.O. (2003) Biochemistry (4th Edition). Thompson.

Celis, J.E., and Gromov, P. (1999) 2D protein electrophoresis: can it be perfected? Current Opinion in Biotechnology, 10, 16-21.

Champion, K.M., Arnott, D., Henzel, W.J., Hermes, S., Weikert, S., Stults, J., Vanderlann, M. and Krummen, L. (1999) A two-dimensional protein map of chinese hamster ovary cells. Electrophoresis, 20, 994-1000.

Chang, C. and Yoshida, A. (1994) Cloning and characterization of the gene encoding mouse mitochondrial aldehyde dehydrogenase. Gene, 148, 331-336.

Chevallet, M., Santoni, V., Poinas, A., Rouquie, D., Fuchs, A., Kieffer, S., Rossignol, M., Lunardi, J., Garin, J. and Rabilloud, T. (1998) New zwitterionic detergents improve the analysis of membrane proteins by two-dimensional electrophoresis. Electrophoresis, 19, 1901-9.

Chevet, E., Cameron, P.H., Pelletier, M.F., Thomas, D.Y. and Bergeron, J.J. (2001) The endoplasmic reticulum: integration of protein folding, quality control, signaling and degradation. Curr Opin Struct Biol, 11, 120-124.

Chik, J.K., Lindberg, U. and Schutt, C.E. (1996) The structure of an open state beta actin at 2.65 A resolution. J. Mol.Biol, 263, 607-623.

Cockett, M.I., Bebbington, C.R. and Yarranton, G.T. (1991) The use of engineered E1A genes to transactivate the hCMV-MIE promoter in permanent CHO cell lines. Nucleic Acids Res, 19, 319-325.

Conlon, I. and Raff, M. (2003) Differences in the way a mammalian cell and yeast cells coordinate cell growth and cell-cycle progression. J.Biol, 2, 7.

Cudna, R.E. and Dickson, A.J. (2003) Endoplasmic reticulum signaling as a determinant of recombinant protein expression. Biotechnol Bioeng, 81, 56-65.

Cull, M., McHendry, C.S. (1990) Preparation of extracts from prokaryotes. Methods in Enzymology, 182, 194-203.

Dalili, M. and Ollis, D.F. (1990) A Flow-Cytometric Analysis of Hybridoma Growth and Monoclonal Antibody Production. Biotechnol Bioeng, 36, 64-73.

Davis, R., Schooley, K., Rasmussen, B., Thomas, J. and Reddy, P. (2000) Effect of PDI overexpression on recombinant protein secretion in CHO cells. Biotechnol Prog., 16, 736-743.

Desilva, M.G., Notkins, A.L. and Lan, M.S. (1997) Molecular characterization of a pancreas-specific protein disulfide isomerase, PDIp. DNA Cell Biol, 16, 269-74.
Dickinson, A.J. (2003) Personal Communication.

Dignam, J.D. (1990) Preparation of Extracts from Higher Eukaryotes. Methods in Enzymology, 182, 193-203.

Domanico, S.Z., DeNagel, D.C., Dahlseid, J.N., Green, J.M. and Pierce, S.K. (1993) Cloning of the gene encoding peptide-binding protein 74 shows that it is a new member of the heat shock protein 70 family. Mol Cell Biol, 13, 3598-3610.

Dorner, A.J., Wasley, L.C. and Kaufman, R.J. (1992) Overexpression of GRP78 mitigates stress induction of glucose regulated proteins and blocks secretion of selective proteins in chinese hamster ovary cells. EMBO, 11, 1563-1571.

Downham, M.R., Farrell, W.E, and Jenkins H.A. (1996) Endoplasmic Reticulum Protein expression in recombinant NS0 Myelomas Grown in batch Culture. Biotechnol Bioeng, 51, 691-696.

Ducommun, P., Kadouri, A., von Stockar, U. and Marison, I.W. (2002) On-line determination of animal cell concentration in two industrial high-density culture processes by dielectric spectroscopy. Biotechnol Bioeng, 77, 316-323.

Dunn, M.J., Gorg, A. (2001) Two-dimensional polyacrylamide gel electrophoresis for proteome analysis. In Pennington, S.R., and Dunn M.J (ed.) Proteomics: from protein sequence to function. BIOS, Oxford, pp. 43-64.

Dutt, M.J. and Lee, K.H. (2000) Proteomic analysis. Current Opinion in Biotechnology, 11, 176-179.

Edman, J.C., Ellis, L., Blacher, R.W., Roth, R.A. and Rutter, W.J. (1985) Sequence of protein disulphide isomerase and implications of its relationship to thioredoxin. Nature, 317, 267-70.

Ellgaard, L. and Helenius, A. (2001) ER quality control: towards an understanding at the molecular level. Curr Opin Cell Biol, 13, 431-437.

Fann, C.H., Guarna, M.M., Kilburn, D.G. and Piret, J.M. (1999) Relationship between recombinant activated protein C secretion rates and mRNA levels in baby hamster kidney cells. Biotechnol Bioeng, 63, 464-472.

Ferrari, D.M. and Soling, H.D. (1999) The protein disulphide-isomerase family: unravelling a string of folds. Biochem J, 339, 1-10.

Fichmann, J. (1999a) Advantages of Immobilized pH Gradients. In Link, A.J. (ed.), Methods in Molecular Biology: 2-D Proteome Analysis Protocols. Humana Press, Vol. 112, pp. 173-174.

Fichmann, J., and Westermeier, R. (1999b) 2-D Protein Gel Electrophoresis: An Overview. In Link, A.J. (ed.), Methods in Molecular Biology: 2-D Proteome Analysis Protocols. Humana Press, Vol. 112, pp. 1-8.

Flick, M.J. and Konieczny, S.F. (2002) Identification of putative mammalian D-lactate dehydrogenase enzymes. Biochem Biophys Res Commun, 295, 910-916.

Flickinger, M.C., Goebel, N.K., Bibila, T. and Boyce-Jacino, S. (1992) Evidence for posttranscriptional stimulation of monoclonal antibody secretion by L-glutamine during slow hybridoma growth. J Biotechnol, 22, 201-226.

Frand, A.R., Cuozzo, J.W. and Kaiser, C.A. (2000) Pathways for protein disulphide bond formation. Trends Cell Biol, 10, 203-10.

Freedman, R.B. (1995) The formation of protein disulphide bonds. Curr.Opin.Struct.Biol, 5, 85-91.

Fu, P. and Barford, J.P. (1994) Methods and strategies available for the process control and optimization of monoclonal antibody production. Cytotechnology, 14, 219-232.

Fuglsang, A. (2003) Codon optimizer: a freeware tool for codon optimization. Protein Expr. Purif., Article in press.

Fussenegger, M., Schlatter, S., Datwyler, D., Mazur, X., and Bailey, J.E. (1998) Controlled proliferation by multigene metabolic engineering enhances the productivity of Chinese hamster ovary cells. Nature Biotechnology, 16, 468-472.

Galeva, N., and Altermann, M. (2002) Comparison of one-dimensional and two-dimensional gel electrophoresis as a separation tool for proteomic analysis of rat liver microsomes: Cytochromes P450 and other membrane proteins. Proteomics, 2, 713-722.

Galfre, G. and Milstein, C. (1981) Preparation of monoclonal antibodies: strategies and procedures. Methods in Enzymology, 73, 3-46.

Geisse, S., Gram, H., Kleuser, B. and Kocher, H.P. (1996) Eukaryotic expression systems: A comparison. Protein. Expr. Purif, 8, 271-282.

Gething, M.J. (1999) Role and regulation of the ER chaperone BiP. Semin Cell Dev Biol, 10, 465-472.

Gething, M.J. and Sambrook, J. (1992) Protein folding in the cell. Nature, 355, 33-45.

Gevaert, K. and Vandekerckhove, J. (2000) Protein identification methods in proteomics. Electrophoresis, 21, 1145-1154.

Gilmore, R. (1993) Protein Translocation across the Endoplasmic Reticulum: A Tunnel with Toll Booths at Entry and Exit. Cell, 75, 589-592.

Glick, B.S. (2000) Organization of the Golgi apparatus. Curr Opin Cell Biol, 12, 450-456.

Gorg, A., Obermaier, C., Boguth, G., Harder, A., Scheibe, B., Wildgruber, R., and Weiss, W. (2000) The current state of two-dimensional electrophoresis with immobilized pH gradients. Electrophoresis, 21, 1037-1053.

Graham, J.M. (1997) Homogenisation of tissues and cells. In Graham, J.M., and Rickwood, D (ed.) Subcellular Fractionation: A practical approach. Oxford University Press, pp. 1-29.

Graves, P.R. and Haystead, T.A.J. (2002) Molecular Biologist's guide to proteomics. Microbiol.Mol.Biol.Rev, 66, 39-63.

Grillari, J., Fortschegger, K., Grabherr, R.M., Hohenwarter, O., Kunert, R. and Katinger, H. (2001) Analysis of alterations in gene expression after amplification of recombinant genes in CHO cells. J Biotechnol, 87, 59-65.

Guarna, M.M., Fann, C.H., Busby, S.J., Walker, K.M., Kilburn, D.G. and Piret, J.M. (1995) Effect of cDNA Copy Number on Secretion Rate of Activated Protein C. Biotechnol Bioeng, 46, 22-27.

Hamman, B.D., Hendershot, L.M. and Johnson, A.E. (1998) Bip maintains the permeability barrier of the ER membrane by sealing the lumenal end of the translocon pore before and early in translocation. Cell, 92, 747-758.

Han, D.K., Eng, J., Zhou, H. and Aebersold, R. (2001) Quantitative profiling of differentiation-induced microsomal proteins using isotope-coded affinity tags and mass spectrometry. Nat Biotechnol, 19, 946-951.

Hauri, H., Appenzeller, C., Kuhn, F. and Nufer, O. (2000) Lectins and traffic in the secretory pathway. FEBS Lett, 476, 32-37.

Haynes, P.A., Gygi, S.P., Figeys, D. and Aebersold, R. (1998) Proteome analysis: Biological assay or data archive? Electrophoresis, 19, 1862-1871.

Haystead, T.A.J. (2003) Personal Communication.

Hearn, A.S., Stroupe, M.E., Cabelli, D.E., Lepock, J.R., Tainer, J.A., Nick, H.S. and Silverman, D.N. (2001) Kinetic analysis of product inhibition in human manganese superoxide dismutase. Biochemistry, 40, 12051-12058.

Hensel, G., Assmann, V. and Kern, H.F. (1994) Hormonal regulation of protein disulphide isomerase and chaperone sythesis in rat exocrine pancrease. Eur J Cell Biol, 63, 208-218.

Herbert, B.R., Sanchez, J and Bini, L. (1997) Two-Dimensional Electrophoresis: The State of the Art and Future Directions. In Wilkins, M.R., Williams, K.L., Appel, R.D., Hochstrasser, D.F (ed.) Proteome Research: New Frontiers in Functional Genomics. Springer, Berlin, pp. 13-33.

High, S. (1995) Protein translocation at the membrane of the endoplasmic reticulum. Prog.Biophys.molec.Biol, 63, 233-250.

Hinton, B.M. (1997) Isolation of subcellular fractions. In Subcellular Fractionation: A practical approach. Graham, J.M., and Rickwood, D (ed.) Oxford University Press, pp. 31-69.

Hjelmeland, L.M. (1990) Solubilization of Native Membrane Proteins. Methods in Enzymology, 182, 253-264.

Hong, W. (1998) Protein transport from the endoplasmic reticulum to the Golgi apparatus. J Cell Sci, 111, 2831-2839.

Hopitzan, A., Himmelbauer, H., Spevak, W. and Castanon, M.J. (2000) The mouse Psma1 gene coding for the alpha-type C2 proteasome subunit: structural and functional analysis, mapping, and colocalization with Pde3b on mouse chromosome 7. Genomics, 66, 313-323.

Horibata, K. and Harris, A.W. (1970) Mouse myelomas and lymphomas in culture. Exp.Cell Res, 60, 61-77.

Huang, W., Suzuki, K., Nagase, H., Arumugam, S., Van Doren, S.R. and Brew, K. (1996) Folding and characterisation of the amino-terminal domain of human tissue inhibitor of metalloproteinases-1 (TIMP-1) expressed at high yield in E.coli. FEBS Lett, 384, 155-161.

Humphreys, D.P., Sehdev, M., Chapman, A.P., Ganesh, R., Smith, B.J., King, L.M., Glover, D.J., Reeks, D.G. and Stephens, P.E. (2000) High-Level Periplasmic Expression in Escherichia coli Using a Eukaryotic Signal Peptide: Importance of Codon Usage at the 5' End of the Coding Sequence. Protein Expr. Purif., 20, 252-264.

Ibarra, N., Watanabe, S., Bi, J., Shuttleworth, J. and Al-Rubeai, M. (2003) Modulation of cell cycle for enhancement of antibody productivity in perfusion culture of NS0 cells. Biotechnol Prog, 19, 224-228.

Ikenaka, Y., Yoshiji, H., Kuriyama, S., Yoshii, J., Noguchi, R., Tsujinoue, H., Yanase, K., Namisaki, T., Imazu, H., Masaki, T. and Fukui, H. (2003) Tissue inhibitor of metalloproteinases-1 (TIMP-1) inhibits tumor growth and angiogenesis in the TIMP-1 transgenic mouse model. Int J Cancer, 105, 340-346.

Irani, N., Wirth, M., Van den Heuvel, J. and Wagner, R. (1999) Improvement of the primary metabolism of cell culture by introducing a new cytoplasmic pyruvate carboxylase reaction. Biotechnol Bioeng, 66, 238-246.

Jan, D.C., Jones, S.J., Emery, A.N. and Al-Rubeai, M. (1994) Peptone, a low-cost growth-promoting nutrient for intensive animal cell culture. Cytotechnology, 16, 17-26.

Jazwinski, S.M. (1990) Preparation of extracts from yeast. Methods in Enzymology, 182, 154-174.

Johnson, M., Yang, H., Johanning, G.L. and Patel, M.S. (1997) Characterisation of the mouse dihydrolipoamide dehydrogenase (Dld) Gene: Genomic sructure, promotor sequence and chromosomal localization. Genomics, 41, 320-326.

Kaghad, M., Dumont, X., Chalon, P., Lelias, J.M., Lamande, N., Lucas, M., Lazar, M. and Caput, D. (1990) Nucleotide sequences of cDNAs alpha and gamma enolase mRNAs from mouse brain. Nucleic Acids Res, 18, 3638.

Kaiser, C. (2000) Thinking about p24 proteins and how transport vesicles select their cargo. PNAS, 97, 3783-3785.

Kao, F.T. and Puck, T.T. (1968) Genetics of somatic mammalian cells, VII. Induction and isolation of nutritional mutants in chinese hamster cells. Proc. Natl. Acad. Sci. USA, 60, 1275-1281.

Kasahara, M., Hayashi, M., Tanaka, K., Inoko, H., Sugaya, K., Ikemura, T. and Ishibashi, T. (1996) Chromosomal localization of the proteasome Z subunit gene reveals an ancient chromosomal duplication involving the major histocompatibility complex. Proc Natl Acad Sci U S A, 93, 9096-9101.

Keen, M.J. and Hale, C. (1996) The use of serum free medium for the production of functionally active humanised monoclonal antibody from NS0 mouse myeloma cells

engineered using glutamine synthetase as a selectable marker. Cytotechnology, 18, 207-217.

Kelley, B.D. (2001) Biochemical engineering: Bioprocessing of therapeutic proteins. Curr Opin Biotechnol, 12, 173-174.

Keown, W.A., Campbell, C.R. and Kucherlapati, R.S. (1990) Methods for introducing DNA into mammalian cells. Methods in Enzymology, 185, 527-537.

Kim, C.H., Oh, Y. and Lee, T.H. (1997) Codon optimisation for high-level expression of human erythropoietin (EPO) in mammalin cells. Gene, 199, 293-301.

Kim, N.S., Kim, S.J. and Lee, G.M. (1998) Clonal variability within dihydrofolate reductase-mediated gene amplified chinese hamster ovary cells: stability in the absence of selective pressure. Biotechnol Bioeng, 60, 679-688.

Klumperman, J. (2000) Transport between the ER and Golgi. Curr.Opin.Cell.Biol, 12, 445-449.

Kozutsumi, Y., Normington, K., Press, E., Slaughter, C., Sambrook, J. and Gething, M.J. (1989) Identification of immunoglobulin heavy chain binding protein as glucose- regulated protein 78 on the basis of amino acid sequence, immunological cross-reactivity, and functional activity. J Cell Sci Suppl, 11, 115-137.

Kozutsumi, Y., Segal, M., Normington, K., Gething, M.J. and Sambrook, J. (1988) The presence of malfolded proteins in the endoplasmic reticulum signals the induction of glucose related proteins. Nature, 332, 462-464.

Kromenaker, S.J. and Srienc, F. (1994) Cell cycle kinetics of the accumulation of heavy and light chain immunoglobulin proteins in a mouse hybridoma cell line. Cytotechnology, 14, 205-218.

Lambert, N., and Merten, O. (1997) Effect of Serum-Free and Serum-Containing Medium on Cellular Levels or ER-Based Proteins in various Mouse Hybridoma Cell Lines. Biotechnol Bioeng, 54, 165-180.

Lee, Y.K., Brewer, J.W., Hellman, R. and Hendershot, L.M. (1999) Bip and Immunoglobulin Light Chain Cooperate to Control the Folding of Heavy Chain and Ensure the Fidelity of Immunoglobulin Assembly. Mol.Biol.Cell, 10, 2209-2219.

Leno, M., Merten, O.W. and Hache, J. (1992a) Kinetic -analysis of hybridoma growth and monoclonal-antibody production in semi-continuous culture. Biotechnol Bioeng, 39, 596-606.

Leno, M., Merten, O.W. and Hache, J. (1992b) Kinetic studies of cellular metabolic activity, specific IgG production rate, IgG mRNA stability and accumilation during hybridoma batch culture. Enzyme.Microb.Technol, 14, 135-140.

Lenstra, J.A., and Bloemendal, H. (1983) Topography of the total protein population from cultured cells upon fractionation by chemical extractions. Eur.J.Biochem, 135, 413-423.

Letourneur, F., Hennecke, S., Demolliere, C. and Cosson, P. (1995) Steric masking of a dilysine endoplasmic reticulum retention motif during assembly of the human high affinity receptor for immunoglobulin E. J Cell Biol, 129, 971-978.

Lewis, S.A., Lee, M.G. and Cowan, N.J. (1985) Five mouse tubulin isotypes and their regulated expression during development. J Cell Biol, 101, 852-861.

Lodish, H. and Kong, N. (1993) The secretory pathway is normal in dithiothreitol treated cells, but disulphide-bonded proteins are reduced and reversibly retained in the endoplasmic reticulum. J Biol Chem, 268, 20598-20605.

Lodish, H., Baltimore, D., Berk, A., Zipursky, S.L., Matsudaira, P., and Darnell, J. (1995) Molecular Cell Biology. Scientific American books, New York.

Lubiniecki, A.S. (1998) Historical reflections on cell culture engineering. Cytotechnology, 28, 139-145.

Maniatis, T., Fritsch, E.F. and Sambrook, J. (1982) Molecular Cloning: A Laboratory Manual. Cold Spring Harbour Press, Cold Spring Harbour, NY.

Mann, M. and Wilm, M. (1994) Error-tolerant identification of peptides in sequence databases by peptide sequence tags. Anal Chem, 66, 4390-4399.

Matsui, N.M., Smith-Beckerman, D. M., and Epstein, L.B. (1999) Staining Preparative 2-D gels: Coomassie Blue and Imidazole-Zinc Negative Staining. In Link, A.J. (ed.), Methods in Molecular Biology: 2-D Proteome Analysis Protocols. Humana Press, Vol. 112, pp. 307-312.

Mayer, M., Kies, U., Kammermeier, R. and Buchner, J. (2000) BiP and PDI cooperate in the oxidative folding of antibodies in vitro. J Biol Chem, 275, 29421-29425.

Mazzarella, R.A., Srinivasan, M., Haugejorden, S.M. and Green, M. (1990) ERp72, an abundant luminal endoplasmic reticulum protein, contains three copies of the active site sequences of protein disulfide isomerase. J Biol Chem, 265, 1094-101.

Meister, A. (1980) Catalytic mechanism of glutamine synthetase; Overview of glutamine metabolism. In J, M. and R, P. (eds.), Glutamine : Metabolism, Enzymology and Regulation. Academic Press, pp. 1-40.

Meister, A. (1985) Glutamate, glutamine, glutathione and related compounds. Methods in Enzymology, 113, 16-27.

Merten, O.W., Moeurs, D., Keller, H., Leno, M., Palfi, G.E., Cabanie, L. and Couve, E. (1994) Modified Monoclonal Antibody Production Kinetics, Kappa/Gamma mRNA levels, and Metabolic Activities in Murine Hybridoma Selected by Continuous Culture. Biotechnol Bioeng, 44, 753-764.

Michalski, W.P. and Shiell, B.J. (1999) Strategies for analysis of electrophoretically separated proteins and peptides. Analytica Chimica Acta, 383, 27-46.

Miller, I.J. and Bieker, J.J. (1993) A novel, erythroid cell-specific murine transcription factor that binds to the CACCC element and is related to the Kruppel family of nuclear proteins. Mol Cell Biol, 13, 2776-2786.

Miller, W.M., Blanch, H.W. and Wilke, C.R. (2000) A kinetic analysis of hybridoma growth and metabolism in batch and continuous suspension culture: effect of nutrient concentration, dilution rate, and pH. Reprinted from Biotechnology and Bioengineering, Vol. 32, Pp 947-965 (1988). Biotechnol Bioeng, 67, 853-871.

Moriyama, K., Matsumoto, S., Nishida, E., Sakai, H. and Yahara, I. (1990) Nucleotide sequence of mouse cofilin cDNA. Nucleic Acids Res, 18, 3053.

Munro, S. (1998) Localization of proteins to the Golgi apparatus. Trends Cell Biol, 8, 11-15.

Neugebauer, J.M. (1990) Detergents: An Overview. Methods in Enzymology, 182, 239-253.

Nishimura, N. and Balch, W.E. (1997) A di-acidic signal required for selective export from the endoplasmic reticulum. Science, 277, 556-558.

Noiva, R. (1999) Protein disulfide isomerase: the multifunctional redox chaperone of the endoplasmic reticulum. Semin Cell Dev Biol, 10, 481-93.

Nothwehr, S.F., and Gordon, J. I. (1990) Targeting of proteins into the eukaryotic secretory pathway: signal peptide structure/function relationships. Bioessays, 12, 479-484.

Novick, P. and Brennwald, P. (1993) Friends and Family: The role of the Rab GTPases in vesicular traffic. Cell, 75, 597-601.

Novick, P., Field, C. and Schekman, R. (1980) Identification of 23 complementation groups required for post- translational events in the yeast secretory pathway. Cell, 21, 205-215.

O'Farrell, P.H. (1975) High Resolution Two-Dimensional Electrophoresis of Proteins. Journal of Biological Chemistry, 250, 4007-4021.

Oliver, J.D., Van der Wal, F.J., Bulleid, N.J. and High, S. (1997) Interaction of the thiol-dependent reductase ERp57 with nascent glycoproteins. Science, 275, 86-88.

O'Malley, K., Mauron, A., Barchas, J.D. and Kedes, L. (1985) Constitutively expressed rat mRNA encoding a 70-kilodalton heat-shock-like protein. Mol Cell Biol, 5, 3476-3483.

Orci, L and Rothman, J.E (1992) Molecular dissection of the secretory pathway. Nature, 355, 409 - 415.

Pahl, H.L. and Baeuerle, P.A. (1997) The ER-overload response: activation of NF-kB. Trends Biochem Sci, 22, 63-67.

Palade, G. (1975) Intracellular aspects of the process of protein synthesis. Science, 189, 347-358.

Pappin, D.J.C., Hojrup, P. and Bleasby, A.J. (1993) Rapid identification of proteins by peptide mass fingerprinting. Curr.Biol, 3, 327-332.

Pelham, H.R. (1990) The retention signal for soluble proteins of the endoplasmic reticulum. Trends Biochem Sci, 15, 483-486.

Potter, M. and Boyce, C.R. (1962) Induction of a plasma cell neoplasma in strain BALB/c mice with mineral oil and mineral oil adjuvants. Nature, 193, 1086-1087.

Presley, R. (1997) Evolutionary biology. Pelvic problems for mammals. Nature, 389, 440-441.

Puck, T.T., Cieciura, S.J. and Robinson, A. (1958) Genetics of somatic mammalian cells. J. Exp. Med, 108, 945-959.

Rabilloud, T. (1999) Silver Staining of 2-D Electrophoresis Gels. In Link, A.J. (ed.), Methods in Molecular Biology: 2-D Proteome Analysis Protocols. Humana Press, Vol. 112, pp. 297-306.

Rabilloud, T., Adessi, C., Giraudel, A., Lunardi, J. (1997) Improvement of the solubilisation of proteins in two-dimesional electrophoresis with immobilised pH gradients. Electrophoresis, 18, 307-316.

Ramagli, L.S. (1999) Quantifying Protein in 2-D PAGE solubilization Buffers. In Link, A.J. (ed.) Proteome Analysis Protocols. Humana Press Inc, Vol. 112, pp. 99-103.

Ramasamy, R., Munro, A. and Milstein, C. (1974) Possible role for the Fc receptor on B lymphocytes. Nature, 249, 573-574.

Rao, C.N., Castronovo, V., Schmitt, M.C., Wewer, U.M., Claysmith, A.P., Liotta, L.A. and Sobel, M.E. (1989) Evidence for a precursor of the high affinity metastasis-associated murine laminin receptor. Biochemistry, 28, 7476-7486.

Rapoport, T.A. (1992) Transport of proteins across the endoplasmic reticulum membrane. Science, 258, 931-936.

Renner, W.A., Lee, K.H., Hatzimanikatis, V., Bailey, J.E. and Eppenberger, H.M. (1995) Recombinant cyclin E expression activates proliferation and obviates surface attachment of Chinese hamster ovary cells (CHO) cells in protein-free medium. Biotechnol Bioeng, 47, 476-482.

Robinson, A.S., Hines, V. and Wittrup, K.D. (1994) Protein disulphide isomerase overexpression increases secretion of foreign protein in saccharomyces cerevisea. Biotechnology, 12, 381-384.

Roitt, I.M. (1985) Essential Immunology. Blackwell Scientific.

Roth, R.A. and Pierce, S.B. (1987) In vivo cross-linking of protein disulphide isomerase to immunoglobulins. Biochemistry, 26, 4179-4182.

Rothblatt, J., Novick, P. and Stevens, T. (eds.). (1994) Guidebook to the secretory pathway. Oxford University Press, New York.

Rothman, J.E. (1994) Mechanisms of intracellular protein transport. Nature, 372, 55-63.

Rothman, J.E. and Orci, L. (1992) Molecular dissection of the secretory pathway. Nature, 355, 409 - 415.

Rothman, J.E. and Wieland, F.T. (1996) Protein sorting by transport vesicles. Science, 272, 227-234.

Santoni, V., Molloy, M. and Rabilloud, T. (2000) Membrane proteins and proteomics: un amour impossible? Electrophoresis, 21, 1054-70.

Saraste, J. and Kuismanen, E. (1984) Pre- and post-Golgi vacuoles operate in the transport of Semliki Forest virus membrane glycoproteins to the cell surface. Cell, 38, 535-549.

Schekmam, R., and Orci, L. (1996) Coat proteins and vesicle budding. Science, 271, 1526-1533.

Schrag, J.D., Procopio, D.O., Cygler, M., Thomas, D.Y. and Bergeron, J.J. (2003) Lectin control of protein folding and sorting in the secretory pathway. Trends Biochem Sci, 28, 49-57.

Schröder M., Körner C., and Friedl P. (1999) Quantitative analysis of transcription and translation in gene amplified chinese hamster ovary cells on the basis of a kinetic model. Cytotechnology, 29, 93-102.

Schröder, M., Schafer, R. and Friedl, P. (2002) Induction of protein Aggregation in an Early Secretory Compartment by Elevation of Expression Level. Biotechnol Bioeng, 78, 131-140.

Schubert, U., Anton, L.C., Gibbs, J., Norbury, C.C., Yewdell, J.W. and Bennink, J.R. (2000) Rapid degradation of a large fraction of newly synthesized proteins by proteasomes. Nature, 404, 770-774.

Shevchenko, A., Wilm, M., Vorm, O. and Mann, M. (1996) Mass spectrometric sequencing of proteins silver-stained polyacrylamide gels. Anal Chem, 68, 850-858.

Singh, R.P., Emery, A.N. and Al-Rubeai, M. (1996) Enhancement of survivability of mammalian cells by overexpression of the apoptotis supressor gene bcl-2. Biotechnol Bioeng, 52, 166-175.

Sitia, R., Neuberger, M.S., Alberini, C., Bet, P., Fra, A.M., Valetti, C., Williams, G. and Milstein, C. (1990) Development regulation of IgM secertion: the role of the carboxy terminal cysteine. Cell, 60, 781-790.

Siuzdak, G. (1994) The emergence of mass spectrometry in biochemical research. Proc Natl Acad Sci U S A, 91, 11290-11297.

Smales, C.M. (2003) Personal Communication.

Smales, C.M., Birch, J.R., Racher, A.J., Marshall, C.T. and James, D.C. (2003) Evaluation of individual protein errors in silver-stained two-dimensional gels. Biochem Biophys Res Commun, 306, 1050-1055.

Söllner, T., Bennett, M.K., Whiteheart, S.W., Scheller, R.H. and Rothman, J.E. (1993) A protein assembly-disassembly pathway in vitro that may correspond to sequential steps of synaptic vesicle docking, activation and fusion. Cell, 75, 409-418.

Steinburg, T.H., Jones, L.J., Haughland, R.P. and Singer, V.L. (1996) SYPRO orange and SYPRO red protein gel stains: One-step fluorescent staining of denatured gels for detection of nanogram levels of protein. Anal. Biochem, 239, 223-237.

Stevens, F.J. and Argon, Y. (1999) Protein folding in the ER. Semin Cell Dev Biol, 10, 443-454.

Stohwasser, R., Kuckelkorn, U., Kraft, R., Kostka, S. and Kloetzel, P.M. (1996) 20S proteosome from LMP7 knock out mice reveals altered proteolytic activities and cleavage site preferences. FEBS Lett, 383, 109-113.

Storrie, B., and Madden,E.A. (1990) Isolation of Subcellular Organelles. Methods in Enzymology, 182, 203-225.

Storrie, B., Pepperkok, R. and Nilsson, T. (2000) Breaking the COPI monopoly on Golgi recycling. Trends Cell Biol, 10, 385-391.

Strausberg, R.L., Feingold, E.A., Grouse, L.H., Derge, J.G., Klausner, R.D., Collins, F.S., Wagner, L., Shenmen, C.M., Schuler, G.D., Altschul, S.F., Zeeberg, B., Buetow, K.H., Schaefer, C.F., Bhat, N.K., Hopkins, R.F., Jordan, H., Moore, T., Max, S.I., Wang, J., Hsieh, F., Diatchenko, L., Marusina, K., Farmer, A.A., Rubin, G.M., Hong, L., Stapleton, M., Soares, M.B., Bonaldo, M.F., Casavant, T.L., Scheetz, T.E., Brownstein, M.J., Usdin, T.B., Toshiyuki, S., Carninci, P., Prange, C., Raha, S.S., Loquellano, N.A., Peters, G.J., Abramson, R.D., Mullahy, S.J., Bosak, S.A., McEwan, P.J., McKernan, K.J., Malek, J.A., Gunaratne, P.H., Richards, S., Worley, K.C., Hale, S., Garcia, A.M., Gay, L.J., Hulyk, S.W., Villalon, D.K., Muzny, D.M., Sodergren, E.J., Lu, X., Gibbs, R.A., Fahey, J., Helton, E., Ketteman, M., Madan, A., Rodrigues, S., Sanchez, A., Whiting, M., Young, A.C., Shevchenko, Y., Bouffard, G.G., Blakesley, R.W., Touchman, J.W., Green, E.D., Dickson, M.C., Rodriguez, A.C., Grimwood, J., Schmutz, J., Myers, R.M., Butterfield, Y.S., Krzywinski, M.I., Skalska, U., Smailus, D.E., Schnerch, A., Schein, J.E., Jones, S.J. and Marra, M.A. (2002) Generation and initial analysis of more than 15,000 full-length human and mouse cDNA sequences. Proc Natl Acad Sci U S A, 99, 16899-16903.

Strutzenberger, K., Borth, N., Kunert, R., Steinfellner, W. and Katinger, H. (1999) Changes during subclone development and ageing of human antibody- producing recombinant CHO cells. J Biotechnol, 69, 215-226.

Sueoka, N. and Kawanishi, Y. (2000) DNA G+C content of the third codon position and codon usage biases of human genes. Gene, 261, 53-62.

Takemoto, H., Yoshimori, T., Yamamoto, A., Miyata, Y., Yahara, I., Inoue, K. and Tashiro, Y. (1992) Heavy chain binding protein (BiP/GRP78) and endoplasmin are exported from the endoplasmic reticulum in rat exocrine pancreatic cells, similar to protein disulfide-isomerase. Arch Biochem Biophys, 296, 129-36.

Taylor, R.S., Wu, C.C., Hays, L.G., Eng, J.K., Yates, J.R., 3rd and Howell, K.E. (2000) Proteomics of rat liver Golgi complex: minor proteins are identified through sequential fractionation. Electrophoresis, 21, 3441-59.

Terashima, M., Kim, K.M., Adachi, T., Nielsen, P.J., Reth, M., Kohler, G. and Lamers, M.C. (1994) The IgM antigen receptor of B lymphocytes is associated with prohibitin and a prohibitin-related protein. Embo J, 13, 3782-3792.

Urano, T., Takamiya, K., Furukawa, K. and Shiku, H. (1992) Molecular cloning and functional expression of the second mouse nm23/NDP kinase gene, nm23-M2. FEBS Lett, 309, 358-362.

Urlaub, G. and Chasin, L.A. (1980) Isolation of Chinese Hamster cell mutants defiecient in dihydrofolate reductase activity. Proc. Natl. Acad. Sci. USA, 77, 4216-4220.

Van Atken, E., Romiji, E.P., Maggioni, C., Mezghrani, A., Sitia, R., Braakman, I. and Hack, J.R. (2003) Sequential waves of functionally related proteins are expressed when B cells prepare for antibody secretion. Immunity, 18, 243-253.

Van Dyk, D.D., Misztal, D.R., Wilkins, M.R., Mackintosh, J.A., Poljak, A., Varnal, J.C., Teber, E., Walsh, B.J. and Gray, P.P. (2003) Identification of cellular changes associated with increased production of human growth hormone in a recombinant Chinese hamster ovary cell line. Proteomics, 3, 147-156.

Varki, A. (1998) Factors controlling the glycosylation potential of the Golgi apparatus. Trends Cell Biol, 8, 34-40.

Venner, T.J. and Gupta, R.S. (1990) Nucleotide sequence of mouse HSP60 (chaperonin, GroEL homolog) cDNA. Biochim Biophys Acta, 1087, 336-338.

Walls, J.D., Berg, D.T., Yan, S.B. and Grinnell, B.W. (1989) Amplification of multicistronic plasmids in the human 293 cell line and secretion of correctly processed recombinant human protein C. Gene, 81, 139-149.

Wells, W.A. (2002) Does size matter? J.Cell.Biol, 158, 1156-1159.

Whiteheart, S.W., Shenbagamurthi, P., Chen, L., Cotter, R.J. and Heart, G.W. (1989) Murine elongation factor 1 alpha (EF-1 alpha) is posttranslationally modified by novel amide-linked ethanolamine-phosphoglycerol moieties. Addition of ethanolamine-phosphoglycerol to specific glutamic acid residues on EF-1 alpha. J Biol Chem, 264, 14334-14341.

Wieland, F and Harter, C. (1996) The secretory pathway: mechanisms of protein sorting and transport. Biochimica et Biophysica Acta, 1286, 75-93.

Wilkins, M.R., Sanchez, A.A., Williams, K.L. and Hochstrasser, D.F. (1996) Current challanges and future applications for protein maps and post-translational vector maps in proteome projects. Electrophoresis, 17, 830-838.

Wong, C.M., Chun, A.C., Kok, K.H., Zhou, Y., Fung, P.C., Kung, H.F., Jeang, K.T. and Jin, D.Y. (2000) Characterization of human and mouse peroxiredoxin IV: evidence for inhibition by Prx-IV of epidermal growth factor- and p53-induced reactive oxygen species. Antioxid Redox Signal, 2, 507-518.

Wu, C.C., Yates, J.R., 3rd, Neville, M.C. and Howell, K.E. (2000) Proteomic analysis of two functional states of the Golgi complex in mammary epithelial cells. Traffic, 1, 769-82.

Wurm, F. and Bernard, A. (1999) Large-scale transient expression in mammalian cells for recombinant protein production. Curr Opin Biotechnol, 10, 156-159.

Yotov, W.V. and St-Arnaud, R. (1993) Cloning and functional expression analysis of the alpha subunit of mouse ATP synthase. Biochem Biophys Res Commun, 191, 142-148.

Zhang, X., Shaw, A., Bates, P.A., Newman, R.H., Gowen, B., Orlova, E., Gorman, M.A., Kondo, H., Dokurno, P., Lally, J., Leonard, G., Meyer, H., van Heel, M. and Freemont, P.S. (2000) Structure of the AAA ATPase p97. Mol Cell, 6, 1473-1484.

Zhou, W., Chen, C., Buckland, B., and Aunins, J. (1997) Fed-Batch Culture of Recombinant NS0 Myeloma Cells with High Monoclonal Antibody Production. Biotechnol Bioeng, 55, 783-792.

Zhou, W., Rehm, J., Europa, A. and Hu, W. (1997) Alteration of mammalian cell metabolism by dynamic nutrient feeding. Cytotechnology, 24, 99-108.